Study of the soil-interaction behaviour with underground structures under unsaturated conditions

By

Omar Hassan Al-Emami

Submitted for the degree of Doctor of Philosophy

(Civil Engineering)

Heriot-Watt University

School of Energy, Geoscience, Infrastructures and Society

May 2020

ABSTRACT

Soil-structure interface behaviour is an interesting topic due to the complexity of the interface mechanics. The interfaces between cohesionless soils and solid structure elements are encountered in different geotechnical engineering projects. The shear strength and stiffness characteristics, the thickness of the interfacial layer, the bonding and slipping properties are playing significant roles in an understanding the mechanical behaviour of such interfaces. One of the key parameters for the design and safety assessment of the engineering structures (e.g. retaining walls, deep and shallow foundations, tunnels and earth reinforcement) is the shear strength at the interface. Suction is an important stress-state variable of unsaturated soils. The magnitude of matric suction affects the shear strength and the volume change of soil and soil-concrete interfaces, thus the adequate characterization of interface behaviour is significant for its precise performance predictions.

The prime aim behind this study is to investigate the behaviour of interface between compacted silty sand soil and concrete counterfaces at (a) different initial void ratios, (b) different surface roughness (smooth and rough) under the influence of different levels of applied vertical stress and test conditions (saturated and constant water content). The second main objective of this study is to investigate the effect of void ratio and the effect of the applied vertical stress level on the variation of matric suction during direct shear tests (matric suction stabilisation, consolidation and shearing stages). To do so, a new loading steel cap of large-scale direct shear apparatus for testing soil-soil and soil-concrete specimens has been manufactured.

Firstly, a series of large-scale (300 mm x 300 mm) direct shear tests were carried out on compacted soil samples under different levels of applied vertical stress, void ratios and test conditions (saturated and constant water content). The experimental results confirm the dependency of shear strength, volumetric behaviour and measured matric suction on the vertical stress and initial void ratio. Secondly, to investigate the interface behaviour with different surface roughness (smooth and rough) and compare it with the behaviour of soil-soil samples, a number of interface direct shear tests were conducted between silty sand and a concrete pad under the same levels of vertical stress, void ratios and test conditions. The trend of behaviour of the shear strength versus horizontal displacement curves of soil-concrete interface tests is similar to those of soil tests. The laboratory tests results show that the surface roughness, vertical stress, void ratio and test

conditions have significant influence on the shearing characteristics of the interface samples. The study noted that the strain softening behaviour of the tested material is noticeably influenced by the initial void ratio of specimens and surface roughness for both test conditions. From the results, it was observed that the initial matric suction has a clear dependency on the void ratio of the specimens. The shearing behaviour of the soil samples was higher than the rough and smooth interfaces for both studied void ratios and test conditions, whereas, the smooth interface showed lower values of shear strength of all the tested samples. It was noted that there is a remarkable decrease in matric suction during shearing stage with the level of applied vertical stress and the most important matric suction evolution was occurred before the horizontal displacement corresponding to the peak/maximum shear strength achieved.

HERIOT WATT UNIVERSITY

Research Thesis Submission

Please note this form should be bound into the submitted thesis.

Name:	Omar Hassan Fakhri AL-Emami		
School:	Energy, Geoscience, Society and Infrastructure (EGIS)		
Version: *(i.e. First, Resubmission, Final)*	Final	Degree Sought:	PhD (Civil Engineering)

Declaration

In accordance with the appropriate regulations I hereby submit my thesis and I declare that:

1. The thesis embodies the results of my own work and has been composed by myself
2. Where appropriate, I have made acknowledgement of the work of others
3. The thesis is the correct version for submission and is the same version as any electronic versions submitted*.
4. My thesis for the award referred to, deposited in the Heriot-Watt University Library, should be made available for loan or photocopying and be available via the Institutional Repository, subject to such conditions as the Librarian may require
5. I understand that as a student of the University I am required to abide by the Regulations of the University and to conform to its discipline.
6. I confirm that the thesis has been verified against plagiarism via an approved plagiarism detection application e.g. Turnitin.

ONLY for submissions including published works

Please note you are only required to complete the Inclusion of Published Works Form (page 2) if your thesis contains published works)

7. Where the thesis contains published outputs under Regulation 6 (9.1.2) or Regulation 43 (9) these are accompanied by a critical review which accurately describes my contribution to the research and, for multi-author outputs, a signed declaration indicating the contribution of each author (complete)
8. Inclusion of published outputs under Regulation 6 (9.1.2) or Regulation 43 (9) shall not constitute plagiarism.

* *Please note that it is the responsibility of the candidate to ensure that the correct version of the thesis is submitted.*

Signature of Candidate:	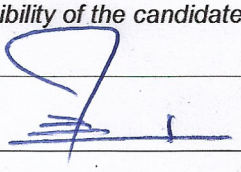	Date:	29/05/2020

Submission

Submitted By *(name in capitals)*:	Omar Hassan Fakhri AL-Emami
Signature of Individual Submitting:	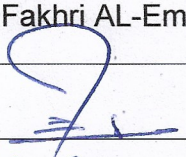
Date Submitted:	29/05/2020

For Completion in the Student Service Centre (SSC)

Limited Access	Requested	Yes		No		Approved	Yes		No	
E-thesis Submitted ***(mandatory for final theses)***										
Received in the SSC by *(name in capitals)*:						Date:				

To my true treasures in life, my parents & wife

For dedicating their life for me and my wellbeing with endless love and support

Acknowledgments

In the Name of Allah, the All- Merciful, the All-Compassionate

The praise is due to Allah, the All-Powerful, the All-Knowing, the All-Wise and the Compassionate for giving me the strength, health, patience and perseverance to complete this work in its best.

I would like to express my sincere gratitude to my supervisor Professor Gabriela Medero for all continuous support, motivation and invaluable academic guidance. My thanks also extended to Professor Fernando Marinho for his collaboration and fruitful discussions. Special thanks are extended to the examination panel, Prof. Omar Laghrouche and Dr. Christopher Beckett for their worth comments and guidance.

I would like to especially thank the Embassy of the Republic of Iraq / Cultural attaché for financial support during my study. I greatly appreciate the support received from the Iraqi Ministry of Higher Education and Scientific research and the University of Technology to give me the opportunity to complete my doctoral study under grant of scholarship.

Great thanks also to the Geotechnical laboratory technician Mr. Alastair McFarlane for his help and support. You often beyond the call of duty in encouraging participation, supporting the aims of this project and providing the necessary expertise especially during the setting up of, and making operational, the large and small scales direct shear apparatus. My special thanks also extended to the mechanical workshops technicians Mr. David Murray and Mr. Tom Buckle for their help with manufacturing different parts of the testing apparatus and are very much appreciated for their works. Mr. Graham Sorley, the laboratory technician at the concrete laboratory is also appreciated for his assistance with manufacturing the concrete pad that was used in this research project.

Finally, and most of all, I would like to thank my parents and brothers for their continuous encouragement and moral support in many ways. This work would have not been possible without the encouragement, patience, and overwhelming support of my wife, Baraa. Finally, the patience of my son, Ryan during the lengthy period of this research is especially acknowledged.

Omar Hassan Al-Emami

TABLE OF CONTENTS

Lists of tables

Lists of figures

List of Acronyms and Symbols plus their Units

Notation	Description	Unit
ψ_{cp}	The capillary potential	kPa
ψ_{ad}	The adsorption potential	kPa
s	Matric suction	kPa
u_a	Pore air pressure	kPa
u_w	Pore water pressure	kPa
R_s	Radius of curvature of the meniscus	m
T_s	Surface tension at the contraktile skin	Nm
A *or* θ	Contact angle between contraktile skin and wall of capillary	o
Δ_u	Pressure difference across the air-water interface	kPa
r_s	Radial distance of the bulk solids arch from hopper virtual apex	m
g	Gravitation acceleration	ms^{-2}
ρ_W	Density of water	kg/m^3
h_c	Height of the capillary rise	m
v	Number of ions from one molecule of solute	----
R_u	Universal (molar) gas constant	J/ mol K
T	Absolute temperature	K
ϕ_0	Osmotic coefficient	----
π	Osmotic suction	kPa
ψ	Total suction	kPa
θ_{1d}	Water content corresponding to the drying path	----
θ_{1w}	Water content corresponding to the wetting path	----
σ'	Effective stress	kPa
σ	Total stress	kPa
σ_{net}	Net normal stress	kPa
β	Croney et al., (1952) pore water pressure factor	----
P''	Insufficiency in the pore water pressure	kPa
χ	Parameter depends on the water content	----
τ	Shear strength of saturated soil	kPa
τ_{us}	Shear strength of unsaturated soil	kPa
ϕ'	Effective angle of friction with respect to the net normal stress	o
c'	Effective cohesion of soil	kPa
ϕ^b	Angle of friction with respect to the changes in matric suction	o
K	Vanapalli et al., (1996) fitting parameter	----
Θ	Normalized water content	----
θ_w	Volumetric water content	----
θ_s	Saturated volumetric water content	----

θ_r	Residual volumetric water content	----
ψ_a	Rassam and Williams (1999) Air-entry value	kPa
β, λ, γ	Rassam and Williams (1999) fitting parameters	----
AEV	Air Entry Value	kPa
K	Garven and Vanapalli (2006) fitting parameter	----
I_p	Plasticity index	%
CDG	Completely Decomposed Granite soil	----
f_c	Potyondy (1961) Coefficient of soil cohesion	----
f_ϕ	Potyondy (1961) Coefficient of interface friction angle	----
σ'_{nf}	Effective normal stress at failure	kPa
δ'	Interface angle of friction with respect to the net normal stress	o
c_a'	Effective adhesion	kPa
δ^b	Interface friction angle with respect to the matric suction	o
ψ_i	Hossain and Yin (2010) interface dilation angle	o
δ_{max}	Hossain and Yin (2010) apparent interface friction angle	kPa
LL	Liquid limit	%
PL	Plastic limit	%
PI	Plasticity index	%
$USCS$	Unified Soil Classification System	----
PSD	Particle Size Distribution	----
c'	Effective soil cohesion	kPa
ϕ'	Effective angle of friction	o
G_s	Specific gravity of soil solids	----
e_{max}	Maximum void ratio	----
e_{min}	Minimum void ratio	----
$\rho_{d\ max}$	Maximum dry unit weight	kg/m^3
D_{50}	Average diameter of the tested soil	mm
OMC	Optimum Moisture Content	%
ω_i	Initial water content of soil sample	%
e_i	Initial void ratio	----
w_f	Water content at the end of direct shear test	%
e_f	Final void ratio at end of saturation stage	----
R_{max}	Maximum vertical distance between the highest and the lowest peaks of the structure asperities	mm
R_n	Normalised surface roughness	----
CP	Collapse potential of soil	%
σ_v	Applied vertical stress	kPa
$e_{f\ cons}$	Void ratio at end of consolidation stage	----
Δ_e	Change in void ratio	----
δ_h	Horizontal displacement at peak/maximum shear strength	mm
τ	Peak/maximum shear strength	kPa
S_{ri}	Initial degree of saturation	%
ρ_d	Dry density	kg/m^3

S_{rf}	Degree of saturation at end of consolidation or shearing stages	%
ΔS_r	Change in degree of saturation	%
$\omega_{f\ she}$	Water content at end of shearing stage	%
Ψ_{peak}	Matric suction corresponding to peak/maximum shear strength	kPa
$\Psi_{residual}$	Residual matric suction corresponding to peak/maximum shear strength	kPa
σ_n	Nominal surcharge load	kPa

CHAPTER ONE

INTRODUCTION

1.1 Introduction and research motivation

The understanding of the soil – structure interaction behaviour is relevant in different geotechnical engineering infrastructure set-ups such as retaining walls, tunnels, shallow foundations and pile foundations. The serviceability of the soil-structure system depends mainly on the hydro-mechanical behaviour of a thin layer formed close to the structure surface. This layer generally referred to as "interface", through which the stress is transferred from solid medium (i.e. structural element) to the softer surrounding soil. Hence, it is commonly exposed to considerable stress concentration and strain localization. The shear strength of the interface is relatively weak in comparison to the shear strength of soils (Gennaro and Frank, 2002; Hamid, 2005; Zhang et al., 2006). For many centuries, engineering structures have been built and relayed on the performance of the infrastructure interaction against the ground. In Iraq, for example, the use of pile foundations is considered appropriate to support many engineering structures. In a foundation like this, the soil-pile interface interaction is greatly affected by the axial response of the pile foundation (Mroueh and Shahrour, 2012). Piles can be classified into friction piles and end bearing piles. The skin friction of the pile is greatly dependant on the behaviour of the interface. In addition, the uplift capability of the piles which is used to resist the uplift forces is affected by the side friction of the piles.

One of the key parameters for the design and safety assessment of many civil engineering projects is the shear strength at the interface between the structure and the surrounding soil surfaces. Many researchers have studied the interface shear strength behaviour between soil (e.g. clay, sand and silt) and different construction materials (e.g. concrete, steel, wood, geotextile etc.) using different types of laboratory equipment including direct shear, simple shear, ring torsion, and annular shear (Potyondy, 1961; Brummund and Leonards, 1973; Acar et al., 1981; Fakharian, 1996). Some have studied

the influence of surface roughness (Yoshimi and Kishida, 1981), soil density (Bosscher and Ortiz, 1987), moisture content of soil (Acar et al., 1982) and different shearing rates (Al-mhaidib, 2006). Up to now most of the experimental research reported in the literature was conducted to examine the interface behaviour either completely dry or with fully saturated. Therefore, there is still a lack of information on the behaviour of the interfaces in unsaturated soils that are more representative of soil structure system in nature.

Unsaturated soil-structure interfaces are popular to many geotechnical engineering structures such as retaining walls constructed over unsaturated compacted soil, pre-cast pile driven (friction pile) in unsaturated soil, buried pipelines and soil nail. It is recognized that the soil properties such as shear strength, volume change and water seepage are influenced by the variation of water content in the soil (Fredlund and Rahardjo, 1993; Ng and Menzies, 2007). In recent years, few experimental studies have been carried out by researchers such as Hamid, (2005), Hossain, (2010) and Borana, (2013) to investigate the characteristics of unsaturated interfaces. These studies developed a small-scale (102 mm x 102 mm and 100 mm x 100 mm) direct shear apparatus for testing the shear strength and the volumetric behaviour of unsaturated soil-structure interfaces under constant matric suction and constant net normal stress conditions. The matric suction in these studies was imposed to the interface specimens by using the axis translation technique. In the work to be presented, an effort has been made to give contribution to the understanding of variation of matric suction during consolidation and shearing stages by means of laboratory works on soil-concrete interface samples tested under constant water content condition and constant applied vertical stress. To do so, a conventional large-scale (300 mm x 300 mm) direct shear apparatus has been developed for real-time matric suction measurements during different test stages.

1.2 Main aim and objectives

To the author's knowledge, this study is one of the first attempts to investigate the interface behaviour of Iraqi soil against concrete interface under constant water content condition. An extensive effort has been made in order to enable a deep understanding of the Iraqi soils. Several soil investigation reports have been collected and assed from different reliable Iraqi government sources. The collected reports examined the physical

and mechanical properties of the main Iraqi soils of different regions located at Baghdad governorate, the capital of Iraq (most populated city in Iraq). A Silty sand soil of Al-Mada'in district was selected due to this site is represent a good generalisation of the soil particle size distribution of Iraqi soils. To be able to develop the main aim of this research, a series of specific objectives were key and are described as follows:

(i) Design and construct a new loading steel cap of the large-scale direct shear apparatus to allow matric suction measurements during testing (from initial equalisation, consolidation and later shear).

(ii) Understand the shear strength and the volume changes behaviour of the studied silty sand soil at saturated and constant water content conditions under different levels of applied vertical stress and void ratios.

(iii) Investigate the shear strength and deformation characteristics of interface between compacted soil and two different concrete counterfaces (smooth and rough) under different vertical stresses, void ratios and test conditions (saturated and constant water content).

(iv) Examine the influence of void ratios, applied vertical stress and surface roughness on the evolutions of matric suction during consolidation and shearing stages.

(v) Undertake a comprehensive comparison of the shear strength of the silty sand soil and the interface shear strength under various vertical stresses and void ratios to build the current understanding of the performance of the soil-concrete interfaces under different values of degree of saturation and different mobilised matric suction.

1.3 Structure of the thesis

This thesis is divided into eight chapters, the review of literature, two chapter presenting the material and methodology and three chapters presenting the experimental tests results and their interpretation, as well as the introduction and conclusions chapters.

Chapter 2 Review of literature

This chapter starts with a brief review of the hydro-mechanical behaviour of unsaturated soils, the main features of shear strength and volumetric behaviour of soil and soil-concrete interface samples under saturated and unsaturated conditions, the effects of different factors on the behaviour of soil-interface specimens, and laboratory equipment available for soil-structure interface testing.

Chapter 3 Material investigation and selection

This chapter explains the procedures adopted to select the proper soil used in this research and its basic characteristics. A brief review of the general country background including topography, population, principal rivers and country boundaries is included. The available soil investigation reports of Baghdad governorate have been collected and re-analyzed and their physical properties are also indicated.

Chapter 4 Experimental equipment development and pilot tests

In this chapter, the physical properties of the prepared soil used in this study and the concrete interface characteristics are presented. The samples preparation procedures and the testing methodology of each test campaign that were adopted in this study are presented, as well. Finally, the details of the laboratory devices used in this study are also described.

Chapter 5 Soil shear strength behaviour

In this chapter, a series of laboratory large-scale (300 mm x 300 mm) direct shear tests were carried out on the compacted silty sand soil samples. The effects of different initial void ratios (e_i = 0.6 and 1.0), the levels of applied vertical stress (100, 200 or 400 kPa) and the test conditions (saturated and constant water content) on the shear strength and volumetric behaviour of the tested material are described. The evolution of matric suction during consolidation and shearing stages has been measured using Equitensiometer suction probes (EQ3) and presented as well. A comparison of saturated and constant water content states was made in order to explore the influence of matric suction on the shearing characteristics. In order to investigate the specimen size effect

on the shear strength of the tested samples, the test results obtained from small-scale (60 mm x 60 mm) direct shear apparatus were compared with those obtained from large-scale apparatus and presented at the end of this chapter.

Chapter 6 Soil-concrete interface shear strength behaviour

This chapter presents the test results and their interpretations of two types of soil-concrete interface specimens with different surface roughness (smooth and rough). These results are presented to explain the influence of many factors such as the level of applied vertical stress, initial void ratio, matric suction, and roughness on the interface shear strength and volumetric behaviour of the tested specimens. Also, the evolution of matric suction during consolidation and shearing stages has been measured and presented. Finally, a comparison is made between the results of saturated and constant water content interfaces.

Chapter 7 Comparison of shear behaviour of soil and soil-concrete interface

The comparisons of behaviour of soil and interfaces (rough and smooth) in terms of shear strength and volumetric behaviour are presented in this chapter. A comparison of the soil and interfaces under saturated condition is firstly presented, and then a similar comparison was made when the specimens are tested under constant water content condition. The effect of void ratio, applied vertical stress and surface roughness on the failure envelopes of soil and soil-concrete interface specimens are presented.

Chapter 8 Conclusions and recommendations

In this chapter, the main findings, relevant remarks and conclusions obtained from the present study are presented followed by the recommendations for future studies in the topic area.

CHAPTER TWO

LITERATURE REVIEW

2.1 Introduction to the unsaturated soils

The higher annual rate of the water evaporation which is greater than the annual rate of the rainfall- causing a third of the earth's surface to be arid or a semi-arid region- leads to the formation of unsaturated soils (Fredlund and Rahardjo, 1993; Lu and Likos, 2004). Hence, the quantity of water in the soil is a primary factor in determining the actual evaporation rate from the earth surface (Wilson, 1990). Other factors that play an important role in the formation of unsaturated soils are weather and environment. The redistribution of water content within a soil mass is caused by the water movement from the soil surface, could be triggered by either infiltration or evaporation (Miller and Miller, 1956). The soil located in the zone between the deepest water table and the earth's surface is usually defined as the unsaturated soil (multi-phases soil) as shown in Figure 2.1. The gaseous phase diminishes as depth is increased finally disappearing or remaining in dissolved state below the water table.

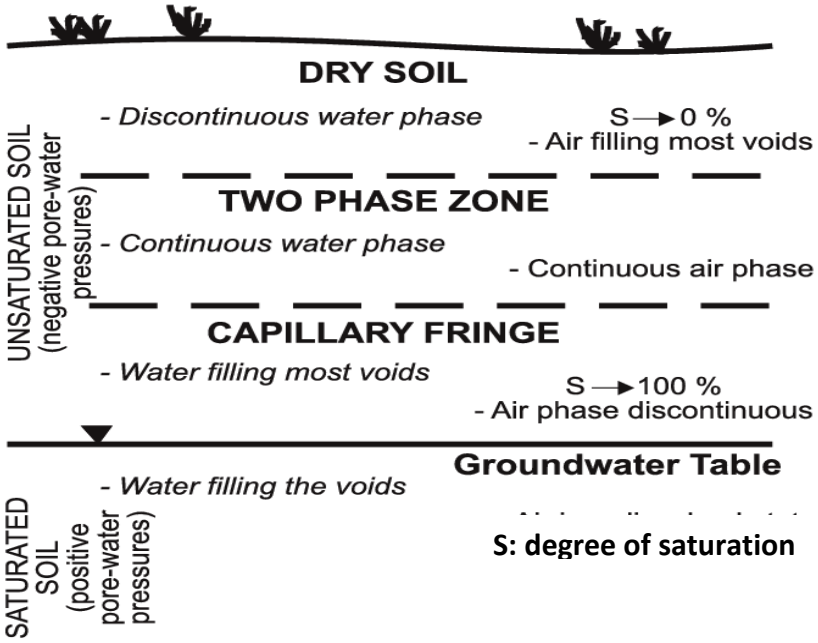

Figure 2.1: Classification of the regions within a saturated– unsaturated soil profile (Fredlund, 2000).

Unsaturated soil consists of three phases: firstly, the liquid phase which commonly exists in the soil voids not occupied by gas. Secondly, the gas phase generally which exists in the pore space not filled with liquid substance. Thirdly, the solid phase which contains different types of soil particles, ranging from fine-grained materials such as clay and silts to the coarse-grained materials such as gravels and sands. Noteworthy, the air-water interface or the contractile skin is known as the fourth phase (Fredlund and Morgenstern, 1977; Fredlund and Rahardjo 1993; Lu and Likos 2004; Ng and Menzies, 2007). A significant effect on the mechanical behaviour of unsaturated soils can be seen as a result of the complex interaction between the three phases (gas, liquid and solid particles).

Several man-made engineering structures for geotechnical applications are constructed using compacted soils (i.e., earth dams, road, housing, airport runways and highways) that are typically in a state of unsaturated condition at the time of placement. Soil compaction is the mechanical process that expels air from voids, complete removal of air voids is impossible and therefore, the end-product will be in the state of unsaturation (Lu and Likos, 2004; Maleki and Bayat, 2012; Elgabu, 2013). Many of these soil structures often do not attain fully saturated conditions during their design life. In nature, collapsible soils, residual soils and expansive soils, which are considered as a problematic soil, are all examples of unsaturated soils encountered in the engineering applications (Gan et al., 1988; Fredlund and Rahardjo, 1993; Lu and Likos, 2004; Maleki and Bayat, 2012).

2.2 The concept of soil suction in the unsaturated soil

2.2.1 Introduction

The suction theory concept emerged in the early 1900's and was developed in soil physics based on energy consideration (e.g. Buckingham, 1907; Gardner and Widtsoe, 1921; Schofield, 1935). In soil physics, soil suction is generally referred to potential energy level in the soil-water phase (Long, 2006; Elgabu 2013). Soil suction is one of the most important parameters widely used to depict the soil moisture stress status in the unsaturated soils. The laboratory measurements of the soil suction are extremely beneficial for estimating the quality of the samples; predicting the effective stress and genuine applications of unsaturated soil mechanics (Krahan and Fredlund, 1972).

2.2.2 Matric suction

Matric suction is closely linked with the capillary phenomenon and occurs as a result of the surface tension of the water phase, arising from the inter-molecular forces on the contractile skin (Fredlund and Rahardjo, 1993). Baker and Frydman (2009) pointed out that the matric suction is an addition of two energy components (per unit volume), namely the capillary potential, ψ_{cp} and the adsorption potential, ψ_{ad} which is related to with the adsorbed water film surrounding soil particles:

$$s = \psi_{cp} + \psi_{ad} \qquad \text{Eq. 2-1}$$

On the other hand, the matric suction, s is usually defined as a difference between the pore air pressure u_a and the pore water pressure u_w within the soil mass (Fredlund and Rahardjo, 1993):

$$s = u_a - u_w \qquad \text{Eq. 2-2}$$

Equation 2-2 is considered valid for the case where the capillary potential dominates; however, questions are raised for the validity of this equation when the major contribution of adsorbed potential onto the soil particles is the major dominate (Baker and Frydman 2009).

The balance of the forces, acting on both sides of any two fluids, is governed by the shape of the interface between them (Lu and Likos, 2004). In the case of three-phase system such as unsaturated soils, the interaction between the surface tension of both air and water phases generates the air-water interface or the contractile skin. The surface tension is tangential to the air-water interface and could be measured as the tensile force per unit length of the contractile skin (Fredlund and Rahardjo, 1993; Wang and Fredlund, 2003; Lu and Likos, 2004; Ng and Menzies, 2007).

As shown in Figure 2.2, surface tension develops along the water surface to equilibrate the inward forces due to an imbalance of intermolecular forces at the air-water interface. Whereas a water molecule inside the liquid experiences equal molecular attraction in all directions the one at the surface has a net attraction towards the water (Figure 2.2(a)).

The surface therefore curves to form an upward concave shape called the meniscus (Figure 2.2(b)). The water meniscus is inversely proportional to the tube diameter. The presence of surface tension (Figure 2.2(b)) enables the water to rise and stay above the atmospheric pressure level in a small-diameter tube (Fredlund and Rahardjo, 1993, Lu and Likos, 2004).

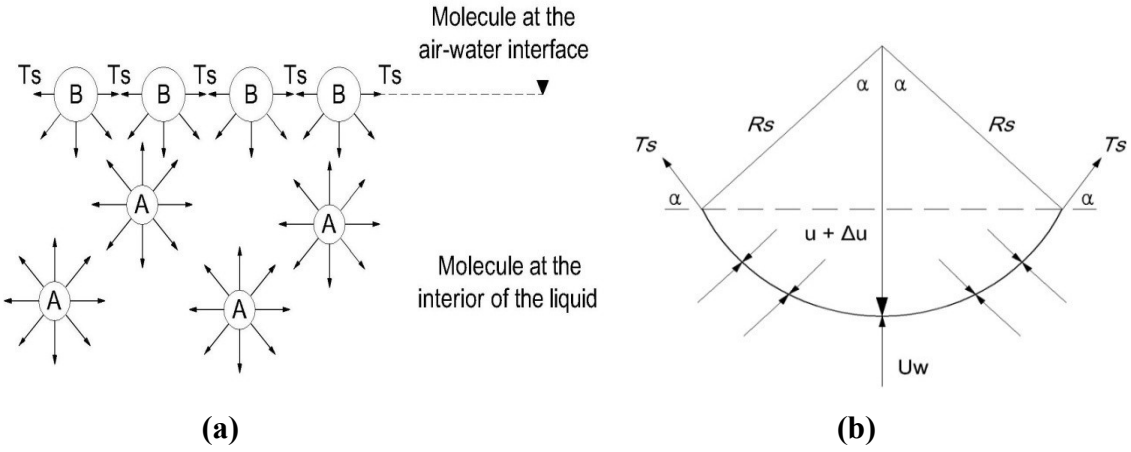

Figure 2.2: Surface tension phenomenon (a) inter-molecular forces; and (b) pressure and surface tension (Fredlund and Rahardjo, 1993).

In the early sixteenth century the capillary phenomenon has been well known when the Leonardo da Vinci noticed lifting of fluid in tight, wetted capillaries, holes and plugs (Lyklema, 2000). The capillary model in Figure 2.3 is used to describe the behaviour of water in a porous medium such as soil (Fredlund & Rahardjo, 1993; Ridley et al., 2003; Lu & Likos, 2004). Water rises and fills the soil voids above the water table leading to a near saturation zone called the capillary fringe as well as the flow during this zone generally describes as a capillary flow. The height of the capillary fringe, h_c , above the water table is a function of the pore sizes which is in turn a function of particle size and distribution within the soil system. Smaller tubes and hence finer soil particles are associated with higher capillary rise and bigger water menisci due to higher surface tension and vice versa (Miller and Miller, 1956; Marshall, 1959; Bear, 1972; Aubertin et al, 1998).

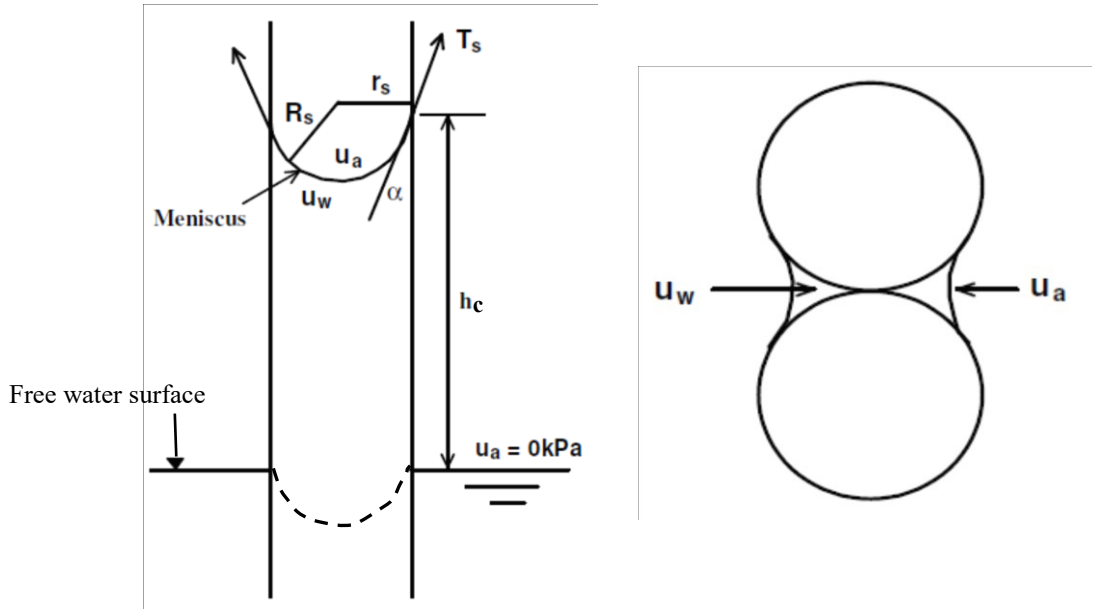

(a) Capillary suction in a tube **(b)** Water meniscus between two soil particles

Figure 2.3: The capillary model (after Kasangaki, 2012).

A liquid with an acute contact angle (e.g., water on glass) will form a concave meniscus, and therefore the water pressure under the meniscus will be smaller than the atmospheric pressure (Figure 2.3(a)). Hence, the water inside the tube will be driven up the tube from its initial location (shown as a dashed curve in Figure 2.3(a)) by the greater pressure of the free water (i.e., water at atmospheric pressure, under a horizontal air–water interface) outside the tube at the same level. When the water surface is concave, the centre of curvature lies outside the water and the curvature is regarded as negative. Thus, for a concave meniscus shown in Figure 2.3(a), the pressure difference between the capillary water (under the meniscus) and the atmosphere is negative with reference to atmosphere. In other words, the height of water above the free surface in the tube is equal to the negative of the capillary-pressure head (Fredlund and Rahardjo, 1993, Hillel, 2005; Ng and Menzies, 2007; Katte and Blight, 2012).

In the capillary tube, the pressure difference between pore-air and pore-water pressure can be calculated by using the Young-Laplace equation:

$$u_a - u_w = \frac{2T_S \cos \alpha}{r_S} \qquad \text{Eq. 2-3}$$

Where the difference ($u_a - u_w$) is the pressure difference across the meniscus and referred to as matric suction, u_a is the pore-air pressure, u_w is the pore-water pressure, T_s is the surface tension at the contractile skin, α is the contact angle between the contractile skin and the wall of capillary tube, R_s is the meniscus radius and r_s is radius of the tube (Fredlund and Rahardjo, 1993). Referring to the Figure 2.3, the corresponding maximum height of the water in the capillary tube, h_c is:

$$h_c = \frac{2\,T_S\,\cos\alpha}{\rho_w\,g\,R_S} \qquad \text{Eq. 2-4}$$

Where h is the height of capillary rise, g is the gravitational acceleration, α is the contact angle between the water meniscus and wall of the capillary tube, and ρ_w the mass density of water. If pure water and a clean tube are assumed then the contact angle is zero so that the maximum height of the water in the capillary clean tube is:

$$h_c = \frac{2\,T_S}{\rho_w\,g\,R_S} \qquad \text{Eq. 2-5}$$

By assuming the contact angle equal to zero, Fredlund and Rahardjo (1993) have explained the surface tension capability to hold the column of water in the capillary tube by plotting the capillary height, h_c versus the pore radius for the different type of soils as shown in Figure 2.4.

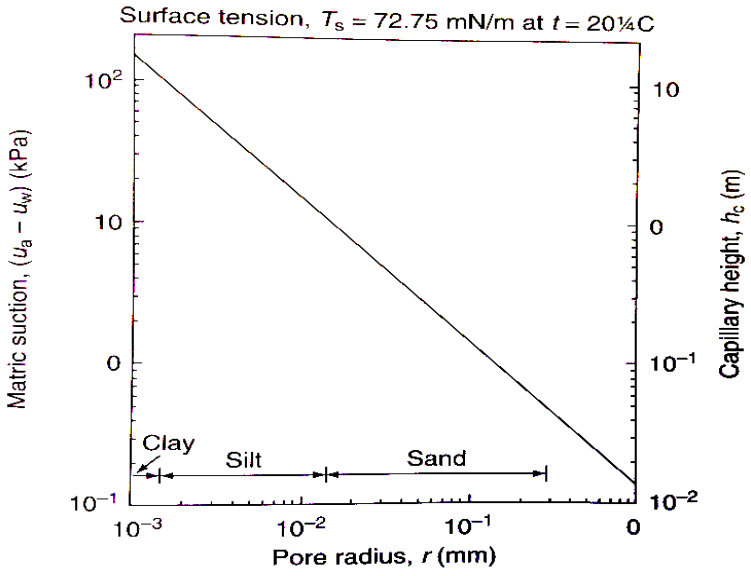

Figure 2.4: Relationship between capillary height, pore radius and matric suction (Fredlund and Rahardjo, 1993).

Capillary rise, that is the movement of pore water against the gravity force, is a prominent phenomenon in unsaturated soil mechanics. Well known samples of capillary rise in geotechnical structures are above the phreatic surface in embankment dams and beneath road pavements (Lu and Likos, 2004; Ghasemzadeh, 2008; Aghajani et al., 2010). The maximum height of capillary rise, h_c, has an important influence on physical and mechanical properties (e.g. matric suction and soil virtual cohesion) of unsaturated soils and is a highly complex system of both the soil and pore-water properties. Hence, the rate, maximum height, and fluid storage capacity of capillary rise are of paramount interest in unsaturated soil mechanics (Lu and Likos, 2004; Shahnazari et al., 2008). Such capillary rise phenomena lead to an increase of the saturation of the soil, which will not only decrease the strength of the soil but also alter the elastic modulus of substructure soils, thereby leading to the corresponding changes in stress and strain response under the external load (Li et al., 2018).

Wheeler and Karube (1995) classified the existing water in the unsaturated soils into three different forms: bulk water, adsorbed water and meniscus (i.e. capillary) water as shown in Figure 2.5. Whereas the bulk water totally occupied the voids between soil particles, the absorbed water surrounds the soil grains entirely due to the electro-chemical forces. The curved meniscus water exists at the contact points between soil particles arising from capillary phenomenon, forming water rings or bridges around them.

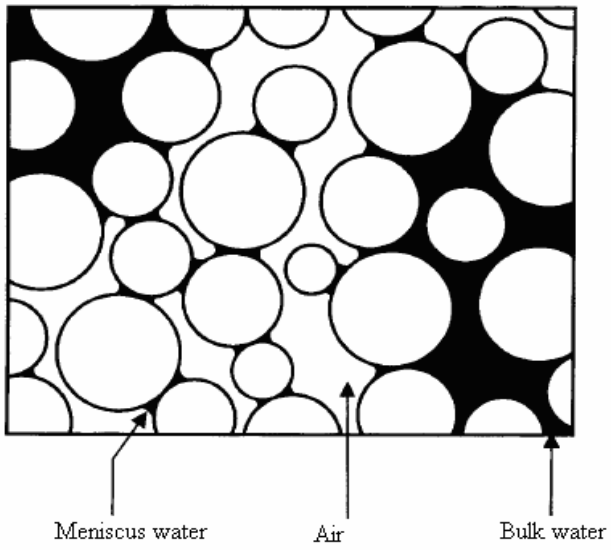

Figure 2.5: Forms of water in unsaturated soils (Wheeler and Karube, 1996).

2.2.3 Osmotic suction

The osmotic suction is a measure of the additional energy required for removing unit volume of water from the water phase due to the presence of dissolved (Leong et al., 2007; Kasangaki, 2012). It's calculated from the Van't Hoff's equation as follows;

$$\pi = - v R T m \phi \qquad \text{Eq. 2-6}$$

Where v is the number of ions from one molecule of solute (i.e., v = 2 for NaCl, KCl, NH_4Cl and v = 3 for Na_2SO_4, etc.); R is the universal (molar) gas constant [i.e. 8.31432 J/ (mol K)]; T is the absolute temperature (K); and ϕ is the osmotic coefficient.

The presence of the dissolved salts in the soil water decreases the relative humidity and results in an increase in the osmotic suction. In other words, an increase in the concentration of the dissolved salts in the water soil will lead to an increase in the energy required to remove a unit volume of the water from the soil water system. Osmotic suction is usually closely linked with the unsaturated soils than the saturated ones (Sowers and Sowers, 1970). Miller and Nelson (1993) conducted several laboratory experiments to study the effect of salt content and osmotic suction on the suction measurements of the naturally compacted clay. Their results showed that at given water content, the volumes of specimen prepared with sodium chloride giving higher osmotic suction are smaller than those of specimen prepared with distilled water. This indicates additional stress acting on the sodium chloride specimen.

Rao and Shivananda (2002) studied the influence of osmotic suction on the swelling of salt-amended clays. They stated that the the osmotic suction is one of the key parameter for understanding the behavior of soils with high salt content in the sense that the specimen with high-osmotic suction showed delay to reach maximum swelling strain due to migration of cation from the soil specimen to the reservoir. The influence of water content on the dissolved salt solution has been investigated by Sreedeep and Singh (2006). The authors concluded that the difference between the total and the matric suctions, which is equal to the osmotic suction, depends strongly on the water content of the soil. At low water content in which there is no dissolved salt in the soil pore-water, the osmotic suction is zero and negligible.

2.2.4 Total suction

Total suction ψ can be defined as the total free energy of soil water, which consists of two components, namely soil matric suction ($u_a - u_w$) and osmotic suction (π):

$$\psi = (u_a - u_w) + \pi \qquad \text{Eq. 2-7}$$

Where the pressure difference across the meniscus refers to the matric suction, u_a is a pore air pressure; u_w is a pore water pressure, and π is osmotic suction. Moreover, Fredlund and Rahardjo (1993) defined the total suction as the energy required to expel a unit volume of water from the unsaturated soil. In the absence of any contaminant in the soil, the total suction is equal to the matric suction (Malaya and Sreedeep, 2012). Total suction under equilibrium conditions is linked to the relative humidity of external gas pressure on the soil water.

2.3 Soil water retention behaviour

The Soil Water Retention Curve (SWRC); also known as soil water characteristic curve (Fredlund and Rahardjo, 1993; Barbour, 1998); soil moisture-retention curve (Kovacs, 1981) or the soil suction curve (Barbour, 1998) represents the graphical relationship between matric suction and water content or degree of saturation of the soil. It is generally determined by drying or moisturizing a soil specimen under pressure with the observation of the changes in the water content of the soil. The water occupying the voids between grains can be represented in three forms: the gravimetric water content ω, which is commonly used in the geotechnical engineering practice; the volumetric water content θ, and degree of saturation S_r, which represents the percentage of water in the soil mass (Fredlund et al., 1994; Rojas 2008; Miguel and Vilar 2009).

The SWRC gives a platform to investigate the ability of soil for adsorption and desorption of water during drying and wetting processes. The gradual drying of the saturated soil specimens generates the main drying curve, whereas, the main wetting curve results from a slow wetting of the soil specimen after air-drying process (Vanapalli et al., 1999). Figure 2.6 shows a typical soil-water retention curve of unsaturated porous materials. Clearly soil can exhibit different values of suction depending on whether it is subjected to drying (decrease in water content) or wetting

(increase in water content). The difference between the wetting and drying paths of the retention curve is called the hysteresis. This is an important phenomenon as hydraulic hysteresis gives rise to different degrees of saturation depending on whether moisture is moving into or out of the soil (wetting/drying paths) at a given suction value. This behaviour can be attributed to different arrangements of water within the voids and consequently different action of matric suction on the soil skeleton (Croney and Coleman, 1954; Lu and Likos, 2004; Haghighi, 2011).

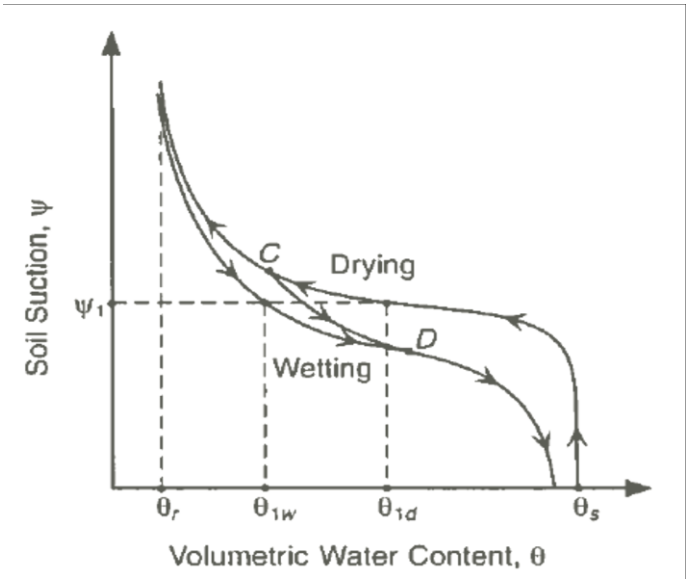

Figure 2.6: Hysteresis phenomenon in soil-water characteristic curve (Lu and Likos, 2004).

There may be several reasons for the hysteresis effect. These include: (1) the ink bottle effect caused by the inhomogeneity of the different shapes and sizes of the interconnected pores. Drying progress is controlled by the smaller pore radius, r, but wetting relies on the larger pore radius R (see Figure 2.7(a)); (2) various liquid–solid contact angles for advancing (wetting) and receding (drying) water meniscus (Figure 2.7(b)); (3) entrapped air in newly wetted soil; and (4) swelling and shrinking of the soil during wetting and drying processes causes various alterations in the soil structure (Wheeler and Karube, 1995; Hillel, 1998; Tinjum et al., 1997; Romero and Vaunet 2000; Lu and Likos, 2004; Birle et al., 2008).

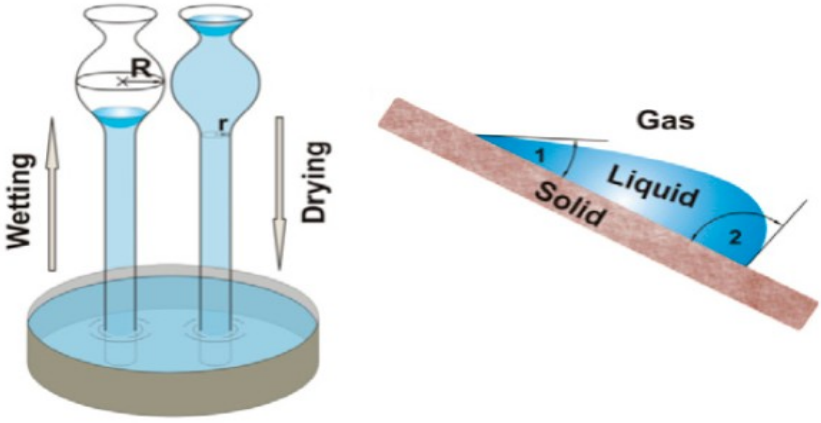

(a) Ink-bottle effect **(b)** contact angle effect

Figure 2.7: Potential mechanisms for hysteresis (Tuller, 2004).

White et al., (1970) has addressed the variation of water content along the drying soil-water retention curve. They reported that there are three main distinctive zones: the boundary zone (saturation), the transition zone (de-saturation), and the residual stage of unsaturation. Later, Vanapalli (1994) proposed a physical model to describe the changes of the water content in different zones of a typical drying soil-water retention curve as shown in Figure 2.8.

In the saturation zone, the voids are fully filled with water and the soils remain saturated to some extent. As the suction increases, the soil starts to de-saturate and hence the decrease in both the degree of saturation and/or the water content and this is known as the transition zone. The residual water content is the water content at residual state, at which the water phase becomes discontinuous. This marks the end of the transition zone and the beginning of the third zone called the residual saturation zone within which water is tightly adsorbed onto the soil particles and any water exchange occurs in the form of vapor. Any water remaining in the soil at the end of this zone is said to be chemically bonded to the soil (i.e. water is only coating soil particles in the form of adsorbed water film) and could be less important with respect to engineering behaviour (e.g. Fredlund et al., 1996; Barbour, 1998; Yang et al., 2004). The soil suction corresponding to the residual water content is called the residual soil suction, and marks the state at which the mechanism of the removal of water from the soil due to suction increase starts to change from drainage (i.e. liquid flow) to vapor migration (Barbour, 1998; Oh and Vanapalli, 2011).

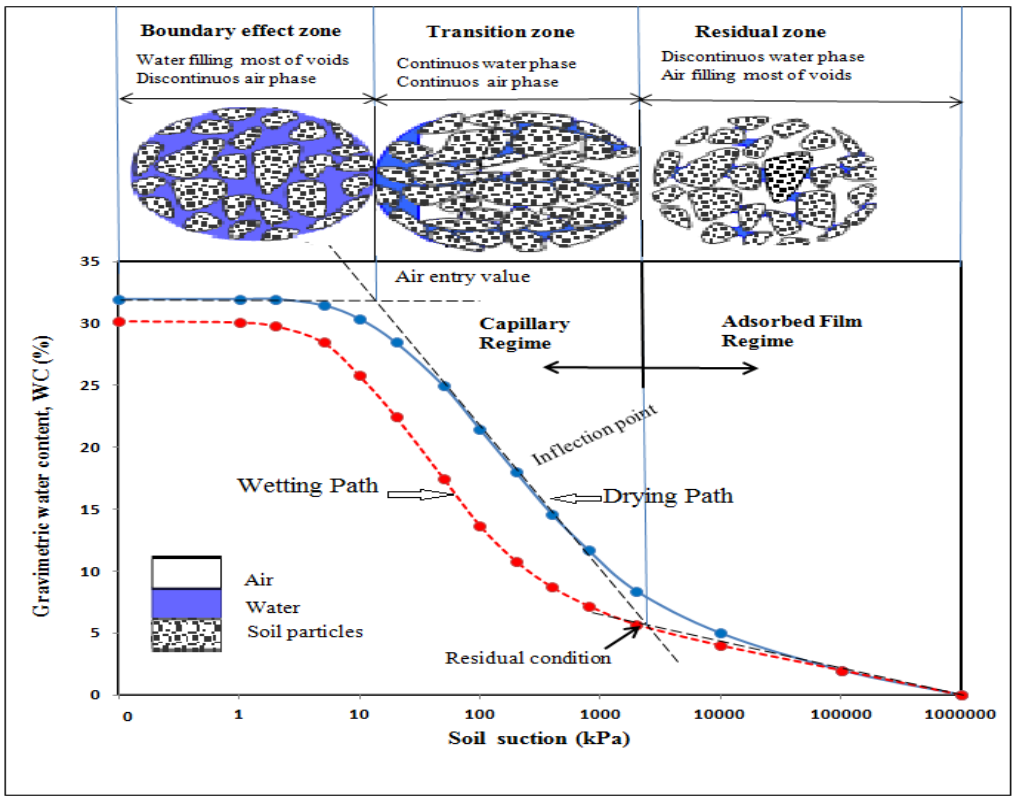

Figure 2.8: A typical soil-water retention curve (Ahmed, 2013).

2.3.1 Factors influencing the soil water retention curve

There is a unique shape of the soil-water retention curve (SWRC) for each type of soil. Several investigations have been performed to study the effect of different factors such as initial dry density, initial water content and the stress history on the shape of the SWRC. In general, the dry density of the soil specimen increases with an increase in the compaction effort, owing to a decrease in the corresponding void ratio. Consequently, some changes in the characteristics of the SWRC are expected.

Miller et al., (2002) investigated the effect of different compaction efforts (standard, modified and reduced) on the behaviour of the SWRC. Their test results, that were performed on the high plasticity compacted clay soil, revealed that the SWRC has been strongly influenced by the changes of the compaction efforts. The SWRC tends to shift rightwards with the increase of the compaction effort as shown in Figure 2.9. The authors attributed this behaviour to that, the specimens compacted with high-compaction efforts have small pores. For the same water content, pore water suctions increase with decreasing pore sizes, leading to the higher-compaction efforts plotting above lower-compaction efforts. This trend behaviour was also observed for all of the

tested specimens, having different initial water content (dry of optimum and wet of optimum).

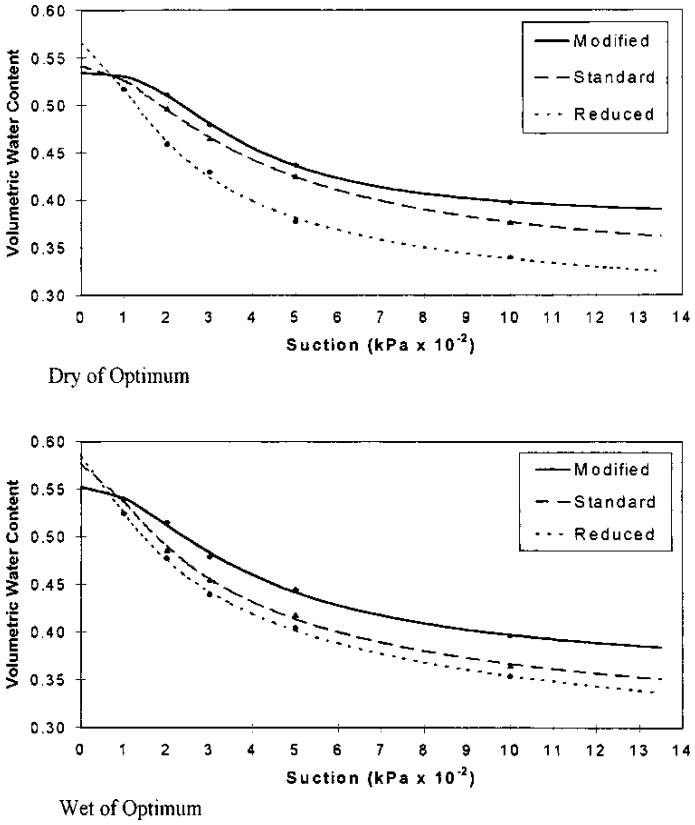

Figure 2.9: Variation in soil water characteristic curve behavior due to compaction effort (Miller et al., 2002).

Tinjum et al., (1997) have noticed similar behaviour when they carried out a series of laboratory pressure plate extractor tests on compacted clayey soils using standard and modified Proctor compaction efforts. They concluded that a slightly higher air-entry suction exists for the soil compacted with modified Proctor effort than those compacted with standard Proctor. Higher compactive efforts also results in a curve that appears to be slightly steeper. This is due to an increasing in the compactive effort results in smaller pores and thus affects the shape of the SWRC. In addition, because of the air-entry suction is higher; the matric suction corresponding to given water content is higher for soils compacted with higher compactive effort. The authors stated that, for a given compaction water content, the air-entry suction is generally higher and the slope is slightly steeper for specimens compacted with greater compactive effort.

Many researchers like Miao et al., (2002); Yang et al., (2004); Gallage and Uchimura (2010) have observed the same effect of the compaction effort on the behaviour of the SWRC. On contrary, Malaya and Sreedeep (2010) demonstrated that the initial dry

density of the sandy soil does not have a significant effect on the SWRC as shown in Figure 2.10.

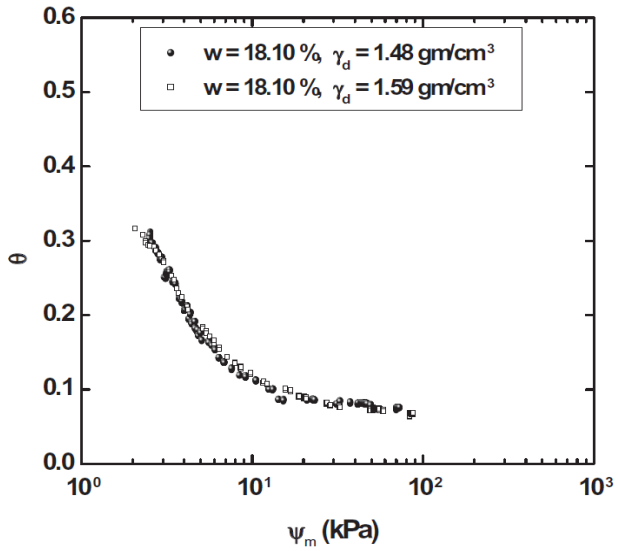

Figure 2.10: Effect of initial dry density of sandy soil on the behaviour of SWRC (Malaya and Sreedeep, 2010).

Kawai et al., (2000) investigated the effect of initial void ratio of the compacted silty clay soil on the behaviour of the soil-water retention curve. They pointed out that the air-entry value is clearly increased as the void ratio of the tested specimens decreased as shown in Figure 2.11.

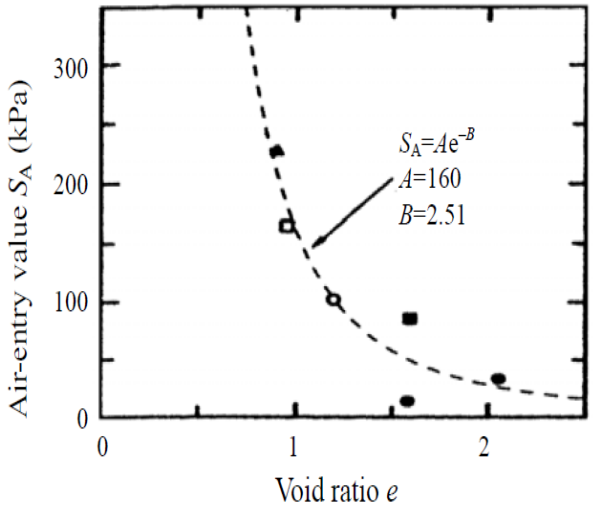

Figure 2.11: Relationship between void ratio and air-entry value (Kawai et al., 2000).

In brief, it can be concluded from the previous literature Tinjum et al., (1997); Kawai et al., (2000); Malaya and Sreedeep, (2010) that the specimens prepared under different

compaction efforts (i.e. different initial density) exhibited different relationship between water content and soil suction.

Vanapalli et al., (1999) have experimentally investigated the effect of different levels of applied pressure (0, 25, 100, and 200 kPa) on the behaviour of SWRC in terms of the effect of stress state. Their results for the tests performed on a compacted sandy clay till soil are presented in Figures 2.12(a) and 2.12(b). The tested specimens, compacted with initial water content, represent the dry and wet of optimum. Figure 2.12(a) shows that there is a remarkable increase in the air-entry value, with increasing level of applied pressure of the specimens prepared dry of optimum. In contrast, specimens compacted wet of optimum showed clearly that the effect of different levels of applied pressure was insignificant as illustrated in Figure 2.12(b). Similar observation was reported by Ng and Pang (2000) and Thu et al., (2007). Their results showed that the air-entry value obviously increased with an increase in the level of applied stress.

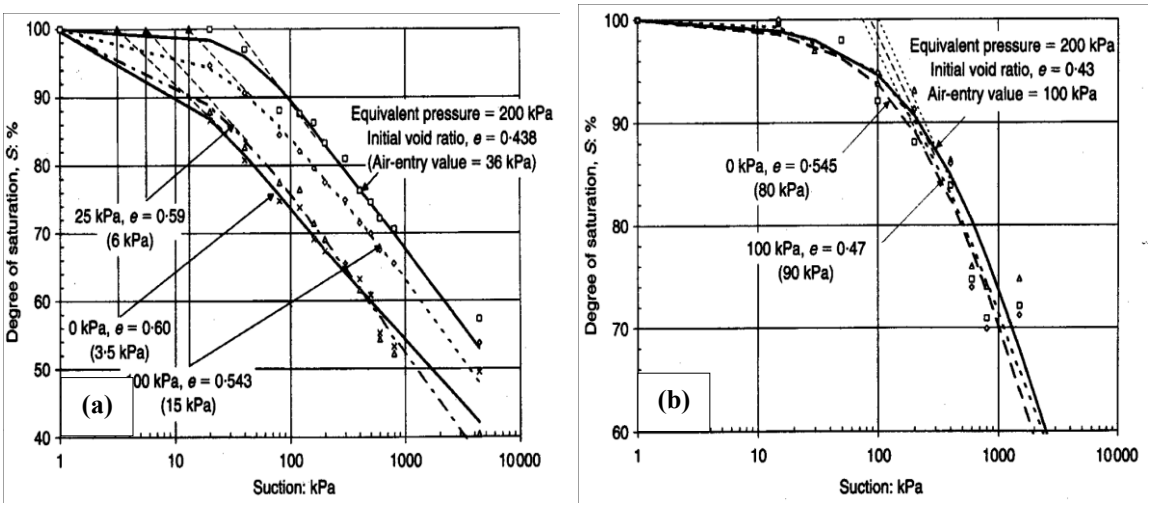

Figure 2.12: Influence of different levels of applied pressure on SWRC of soil compacted: **(a)** dry of optimum; **(b)** wet of optimum (Vanapalli et al., 1999).

2.4 Hydro-mechanical behaviour of unsaturated soil

2.4.1 Stress state variables in unsaturated soil

It is well recognized that the Terzaghi's effective stress theory, for studying the saturated soil mechanics, has a significant impact in the civil and geotechnical engineering practices. Terzaghi (1936) founded the fundamentals of the effective stress theory of saturated soils. He set up his theory based on assumptions that both soil

particles and the water occupying voids are incompressible. He added that the contact area between soil particles can be ignored. For saturated soil, the equation is as follows:

$$\sigma = \sigma' + u_w \qquad \text{Eq. 2-8}$$

Therefore;

$$\sigma' = \sigma - u_w \qquad \text{Eq. 2-9}$$

Where σ' is the effective stress, σ is the total stress and u_w is the pore-water pressure.

As shown in Eq. 2-8, the total stress consists of two components; the first one is the pore-water pressure u_w which is directly generated to equalise a part of the total applied stress, while the second one is the effective stress σ' which represents the remaining part of the applied stress and contributes to the soil deformation (Karube and Kawai, 2001). Terzaghi's effective stress is reasonable as long as the existing air in the soil mass has a bubble form and could be isolated from the soil mass even if the soil is in unsaturated condition (Karube and Kawai, 2001; Lee et al., 2005). Therefore, the pore-water pressure u_w in Eq. 2-8 can be replaced by the pore-air pressure u_a in the case that the air exists in the soil as a continuous phase as follows:

$$\sigma = \sigma_{net} + u_a \qquad \text{Eq. 2-10}$$

Therefore;

$$\sigma_{net} = \sigma - u_a \qquad \text{Eq. 2-11}$$

Where σ_{net} is the net normal stress.

Since 1950s, many studies have been conducted to understand the relationship between the effective shear stress and the soil suction. Croney et al (1952) attempted to develop an effective stress equation for unsaturated soils. They suggested that the effective stress equation is:

$$\sigma' = \sigma - \beta u_w \qquad \text{Eq. 2-12}$$

Where σ' is the effective stress, σ is the total stress, β is a factor and u_w is the pore-water pressure. Jennings (1961) and Aitchison (1961) have considered the presence of the air

pressure in the soil voids. Therefore, they suggested that the effective stress equation is as follows:

$$\sigma' = \sigma - \psi P'' \qquad \text{Eq. 2-13}$$

Where P″ was known as an insufficiency in the pore water pressure by Aitchison, while by Jennings known as the absolute value of the negative pore-water pressure.

In 1959, Bishop modified Terzaghi's effective stress theory and suggested the first equation for unsaturated effective stress which, accounting for both pore-water pressure u_w and pore-air pressure u_a, can be expressed as:

$$\sigma' = (\sigma - u_a) + \chi\,(u_a - u_w) \qquad \text{Eq. 2-14}$$

In the above formula σ' represents the effective stress; u_w is the pore-water pressure; u_a is the pore-air pressure; the term $(\sigma - u_a)$ is known as the net normal stress; the term $(u_a - u_w)$ is the matric suction. The latter is negative due to $u_a < u_w$ and χ is a parameter ranging from zero (when the soil is completely dry) and 1 (when the soil is completely saturated). Also, the negative value depends on other factors such as: the soil type, degree of saturation, stress variation and wetting and drying cycles (Aitchison and Donald, 1956; Aitchison, 1961; Blight, 1967).

Later, researchers have tried to enhance the effective stress equation in the early 60s of the twentieth century. In their work, Bishop and Blight (1963) proposed that the two independent stress state variables, the net normal stress $(\sigma - u_a)$ and the matric suction $(u_a - u_w)$ must be considered to understand the stress-strain behaviour of unsaturated soils. Matyas and Radhakrishna (1968) examined the validity of the stress state variables that were suggested by Bishop and Blight (1963). They performed a series of suction-controlled compression tests to establish the state surfaces for a mixture of Kaolin and flint powder. They presented the results in term of void ratio versus suction and degree of saturation versus net normal stress. Their results suggested that the variations in both degree of saturation and void ratio could be clarified by unique surfaces in term of stress-degree of saturation and stress-void ratio respectively.

Later on, Fredlund et al., (1978) proposed the first mathematical equation for the state surfaces in terms of water content ω, and degree of saturation S_r. Similarly, Lioret and Alonso (1985) also suggested a state surface equation for both degree of saturation S_r and void ratio is as follows:

$$S_r = a - \tanh(bs)(c + dp') \qquad \text{Eq. 2-15}$$

The letters a, b, c, and d represent the soil constants. They showed that the above equation is adequate at low stress level. Gallipoli et al., (2003) and Wheeler et al., (2003) noted that the degree of saturation, soil density, matric suction and the stress level have a significant effect on the stress-strain behaviour of unsaturated soil.

2.4.2 Volumetric behaviour of unsaturated soil

The measurement of the volume changes in unsaturated soil is usually complex and difficult in comparison to the volume change measurements in the saturated soil. Due to both soil particles and water being approximately incompressible materials, the volume change is equal to the water volume change in saturated soil. In other words, the volume changes occur due to flow of water inside or outside the soil. Whereas, in an unsaturated soil, because of the existence of the air in the voids, the volume changes are of two components: the volume change of water and the overall volume change (Fredlund and Rahardjo, 1993; Aziz et al., 2006; Elgabu, 2013). Fredlund and Morgenstern (1977) defined the volumetric changes in an unsaturated soil as the changes in both void ratio and water content due to changes of the stress state variables (net normal stress and matric suction).

The volume change behaviour of unsaturated soil has been investigated by many researchers (e.g. Matyas and Radhakrishna, 1968; Josa et al., 1987; Huat et al., 2006). Matyas and Radhakrishna (1968) performed a series of tests on a partially saturated soil. They reported that, at high matric suction, the tested specimens showed stiff behaviour and a small amount of compressibility.

Huat et al., (2006) conducted a series of suction-controlled compression tests to examine the volume change behaviour of unsaturated sandy clay soil. The authors showed that the tested specimens displayed a noticeable volume reduction in the soil

mass with decreasing suction. This behaviour is caused by the suction decrease; the bonding stresses at the contact points between soil particles that contribute in the stiffness of the specimens decrease and the subsequent stiffness of the specimens decreases. Aziz et al., (2006) investigated the influence of various levels of applied matric suction and net normal stress on the volume change of the compacted specimens. Their results showed that the tested specimens exhibited small amount of compressibility with increasing the applied matric suction. Similar trend of behaviour can be noticed from the results of Josa et al., (1987). They reported that, at a given value of applied net normal stress, the tested specimens showed a noticeable reduction in their volume when the matric suction decreased up to 25 kPa.

Geiser et al. (2000) classified some of the relevant methods used for the measurement of the volume change in an unsaturated soil into three groups. The first group contains the methods devoted for measuring the volume of the liquid in the cell, whereas, the methods used for measuring the volume of water and the volume of air separately are collected in the second group. Finally, the third group contains the direct measurement methods of the soil specimen. In the first group, the volume change of the tested specimen is calculated based on the variation of the confining liquid cell in the standard triaxial apparatus. Many barriers are usually associated with the use of these methods such as dilation-shrinkage in the triaxial cell wall and in the cell liquid due to the changes in pressure and temperature. To overcome that, Bishop and Donald (1961), and Cui and Delage (1996) added an additional internal cell (double wall) to minimize this effect.

In the second group, the process of measuring the volume change of the air is inaccurate because the volume of air is significantly influenced by the atmospheric pressure and temperature. Therefore, this method is impractical in the triaxial testing of unsaturated soils. The methods in the third group are more appropriate for measuring the total volume change by using displacement transducers to measure the vertical and diagonal deformations of unsaturated soil specimens.

Estabragh and Javadi (2012) conducted a series of suction-controlled triaxial tests to examine the influence of suction and net stress on the volumetric behaviour of the unsaturated compacted silty soil. They concluded the tests at any given value of matric suction, the specific volume of the tested specimens decreased (collapse) with increasing mean net stress. In addition, the specimens showed more yield with further

increasing in the mean net stress. Consistent behaviour regarding to the effect of suction was observed as shown in Figure 2.13.

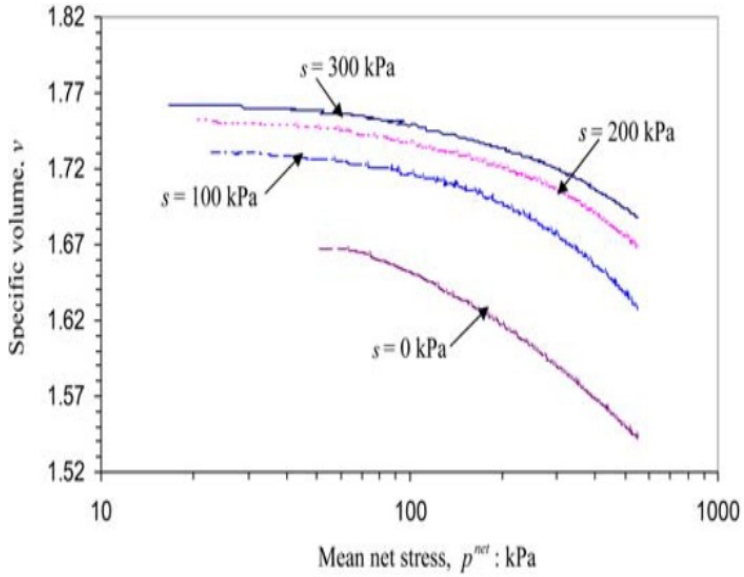

Figure 2.13: Effect of suction and mean net stress on the specific volume (Estabragh and Javadi, 2012).

2.5 Shear strength of unsaturated soils

The shear strength of the soil is one of the most important parameters used in analyzing and addressing many geotechnical problems such as retaining walls, tunnels, shallow foundations, pile foundation and slope stability. It is well recognized that the stress state of the soil is governed by the shear strength behaviour. In unsaturated soil, it is well known that the stress state variables are the net normal stress and matric suction (Fredlund et al., 1978; Fredlund and Rahardjo, 1993; Borana et al., 2013). Experimental studies reported that, for a given soil and under same net normal stress, the unsaturated shear strength is higher than the saturated one (e.g. Arunasalam, 2009).

Many efforts have been made to understand the shear strength behaviour of unsaturated soils. In the early days, Bishop (1959) extended Terzaghi's effective stress equation of saturated soil and suggested one of the well-known unsaturated shear strength equations as follows:

$$\tau = c' + [(\sigma - u_a) + \chi (u_a - u_w)] \tan \phi' \qquad \text{Eq. 2-16}$$

Where τ is the shear strength of unsaturated soil, c' is the effective cohesion and ϕ' is the effective angle of internal friction with respect to the net normal stress. Eq. 2-16 consists of two parts; the first part is a function of the normal stress and related to the shear strength of saturated soil, whereas the second part represents the suction strength τ_{us} and related to the matric suction. The suction strength is defined as follows:

$$\tau_{us} = \chi\,(u_a - u_w)\tan\phi' \qquad \text{Eq. 2-17}$$

Many researchers (e.g. Aitchison, 1961; Jennings and Burland, 1962; Burland, 1965) have previously reported that the shear strength equation proposed by Bishop was unsuccessful. They highlighted some difficulties related to the determination of the χ parameter whether theoretically or experimentally. In addition, the equation was found unsatisfactory in terms of describing the behaviour of unsaturated soil due to wetting (swell or collapse), as a function of applied stress. In other terms, at a relatively low normal stress, the unsaturated soil specimen will swell due to wetting. Hence, the single effective stress approach cannot be used to clarify these two different aspects of mechanical behaviour (Arunasalam, 2009).

Eventually, to overcome such limitations in Eq. 2-16, Fredlund et al., (1978) proposed a relationship between the two independent stress state variables and the shear strength of unsaturated soil as follows:

$$\tau = c' + (\sigma - u_a)\tan\phi' + (u_a - u_w)\tan\phi^b \qquad \text{Eq. 2-18}$$

Where τ is the shear strength of unsaturated soil, c' is the effective cohesion, ϕ' is the angle of friction with respect to the net normal stress, and ϕ^b is the angle of friction with respect to the changes in matric suction.

According to the basic geotechnical concept, the shear strength of saturated soil includes two components, frictional component and the soil cohesion component. On the contrary to the saturated soil, the shear strength of unsaturated soil has a third component besides the two components of the saturated soil. Hence, Fredlund et al., (1978) presented the Mohr-Coulomb envelope failure envelopes of unsaturated soils in three-dimensional form, in which the y-axis represents the shear stress at failure, while

the x-axis represents the net normal stress, and the z-axis represents the matric suction (Figure 2.14).

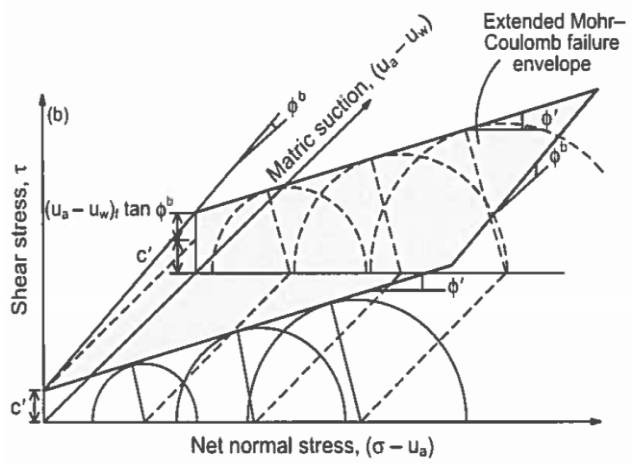

Figure 2.14: Extended Mohr-Coulomb failure envelope for unsaturated soils (Fredlund et al., 1978).

In earlier studies, many believe that the angle of friction with respect to the matric suction ϕ^b is equal to the angle of friction with respect to the net normal stress ϕ', resulting in a linear change in the unsaturated shear strength with suction. Later on, several experimental studies (e.g. Escario and Saez, 1986; Gan, 1986; Gan and Fredlund 1988; Escario and Juca, 1989; Toll, 1990; Nishimura and Toyota, 2002) pointed out that the relationship between the shear strength and the matric suction is nonlinear (i.e. non-linear failure envelope). They revealed that the angle of friction ϕ^b varied nonlinearly with the matric suction.

Nishimura and Toyota (2002) examined the effect of applied matric suction on the shear strength behaviour of silty soil and low plasticity silty soil. Their results clearly showed that the shear strength changed nonlinearly with respect to the matric suction as shown in Figure 2.15. The authors also indicated that, instead it peaks for some value of suction; further drying may lead to a decrease in the shear strength from that peak value.

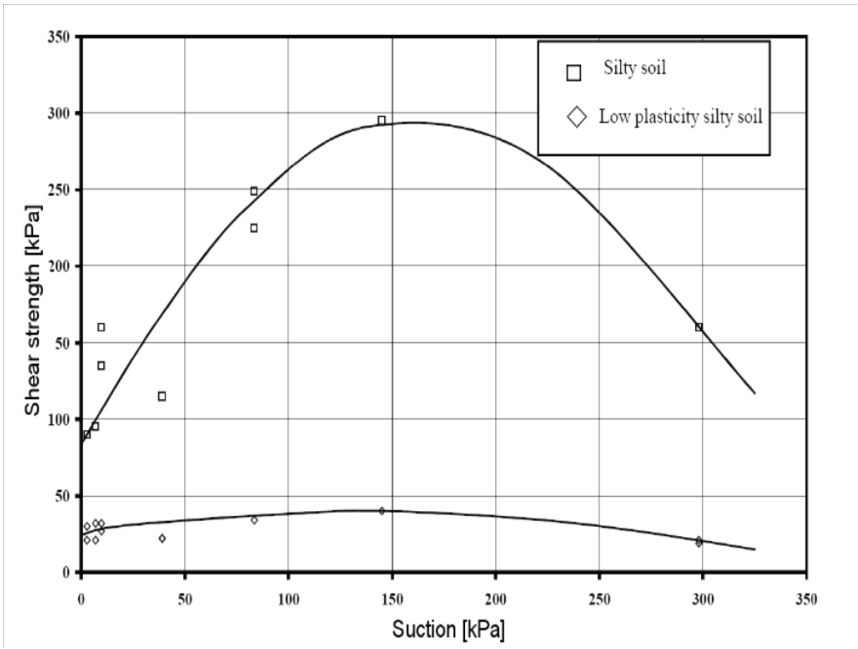

Figure 2.15: Changes in shear strength with the soil suction (data from Nishimura and Toyota, 2000).

Gan (1986) performed a series of multi-stage direct shear tests on unsaturated specimens of a compacted glacial till using a modified direct shear apparatus. He has observed that the failure envelope with respect to the matric suction was nonlinear. In addition, the results showed that the shear strength increased with the increase in matric suction. Gan and Fredlund (1992) also studied the effect of matric suction on the shearing behaviour of completely decomposed granite soil and they found that the stiffness of the tested specimens as well as the shear strength increased with an increase in matric suction. Similar findings were indicated by other researchers (e.g. De Campos and Carrillo, 1995; Gan and Fredlund, 1996; Feuerharmel et al., 2006).

A series of suction-controlled direct shear tests were performed by Hamid (2005) using a locally available soil from central Oklahoma known as Minco silt. The experimental results showed an increase in the shear strength of the tested specimens as the matric suction increases. He also reported that the unsaturated shear strength parameters increased as the matric suction increases. Similar trend of behaviour was reported by Hossain and Yin (2010) and Borana (2014). Their findings revealed that the shear strength of completely composite granite soil is significantly influenced by the changes in both net normal stress and matric suction.

Noteworthy, the previous listed experimental studies to investigate the shearing behaviour of unsaturated soil were done by using axis-translation method for imposing the matric suction, which is relatively covering a low range of matric suction corresponding to high degree of saturation for fine grained soils (Rassam and Williams, 1999; Rahardjo et al., 2004; Lee et al., 2005; Hamidi et al., 2013). The axis-translation technique was developed by Hilf (1956), and since then become the most common method used in unsaturated soil mechanics. The basic principle of axis-translation technique is to elevate pore-air pressure u_a to increase pore-water pressure u_w to be positive, preventing cavitations in water drainage system. Total stress σ is increased with air pressure u_a at the same amount to remain net normal stress ($\sigma - u_a$) unchanged. Axis-translation is accomplished by separating air and water phases in a soil through porous material with high air-entry value. In axis-translation technique, both pore-air pressure and pore-water pressure are controlled and measured independently, which enables measured and controlled variation of suction. One limitation of axis-translation technique relates to maximum value of suction can be applied. It is limited by the maximum value of cell pressure and the air-entry value of the porous material (Bishop and Blight, 1963; Fredlund and Morgenstern, 1978; Fredlund and Rahardjo, 1993; Hossain, 2010).

Hamidi et al. (2013) studied the influence of a wide range of suction values (up to 800 kPa) on the unsaturated shearing behaviour of Iranian silty clay soil by using a modified direct shear apparatus. In this study, the targeted suction imposed by employing osmotic suction method, in which the desired matric suction was imposed based on the concentration of a Polyethylene glycol (PGE) solution. The authors observed that the shear strength and shear induced dilation of the tested specimens increased with suction.

2.5.1 Various shear strength equations for unsaturated soil

Many efforts have been made in order to propose a number of empirical equations to predict the shear strength of unsaturated soil. Karube (1988) performed a series of triaxial compression tests for low-plasticity clays compacted on the dry side of optimum water content to express a new concept for effective stress based on e1asto-p1astic behaviour of unsaturated soils. The author postulated that the matric suction component can be considered constant compared to the net normal stress component in the stress-strain equations of unsaturated soil. Based on the test results obtained from the laboratory tests, he derived the following equation for the unsaturated shear strength:

$$q_{f} = M\,(p - u_a) \text{ where } M = M'\left(\frac{1}{\alpha}\right) + \left(-\frac{\Delta v}{\Delta \varepsilon}\right)_f \text{ and } \left(\frac{1}{\alpha}\right) = \left(1 + \frac{f_{(s)}}{p}\right) \qquad \text{Eq. 2-19}$$

M' is the slop of the failure lines, $f_{(s)}$ is the intercept of the failure lines with the $(p - u_a)$ axis, ε is the shear strain defined as $\varepsilon = 2\,(\varepsilon_1 - \varepsilon_3)/3$, and $\left(-\frac{\Delta v}{\Delta \varepsilon}\right)_f$ is the dilatancy index. Also, the model obtained, however, could not apply to soils on the wetter side in which consolidation was induced by increasing suction. Figures 2.16 (a) and (b) show the isotropic stress paths and the variation of the specific volume of samples compacted at a water content of 6% dry side of optimum.

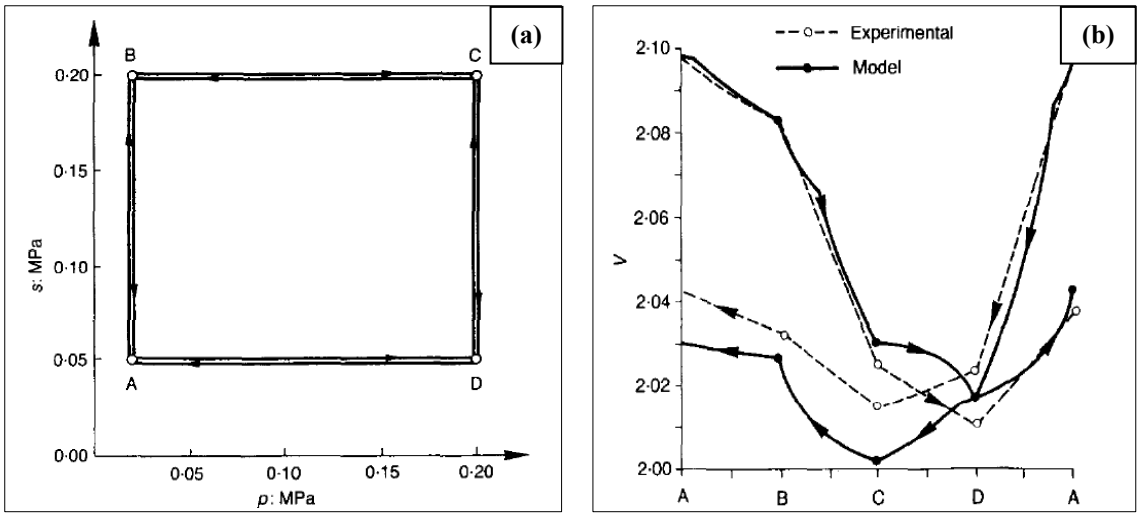

Figure 2.16: Shear tests on partially saturated compacted kaolin: (a) stress paths, (b) comparison between experimental and computed results (Karube, 1988).

Toll (1990) performed a series of suction-controlled triaxial tests on Kiunyu gravel. The author established a critical state framework to explain the unsaturated shear strength behaviour based on the assumption that the two stress state variables (net normal stress and matric suction) are taken into consideration separately to avoid problems resulting from the coupling of the two variables. The author explained the behaviour of compacted unsaturated soils in terms of a two level structure involving compression of the packing arrangement of different packets and swelling of each individual packet. These two different aspects of behaviour will cause different volume change or pore water pressure response and the overall behaviour is dependent on the relative contributions of each effect. The proposed critical state formula of unsaturated shear strength is written as follows:

$$q = M_a (p - u_a) + M_w (u_a - u_w) \quad \text{Eq. 2-20}$$

Where q is the deviator stress ($\sigma_1 - \sigma_3$), p is the mean total stress ($\sigma_1+\sigma_2+\sigma_3$)/3, M_a is the critical stress ratio with respect to net mean stress, ($p - u_a$), and M_w is the critical stress ratio with respect to suction, ($u_a - u_w$). The last two parameters are highly influenced by the degree of saturation as shown in Figure 2.17.

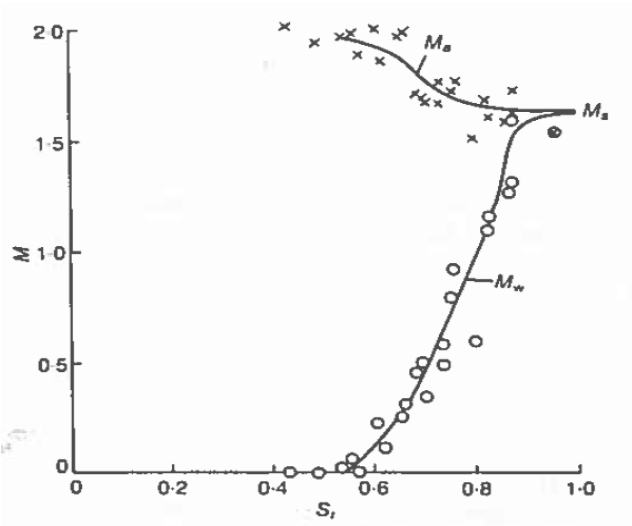

Figure 2.17: Variation of the critical state stress ratios with degree of saturation (Toll, 1990).

The author observed that the contribution of the net mean stress, M_a, increased as the degree of saturation increased. A simple technique to evaluate the values of M_a and M_w cannot be used directly. A multiple linear regression technique was proposed by the author to separate the contributions of the two stress components.

Vanapalli et al., (1996) extended the shear strength equation proposed by Fredlund et al., (1978) and established two non-linear equations of unsaturated shear strength using the entire suction range from 0 to 10^6 kPa and the saturated shear strength parameters, as shown below:

$$\tau = [c' + (\sigma_n - u_a) \tan \phi'] + [(u_a - u_w)\{(\Theta^K) (\tan \phi')\}] \quad \text{Eq. 2-21a}$$

$$\tau = [c' + (\sigma_n - u_a) \tan \phi'] + [(u_a - u_w) \tan \phi' (\frac{\theta_w - \theta_r}{\theta_s - \theta_r})] \quad \text{Eq. 2-21b}$$

Where ($\sigma_n - u_a$) is the net normal stress, ($u_a - u_w$) is the soil suction, K is the fitting parameter used to obtain a good correlation between the experimental and the predicted values; Θ is the normalized water content (θ_w / θ_s); θ_w is the volumetric water content; θ_s is the saturated volumetric water content and θ_r is the residual volumetric water content. The results obtained from the model developed for predicting the shear strength (Eq. 2.21a and 2.21b) are compared with experimental results for a glacial till. Specimens were prepared at three different water contents and densities (i.e., corresponding to dry of optimum, at optimum, and wet of optimum conditions). The authors pointed out that there is a good correlation between the predicted and measured values of shear strength for the unsaturated soil. Researchers indicated that the changes in the values of Θ, θ_r and θ_s can be measured from the soil water retention relationships. In addition, the variation of shear strength with respect to the matric suction can be obtained using one of the above equations.

The relationship between the shear strength and matric suction is linear up to the air-entry value. After that, the shear strength displayed non-linear behaviour as a result of an increase in the matric suction (Rassam and Williams, 1999). Rassam and Williams (1999) proposed an empirical equation to demonstrate the failure envelope transition from saturated to unsaturated shear strength of the soil. The authors presented the shear strength formula taking into consideration the contribution of the net normal stress and the matric suction on the shear strength behaviour, as follows:

$$\tau = c' + (\sigma - u_a) \tan \phi' + s \tan \phi' - (s - \psi_a)^{\beta} [\gamma + \lambda (\sigma - u_a)] \qquad \text{Eq. 2-22}$$

Where s is the matric suction of soil ($u_a - u_w$), ψ_a is the air-entry value; β, λ and γ are the fitting parameters. It can be observed that the shear strength formula (Eq. 2.22) consists of two terms; the first one is the basic Mohr-Columb criterion and represents the matric suction contribution to the shear strength up to the AEV in the sense that, the soil maintains saturating under any value of matric suction. The second one is the correction term where the soil starts to desaturate beyond the AEV. In their work, Rassam and Williams (1999) indicated that the air-entry value changes linearly with the net normal stress, as well as the shape of the soil-water retention curve changes with the net normal stress. At a given value of net normal stress, Eq. 2.23 estimates the air-entry value as follows;

$$AEV = AEV_1 + AEV_s\,(\sigma - u_a) \qquad \text{Eq. 2-23}$$

Where AEV is the air-entry value, AEV_1 is the intercept of the line, AEV_s is the slope of the line, and $\sigma - u_a$ is the net normal stress.

2.6 Behaviour of soil-structure interaction

The interaction between the structural element (e.g. concrete, steel, wood) and a soil forms an interface (Potyondy, 1961; Fakharian, 1996; Hamid, 2005; Lashkari, 2010; Borana, 2014). One of the key parameters for the design and safety assessment of the engineering structures (e.g. retaining walls, deep and shallow foundations, tunnels and earth reinforcement) is the shear strength at the interface between the structure and the surrounding soil surfaces. The interface layer transfers the loads from the structure to the soil mass and exhibited to the significant strain localization and stress concentration (Hamid, 2005). Many experimental investigations have been made to understand the mechanical behavior of the interface because it is difficult and complex to model the interface behaviour mathematically (Hossain, 2010). Most of the available literature was undertaken to examine the interface behaviour for either fully dry or fully saturated condition, whereas, few studies can be found in the literature while were conducted to understand the interface shear strength behaviour under unsaturated condition.

2.6.1 Interface shear behaviour at fully dry and fully saturated condition

Several investigations have been conducted to study the effect of different parameters such as various types of soil (e.g. clay, sand, and silt), surface condition (e.g. rough, intermediate, and smooth), type of construction materials (e.g. concrete, steel, wood, geotextile etc.), water content of soil, different applied vertical stress, void ratio of soil, grain size distribution, and rate of shearing on the interface shearing behaviour using different types of laboratory equipment including direct shear, simple shear, ring torsion, and annular shear (Potyondy, 1961, Brummund and Leonards, 1973; Acar et al., 1981; Fakharian, 1996).

Potyondy (1961) performed an extensive laboratory testing programme under different test conditions (saturated and dry) to study the effect of different factors (e.g. various

construction materials, different surface condition, various types of soil, different applied vertical stress) on the magnitude of skin friction using direct shear apparatus. The experimental results revealed that for cohesive soils both cohesion and internal friction should be considered in the evaluation of skin friction. Acar et al., (1982) examined the interface shearing behaviour between quartz sand and different construction materials (concrete, steel, and wood) using direct shear apparatus. They conducted all the tested specimens under constant rate of shearing and concluded that the normal stress and soil density of sand have a significant influence on the angle of friction between sand and construction materials.

Brummund and Leonards (1973) reported that the interface friction angle increased with increasing surface roughness and the angularity of the sand particles. The authors also indicated that the dynamic friction coefficient is greater than the static friction coefficient by about 20% in the case of unlubricated surfaces. In support of these observations, Yoshimi and Kishida (1981) performed several laboratory tests between dry sand and steel plate using ring torsion apparatus in order to study the effect of surface roughness and soil density. The authors concluded that surface roughness of the steel plate primarily governed the frictional resistance behaviour, regardless of the sand density. Similar behaviour was observed by Uesugi and Kishida (1986) by employing simple shear apparatus. Bosscher and Ortiz (1987) investigated the interface shearing behaviour between sand and different types of bedrock and construction materials under cyclic loading. They concluded that the coefficient of friction depends mainly on the surface roughness of the counterface.

Frost and Han (1999) concluded that the normal stress level, interface surface roughness, mean grain size of granular materials, initial density of soil specimen and the angularity of the particles have a clear effect on the interface shear strength behaviour. The test results showed that the rate of shearing, specimen preparation method and the thickness of the soil specimen have insignificant influence on the interface behaviour.

Al-Mhaidib (2006) studied the effect of different shearing rates on the angle of friction between sand and two different steel surfaces (smooth and rough). He examined five different shearing rates under three different values of applied vertical stress using a conventional direct shear test apparatus. The experimental results showed that, at any level of vertical stress, the interface shear strength increased with increasing rate of soil shearing, and thus leading to an increase in the angle of friction between sand and steel

interface. This trend of behaviour was observed for both rough and smooth interfaces specimens, as shown in Figures 2.18(a) and 2.18(b). In contrast, Lemos and Vaughan (2000) performed a series of shearing tests using a ring shear device. The authors reported that the shearing rate has insignificant effect on the shear resistance between sand and steel interface.

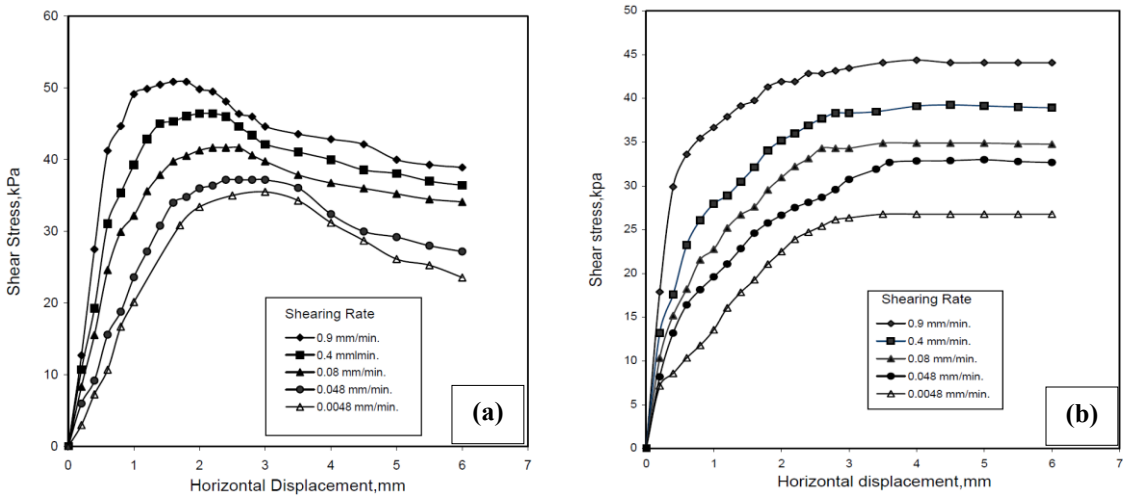

Figure 2.18: Shear stress versus horizontal displacement curves for dry sandy soil sheared under 100 kPa normal stress; **(a)** sand-rough interface, **(b)** sand-smooth interface (Al-Mhaidib, 2006).

The effect of surface roughness on the angle of skin friction between soil and construction material has been studied by Laskar and Dey (2011). They carried out a series of large scale direct shear tests between steel and sand at the relative density of 85 per cent. The experimental results showed that the friction angle increased with increasing surface roughness. Likewise, the interface shear strength increases approximately by 10% when the surface roughness of the steel plates is doubled. Gireesha and Muthukkumaran (2011) also studied the effect of different relative densities and soil gradation (poorly-graded and well-graded sand) on the interface strength behaviour using direct shear apparatus. The test results indicated that the skin friction angle clearly influenced by soil gradation in the sense that the well-graded specimens revealed higher skin friction value than those of poorly-graded specimens. The authors also found that the interface friction angle increased with increasing relative density. This behaviour was observed for poorly-graded and well-graded specimens.

Recently, Tiwari and Al-Adhadh (2014) performed a comprehensive experimental programme to investigate the influence of different types of soil, different soil gradation, different test conditions (dry and saturated), and different values of relative density ranging from 10 – 95% (i.e. very loose to very dense) on the frictional resistance between soil specimen and various construction materials (concrete, steel, and wood) by employing direct shear apparatus. They concluded that the soil shear strength is greater than the interface shear strength regardless of the test condition (fully dry or fully saturated). In addition, the soil-wood interface specimen showed lower shear strength value compared to the soil versus concrete or steel. The test results showed that the soil friction angle increased by 23% when the density of the tested specimen changed from loosest to the densest condition. Likewise, the friction angle of the soil-concrete interface specimen was increased by 7% when the density of the soil changed from the loosest to the densest condition. However, the effects of such change in density were inconsistent for the skin friction angle between soil and wood or steel. Investigations performed on completely decomposed granite (CDG) soil by using direct shear apparatus show that the interface shear strength clearly depends on the level of the applied vertical stress, the interface surface roughness, and the soil suction (Hossain, 2010; Borana, 2014)

It is noteworthy to mention here that most of the previous studies examined the effects of different parameters on the angle of skin friction between the cohesionless soils and structural materials. Many efforts have been performed to investigate the interface shearing behaviour between cohesive soil and different construction materials. For example, Tsubakihara and Kishida (1993) used two types of direct shear apparatuses of simple shear type and shear box type to evaluate friction resistance between normally consolidated Kawasaki clay and mild steel over wide ranges of surface roughness and rate of shear displacement. The laboratory test results indicated that the maximum resistance of friction is primarily governed by the roughness of the steel surface, irrespective of the apparatus used. In addition, the rate of shear displacement is influential in the maximum resistance of friction, while less influential for smoother steel surface. In support of these observations, Tika-Vassilikos (1999) examined the effect of rate of shearing on the shearing resistance of London clay against steel interfaces. The author concluded that, the coefficient of friction between clay and steel for shaft friction is significantly dependent on the rate of shearing. The shear behaviour of clays having different plasticity against interfaces of different materials and varying

roughness has been investigated by Lemos and Vaughan (2000) by performing a series of laboratory tests using ring shear apparatus. The experimental results showed that the shearing resistance of interface depends on many factors such as the interface surface roughness, the grain size distribution of the soil, soil properties, rate of shearing, the applied vertical stress, and the shape of the soil particles. Zimnik et al., (2000) studied the adherence behaviour of clay by measuring the shear stress required to shear two different types of clay (Speswhite and Bloom clay) over five different stainless steel plates of various roughness in a direct shear apparatus. The adhesive shear strength was increased with increasing normal stress, roughness of the steel plate, and the contact time between clay and steel. The authors reported that the direct shear test gives a good quantitative impression of the adhesive shear strength. The frictional characteristics of various roughnesses of construction materials (steel and concrete) against cohesive soils were studied by Hammoud and Boumekik (2006) using ring shear apparatus. The authors pointed out that that the surface roughness and the average diameter of particles, which are combined into the influence of relative roughness have a significant effect on the interfacial shear strength at a given normal stress level. Rouaiguia (2010) demonstrated that the interface material, surface roughness and soil composition are significantly affected by the interface residual shear strength. They conducted a series of laboratory drained shear tests on two groups of clay; the first one consists of three types of Algerian clay, while the second one consists of three types of British clay. The author concluded that, at same stress condition, the shear strength of clay specimen is higher than those of clay-interface specimen.

Recently, Taha and Fall (2014) performed several direct shear test on sensitive Leda clay and steel, with special emphasis on surface roughness of steel counterface. The results indicated that Leda clay interface shear behaviour not only depends on the surface roughness of the steel but also on the dry density and Leda's clay Over Consolidation Ration (OCR).

2.6.2 Interface shear strength equation under fully saturated condition

The interface shear strength behaviour before failure point, from geotechnical point of view, exhibits two different models either rigid-perfectly plastic or elastic-perfectly plastic. In the case of saturated condition, the Mohr-Coulomb failure criterion can be employed to the interfaces in the same way as soils (Hamid, 2005; Hossain, 2010, Borana, 2014). Potyondy (1961) determined the ratio between skin friction and shearing

stress by modifying the Mohr-Coulomb's equation with establishing the coefficient of soil cohesion $f_{c,}$ and coefficient of interface friction angle f_{ϕ}. The equation of skin friction becoming:

$$\tau_f = f_c\, c' + \sigma' \tan (f_\phi\, \phi') \qquad \text{Eq. 2-24}$$

Where τ_f is the interface shear stress at failure, c' is the effective cohesion of soil, ϕ' is the effective angle of friction, $f_c = \frac{c_{a'}}{c'}$; $f_\phi = \frac{\delta'}{\phi'}$; $c_a{}'$ is the effective adhesion, δ' is the effective interface friction angle.

Later, Chandler (1968) presented shear strength equation used of an interface structure,

$$\tau_f = \sigma'_{nf} \tan \delta' + c_a' \qquad \text{Eq. 2-25}$$

Where τ_f is the interface shear strength, σ'_{nf} is the effective normal stress at failure, δ' the interface angle of friction, and c_a' is the effective adhesion. Figure 2.19 shows the Mohr-Coulomb failure envelope of an interface (Fakharian, 1996).

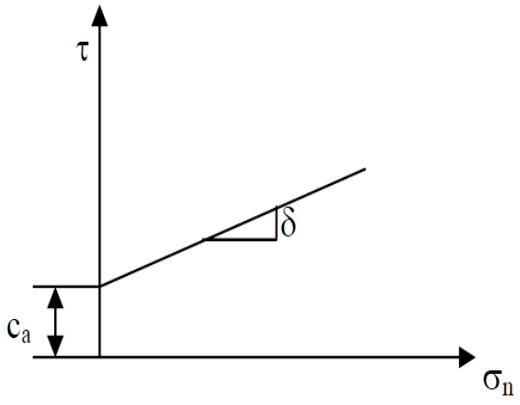

Figure 2.19: Mohr-Coulomb failure criterion for an interface (Fakharian, 1996).

2.6.3 Interface shear behaviour at unsaturated condition

Many researchers have performed a series of laboratory experiments in order to examine the effect of the net normal stress and matric suction (Hamid and Miller 2009; Hossain and Yin, 2010, Borana et al., 2013) and hydraulic hysteresis (Khoury et al., 2010) on the interface shear strength characteristics of the unsaturated soils. A common

conclusion from these works is that the interface shear strength increases with increasing net normal stress and matric suction.

Fleming et al., (2006) have performed a series of soil-geomembrane interface shear tests using a newly developed interface direct shear apparatus. The authors used a miniature pore pressure transducer to measure the pore-water pressure in the vicinity of geomembrane-soil interface during shearing. The effect of initial water content, dry density and different rate of shearing on the interface shearing behaviour are investigated in this study. The test results revealed that the studied parameters have a considerable influence on the interface shear strength as well as the interface angle of friction. The authors pointed out that, at lower normal effective stresses; however, it was possible to predict interface shear strength values using unsaturated soil mechanics concepts and matric suction measured in the vicinity of geomembrane–soil interface during the shearing process. At high normal stresses, the use of unsaturated soil mechanics concepts resulted in calculated shear strength values that were significantly lower than the measured values.

Hamid and Miller (2008) modified a conventional direct shear apparatus to perform a series of direct shear interface tests between unsaturated low plasticity Minco silt and stainless steel plate. The effect of surface roughness was also investigated in this study by employing two interfaces being rough and smooth. The authors reported that the peak shear strength increased with increasing the level of applied vertical stress. Consistent trends of behaviour corresponding to different values of matric suction were observed. The test results indicated that, at any level of applied vertical stress, the soil shear strength was greater than the shear strength of smooth and rough interfaces. The presented results also showed that the pre-peak shear strength for soil and interfaces are largely affected by the matric suction in the sense that the matric suction clearly contributes up to the peak shear strength. However, post-peak shear strength did not appear to vary with changes in matric suction, as shown in Figure 2.20. In contrast, the changes in the net normal stress clearly affected the peak and post-peak shear strength. The shear strength parameters are also studied in this research. The test results showed that the friction angle of the smooth interface with respect to the net normal stress was lower than the friction angle of soil and rough interface (see Figure 2.21). Likewise, the value of the cohesion with respect to the net normal stress of soil was greater than the adhesion for smooth and rough interfaces.

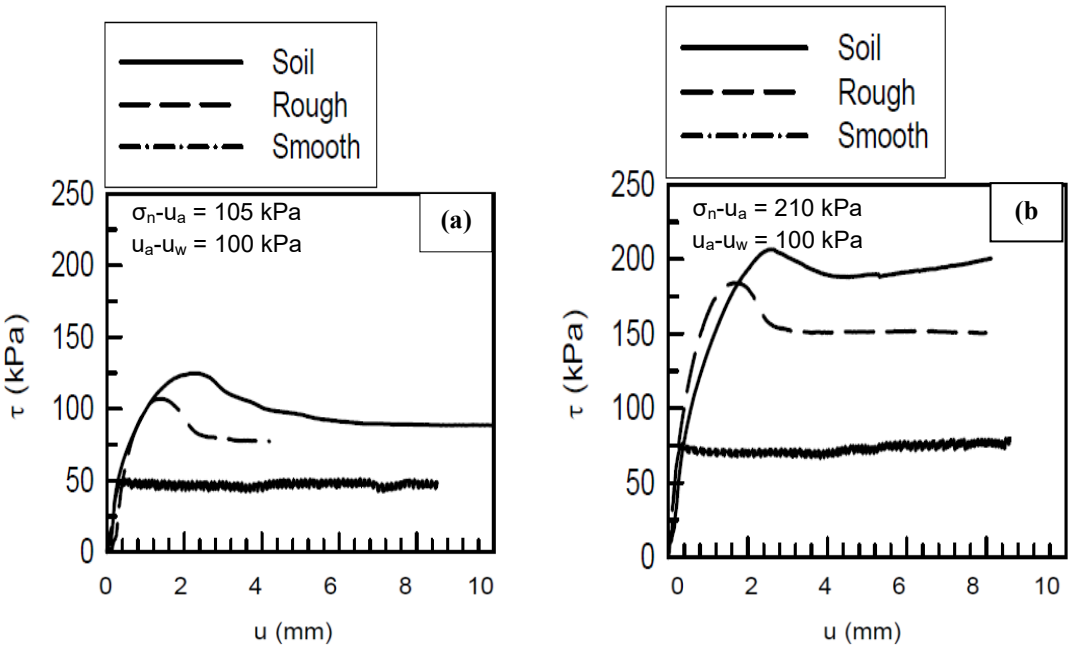

Figure 2.20: Comparison of soil, rough interface and smooth interface test results during shearing process at **(a)** σ_n-u_a = 210 kPa; **(b)** σ_n-u_a = 105 kPa (Hamid and Miller, 2008).

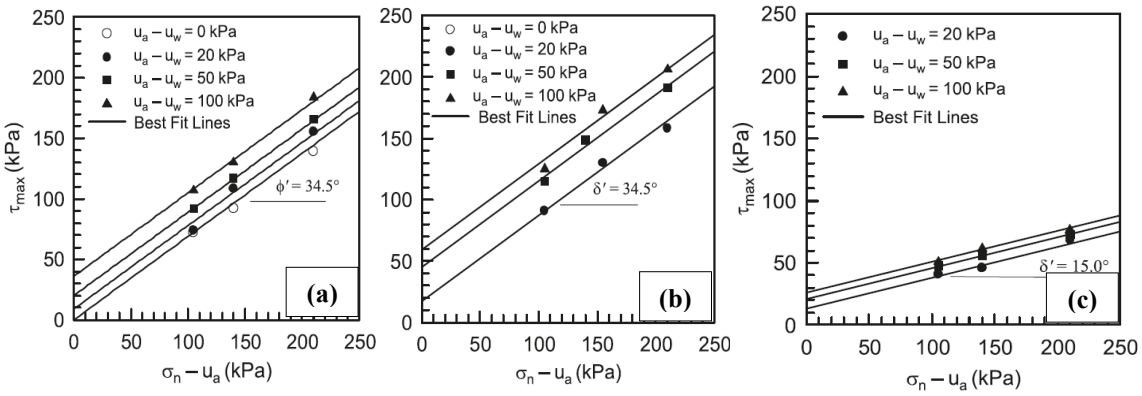

Figure 2.21: Linear failure envelopes for, (a) soil, (b) rough, (c) smooth surface (Hamid and Miller, 2008).

Hossain (2010) conducted suction-controlled direct shear tests to study the interface shearing behaviour between completely decomposed granite soil and cement grout under different net normal stresses, matric suctions, and grouting pressures. The author reported that interface shear strength of soil-cement grout specimen obviously increases with net normal stress and matric suction. Similarly, the test results revealed that the grouting pressure has a significant influence on the behaviour of the interface and on the dilation angle and apparent cohesion. Khoury et al., (2010) reported that the interface

shear strength increases nonlinearly with increasing matric suction. However, the role of matric suction on the interface post-peak shear strength is negligible.

Borana et al., (2013) investigated the effect of surface roughness (smooth, medium, and rough) of steel interface and different shearing planes on the interface shearing behaviour of completely decomposed granitic (CDG) soil using a modified suction-controlled direct shear apparatus. The researchers indicated that the net normal stress and matric suction noticeably influence the shearing behaviour of soil and soil-steel interface specimens sheared at different shearing planes. However, the soil specimen gains higher strength than those of soil-steel interface specimens as a result of an increase in the matric suction. The authors also observed that the variation in the interface roughness has a clear influence on the interface shearing behaviour. The test results showed that, at a given value of matric suction, the interface shear strength increased with increasing the interface thickness (i.e. the distance between shear plane and the counterface) as shown in Figure 2.22.

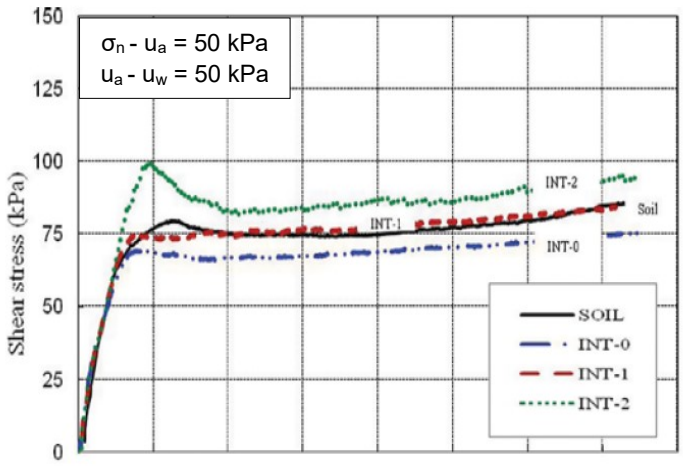

Figure 2.22: Variation of shear stress versus horizontal displacement of, INT-0, INT-1, INT-2 and soil (Borana et al., 2013).

Table (A-1) shows summary of the previous studies related to the interface shear strength behaviour under different conditions (see Appendix A).

2.6.4 Interface shear strength equation under unsaturated condition

Hamid (2005) presented an interface shear strength formula for an unsaturated soil by modifying the shear strength equation proposed by Fredlund et al., (1978) to examine the interface behaviour between unsaturated Minco silt and steel interface. The equation is as shown below:

$$\tau_s = c_a' + (\sigma_n - u_a) \tan \delta' + (u_a - u_w) \tan \delta^b \quad \text{Eq. 2-26}$$

Where σ_n is the normal stress on the interface at failure, u_a is the pore air pressure at failure, u_w is the pore water pressure at failure, δ' is the interface friction angle with respect to the net normal stress, δ^b is the interface friction angle with respect to the matric suction, and c_a' is the adhesion intercept.

Sharma et al., (2007) considered the effective stress equation for unsaturated soil proposed by Bishop (1959) to investigate the shear strength at the soil-geomembrane interface under unsaturated condition, as follows:

$$\tau = \alpha + [(\sigma - u_a) + \chi (u_a - u_w)] \tan \delta \quad \text{Eq. 2-27}$$

where τ is the interface shear strength, α is the adhesion, δ is the angle of shearing resistance at the soil-geomembrane interface, $(\sigma - u_a)$ is the net normal stress, $(u_a - u_w)$ is the matric suction, and χ is a parameter depending on degree of saturation and ranged from 0 to 1. The authors adjusted the value of χ to minimize the root mean square error between the calculated and measured shear stresses. In other words, to obtain a calculated shear stress value closed to the measured shear stress value. The resulting χ values ranged from 0.4 to 2.1. Noteworthy, despite the adjustment of χ value, the author pointed out that the measured shear strength values obtained by equation (Eq. 2-27) are inaccurately and highly dependent on the level of applied normal stress. At normal stresses greater than 20 kPa, the shear strength at the interface obtained by Eq. 2-27 resulted in unrealistically high values of χ (i.e. >2). Therefore, the shear strength model represented by Eq. 2-27 is appropriate only for low normal stresses. At high normal stresses, it is likely that a different mechanism of failure occurs.

To date, the interface shear strength equation proposed by Hamid and Miller (2008) was modified by Hossain and Yin (2010) by taking into consideration the dilatancy induced by matric suction. The authors proposed a mathematical formula to evaluate the

interface shear strength between completely decomposed granite soil and cement grout as follows;

$$\tau_f = c_a + (\sigma_n - u_a)_f \tan(\delta' + \psi_i) \quad \text{Eq. 2-28}$$

Where the interface shear strength (τ_f) and the adhesion intercept (c_a) can be defined as $c_a = c_a' + (u_a - u_w)_f \tan \delta^b$, δ' is the effective interface friction angle at saturated condition, ψ_i is the interface dilation angle, and $(\delta' + \psi_i) = \delta_{max}$ is the apparent interface friction angle.

2.7 Laboratory measurement devices

In this section, the laboratory devices used to study the behaviour of unsaturated soil, particularly the shear strength, are first briefly presented followed by interface testing devices used to investigate the interface shearing behaviour between unsaturated soil and the counterface.

2.7.4 Triaxial device

Triaxial testing of unsaturated soil is more difficult than testing the saturated specimens. For unsaturated soil, a test conducted under undrained conditions is no longer a constant volume test and the sample volume change in a drained test cannot be measured simply by the flow of water from the sample (Leong et al., 2003). Two types of volume change need to be measured in triaxial testing of unsaturated soils. These are the total sample volume change and the water volume change. The water volume change can be measured in the usual manner with a burette or automatic volume change device connected to the drainage line from the sample (Ng and Chui, 2001; Ng et al., 2002). The overall sample volume change, due to changes in both air and water volumes, can be measured in two ways: by measuring the flow of cell fluid into or out of the cell, or by measuring axial and lateral strains of the sample and calculating volumetric strain (Thu et al., 2007).

Bishop and Donald (1961) developed a modified triaxial cell to test unsaturated soil at Imperial College. The modified apparatus consisted of a double-walled cell with an acrylic jacket forming an inner cell wall. Mercury was used as the cell fluid in the lower part of the inner cell. The design of triaxial cell developed by Bishop and Donald (1961)

was also used by Matyas and Radhakrishna (1968) to perform isotropic consolidation tests on unsaturated soil. Wheeler (1986) developed a double-walled triaxial cell to test unsaturated soils in the laboratory. The basic idea of the double-walled triaxial cell was that volume change of the sample could be measured by measuring the flow of water into or out of the inner cell.

The axis translation technique has been used in most laboratory research involving triaxial testing of unsaturated soil. Elevated values of pore air pressure are applied to one part of the sample boundary via a low air entry filter and lower (but still positive) values of pore water pressure are applied or measured on a different part of the sample boundary via a high air entry porous disk. Use of a high air entry porous disk does not solve the difficulty of air getting into the water drainage line. Dissolved air within the pore water can still penetrate through the porous stone by diffusion and this air may then come out of solution in the drainage line beneath the porous stone. Bishop and Donald (1961) developed a bubble pump and Fredlund (1975) developed the Diffused Air Volume Indicator (DAVI) to remove and measure the amount of diffused air collected beneath a high air entry porous stone.

2.7.5 Oedometer device

Testing of unsaturated soil in an Oedometer is easier than testing in a triaxial cell because in this test movement of sample takes place only in one direction. Barden and Sides (1970) developed a modified Rowe cell to conduct one-dimensional consolidation tests on unsaturated soils. They used the axis translation technique to control or measure the matric suction. Other researchers, including Fredlund and Morgenstern (1977) and Escario and Juca (1989), used the same type of apparatus with some modifications. Rahardjo and Fredlund (1996) designed an apparatus for performing consolidation tests to study the pore pressure and volume change behaviour under K_o (coefficient of earth pressure at rest) conditions of unsaturated silty sand soils.

2.7.6 Direct Shear device

In the direct shear test, a soil sample is sheared on a predetermined shear plane. This apparatus has been used for testing shear strength of both saturated and unsaturated soils for many years. Escario (1980) developed a direct shear apparatus to examine the shear strength of Madrid grey clay under unsaturated state. To apply the matric suction, the axis translation technique was employed. Elevated pore air pressure was applied to a

container surrounding the whole apparatus. The pore water pressure was then applied or measured by using the High Air Entry Porous Disk (HAEPD) at the sample base. The same type of apparatus was used by Gan and Fredlund (1988) to determine the shear strength parameters of compacted glacial till under unsaturated condition. Gachet et al., (2003) described a modified direct shear box to measure the shear strength of sand-glass and sand-Plexiglas interfaces for different degrees of saturation. The authors studied the effects of friction and cohesion at the interface between soil and model on the experimental results. They suggested that in any experiment of limited lateral extension, side effects may play a dominant role. Their results revealed that the degree of saturation seems to govern the interface behavior and dependence could be established between degree of saturation, suction in the sand, and the border effect intensity. Degree of saturation was changed by using water aspiration on half of a Casagrande shear box that contained saturated sand. By using water aspiration, they estimated the degree of saturation in the sand and correlated it to the suction.

2.7.7 Interface direct shear device

The direct shear testing of interfaces is similar to direct shear testing of soil. A hollow box, containing the soil specimen, rests on a construction material such as steel and concrete. A normal load is applied to the top of the soil specimen, and then a horizontal force is applied to shear the interface between the soil and the construction material. Potyondy (1961) used the direct shear box to determine the skin friction between different types of soils and construction materials, both by stress control and strain control methods. In this study, the specimens of construction materials were placed in the lower part of the box, and the soil was placed in the upper part.

Desai et al., (1985) have also used a shear box device to study the friction between sand and steel/concrete under cyclic interface condition. The lower half of the shear box had a square cross-section and was made from steel plates with inner dimension of 410 mm x 410 mm. One of the materials such as concrete, ballast, and rock was inserted in the lower half. The top part consisted of a square box (310mm x 310 mm) and contained the other material. Recently, Hamid (2005), Hossain (2010) and Borana et al., (2013) modified a conventional direct shear apparatus to perform a series of direct shear interface tests (Figures 2.23 and 2.24). The new device has several features like the capability to apply and maintain suction ($u_a - u_w$) via axis translation and capability to apply and maintain net normal stress ($\sigma - u_a$).

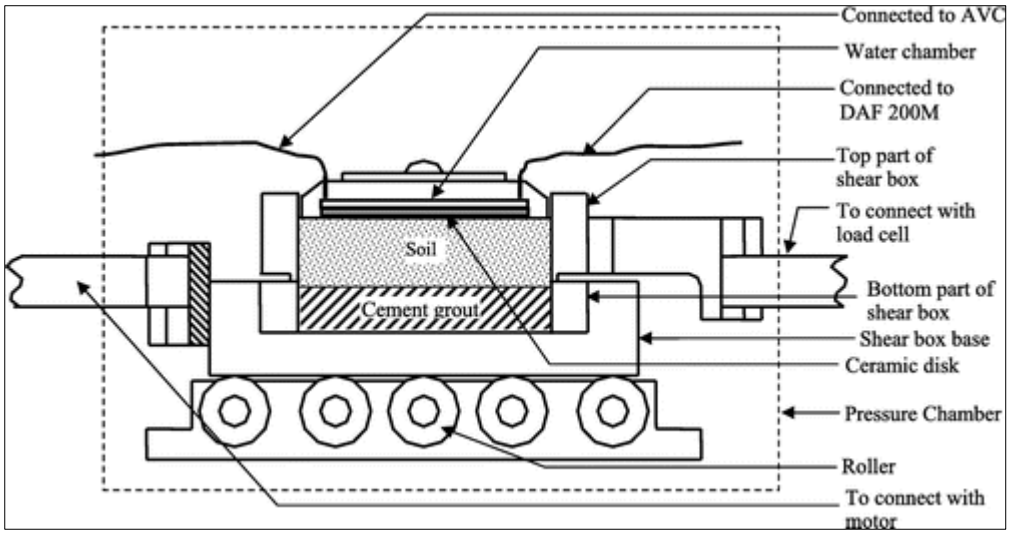

Figure 2.23: Schematic diagram of modified direct shear apparatus used for soil-cement grout interface test (Hossain, 2010).

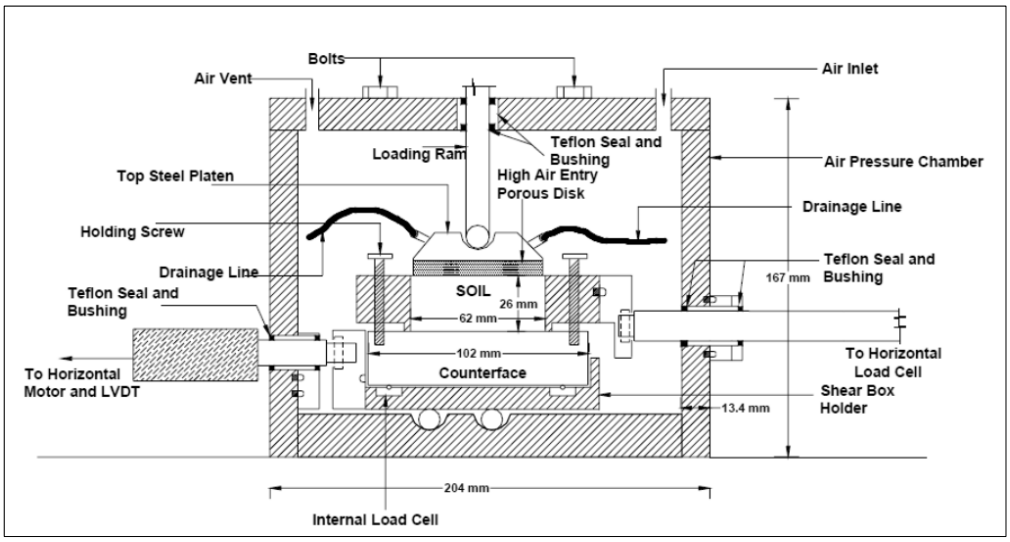

Figure 2.24: Cut away cross-section view of the air chamber, shear box holder, and shear box (Hamid, 2005).

2.7.8 Interface annular shear device

The annular shear device was used by Brummund and Leonards (1973) for experimental study of static and dynamic friction between sand and construction materials. It consists of a cylinder of sand encased in rubber membrane with a 28.6mm diameter, 356mm long rod located along its axis. By evacuating air from within the membrane, a normal stress was applied to the sand-rod interface that ranged from 8.6 kPa to 86 kPa. The rod was then caused to slip relative to the sand by gradually applying static forces to the rod in the axial direction. The coefficients of friction between sand and different materials such as steel, Teflon, cement mortar, and graphite were measured using this apparatus.

The coefficient of friction increases with the surface roughness and angularity of the sand grains, and as the roughness of the contact surface increases with respect to the size of the sand particles. In addition, Teflon and graphite reduced wall friction by one-half to one-third at high loading rates

2.7.9 Interface ring torsion device

Yoshimi and Kishida (1981) used a ring torsion apparatus to study the behavior of the interfaces between sand and steel. Dry sand was rained into an annular container lined with a 0.3mm thick rubber membrane. A ring shaped metal specimen was placed on the sand as the construction material and a static torque was applied to shear the interface under constant normal load applied with weights. In addition to measurements of circumferential and vertical displacements of the metal ring, the deformation of the sand and the slippage at the soil-metal contact were measured in some tests using x-ray radiography.

2.7.10 Interface simple shear device

Uesugi and Kishida (1986) modified a simple shear type device that was capable of measuring both sliding displacement between steel and soil as well as shear deformation of the soil mass (Figures 2.25(a) and (b)). The contact surface between steel and sand was originally 40 mm in wide and 100 mm in length. The area of friction surface remained constant during a test even if sliding occurred, since the steel plate was longer than the friction surface. Normal and tangential loads were applied by vertical and horizontal hydraulic actuators.

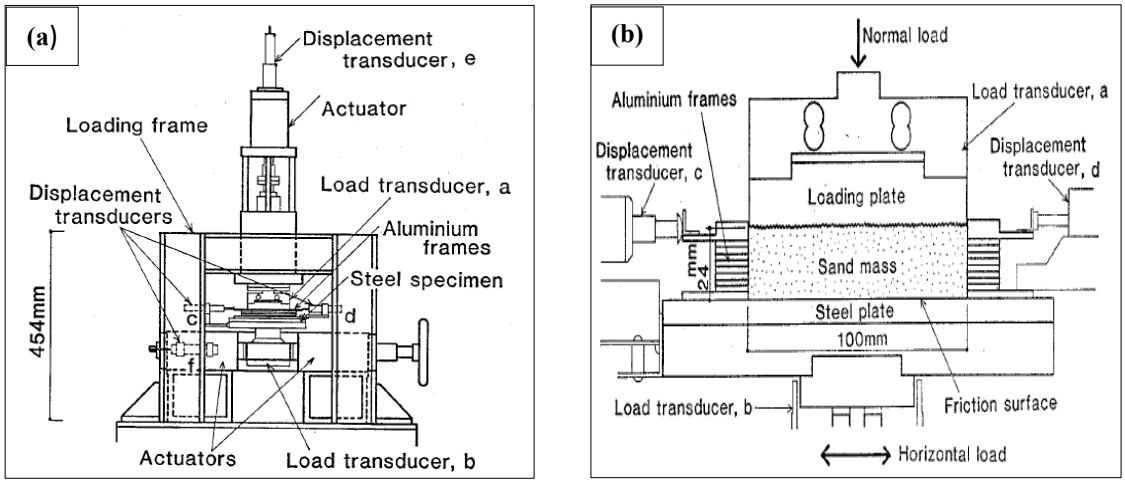

Figure 2.25: Simple shear type testing apparatus (a) schematic view, (b) cross-sectional detail of frictional cell (Uesugi and Kishida, 1986).

2.7.11 Three-dimensional interface testing device

Fakharian and Evgin (1996) developed a computer controlled apparatus to study the behaviour of three dimensional monotonic and cyclic loading conditions. Figures 2.26(a) and (b) depicts the schematic diagram and photographical view of the three-dimensional interface apparatus. The apparatus was capable to apply normal stress, σ_n, and two shear stresses, τ_x and τ_y. It had the capability for direct shear and simple shear testing in 3-dimensions. A reaction frame was designed to withstand a vertical or horizontal load up to 25 kN. The actuators used to apply the normal and tangential loads had capacities of 10 kN each. The soil was placed in a 25mm thick hollow aluminium box, with inside area of 100 mm x 100 mm. The sand was deposited by using a multiple-sieving-pulviation method. The sand surface was levelled off by means of a vacuum so that the initial height of the sample was 20mm. First the interface was sheared in one tangential direction up to a shear stress level less than the peak value. Then, the interface was sheared in a perpendicular direction, while the shear stress in the previous direction was maintained at a constant level. The authors also reported that the shear stress and shear displacement increments experienced different paths, while the resultant shear stress-shear displacement curves remained the same irrespective of stress paths.

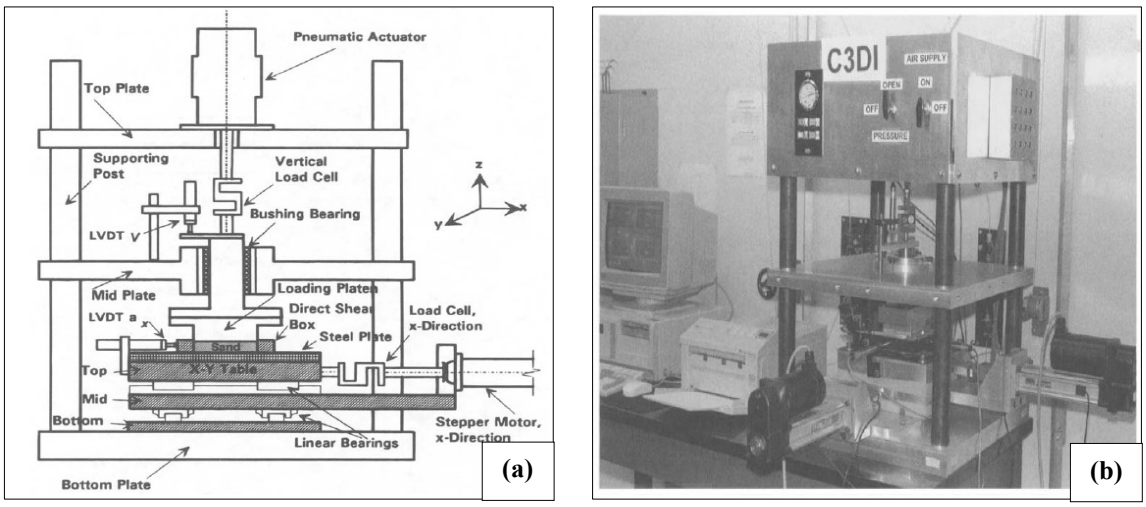

Figure 2.26: Three-dimensional (C3DI) interface apparatus (a) schematic view, (b) photograph of C3DI (Fakharian and Evgin, 1996).

2.8 Direct and indirect methods of soil suction measurements

The measurement of negative pore-water pressure (or soil suction) is an essential challenge in the geotechnical engineering field, particularly when measuring high

values of matric suction. Soil suction has a greater effect on the shear strength and volume change behaviour of unsaturated soils.

Significant contributions have been made by several researchers to develop new tools and techniques for measuring soil suction over various ranges and with different degrees of accuracy in both laboratory and field (Fredlund and Rahardjo, 1993; Ridley, 1993). Ridley and Wray, (1995) and Fredlund et al., (2012) summarized the most common suction measurement devices used for measuring matric suction, osmotic suction, and total suction in Table 2-1 along with restrictions associated with these methods.

Table 2-1: Devices for measuring soil suction and its components (Ridley and Wray, 1995 and Fredlund et al., 2012)

Name of device	Suction measured	Range (kPa)	Comments
Psychrometers (Peltier type)	Total	100 to ≈ 8000	Constant-temperature environment required
Filter paper	Total	Entire range	May measure matric suction when in good contact with mist soil
Null-type pressure plate (Axis translation)	Matric	0 - 1500	Range of measurement is a function of the air-entry value of ceramic disk
Thermal conductivity sensors	Matric	10 to ≈ 1500	Indirect measurement using variable-pore-size ceramic sensor
Pore fluid squeezer	Osmotic	Entire range	Used in conjunction with psychrometer or electrical conductivity measurement
Imperial College tensiometers	Matric	0 to 1800	Range of suction is limited by the air-entry value of the ceramic
Osmotic tensiometer	Matric	0 to 1500	Reference pressure can deteriorate with time, and temperature dependent
Suction probe	Matric	Up to 1500	There may be cavitation and air diffusion through the ceramic head during the suction measurement

It is obvious from Table 2-1, that each of these tools or techniques has its own limitations and disadvantages. In other meaning, there is no single piece of tool covering the entire range of total suction measurements. Hence, two or more methods may be used to measure wide-range of soil suction. The basic concepts and the application of the suction measurement tools are discussed in details in the literature like (Fredlund and Rahardjo, 1993; Ridley and Burland, 1995; Bulut and Leong, 2008; Hu et al., 2010; Fredlund et al., 2012).

2.8.4 Suction probe

The direct measurement of matric suction is preferred in unsaturated soil tests since measured pore water pressures are more rapidly reflected. Ridley and Burland (1993) developed a suction probe for measuring matric suction of soil. The principle of making suction measurements using a suction probe is based on the equilibrium between the pore-water pressure in the soil and the pore-water pressure in the water reservoir. Before equilibrium is attained, water flows from the water reservoir into the soil, or vice versa as shown in Figure 2.27. The suction probe measures the pore-water pressure (u_w). The matric suction can be computed since the applied air pressure (u_a) is known, and the matric suction is the difference between the pore-air pressure and the pore-water pressure ($u_a - u_w$). Basically, a suction probe consists of a pressure transducer with a high-air entry ceramic disk mounted at the tip of the transducer. The diaphragm of the pressure transducer responds to the applied pressure. In the suction probe, the volume of water reservoir beneath the ceramic disk or ceramic cup is minimized. Water in the water reservoir is pre-pressurized such that benefit of the high tensile strength of water can be utilized (Marinho and Chandler, 1995). Recently, Meilani et al. (2002) developed a mini suction probe for measuring matric suction along the specimen's height during triaxial test on an unsaturated soil. It is unique in its ability to make direct measurements over a wide range of soil suctions (i.e. up to 1500 kPa) and has been used extensively in both laboratory and field applications for a variety of clients and on a range of soil types. Measurements can be made in a borehole at depths between 0 and 5m or on samples after they have been recovered from the ground. Similar to the null-type axis-translation technique, the upper limit of matric suction that can be measured using this technique is governed by the air-entry value of the ceramic disk or ceramic cup used.

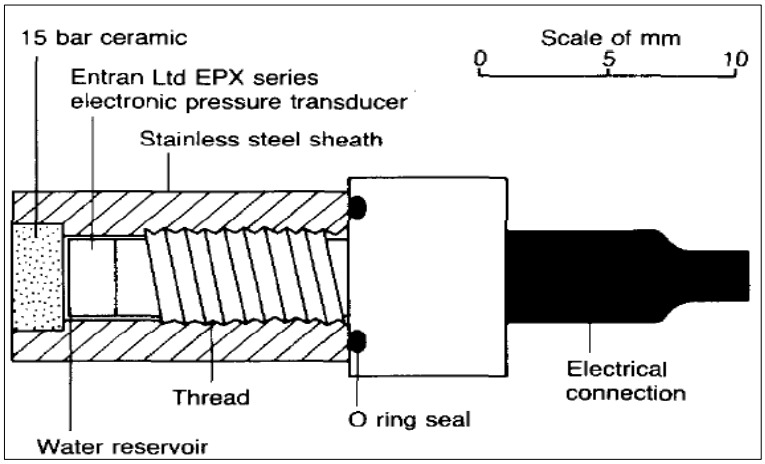

Figure 2.27: Schematic plot of the developed suction probe (Ridley and Burland, 1993).

2.9 The effect of shear box size on the shear strength behaviour

In the middle of the last century, the specimen size effects on the shear strength behaviour have been investigated experimentally by Parsons (1936). The author performed a series of different sizes of shear boxes (60 mm x 60 mm, 120 mm x 100 mm and 120 mm x 200 mm) direct shear tests on crushed quartz and Ottawa clean uniform sand. The laboratory results revealed that the angle of friction slightly decreased with increasing the size of the shear box, as shown in Figure 2.28.

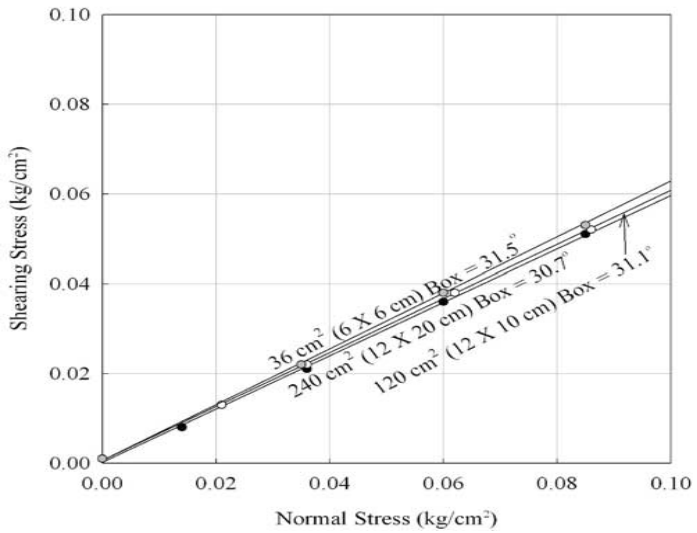

Figure 2.28: Effect of shear box size on the friction angle of crushed quartz (Parsons, 1936 cited in Moayed and Alizadeh, 2012).

Results presented in Table 2-2 showed that friction angles obtained for the crushed quartz ranged from 30.7˚ to 31.5˚ and the Ottawa sand ranged slightly more from 28.5˚ to 31.0˚ and the friction angle resulted from testing the crushed quartz ranged from 30.7˚ to 31.5˚.

Table 2-2: Scale effect of crushed quartz and Ottawa sand (Parsons, 1936)

Shear box dimensions L (mm) x W (mm)	Ottawa sand	Crushed quartz
	ϕ (deg)	ϕ (deg)
60 x 60	31.0	31.5
120 x 100	29.6	31.1
120 x 200	28.5	28.5

Dadkhah et al., (2010) studied the effect of shear box size on the shear strength parameters of clayey sand in Isfahan city, Iran. The specimens were performed by using large, medium and small scale direct shear test apparatus with shear box dimensions of 60, 100 and 300 mm. Their results revealed that the shear strength parameters can be dependent on shear box size, in the sense that the large and medium scale direct shear produce a higher cohesion and lower friction angle compared with the small scale direct shear test results. In support of these observations, Moayed and Alizadeh, (2012) investigated the specimen size effects on the shear strength properties of Firuzkuh #161 crushed silica sand with different silt percentages by employing different sizes of shear box. The authors concluded that the peak shear strength and friction angle decreased as the shear box size increased. So the tests indicated that the scale effect can be seen in silty sands but the rate of its effect reduces with increasing the silt percentages, as shown in Table 2-3. In addition, their conclusion showed that larger shear boxes can be more accurate to determine the shear strength properties of the cohesionless soils performed under unsaturated condition.

Recently, similar behaviour was observed by Shakri et al., (2017). They performed a series of direct shear tests of two shear box sizes (60 mm x 60 mm and 300 x 300 mm) on modified sand-column (PFA-sand mixture) and soft soil. Their results showed that that the shear strength decreases as the size of shear box increase.

Table 2-3: Direct shear box test results using the peak shear strength (after Moayed and Alizadeh, (2012))

Soil Type	Shear box sizes, (mm)	
	60 x 60	100 x 100
	ϕ (deg)	ϕ (deg)
Pure Sand	42.46	38.88
Silty Sand I (10% Silt)	39.18	36.06
Silty Sand II (20% Silt)	35.35	34.51
Silty Sand III (30%Silt)	33,27	32.76

Conversely, Palmeira and Milligan (1989) reported no significant difference in frictional angle with increasing the size of the shear box (see Table 2-4). The authors obtained their results by performing several laboratory tests on dense Leighton Buzzard Sand using three different sizes of shear boxes (small, medium and large).

Table 2-4: Influence of scale on the friction angle of Leighton Buzzard Sand (after Palmeira and Milligan (1989)

Shear box	Dimensions (L*W*H) mm	Friction angle, ϕ' (deg)
Small	60 x 60 x 32	50.1
Medium	252 x 152 x 152	50.2
Large	1000 x 1000 x 1000	49.4

2.10 Concluding remarks

In this chapter, literature relevant to the current research project has been reviewed and presented. Emphasis was placed on the review of unsaturated soils and suction concepts, hydro-mechanical behaviour including stress state variables and volumetric behaviour. General information on the soil-water retention curve (SWRC) and its features and factors affecting the SWCC were covered. The review of literature regarding the shear strength behaviour of saturated and unsaturated interface was included. The laboratory testing of unsaturated soils and interfaces is also reviewed and presented. The main observations from this chapter can be summarised as follows:

1. Several methods are currently available for suction measurements; however each method has its own limitations and advantages.

2. Behavior of unsaturated soil cannot be described using the traditional single effective stress variable for saturated soils.
3. Two stress state variables, matric suction ($u_a - u_w$) and net normal stress ($\sigma_n - u_a$) can be used to explain the behaviour of unsaturated soils.
4. Conventional laboratory devices (e.g. Triaxial, direct shear and Oedometer) have been modified to examine the behaviour of unsaturated soils.
5. Most of the modified laboratory devices used axis-translation technique to apply and maintain matric suction.
6. Major factors influencing the shear strength behaviour of a given interface are type of soil, void ratio, water content, rate of shear displacement and surface roughness.
7. Direct shear, simple shear, annular shear, and torsional shear apparatuses can be used to test the interfaces between soil and different construction materials.
8. The previous review of literature shows that, the shear strength behaviour between unsaturated soils and construction materials have been investigated using modified small-scale direct shear devices (dimensions of the shear cell e.g. 60 x 60 mm^2 and 100 x 100 mm^2).
9. The strength and volumetric behaviour of unsaturated interface have been investigated by imposing different levels of net normal stress and matric suction.

However, based on the literature review, there is still a lack of knowledge and open questions concerning the behaviour of soil-structure interaction under unsaturated condition. In the following chapters, this study addresses the following research questions:

1. What is the effect of different levels of vertical stress and void ratios on the strength characteristics of the unsaturated soils, especially artificial silty sand soil?
2. How do the real-time matric suction measure during large-scale (300 x 300 mm^2) direct shear tests?
3. How do the variations of matric suction behave during direct shear tests (matric suction stabilisation, consolidation and shearing stages)?
4. How do the different levels of vertical stress, void ratio and surface roughness affect the interface strength behaviour and variation of matric suction?

CHAPTER THREE

MATERIAL INVESTIGATIONS AND SELECTION

3.1 Introduction

Unsaturated soils are commonly found in most parts of the World, especially at shallow depths from the surface and in arid and semi-arid areas where the ground water table typically is often many meters deep (Fredlund and Rahardjo, 1993; Fredlund, 2000; Lu and Likos, 2004). Very limited research studies have been reported in the literature concerning the behaviour of unsaturated Iraqi soils. For this reason, an extensive experimental program was undertaken in order to investigate the unsaturated characteristics of Iraqi soils and their behaviour when interact with the structural elements.

This chapter covers the procedures adopted to select the proper soil used in this research and its basic characteristics. A brief review of the general country background including topography, population, principal rivers and country boundaries is included. The available soil investigation reports of Baghdad governorate have been collected and re-analyzed and their physical properties are also indicated.

3.2 Adopted soil selection procedure

3.2.1 General country background of Iraq

Several regions of the earth's surface are classified as arid and semi-arid, which covers approximately 33% of the total area of the world (Dregne, 1974; Fredlund and Rahardjo, 1993). The soils in these regions are receiving annual precipitation below the annual

potential evaporation. Hence, the soil nearest to the ground surface is very dry. Typically, the soils in these regions are in a state of unsaturated conditions.

The map of Iraq is as shown in Figure 3.1. Iraq is positioned in the Middle East, a recognized geographical region of South-west of continent Asia, and is situated in both the northern and eastern hemispheres. The geographic location of Iraq lies between longitudes 38° 45′ and 48° 45′ and latitudes of 29° 15′ and 37° 15′ in arid to semi-arid region. It shares land borders with six countries, in the east by Iran, in the west by Syria and Jordan, and Turkey in the north, and Kuwait, Saudi Arabia and the small stretch of Arabian Gulf, in the south. The climate of Iraq is arid and dry, distinguished by hot summers and short cold winters. The average of hotness and coldness in Iraq is approximately higher than 48 degrees ºC in July and August and below freezing in January. A majority of the rainfall happens from December through April and is more plentiful in the mountainous region. Tigris and Euphrates are the main water resources in Iraq and these two rivers stem from Turkey and join together in the south of Iraq to create Shatt Al-Arab which drains to the Arabian Gulf (Al-Ansari et al., 2014).

According to the United Nation Development Department statistical data, Iraq's population was at 34 million in 2007, nearly 20% of the population concentrate in Baghdad governorate (the capital of Iraq) according to the population distribution in Iraq based on 2007 estimation. Geologically, landforms in Iraq can be classified into four major categories, sedimentary plain, desert plateau, mountain region and undulating terrain. The sedimentary plain area occupies about 30% of the total area of the country with a low annual rate of rainfall ranging from 50-200 mm compared with the other region in Iraq (e.g. mountain region with annual rainfall ranging from 400-1000 mm). The sedimentary plain region is a geological depression filled with river sediments, which cover the central and southern parts of Iraq. The soils are mostly silty clay loams and silty clays formed in river basins. They are layered with soil materials ranging in textures from silty clay loam and silty clay to very fine sand. In addition, they occur along the rivers in narrow strips. These are the most important soils in the lower Mesopotamian plain (Buringh, 1960; Food and Agricultural Organization, FAO, 1990).

The climate of Iraq is strongly affected by the location of the country between the sub-tropical dryness of the Arabian Desert areas and the sub-tropical wetness of the Arabian

Gulf. Therefore, the greater part of the country (about 62 %) has an arid climate and suffering from high rate of evapotranspiration that exceed the annual rate of rainfall leads to the formation of unsaturated soils (Jassim and Goff, 2006). For that reason a special attention was given to study the behaviour of such soils.

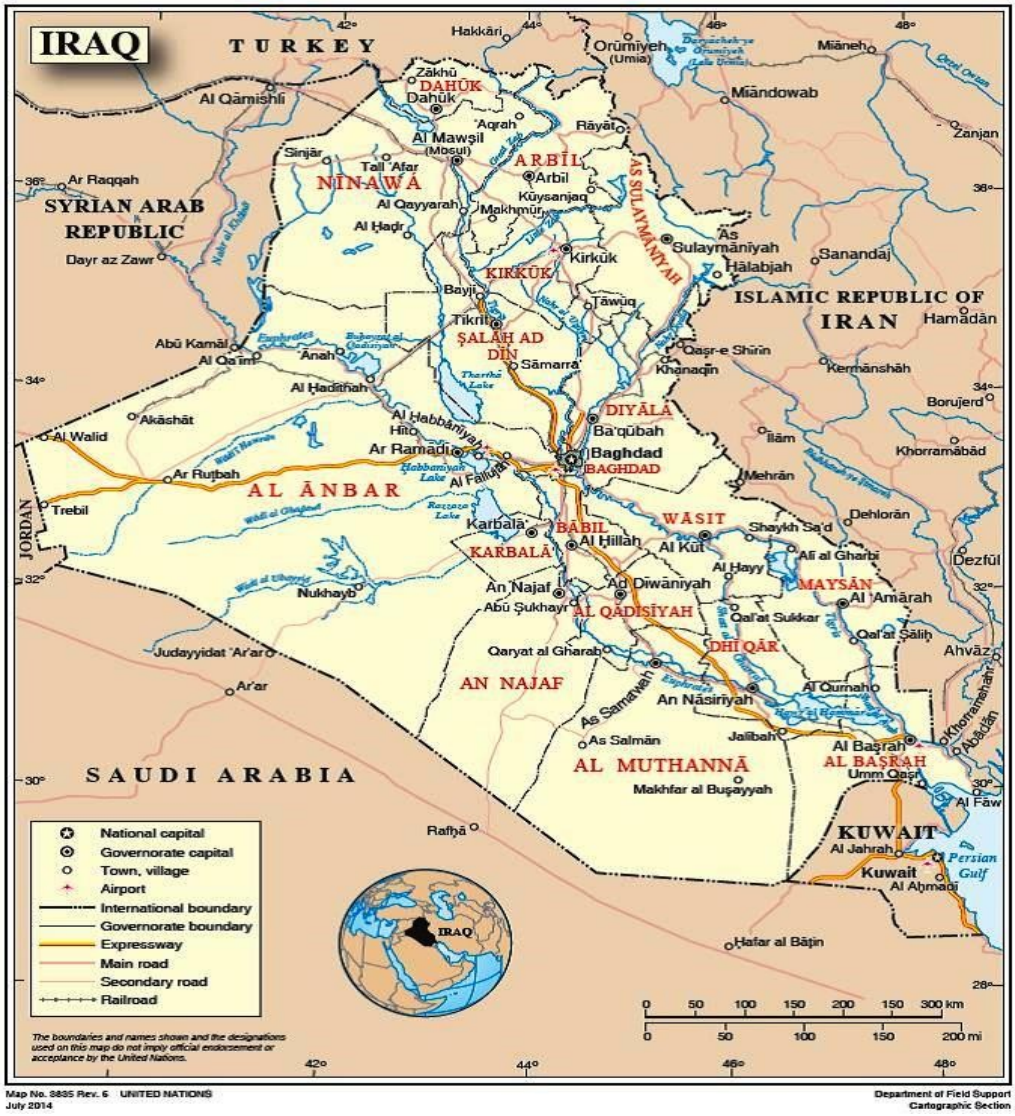

Figure 3.1: Location of Iraq in the world and region (www.un.org).

3.3 Collection and assessment of site investigation reports

Several major problems were encountered during this research. Of these, the most significant was the inability to collect and transport the soil samples from Iraq to the geotechnical laboratory of the Heriot-Watt University (Edinburgh, UK). To overcome this problem, extensive effort has been made in order to enable a deep understanding of the

Iraqi soils. Several soil investigation reports have been collected and assessed from different reliable Iraqi government sources such as University of Technology (Building and Construction Engineering Department), Ministry of Construction and Housing (National Centre for Construction Laboratories, NCCL), and Al-Mustansiriya University. The collected reports examined the physical and mechanical properties of the main Iraqi soils of different regions located at Baghdad governorate, the capital of Iraq (most populated city in Iraq). Figure 3.2 shows the locations of sites that have been explored on Baghdad governorate map. As can be seen from Figure 3.2, the Tigris River divides Baghdad governorate into two districts, western district namely Al-Karkh and Al-Rasafa is the eastern district. According to the geotechnical investigation reports, it was clearly noted that the sampling locations covered a wide range of areas in Baghdad. Accordingly, the locations of the investigated soil can be divided into five groups; two groups (3 and 4) are located within Al-Rasafa district and contain five sampling sites (A, B, C, F, and J), and seven sampling sites (D, E, G, H, I, K, and L) distributed within three groups (1, 2, and 5) located in Al-Karkh district.

Generally, the main conclusion can be drawn from the results indicated that the soil particle size distribution shown higher percentage of silt than sand with clay and almost no gravel. The majority of soil profile composed by three different types of soil; the first one is silty clay soil (CL), the second is clayey silt soil (ML) and the third one is silty sand soil (SM). In the following subsections, the Particle Size Distribution (PSD) curves of soils obtained at different depths for twelve sites are presented. In addition, the summary of field and laboratory tests results and the main properties of the investigated soils are also indicated. The general trend of particle size distribution curves for each site is shown in Figure 3.15.

Based on the results recorded by the geotechnical investigation reports (Figures 3.3 to 3.14), the soil characteristics of site J was chosen. The investigated site selected is located in the east of Tigris River, 27 kilometres east south of Baghdad city. The reasons for selecting this site is the low plasticity of the soil due to its low clay content (less than 5 %) facilitated the suction stabilisation time for the tests and made viable the research in the available timeframe. In addition, the pre-cast driven concrete piles having an outer cross-section of 27.5 cm by 27.5 cm have been used as a deep foundation due to the high amount of working loads applied from the superstructure (Al-Madaen water treatment plant) to the

soil beneath. The pile foundation system has been found the most relevant because of the site condition, soil properties, structures arrangements, loading distribution which was collected from design criteria report for structural foundation and discussion of the test results. As well as, safety and the stability of the structure depend upon proper design and performance of its foundation. The structures at Al-Madaen water treatment plant site have been supported by pile foundation with tip of piles resting below natural ground surface to a depth of 19 – 20 m and the pile having allowable bearing capacity ranged from 35 – 40 ton.

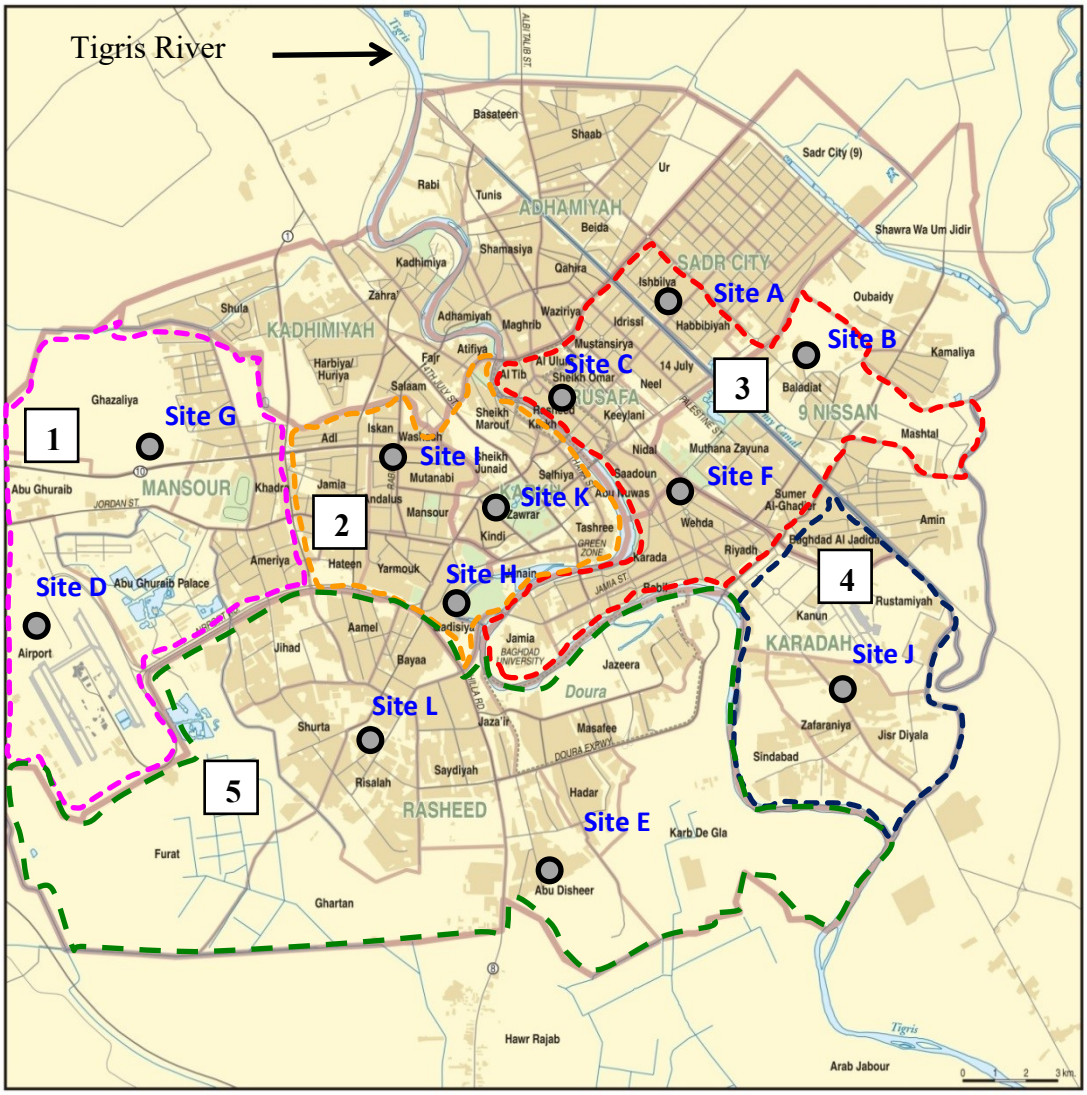

Figure 3.2: Baghdad governorate map and sites locations (www.understandingwar.org).

3.3.1 Site investigation report for multi-story building at Al-Mansour district (site G)

Site investigation was carried out and undertaken by the University of Technology, to carry out the geotechnical investigation of multi-story commercial building located at Al-Mansour distract west of Baghdad city. Laboratory soil testing was carried out on soil samples taken from boreholes at the site location in order to categorize soils according to their probable engineering behavior. The main properties of the investigated soil are shown as follows:

- The soil classified as Silty clay (CL) according to USCS.
- Atterberg limits: Liquid limit, LL ranged from (34 – 72 %), and plastic limit, PL ranged from (18 – 31 %).
- The in-situ dry density, $\gamma_{in\text{-}situ}$ ranged from (13.6 – 15.9 kN/m^3).
- The maximum dry density ranged from (18.3 – 24.1 kN/m^3).
- Shear strength parameters: angle of friction, ϕ ranged from (3 - 12º), and soil cohesion, c ranged from (30 – 39 kPa).

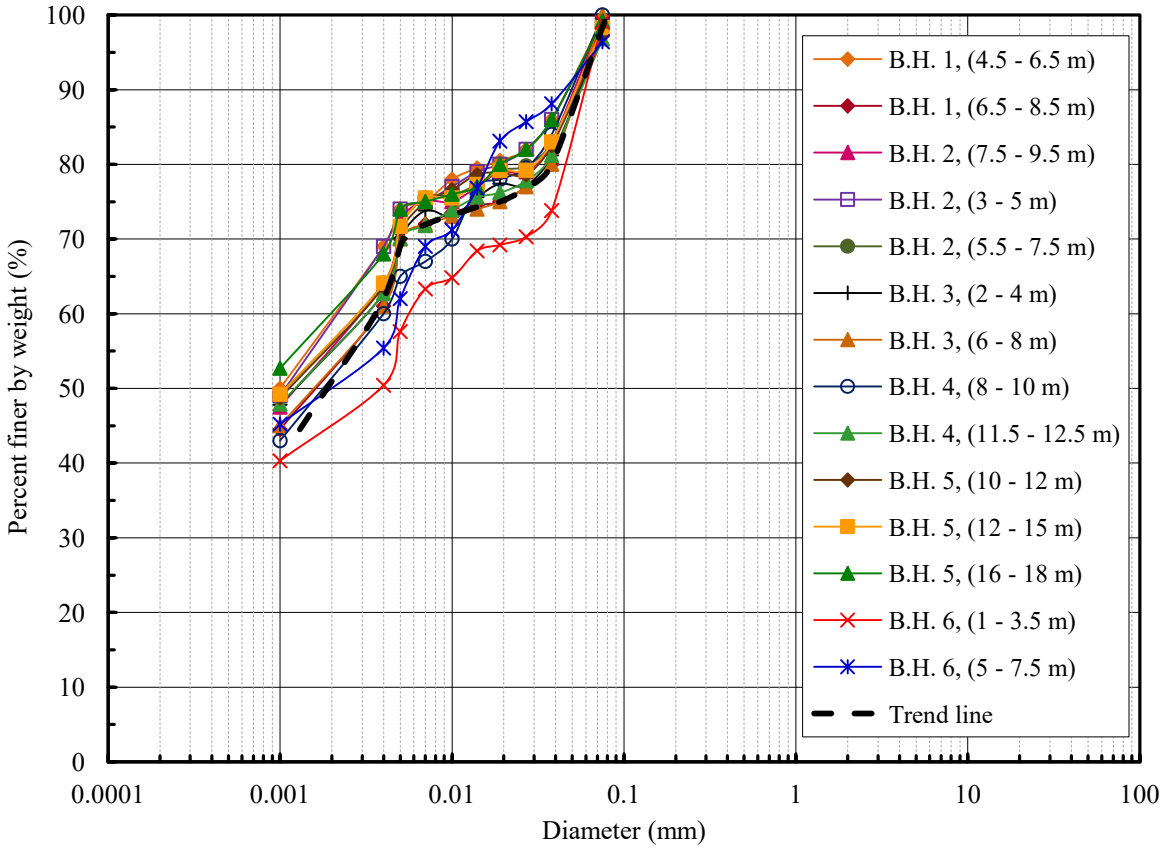

Figure 3.3: Particle size distribution curves at different depths for AL-Mada'an treatment plant site (site G).

3.3.2 Site investigation report of maintenance aircraft hanger for B-737 NG & GRJ at Baghdad International Airport (BIAP) (site D)

The maintenance hanger for B-737 NG & GRJ is a part of Pleistocene terrace physiographic region. This Pleistocene terrace is closely related to Pleistocene evolution of the main river sources. The purpose of this investigation was to explore the subsoil conditions of the site to facilitate and evaluate the foundation design for the structures. The field investigation was carried out in the site by the geotechnical group of AL-Mustansiriya University and included the drilling of different boreholes (Shelby and SPT) with suitable depths till encountered the firm soil. The summary of the laboratory test results as follows:

- The soil classified as Silty clay of intermediate to high plasticity according to USCS.
- Atterberg limits: Liquid limit, LL ranged from (35 – 55 %), and plastic limit, PL ranged from (15 – 25 %).
- The in-situ dry density, $\gamma_{in\text{-}situ}$ ranged from (15.1 – 15.9 kN/m^3).
- The maximum dry density, $\gamma_{dry\ max}$, ranged from (17.5 – 18.5 kN/m^3).
- Shear strength parameters: angle of friction, ϕ ranged from (3 - 8º), and soil cohesion, c ranged from (25 – 65 kPa).

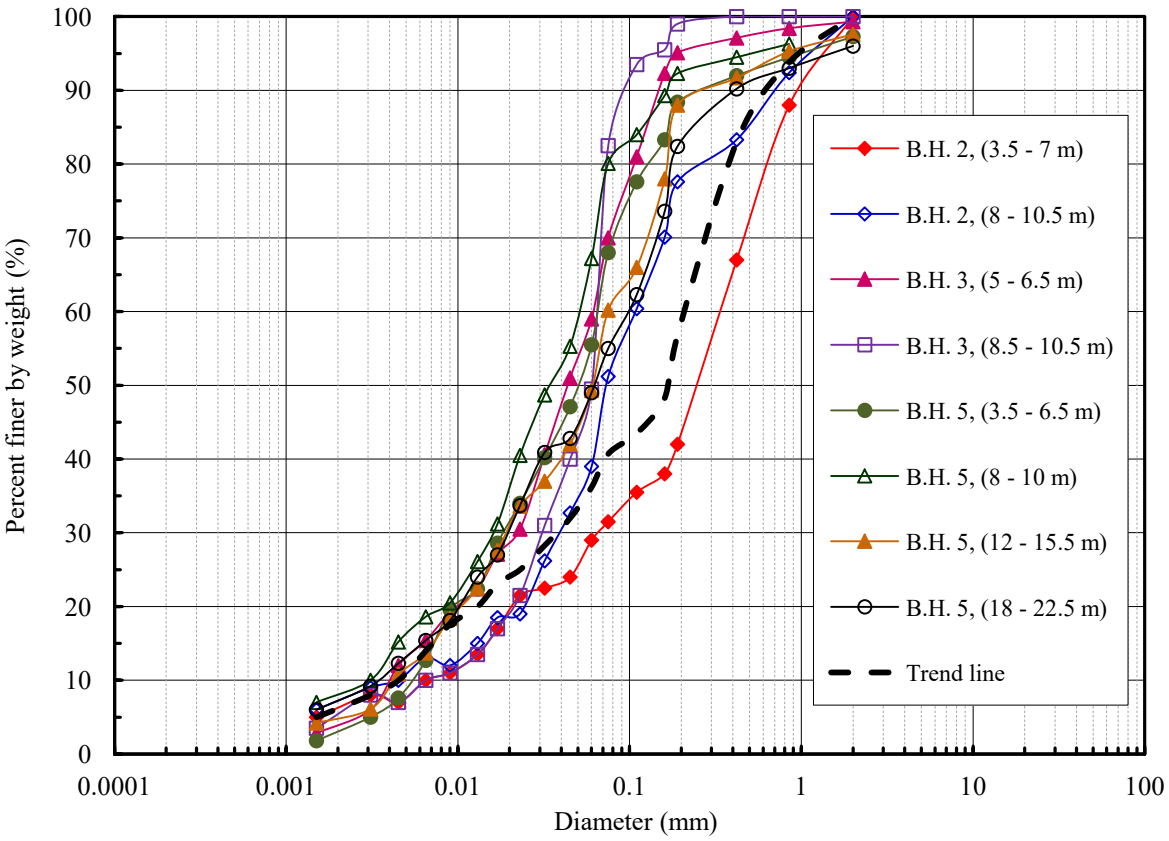

Figure 3.4: Particle size distribution curves at different depths for Maintenance Aircraft Hanger for B-737 NG & GRJ site (site D).

3.3.3 Site investigation report of communication tower site at Hay Al-Yarmouk district (site H)

was The purpose of this investigation to explore the subsoil conditions of the proposed location of the communication tower at Baghdad city, hence, lay down certain recommendations regarding the properties of soil with respect to the proposed system of foundations. The field investigation was carried out on December 2012, and included the drilling of (4) boreholes to a depth of (25 m) below the existing ground surface. At the laboratory, a program was set up to test the obtained samples in order to reveal the pertinent physical properties of the soil, and listed as below:

- The soil classified as clayey silt (SC) according to USCS.
- Atterberg limits: Liquid limit, LL ranged from (41 – 60 %), and plastic limit, PL ranged from (20 – 24 %).
- The maximum dry density, $\gamma_{dry\ max}$, ranged from (15.4 – 17.1 kN/m^3).
- Shear strength parameters: angle of friction, ϕ ranged from (16 - 20º), and soil cohesion, c ranged from (28 – 37 kPa).

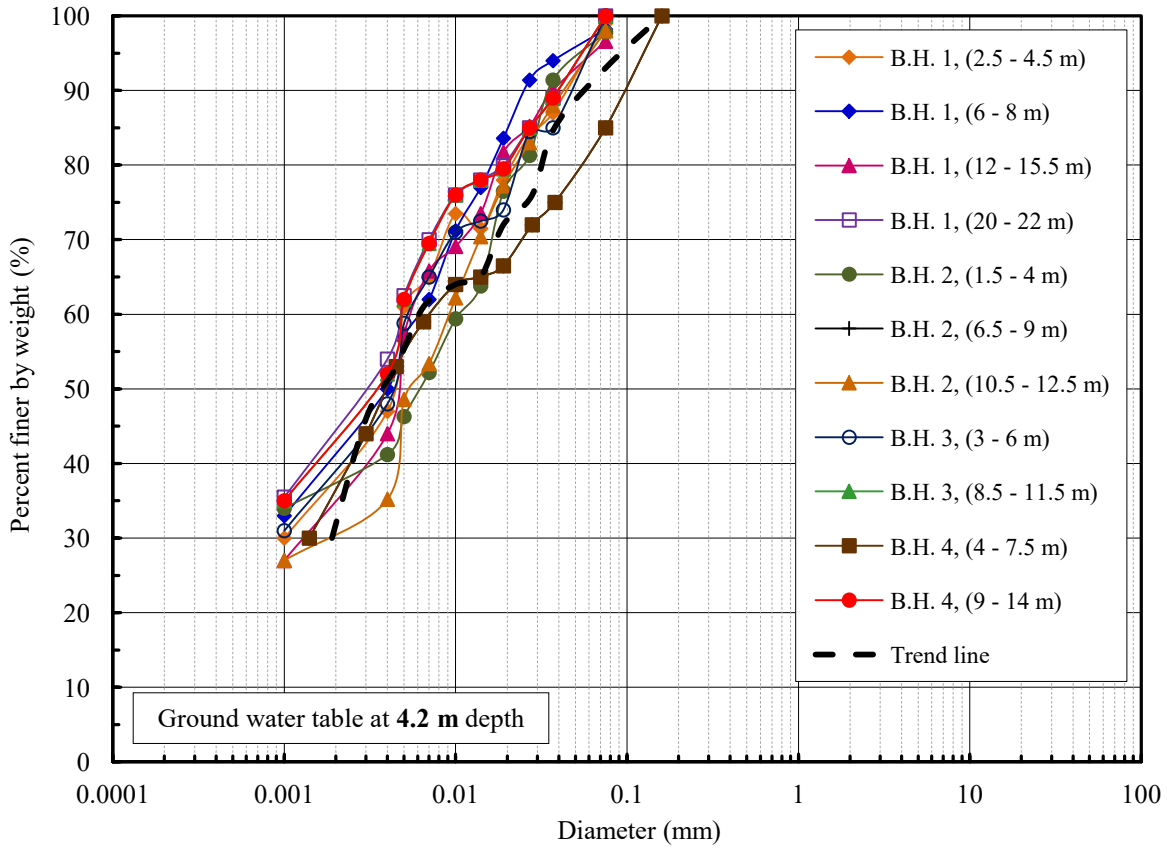

Figure 3.5: Particle size distribution curves at different depths for communication tower site (site H).

3.3.4 Site investigation report of multi-story car park building site at Al- Karkh district (site I)

The purpose of this investigation was to explore the subsoil conditions for multi-story car park site in east of Baghdad to facilitate and evaluate the foundation design for the main structures. The field investigation consists of drilling (5) boreholes to depth of (25 m). Field and laboratory works were carried out by a group of geotechnical engineers from AL-Mustansiriya University. The main properties of the investigated soil are shown as follows:

- The soil classified as silty sand of intermediate plasticity according to USCS.
- Atterberg limits: Liquid limit, LL ranged from (38 – 49 %), and plastic limit, PL ranged from (19 – 21 %).
- The maximum dry density, $\gamma_{dry\ max}$, ranged from (15.1 – 15.6 kN/m^3).
- Shear strength parameters: angle of friction, ϕ ranged from (2 – 5.5º), and soil cohesion, c ranged from (25 – 33 kPa).

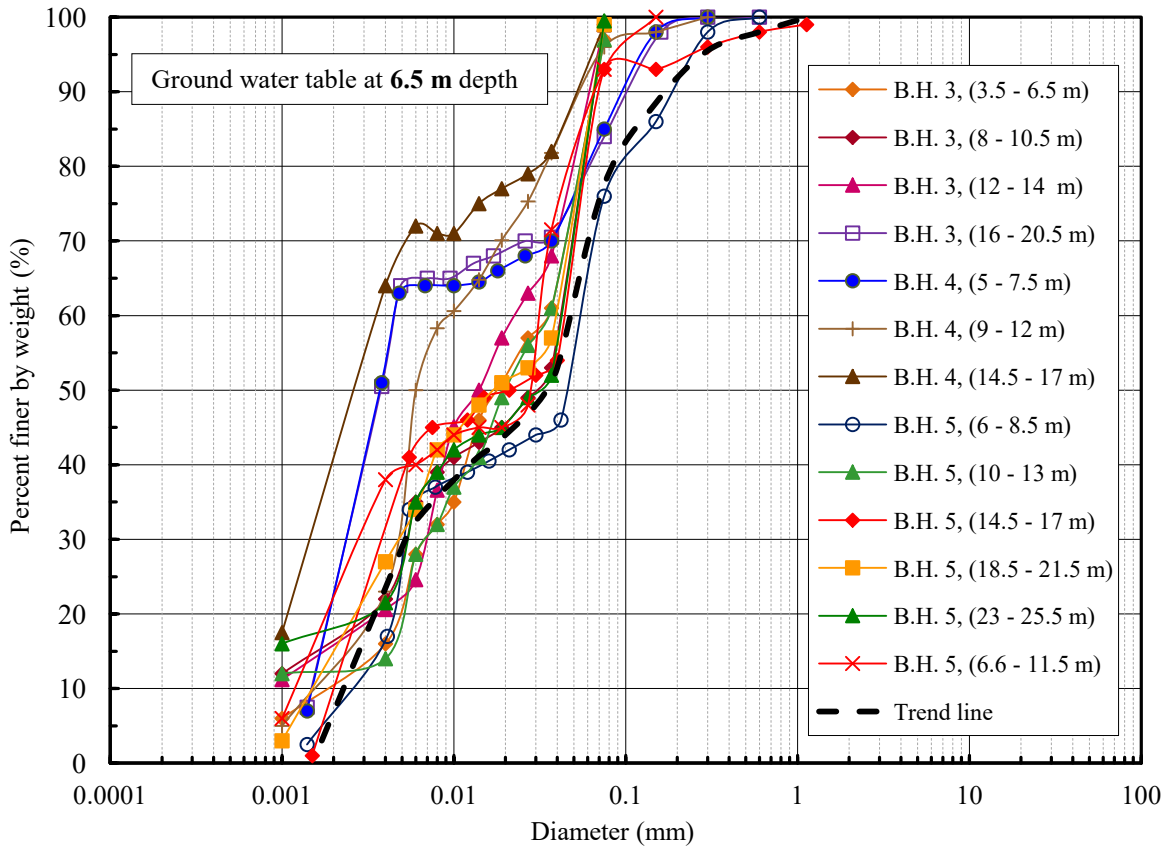

Figure 3.6: Particle size distribution curves at different depths for multi-story car park site (site I).

3.3.5 Site investigation report of Qasar Al-Hamra'a primary school site at AL-Amel district (site K)

Generally, the subsurface condition of the area explored by drilling of (4) boreholes is seemed to consist of the following two major strata: The first layer is medium stiff brown silty clay. This layer extends to a depth ranging between (4 to 11.5 m). The second layer consists of stiff brown silty clay with an extension to a depth of about (20 m). The physical characteristics of the investigated soil are listed below:

- The soil classified as silty clay (CL) according to USCS.
- Atterberg limits: Liquid limit, LL ranged from (37 – 53 %), and plastic limit, PL ranged from (15 – 26 %).
- The maximum dry density, $\gamma_{dry\ max}$, ranged from (15.3 – 15.8 kN/m^3).
- Shear strength parameters: angle of friction, ϕ ranged from (3 – 5º), and soil cohesion, c ranged from (28 – 35 kPa).

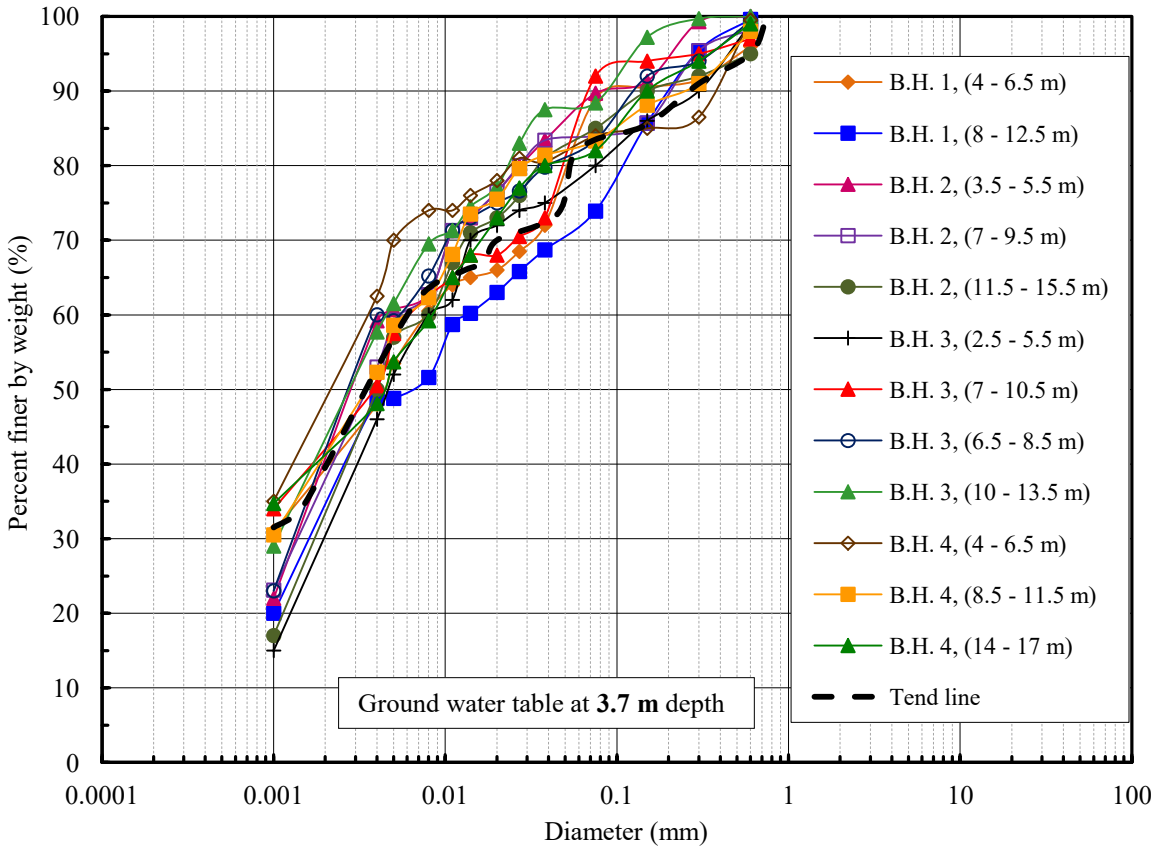

Figure 3.7: Particle size distribution curves at different depths for Qasar Al-Hamra'a primary school site (site K).

3.3.6 Site investigation report of multi-story commercial building site at Al- Rasafa district (site A)

Site investigation was performed by the University of Technology, to examine the geotechnical properties of a multi-story commercial building located at Al-Rasafa distract east of Baghdad city. Laboratory soil testing was carried out on soil samples taken from boreholes at the site location in order to categorize soils according to their probable engineering behavior. The main properties of the investigated soil are shown as follows:

- The soil classified as silty clay (CL) according to USCS.
- Atterberg limits: Liquid limit, LL ranged from (38 – 76 %), and plastic limit, PL ranged from (24 – 32 %).
- The in-situ dry density, $\gamma_{in\text{-}situ}$ ranged from (17.7 – 17.9 kN/m^3).
- The maximum dry density, $\gamma_{dry\ max}$, ranged from (18.5 – 19.3 kN/m^3).
- Shear strength parameters: angle of friction, ϕ ranged from (1 – 3.5º), and soil cohesion, c ranged from (26 – 43 kPa).

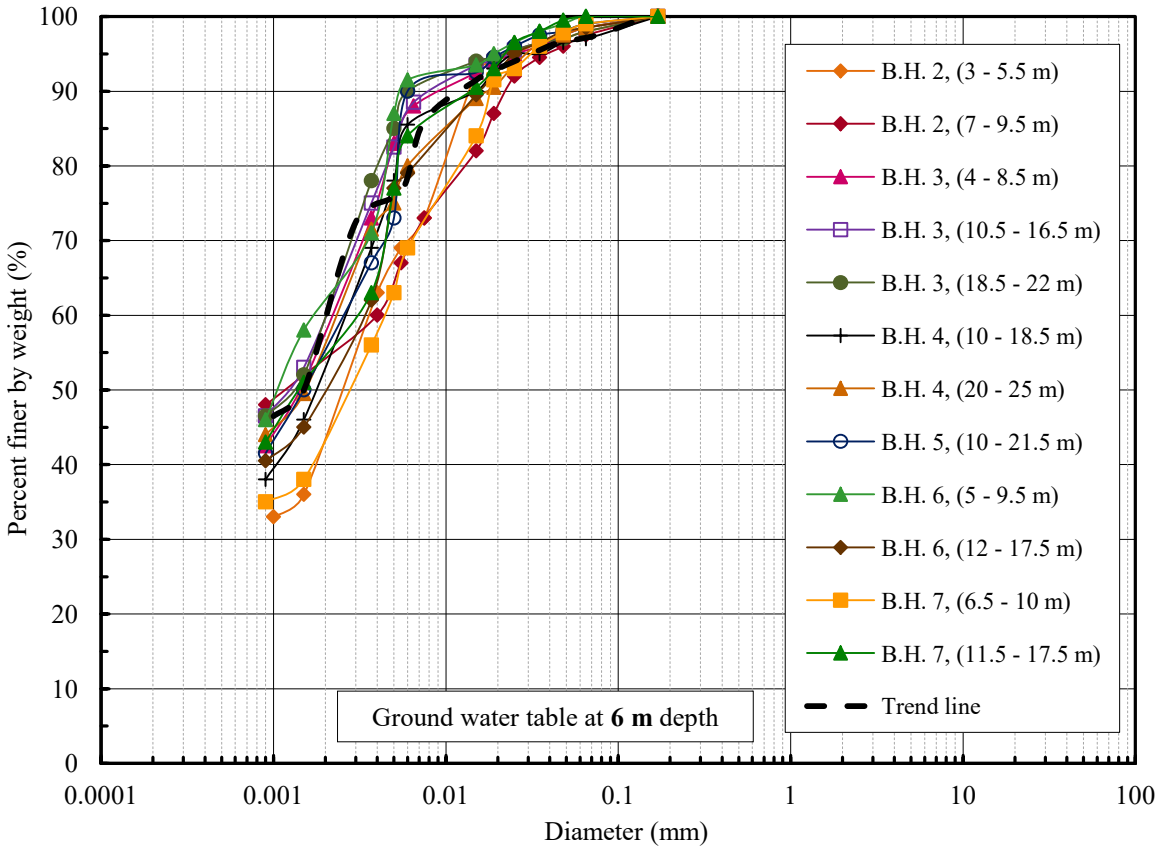

Figure 3.8: Particle size distribution curves at different depths for multi-story commercial building site (site A).

3.3.7 Site investigation report of multi-story residential building site at Al- Rasafa district (site B)

The purpose of this investigation was to explore the subsoil conditions for 8-storey residential building site at Karada Kharich east of Baghdad to facilitate and evaluate the foundation design for the main structures. The field investigation consists of drilling (5) boreholes to depth of (30 m). Field and laboratory works were carried out by a group of geotechnical engineers from University of Technology. The main properties of the investigated soil are shown as follows:

- The soil classified as silty clay (CL) according to USCS.
- Atterberg limits: Liquid limit, LL ranged from (42 – 49 %), and plastic limit, PL ranged from (21 – 24 %).
- The maximum dry density, $\gamma_{dry\ max}$, ranged from (17.1 – 18.2 kN/m^3).

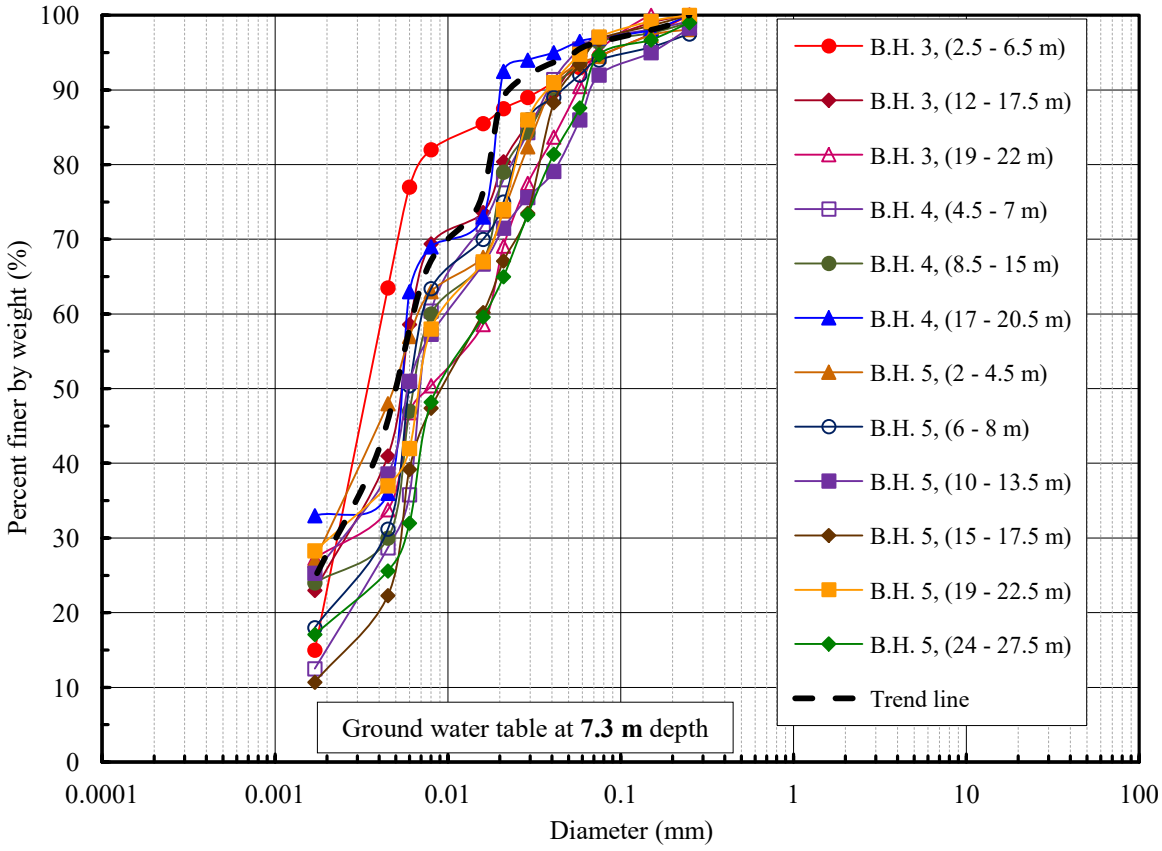

Figure 3.9: Particle size distribution curves at different depths for 8-storey residential building site (site B).

3.3.8 Site investigation report of AL-Karama multi-storey commercial building at Al-Rasafa district (site C)

Site investigation was carried out by the University of Technology, to examine the geotechnical properties of AL-Karama multi-storey commercial building at Al- Rasafa district North West of Baghdad city. Laboratory soil testing was carried out on soil samples taken from boreholes at the site location in order to categorize soils according to their probable engineering behavior. The main properties obtained from the field and laboratory tests of the investigated soil are shown as follows:

- The soil classified as silty clay (CL) according to USCS.
- Atterberg limits: Liquid limit, LL ranged from (30 – 50 %), and plastic limit, PL ranged from (20 – 25 %).
- The maximum dry density, $\gamma_{dry\ max}$, ranged from (17.3 – 18.8 kN/m^3).

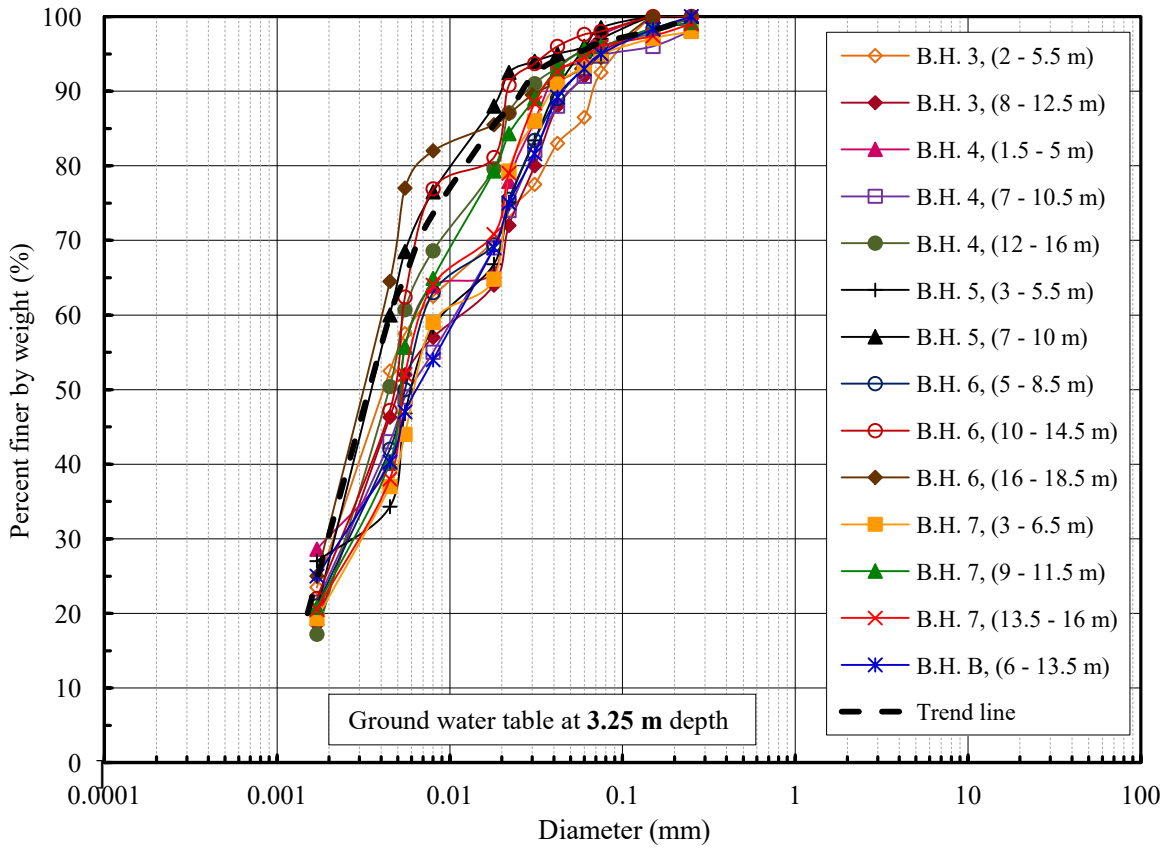

Figure 3.10: Particle size distribution curves at different depths for AL-Karama multi-storey commercial building site (site C).

3.3.9 Site investigation report of Sahat Al-Wathiq commercial building at Al-Rasafa district (site F)

The purpose of this investigation was to explore the subsoil conditions for commercial building site at Al-Rasafa district east of Baghdad to facilitate and evaluate the foundation design for the main structures. The field investigation consists of drilling (3) boreholes to depth of (25 m). Field and laboratory works were carried out by a group of geotechnical engineers from AL-Mustansiriya University. The main properties of the investigated soil are shown as follows:

- The soil classified as silty clay of high plasticity according to USCS.
- Atterberg limits: Liquid limit, LL ranged from (34 – 54 %), and plastic limit, PL ranged from (19 – 27 %).
- The maximum dry density, $\gamma_{dry\ max}$, ranged from (18.8 – 20.1 kN/m^3).
- Shear strength parameters: angle of friction, ϕ ranged from (0 – 2º), and soil cohesion, c ranged from (28 – 41 kPa).

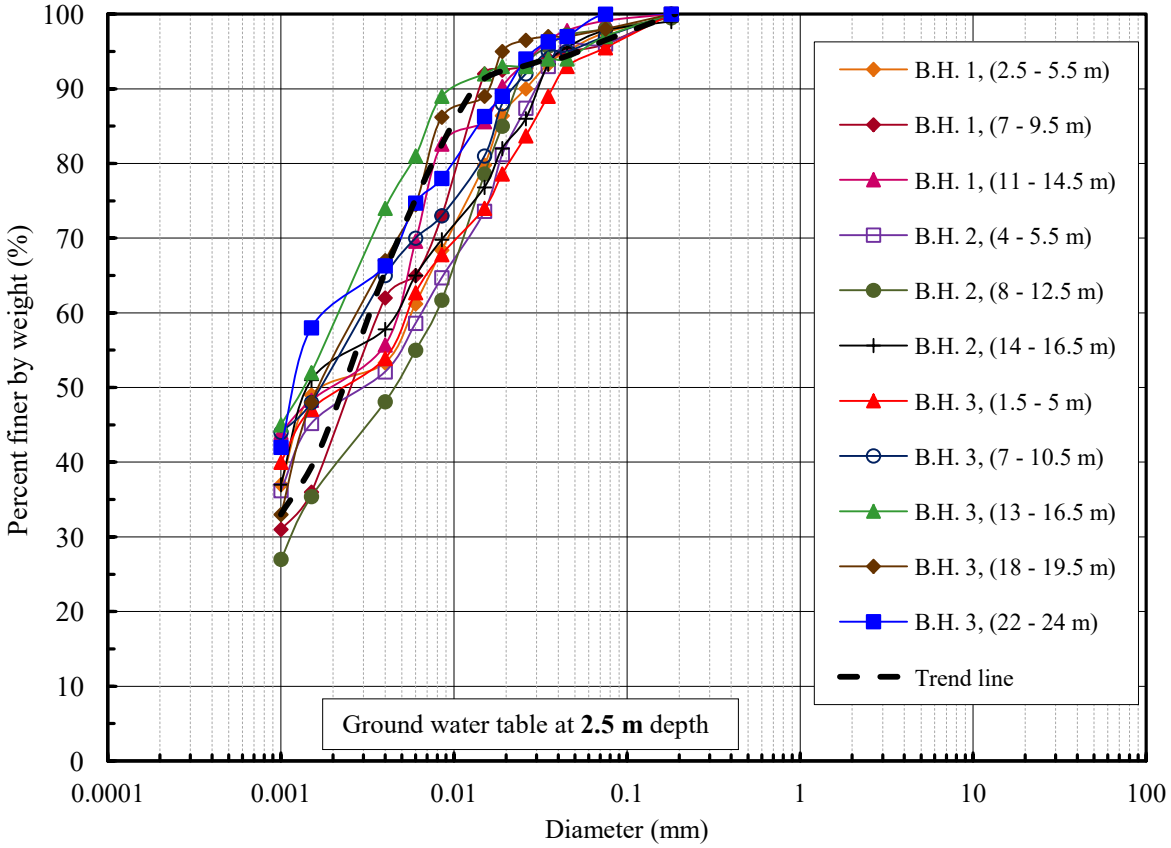

Figure 3.11: Particle size distribution curves at different depths for Sahat Al-Wathiq commercial building site (site F).

3.3.10 Site investigation report of Al-Madaen water treatment plant at Al-Rasafa district (site J)

The purpose of this investigation was to explore the subsoil conditions for Al-Madaen water treatment plant site located at south east of Baghdad to facilitate and evaluate the foundation design for the main structures. Generally, the subsurface condition of the area explored by drilling of (2) boreholes by a group of geotechnical engineers from University of Technology is seemed to consist of the following major strata: The first layer is medium dense silty sand. This layer extends to a depth of about (4 – 5 m). This layer is followed by a dense silty sand layer extending to the end of boring at (40 m) depth. The main characteristics of the investigated soil are listed below:

- The soil classified as silty sand (SM) according to USCS.
- Atterberg limits: Liquid limit, LL ranged from (22 – 27 %), and plastic limit, PL ranged from (18 – 22 %).
- The maximum dry density, $\gamma_{dry\ max}$, ranged from (18.1 – 19.9 kN/m^3).
- Shear strength parameters: angle of friction, ϕ ranged from (30 – 36º), and soil cohesion, c ranged from (0 – 2 kPa).

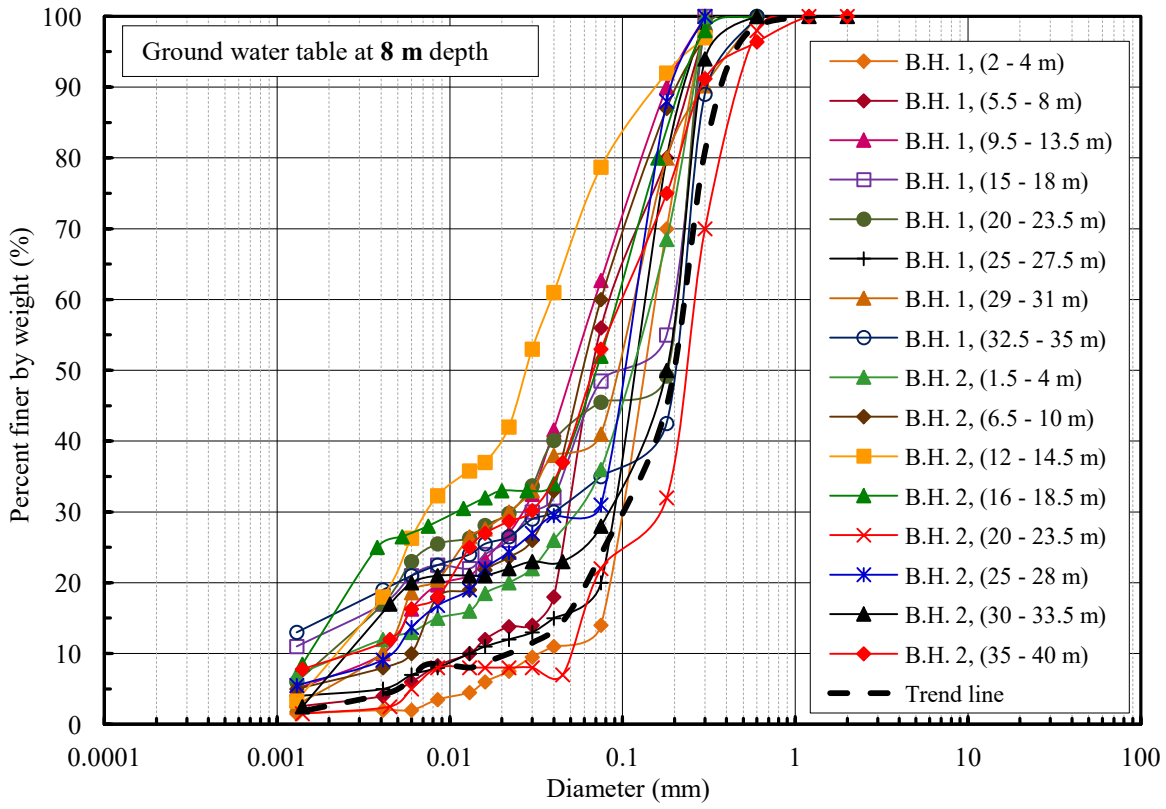

Figure 3.12: Particle size distribution curves at different depths for Al-Madaen water treatment plant site (site J).

3.3.11 Site investigation report of multi-story commercial building at Al-Karkh district (site L)

The aim of this investigation was to explore the subsoil conditions for commercial building site at Hay Al-Risalah south west of Baghdad to facilitate and evaluate the foundation design for the main structures. Laboratory soil testing was carried out on soil samples taken from boreholes at the site location in order to categorize soils according to their probable engineering behavior. Field and laboratory works were carried out by a group of geotechnical engineers from University of Technology. The geotechnical properties of the soil are shown as follows:

- The soil classified as clayey silt (SC) according to USCS.
- Atterberg limits: Liquid limit, LL ranged from (43 – 55 %), and plastic limit, PL ranged from (23 – 26 %).
- The maximum dry density, $\gamma_{dry\ max}$, ranged from (16.0 – 17.4 kN/m^3).
- Shear strength parameters: angle of friction, ϕ ranged from (14 – 18º), and soil cohesion, c ranged from (24 – 29 kPa).

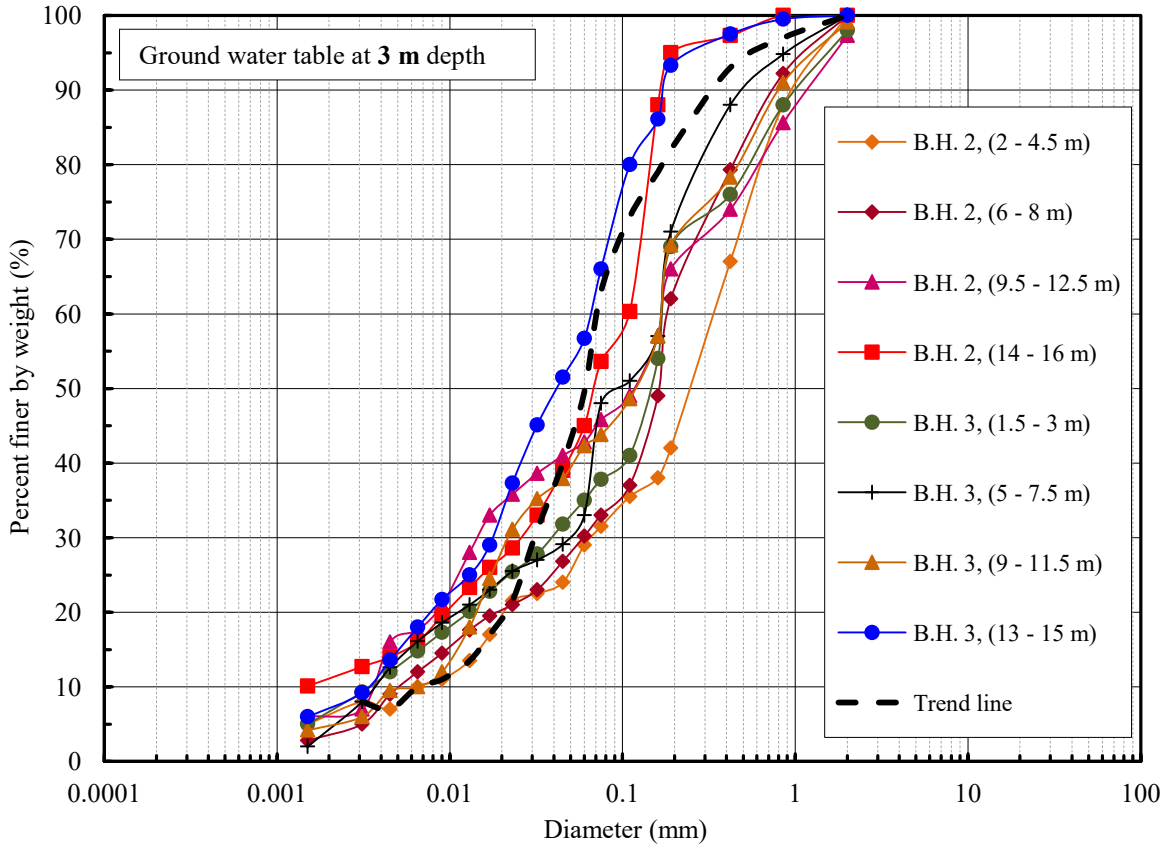

Figure 3.13: Particle size distribution curves at different depths for Hay Al-Risalah multi-story commercial building site (site L).

3.3.12 Site investigation report of multi-story residential building at Al-Karkh district (site E)

The purpose of this investigation was to explore the subsoil conditions of 5-storey residential building site at Abu Disheer south of Baghdad to facilitate and evaluate the foundation design for the main structures. The field investigation consists of drilling (4) boreholes to depth of (25 m). Field and laboratory works were carried out by ministry of construction and housing. The physical properties of the investigated soil are listed as follows:

- The soil classified as silty sand (SM) according to USCS.
- Atterberg limits: Liquid limit, LL ranged from (18 – 21 %), and plastic limit, PL ranged from (16 – 19 %).
- The maximum dry density, $\gamma_{dry\ max}$, ranged from (18.6 – 19.8 kN/m^3).

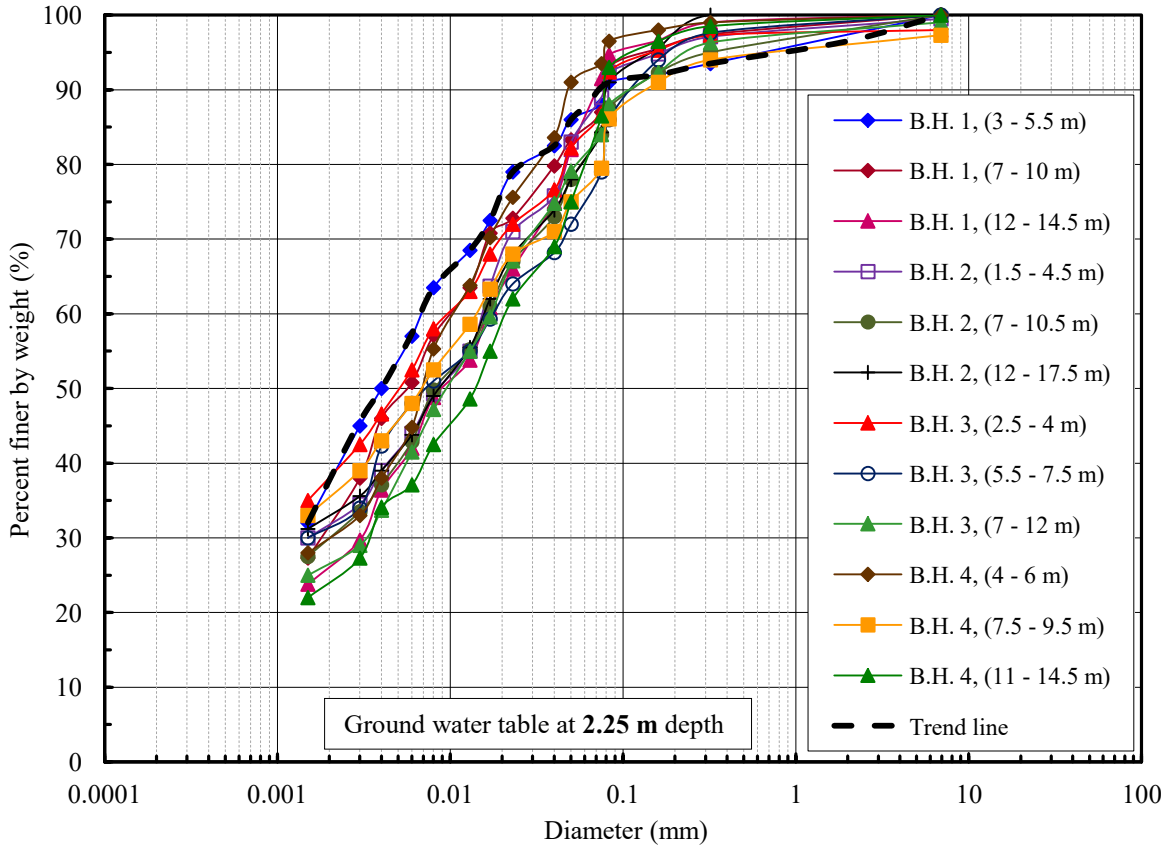

Figure 3.14: Particle size distribution curves at different depths of 5-storey residential building site at Abu Disheer south of Baghdad (site E).

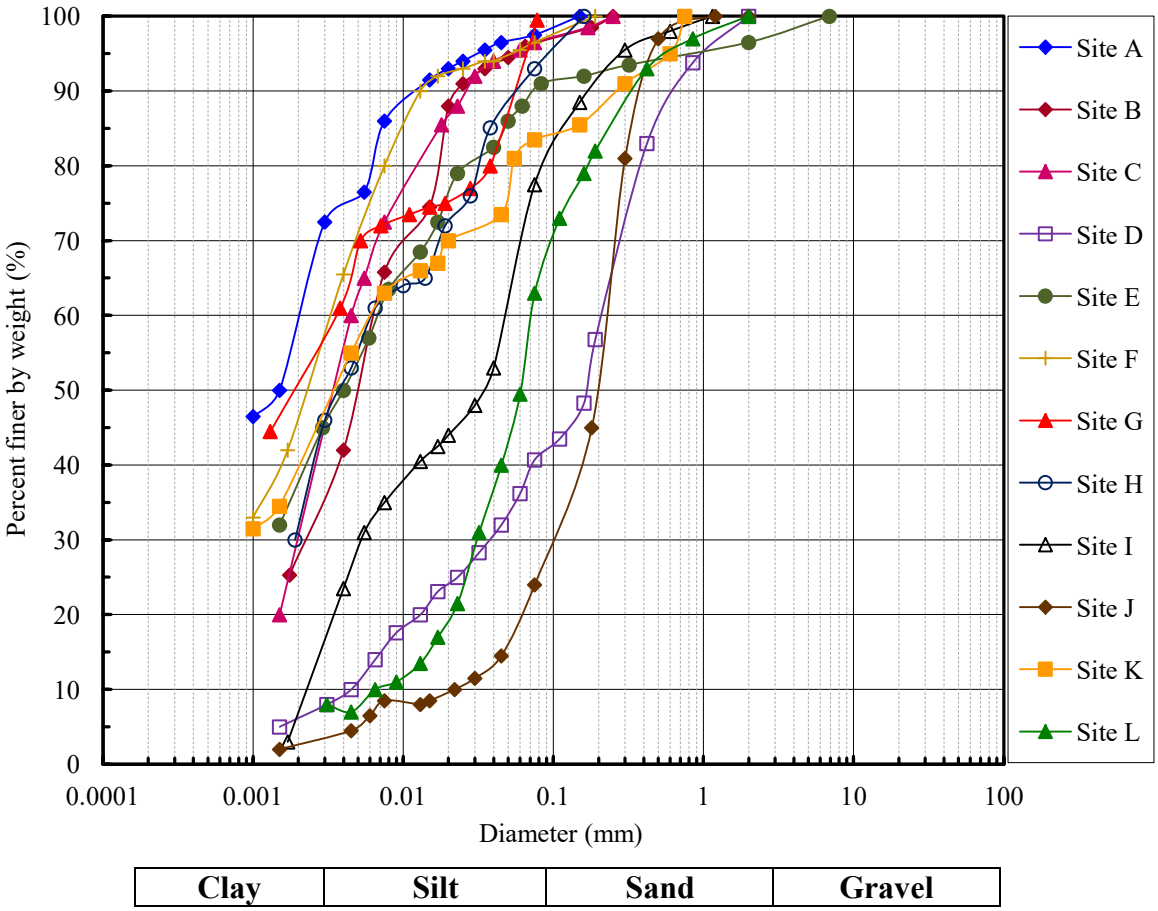

Figure 3.15: General trend of particle size distribution curves of soils at different sites

CHAPTER FOUR

EXPERIMENTAL EQUIPMENT DEVELOPMENT AND PILOT TESTS

4.1 General view

The primary objective of this study is to introduce a newly modified large-scale (300 mm x 300 mm) direct shear apparatus for measuring the evolution of matric suction during direct shear stages (equalisation, consolidation and shearing). This chapter also presents the basic properties of the artificial soil used within the experimental programme. The chapter then continues with the description of the experimental techniques and test procedures which was carried out by using the newly modified device including soil – soil and soil – concrete interface direct shear tests. As a second objective of these tests was to demonstrate the reliability and precision of the modified device in measuring the unsaturated soils. Finally, the chapter closes with concluding remarks.

4.2 Soil and interface materials

4.2.1 Geotechnical characterization of the used soil

The characterisation properties of the adopted and prepared soil were determined following the British Standard (BS 1377-2: 1990). These tests concern the particle size distribution (dry sieving), the Atterberg limits including the liquid limit and the plastic limit, and the specific gravity of the soil solids. The light and heavy efforts compaction tests were performed following the procedure in the British standard (BS 1377-4: 1990). The minimum and maximum index density tests were carried out by using American Society for Testing and Materials (ASTM D 4254-00 and ASTM D 4253-00)

respectively. The physical and the geotechnical properties of the adopted soil and the original soil are presented in Table 4-1.

Table 4-1: Basic properties of the adopted and original soils

Soil property	Adopted soil	Original soil
Specific gravity of soil solids, G_s	2.66	2.67
Particle size distribution		
Gravel (%)	0	0
Sand (%)	81	82
Silt (%)	17	15
Clay (%)	2	3
Atterberg Limits		
Liquid Limit, *LL* (%)	9.50	11.75
Plastic Limit, *PL* (%)	7.10	8.30
Plasticity Index, PI	2.4	3.45
Maximum void ratio, e_{max}	0.965	--------
Minimum void ratio, e_{min}	0.354	--------
Standard Proctor compaction		
Maximum dry unit weight, $\rho_{d\,max}$ (Mg/m^3)	1.922	--------
Optimum moisture content, (%)	9.5	--------
Modified Proctor compaction		
Maximum dry unit weight, $\rho_{d\,max}$ (Mg/m^3)	2.012	--------
Optimum moisture content, (%)	8.6	--------

The results of the particle size distribution are shown in Figure 4.1. To account for any heterogeneity in the prepared soil, the sieve analysis tests were carried out three times during the experimental programme and the average grain size distribution curve was produced. The artificial soil was created using sand having different grain sizes obtained from Geotechnical laboratory of the Institute of Infrastructure & Environment, Heriot-Watt University, United Kingdom and kaolin clay (supplied by Whitfield & Son Ltd., England). The adopted soil contains 0% gravel, 81% sand, 17% silt and 2% clay. The soil can be classified as silty sand and designated as SM according to the Unified Soil Classification System (ASTM D 2487-06). Furthermore, the sand percentage in the adopted soil contains 2%, 54% and 25% of coarse, medium and fine sand of particle size between 0.6-2 mm, 0.6-0.2 mm, and 0.06-0.2 mm, respectively. The average diameter of the tested soil (D_{50}) is 0.2 mm. The liquid limit (LL), the plastic limit (PL) and the plasticity index (PI) of the soil are 9.50%, 7.10% and 2.40%, respectively. It

should be noted that the soil investigation report of site J is only indicated some of the relevant physical properties of the tested soil (specific gravity, particle size distribution, Atterberg limits and shear strength parameters) as presented above in Table 4-1 and did not contains the analysis of the mineral compositions. In general, the main purpose of site investigation reports carried out in Iraq is to explore the subsoil conditions of the site to facilitate and evaluate the foundation design for the main structures.

The compaction test of the silty sand soil was carried out following the procedures outlined in the British Standard BS 1377 (1990). Figure 4.2 shows the obtained compaction curve along with the zero air void line of the studied material. The obtained maximum dry density, $\rho_{d\ max}$, was 1.922 Mg/m^3 with a corresponding optimum water content of 9.50%.

The specific gravity tests were performed by using small pycnometer method which is the most preferable method for soils containing clay, silt and sand size particles. The specific gravity, G_s, of the soil solids was found to be 2.66 at 22 °C.

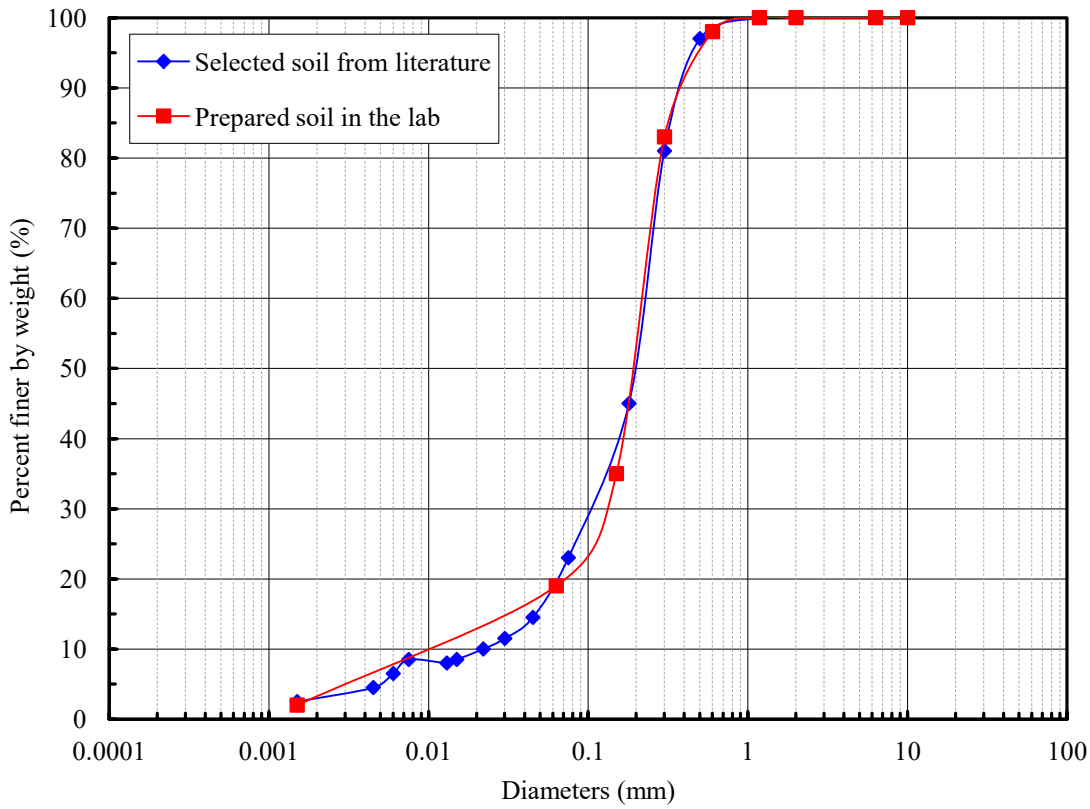

Figure 4.1: Particle size distribution of the selected and prepared soils.

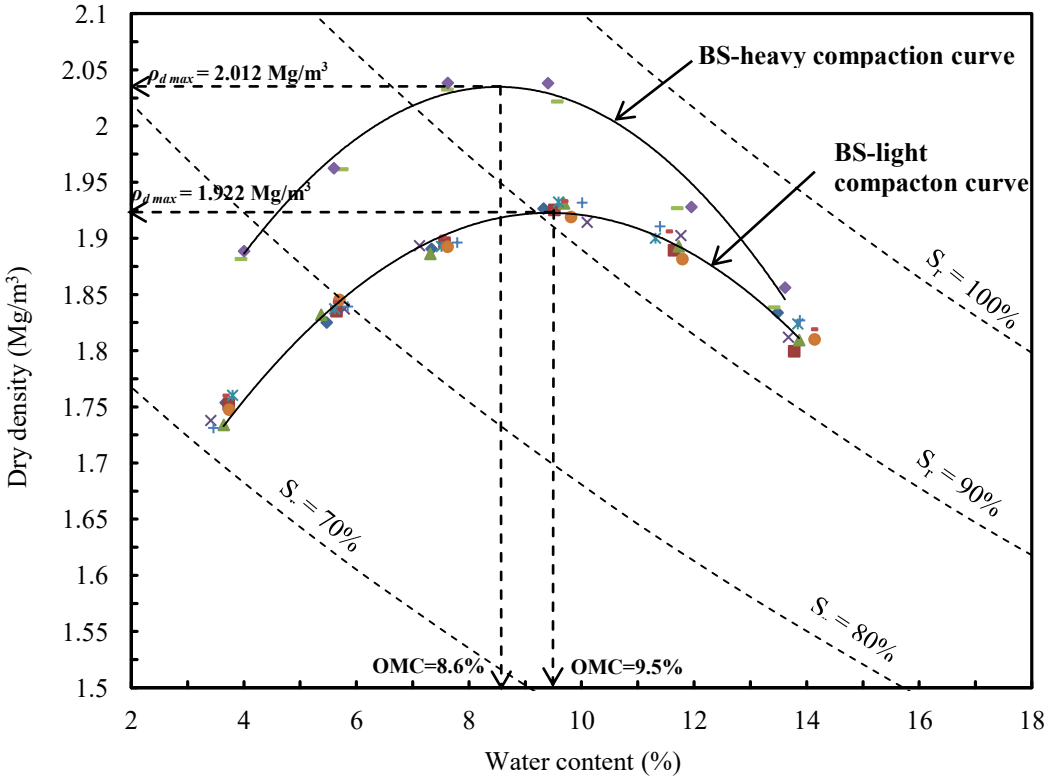

Figure 4.2: Compaction curves of the selected soil (BS-light and BS-heavy).

4.2.2 Concrete interface

Several authors (e.g. Briaud et al., 1982; Smith and Ray, 1986) show that the soil-pile interface (skin friction) plays a major part in supporting the applied load. One of the most important parameters which govern the soil-structure interface response is the structure surface roughness. As proposed by Uesugi and Kishida, 1986, the surface toughness is defined through normalised surface roughness, R_n as follows:

$$R_n = R_{max} / D_{50} \qquad \text{Eq. 4-1}$$

Where R_{max} is the maximum vertical distance between the highest and the lowest peaks of the structure asperities over a gage of a fixed length and D_{50} the soil mean particle size (Figure 4.3). A value of 0.0025 mm was used as a peak to valley height for smooth concrete interface by Di Donna (2014) and adopted in this study. The author prepared the smooth concrete interface in a manner similar to that used in this study. In addition,

the maximum peak to valley height, R_{max}, for rough concrete interface was 1.1 mm. Based on the particle size analysis of silty sand, R_n= 55 and 0.0125 was calculated for rough and smooth concrete interface, respectively.

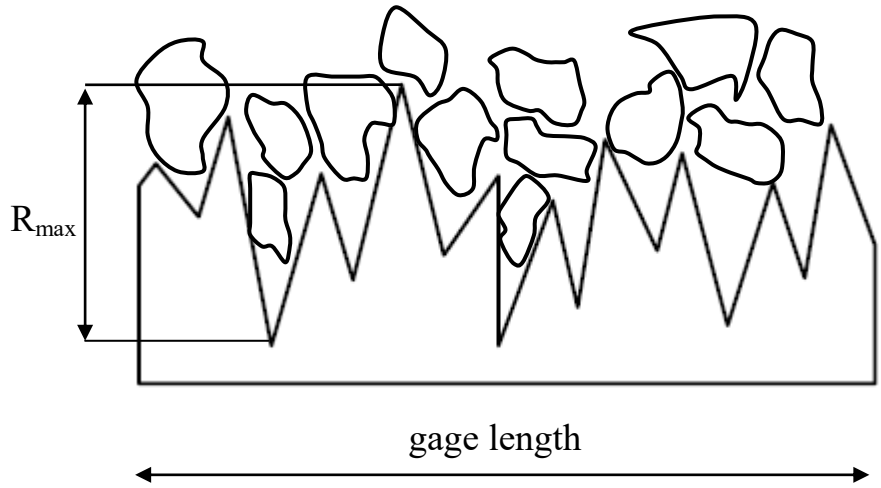

Figure 4.3: Example of soil-structure interface roughness (Uesugi and Kishida, 1986).

Two different square concrete counterfaces (299 mm x 299 mm x 70 mm) with different surface roughness were produced for this study as shown in Figure 4.4. The concrete pad was prepared in the concrete laboratory by mixing fine aggregate (i.e. sand), coarse aggregate, cement, and water according to the British Standards (BS 8110-1:1997). To produce one cubic meter of concrete to be used for foundation constructions, the British Standards propose the following values: (i) minimum quantity of cement 240 kg/m^3, (ii) maximum aggregate diameter of 20 mm, (iii) maximum water to cement ratio (w/c) 0.65, (iv) minimum compressive strength C25/30 and (v) maximum fine aggregate diameter of 300 μm. The amount of materials required to fill the mould was calculated before mixing and is summarized in Table 4-2. It should be noted that, the aim of this study is to investigate the influence of surface roughness of the concrete interface on the behaviour of the silty sand soil, whereas the characteristics of the material does not play significant role.

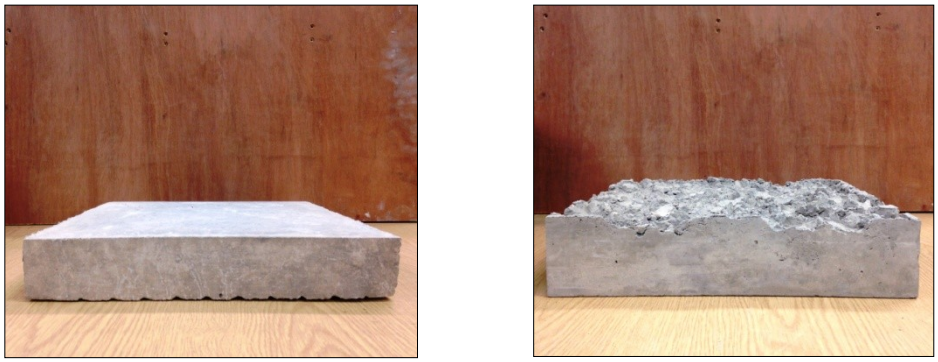

(a) **(b)**

Figure 4.4: Interfaces used in this study: **(a)** smooth; **(b)** rough.

In order to facilitate handling of the concrete pad, two anchor bolts of 10mm diameter and 40mm length were fixed inside the mould as shown in Figure 4.5. The concrete specimens were cured in water tank for 28 days at 23 °C ± 2. Uniaxial compressive strength tests were performed on 150mm cubes of concrete according to the British Standards (BS 1881: Part 116: 1983) before casting the concrete interfaces. The average compressive strength from three specimens was 34.2 MPa.

One concrete pad was prepared with a smooth surface by pouring the appropriate amount of concrete mixture inside the wooden mould. In parallel, a rough surface square concrete pad was also fabricated for investigating the interface behaviour. To do so, the sieve analysis firstly was carried out on the different diameters of the coarse aggregate which are available at the University site and the aggregate passing sieve 31.5 mm and retained on the 20 mm sieve was selected, as shown in Figure 4.5(a). After that, the aggregate was glued one by one using super glue on the surface of the square piece of the plywood and left for 24 hours for hardening. Then, the same procedure was followed as that of the smooth surface of the concrete pad (see Figure 4.5(b)).

Table 4-2: Quantity of materials for concrete mixture

Cement mass (g)	Fine aggregate mass (g)	Coarse aggregate mass (g)	Water mass (g)	Water/cement ratio (w/c)
1515	2500	5000	985	0.65

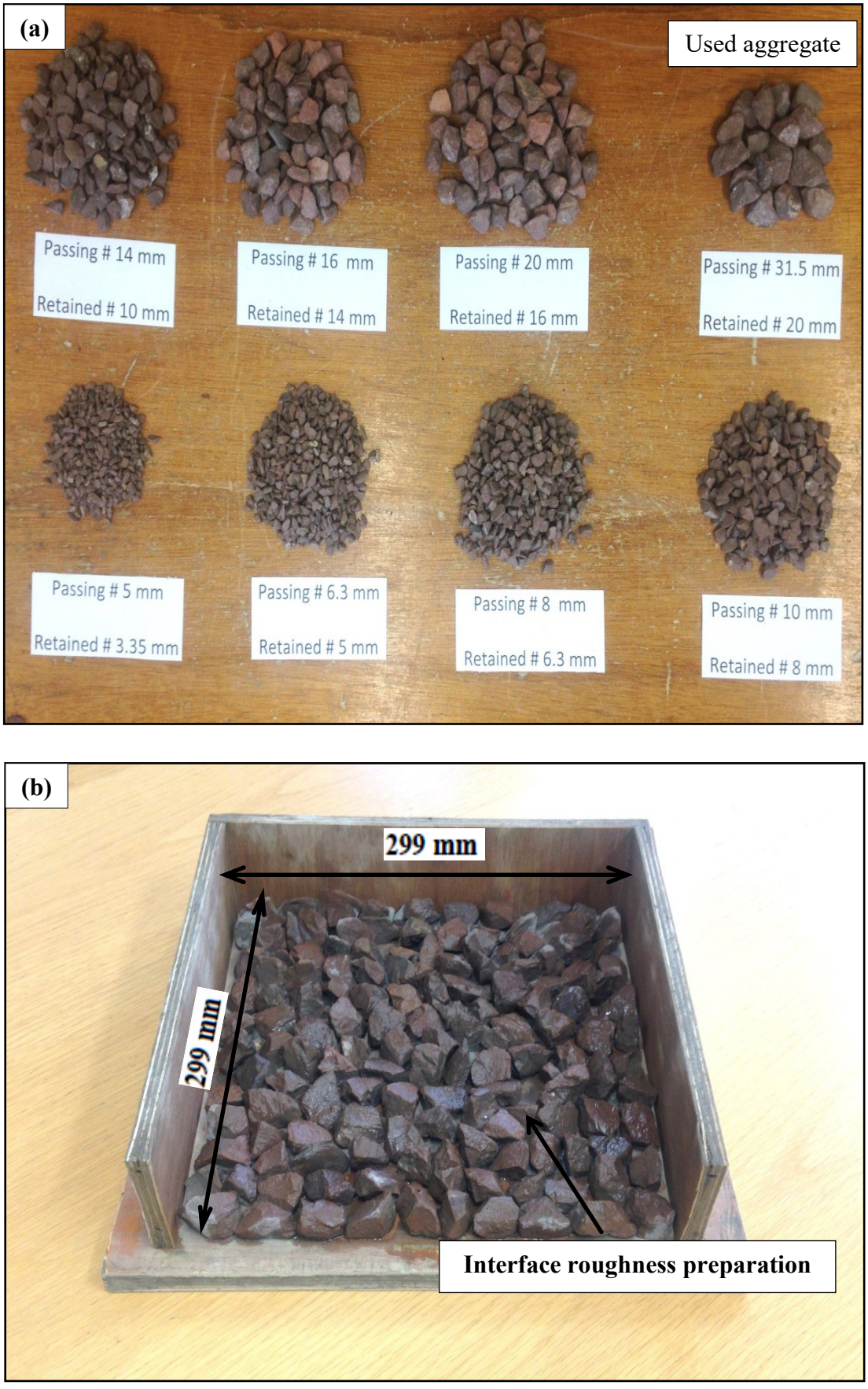

Figure 4.5: Concrete pad with rough interface: **(a)** particle size distribution; **(b)** rough surface preparation.

4.3 Direct shear tests

4.3.1 Small-scale direct shear sample preparation and apparatus

The dried soil (24 hours in 105 °C) was mixed with water at a target moisture content (ω = 8 ±1%) and then statically compacted into a mould with the same internal dimensions of the direct shear box at a target void ratio (e_i = 0.6 and 1.0). In fact, this value of water content was selected in order to facilitate the compaction process and hence improve the workability of the soil samples especially when a relatively low void ratio samples had to be tested. The soil was compacted into four layers of 5mm thickness each inside the mould. To ensure a good contact between the layers, the surface of each layer was scratched by using 1 mm diameter stainless steel wire before compacting the following layer. The target water content was checked by oven drying method (BS 1377-2:1990). The California Bearing Ratio (CBR) frame machine was used to apply the static load with a constant displacement rate of 1.27 mm/min. A schematic drawing showing the components of the compaction mould and their assembling is shown in Figure 4.6. The schematic view of the small-scale direct shear box is shown in Figure 4.7. It should be noted that the drawings presented in Figures 4.6 and 4.7 are not to scale.

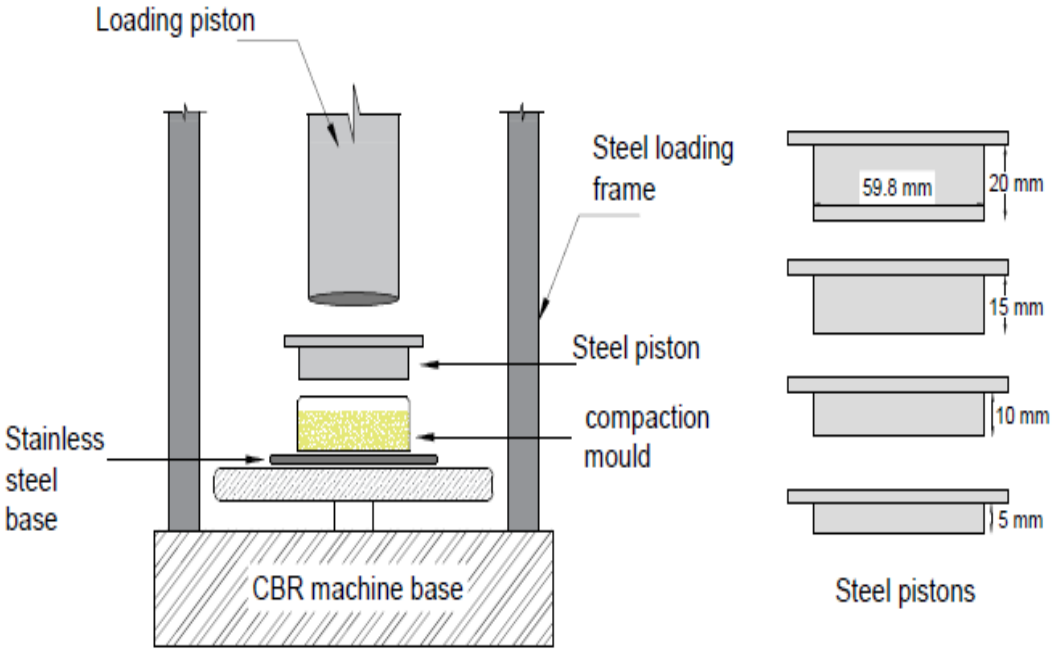

Figure 4.6: Schematic drawings of static compaction mould for small-scale direct shear test specimens.

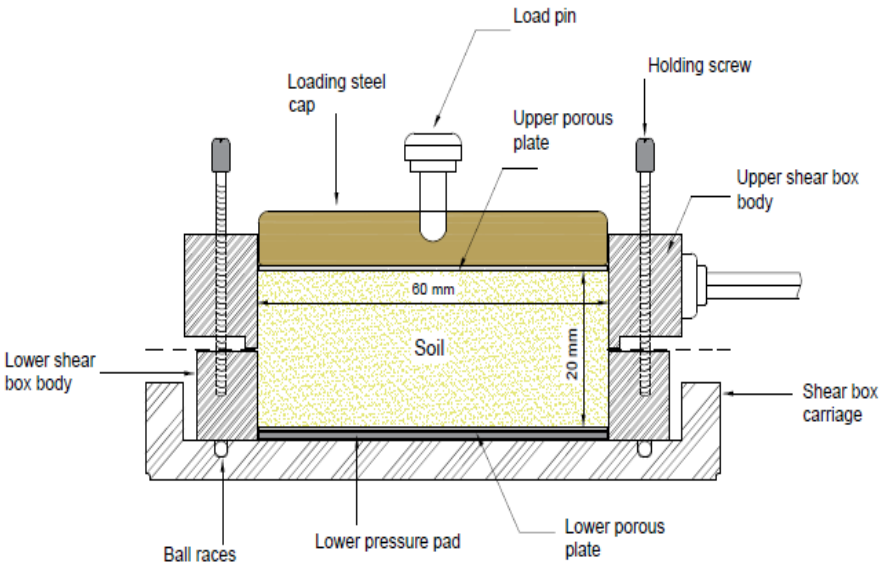

Figure 4.7: Schematic drawing of the soil-soil direct shear cell (small-scale apparatus).

4.3.2 Large-scale direct shear sample preparation and apparatus

Soil-soil and soil-concrete large-scale direct shear tests were described in this section. The same water content and void ratios were targeted ($\omega = 8 \pm 1\%$ and $e_i = 0.6$ and 1.0) and obtained following the same procedure as explained in 4.3.1. For soil-soil tests, the soil specimens were directly compacted inside the shear box into four layers (35mm thickness each) by dynamic compaction. The required mass of wet soil for a particular layer was calculated, then placed and compacted. The compaction is done by dropping 3.2 kg rammer having a square section of 285 x 285 mm from a constant height (45 cm) until achieve the required void ratio as shown in Figure 4.8.

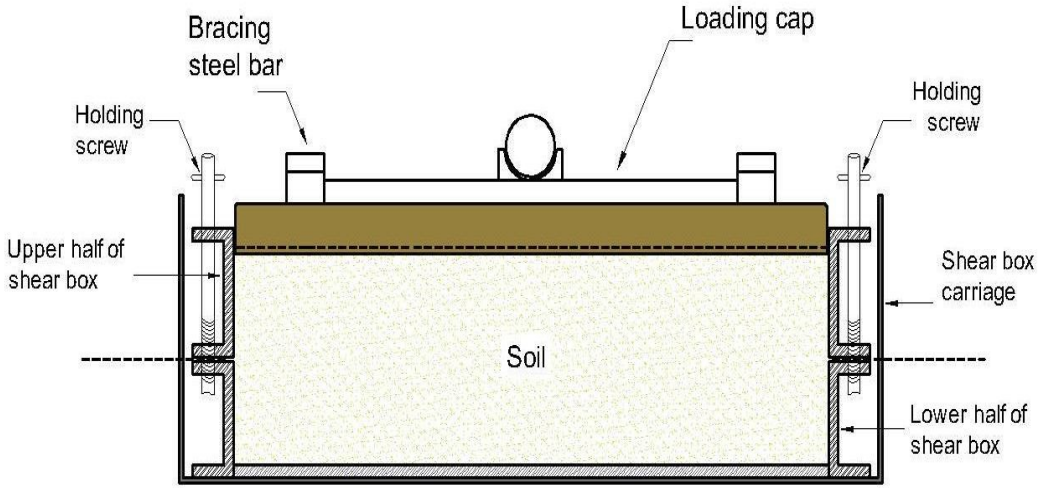

Figure 4.8: Schematic diagram of the large-scale direct shear box for testing soil sample (not to scale).

In this study, for soil-interface specimens, the concrete counterface was placed in the lower half of the shear box instead of soil. The soil was compacted over a concrete pad into two layers having a thickness of 35 mm each. After samples were ready, the loading steel pad was placed over the specimen. Figures 4.9(a) and (b) show the schematic view of the direct shear box used for smooth and rough interface testing, respectively. Similar to that, several researchers (e.g. Sharma et al., 2007; Hamid and Miller, 2009; Hossain and Yin, 2013; Borana et al., 2015; Liu and Vanapalli, 2018) have been used the procedure adopted in this study to prepare the specimens for soil-structure interface direct shear test.

Hamid and Miller, 2009 have been performed the interface specimens by compacting soil mixture over the steel counterface to the required density by using a tamping rod in two layers. Yin and Borana, 2013 have been made the interface specimens by placing the square steel counterface in the lower half of the shear box. Following, the pre-treated soil compacted at optimum water content and maximum dry density over the interface into two layers (each of 10 mm thickness). After compacting the first layer of soil, its top layer was scratched to ensure proper bonding between two layers. Liu and Vanapalli (2018) statically compacted the expansive soil of different densities in the upper half of the shear box into two layers over prefabricated steel block with the rough surface.

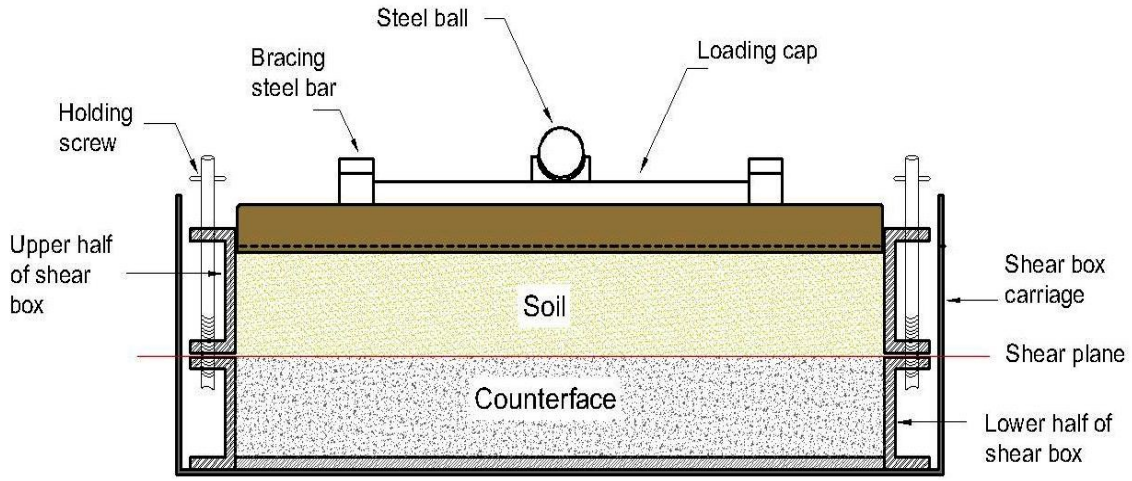

(a)

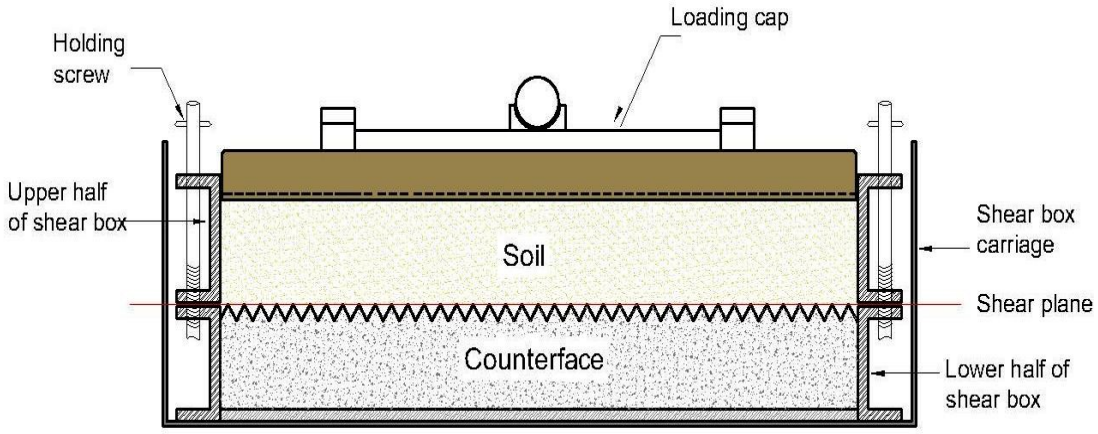

(b)

Figure 4.9: Schematic diagram of the large-scale direct shear box for testing: **(a)** soil - smooth interface and **(b)** soil - rough interface (not to scale).

4.4 Testing procedures

4.4.1 Direct shear tests at saturated condition

The direct shear test at saturated condition comprises of three stages; saturation, consolidation and shearing. Firstly, the soil specimen placed inside the shear box and ample amount of de-aired water was added in the direct shear carriage to the marked level. The soil specimen in the direct shear cell was allowed to soak water for 24 hours under a nominal surcharge load (loading steel pad). It should be noted that, the time required for soaking was adopted according to different pilot tests carried out before running the real test to ensure that the fully saturated condition was fulfilled. Results of degree of saturation corresponding to different soaking period are listed Table 4-3. Furthermore, the degree of saturation of the compacted specimen was investigated after saturation and found that more than 98.6% saturation was achieved by soaking. The height of the specimen before and after saturation was monitored to indicate any change in the specimen height at the end of saturation stage.

After reaching saturation, it is to be consolidated under the pre-decided vertical load and this represents the second stage of test. Consolidation of the specimen was noticed to be achieved when no further increase in the vertical displacement was noticed (approximately steady state). Six hours of consolidation was found to be satisfactory for all tested specimens under saturated condition. After attaining the consolidation, the soil specimen was sheared under constant vertical load and constant rate of shear displacement.

Table 4-3: Values of degree of saturation corresponding to different soaking period of two shear box sizes (60 x 60 and 300 x 300 mm^2)

Shear box dimensions, L (mm) x W (mm)	Initial void ratio, e_o	Time, (hrs)	Degree of saturation, Sr, (%)
Small – scale (60 x 60)	0.6	0.3	73.31
		1.0	88.48
		2.0	95.11
		3.0	99.26
		24	99.88
	1.0*	0.3	81.57
		1.0	95.70
		2.0	98.08
		3.0	99.57
		24	99.73
Large – scale (300 x 300)	0.6	0.3	57.14
		1.0	71.67
		2.0	88.11
		3.0	95.46
		24	99.33
	1.0*	0.3	73.60
		1.0	91.03
		2.0	98.60
		3.0	99.05
		24	99.80

* Collapse behaviour noticed during saturation.

Before starting the shearing stage, it should be mentioned that the rate of shear displacement has a significant impact while testing the specimens. Previous studies (e.g. Al-Mhaidib, 2006; Ahmed, 2013) show that rapid rate of shear displacement is associated with positive pore water pressure generation for loose soils. In contrast, dense soils might exhibit negative pore water pressure generation following rapid shearing. Consequently, rapid shear of a saturated soil may cause a decrease in the strength of a loose soil or an increase in the strength of a dense soil. Thus, the adequate rate of shearing displacement was very important to decide before starting the shearing process. Several pilot experiments were carried out to select the appropriate rate of shearing for this study. The specimens were compacted at e_i = 0.6 and tested under 200 kPa applied vertical stress. At saturated conditions, the specimens were then sheared at different rates of shearing (0.04, 0.06, 0.08, 0.10, 0.15 and 0.20 mm/min) as shown in Figures 4.10(a), (b), (c), (d), (e) and (f).

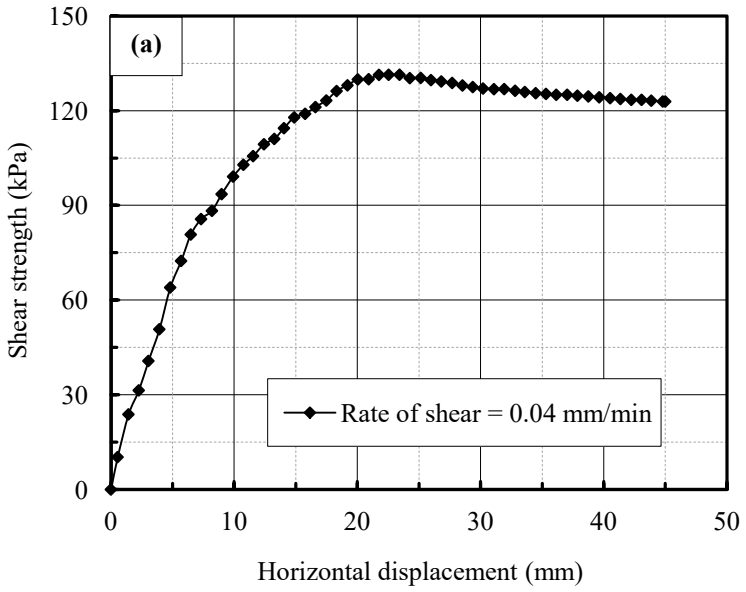
(a)
Shear strength (kPa)
Horizontal displacement (mm)
Rate of shear = 0.04 mm/min
0
30
60
90
120
150
0
10
20
30
40
50

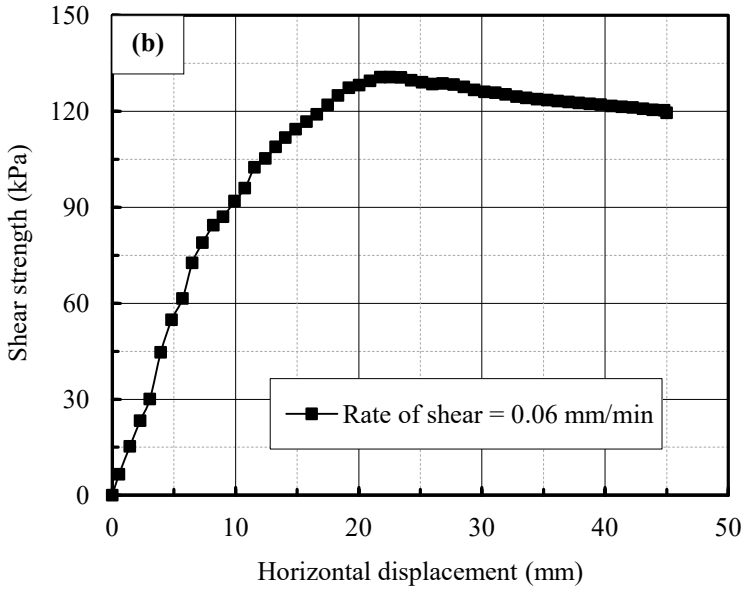
(b)
Shear strength (kPa)
Horizontal displacement (mm)
Rate of shear = 0.06 mm/min
0
30
60
90
120
150
0
10
20
30
40
50

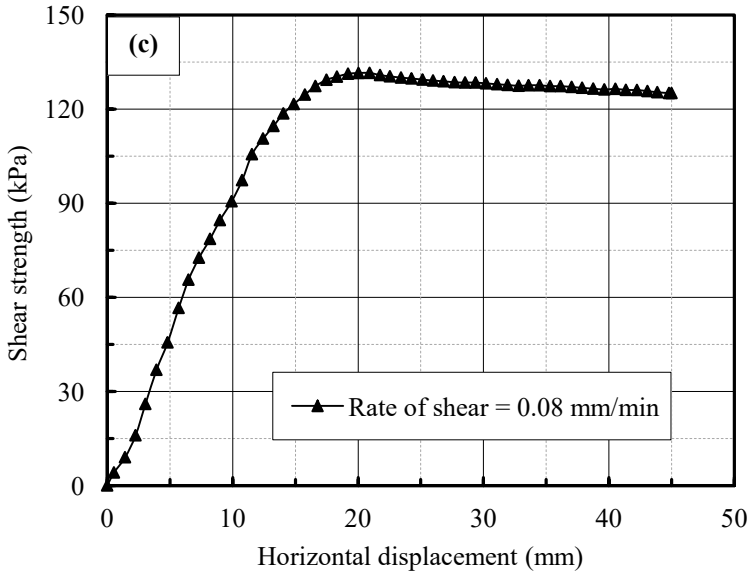
(c)
Shear strength (kPa)
Horizontal displacement (mm)
Rate of shear = 0.08 mm/min
0
30
60
90
120
150
0
10
20
30
40
50

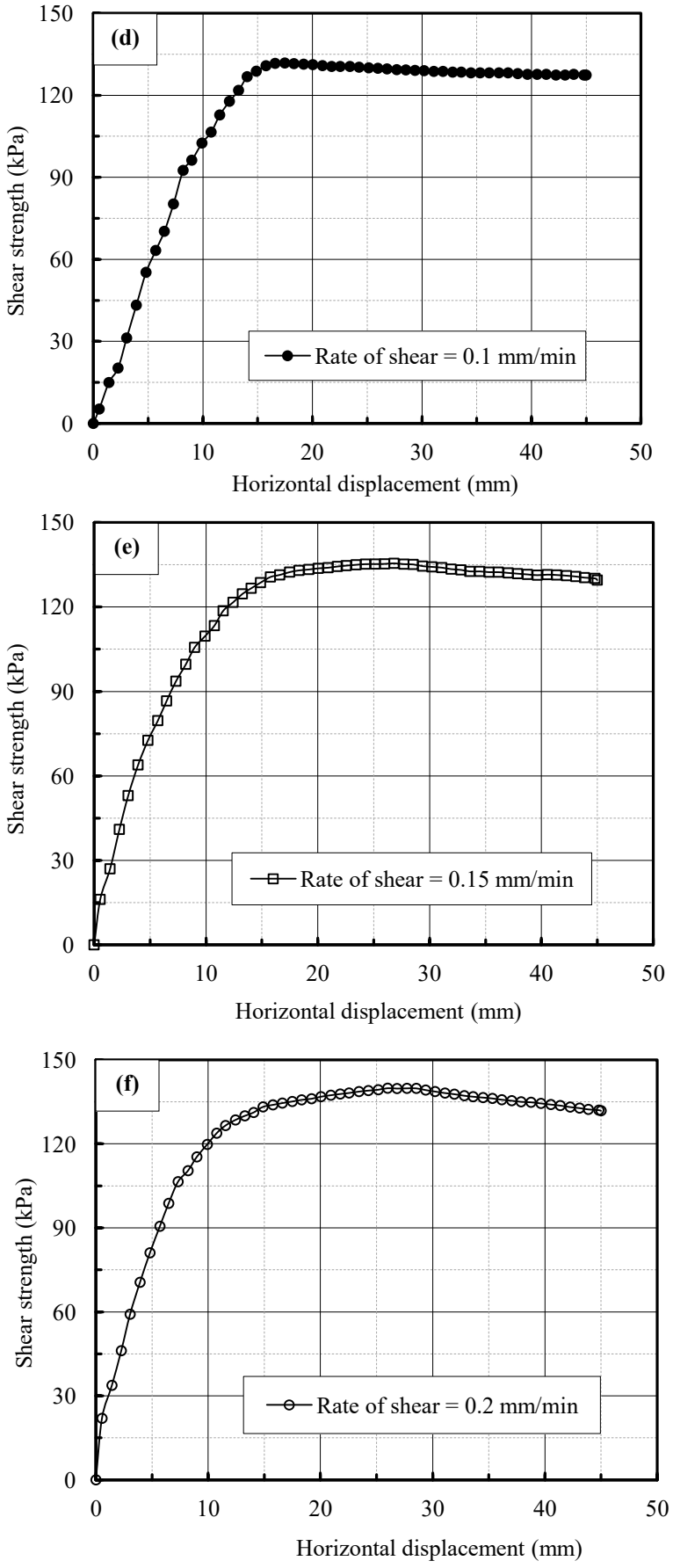

Figure 4.10: Shear strength versus horizontal displacement for saturated silty sand at e_i = 0.6 sheared under 200 kPa vertical stress at different shear rates (mm/min) of: **(a)** 0.04 , **(b)** 0.06 , **(c)** 0.08 , **(d)** 0.1 , **(e)** 0.15 , and **(f)** 0.20.

Figure 4.11 shows the influence of rate of shear on the peak shear strength of the tested material. It can be observed that the peak shear strength remains approximately constant until the rate of shearing equal to 0.1 mm/min. Based on these experimental results, a rate of 0.05 mm/min was adopted for all saturated soil and interfaces direct shear tests.

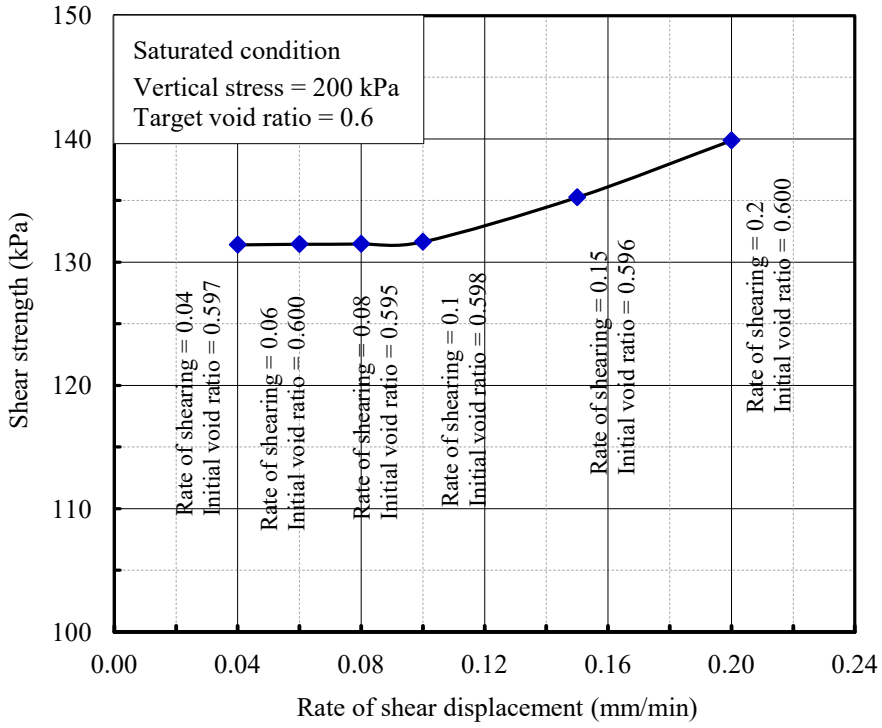

Figure 4.11: Results of shear rate tests on saturated silty sand soil.

During the shearing stage, the values of shear force, the horizontal displacement, and the vertical displacement were measured and recorded automatically in a computer at regular intervals of one minute. The shearing process continues until the full travel of shear box was achieved (10 mm of small-scale and 45 mm of large-scale direct shear apparatus). The above procedure presented in this section was adapted to performed soil-soil and soil-concrete interface tests under saturated condition using two different shear box sizes used in this study. It should be mentioned that the pore water pressure does not measured during shearing stage.

4.4.2 Direct shear tests at constant water content condition

The shear strength of unsaturated soils has normally been performed by either triaxial tests or direct shear tests. The majority of shear tests have been carried out using the

triaxial apparatus (Ho and Fredlund, 1982). However, the time required for triaxial testing of unsaturated soils for performing one experiment is quite long due to the length of the drainage path in comparison with the direct shear test. In addition, during triaxial shearing, an increase in the deviator stress results in an increase in not only shear stress but also mean net stress, and the latter tends to cause the contraction of the specimens. Consequently, the effect of suction on the dilation tendency may be masked by the contraction (Zhen and Ng, 2006). For these reasons, a number of experimental studies have been performed using direct shear apparatus (Escario, 1980; Escario and Saez, 1986; Gan, 1986; Gan et al., 1988; Gachet et al., 2003; Hamid, 2005; Hossain, 2010).

The experimental procedure of soil-soil and soil-concrete tests consists of three stages: matric suction stabilisation, consolidation under predetermined vertical load and shearing at a constant vertical load and constant rate of shear displacement. During suction stabilisation stage, the specimen was allowed to achieve soil suction equilibrium. Equilibration of the specimen was noticed to be achieved when the measured suction was approximately constant (≤ 1% changes of the recorded suction). It should be noted that the time required for suction equilibration was adopted according to different pilot tests carried out before running the real test as shown in Figures 4.12 (a), (b) and (c). Nine days of matric suction stabilisation were found to be satisfactory for all tested specimens. The evolution of matric suction with time during suction stabilisation stage of soil and interfaces (smooth and rough) of e_i = 0.6 and 1.0 specimens is presented in Figure A, Appendix A.

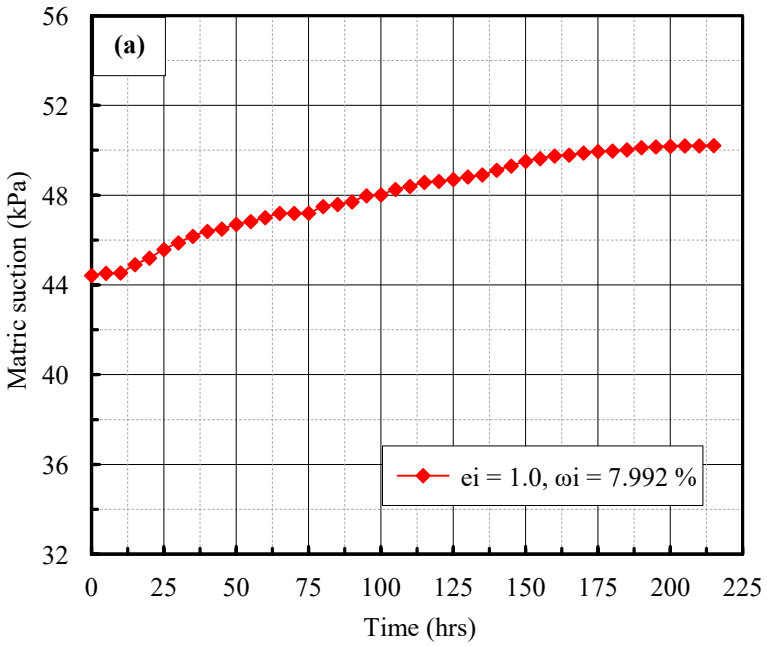

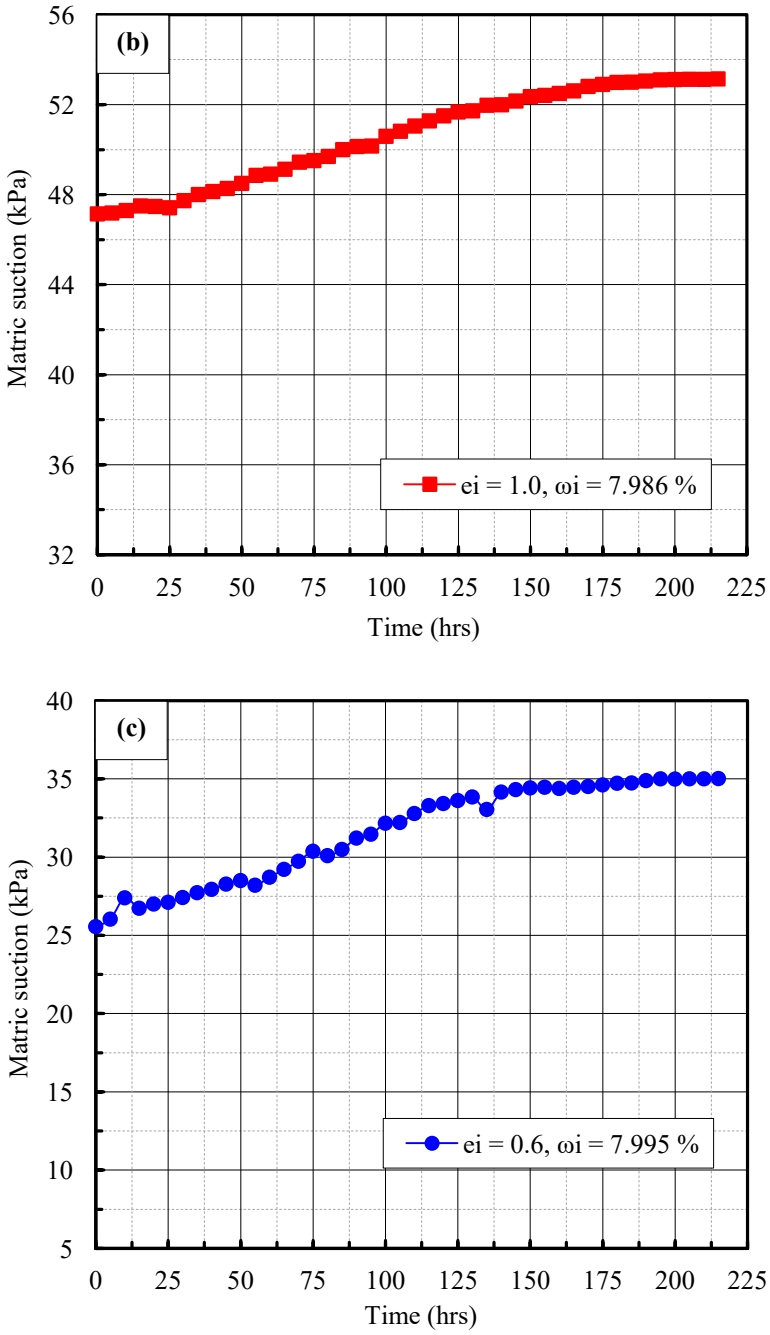

Figure 4.12: Variation of matric with time during stabilisation stage of soil samples: **(a)** e_i = 1.0, ω_i = 7.992 %, **(b)** e_i = 1.0, ω_i = 7.986 % and **(c)** e_i = 0.6, ω_i = 7.995 %.

It is noteworthy to mention here that the suction stabilisation stage was performed under nominal surcharge load (i.e. weight of loading pad only), and the values of stress level were used in this figure to differentiate the plots.

After achieving equilibration, the specimen was allowed to consolidate under the pre-decided vertical load and this represents the second stage of test. Consolidation of the

specimen was noticed to be achieved when no further increase in the vertical displacement was observed. Ten hours of consolidation were found to be satisfactory for all tested specimens. The specimen was left for a further two hours to ensure that there is no further increase in the vertical displacement. The changes in matric suction associated with loading with respect to time (i.e. during 12 hours) were measured and recorded. Due to limitation of required time, matric suction was not re-equilibrated prior to shearing. After consolidation, the specimen was subjected to the shearing force at constant vertical load and rate of shear displacement. During shearing, the vertical and horizontal displacements as well as the shear force were recorded.

Table 4-4: Shearing rate used by various researchers for testing specimens under unsaturated condition

Reference	Physical properties	Soil composition	Type of soil	Shearing rate (mm/min)
Gan, 1986	LL = 35.5 % PL = 16.8 % Pl = 18.7 %	Sand = 28 % Silt = 42.8 % Clay = 30 %	Glacial till	0.01
Escario and Saez (1986)	LL = 71 % PI = 35 %	--------	Madrid clay	0.0017
Escario and Saez (1986) and Gan and Fredlund (1986)	--------	--------	Two types of soil; clay and sand	0.0016 – 0.01
Gan and Fredlund (1988)	LL = 35.5 % PL = 16.8 % PI = 18.7 %	Sand = 28% Silt = 42.8% Clay = 30%	Glacial till	0.0132
Gan and Fredlund (1994)	LL = 32.8 % PL = 22.7 % PI = 10.1 %	Gravel = 5.8% Sand = 44.1% Silt = 36.8% Clay = 13.3%	Completely Decomposed Granite	0.005
Han, (1997)	LL = 47 % PL = 29 % PI = 18 %	Sand = 49 % Silt = 25 % Clay = 26 %	Residual soil	0.004
Hamid, (2005)	LL = 28 % PI = 8 %	Fines = 73 %	Minco silt	0.005
Hossain, (2010)	LL = 22.7 % PL = 32.8 % PI = 10.1 %	Gravel = 5.8% Sand = 44.1% Silt = 36.8% Clay = 13.3%	Completely Decomposed Granite	0.004
Borana et al., (2013)	LL = 31 % PL = 21 % PI = 10 %	Sand = 50 % Silt = 38 % Clay = 12 %	Completely Decomposed Granite	0.004

The calibration was done to check the accuracy of the measurements of the direct shear components (vertical and horizontal LVDTs and load cell) as given in Appendix C. Similar to saturated soil tests, the rate of shearing is an important factor while testing soil at constant water content condition. Table 4-4 presents a summary of the unsaturated direct shear experiments performed by various researchers along with the values of shearing rate used in these studies.

Considering the values presented in Table 4-4, in the present study the specimens was sheared with a constant shearing rate of 0.01 mm/min for both soil and interfaces until the horizontal displacement reached to 45 mm. Approximately less than 1% change in water content occurred during shearing, which indicates that shearing rate was reasonably slow. Once the shearing stage was completed, the shear box cell was dismantled and the specimen was extruded for the determination of water content by drying method (BS 1377-2:1990). The initial and final water content of the soil and interfaces specimens (smooth and rough) under constant water content condition are summarised in Table 4-5. It should be noted that, the soil suction was monitored and recorded throughout the testing stages (i.e. suction stabilisation, consolidation and shearing).

Table 4-5: Values of initial water content, ω_i and at the end of shearing stage, ω_f for soil and interfaces (smooth and rough) under constant water content condition

Type of test	Target void ratio	Vertical stress (kPa)	Initial water content, ω_i (%)	Final water content at end of shearing stage, ω_f (%)
Soil – soil	0.6	100	8.004	7.988
			7.993	7.960
		200	7.995	7.941
			8.006	7.927
		400	7.997	7.955
			8.000	7.941
	1.0	100	7.996	7.967
			7.991	7.938
		200	8.003	7.946
			7.994	7.966
		400	8.008	7.962
			8.003	7.943
Soil – smooth interface	0.6	100	7.997	7.943
			8.005	7.931
		200	8.002	7.959
			7.997	7.962
		400	7.998	7.938
			7.991	7.957
	1.0	100	8.000	7.956
			7.998	7.925
		200	8.003	7.957
			7.994	7.941
		400	7.997	7.937
			8.002	7.953
Soil – rough interface	0.6	100	7.995	7.968
			7.993	7.933
		200	8.003	7.956
			7.991	7.953
		400	7.996	7.965
			8.006	7.934
	1.0	100	7.991	7.939
			7.998	7.960
		200	7.995	7.954
			7.994	7.948
		400	8.003	7.952
			8.008	7.936

4.4.3 Modifications of conventional direct shear apparatus for constant water content tests

The main obstacle to perform direct shear test at a constant water content condition is to prevent the evaporation of water from the soil specimen during the testing stages. To do so, the gaps between the lower half of the shear box and the base of carriage were sealed with waterproof silicon sealant. The surfaces of contact between the two halves of shear box were filled with a thick layer of grease. A plenty of grease was smeared on the external boundary of the contact surface between the two halves to prevent any evaporation of water during the testing process. In addition, the space between the upper part of the shear box and the loading steel cap was firstly filled with a light layer of low density grease then was covered by the jacket of latex membrane, which was sealed to the edges of the loading cap and the upper half of the shear box using super glue. The grease layer did not affect the vertical displacement measurements. It should be noted that the length of latex membrane is adequate for free movement of loading cap during consolidation and shearing stages.

After that, the two suction probes were inserted into the loading steel cap and fixed well to the steel tube by screws. The upper space between the suction probe and the steel tube was sealed with the waterproof silicon sealant. To check the efficiency of the anti-evaporation system, the soil suction of the two specimens were measured with the suction probes.

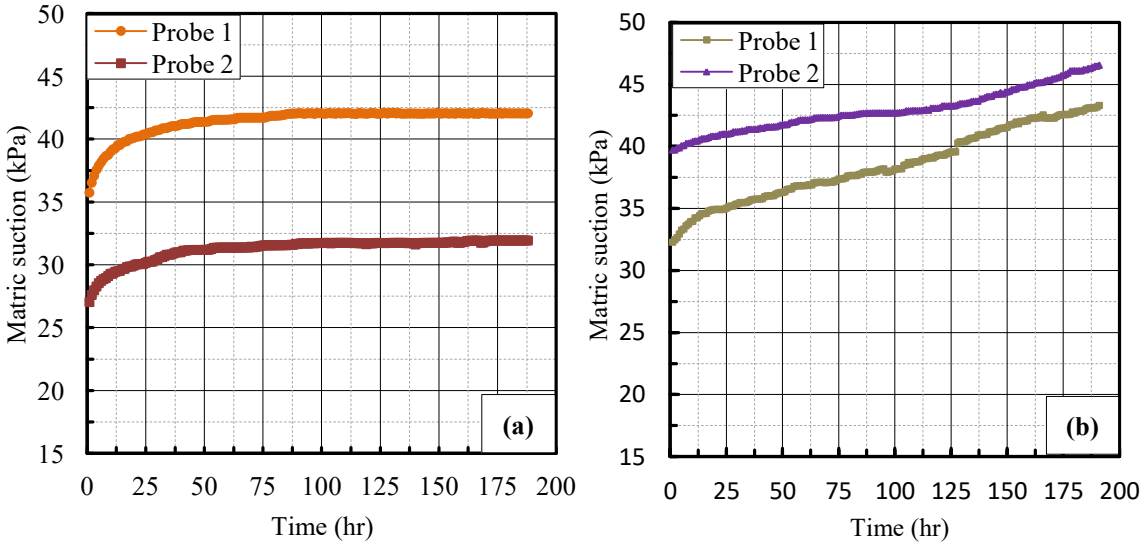

Figure 4.13: Evolution of the measured matric suction: **(a)** isolated with anti-evaporation system, and **(b)** non-airtight tested specimen.

One test was performed when the soil specimen was isolated by using the proposed anti-evaporation system as shown in Figure 4.13(a). It can be noted that the soil suction recorded by the suction probe remains approximately constant. In contrast, an increase in the matric suction with time was observed for the non-airtight tested specimen, as shown in Figure 4.13(b).

One of the primary aims of this study is to measure the evolution of matric suction during direct shear tests. To achieve this aim, a new loading steel cap of large-scale direct shear apparatus for testing soil-soil and soil-concrete specimens has been manufactured. The design and construction details of the new loading steel cap have been supplied to the technical staff in the mechanical workshop at Heriot-Watt University where it's manufactured (Figure 4.14). The loading cap has a thickness of 20 mm and an external dimension of 297 mm x 297 mm which is consistent with the conventional one used for saturated soil testing. The bottom face of the loading cap has seventeen machined symmetrical longitudinal grooves. Each groove has a dimension of 10 mm by 297 mm, and a thickness of 4 mm. The design of the grooves is in such way it provides a good contact between the loading cap and the compacted soil specimen during test process.

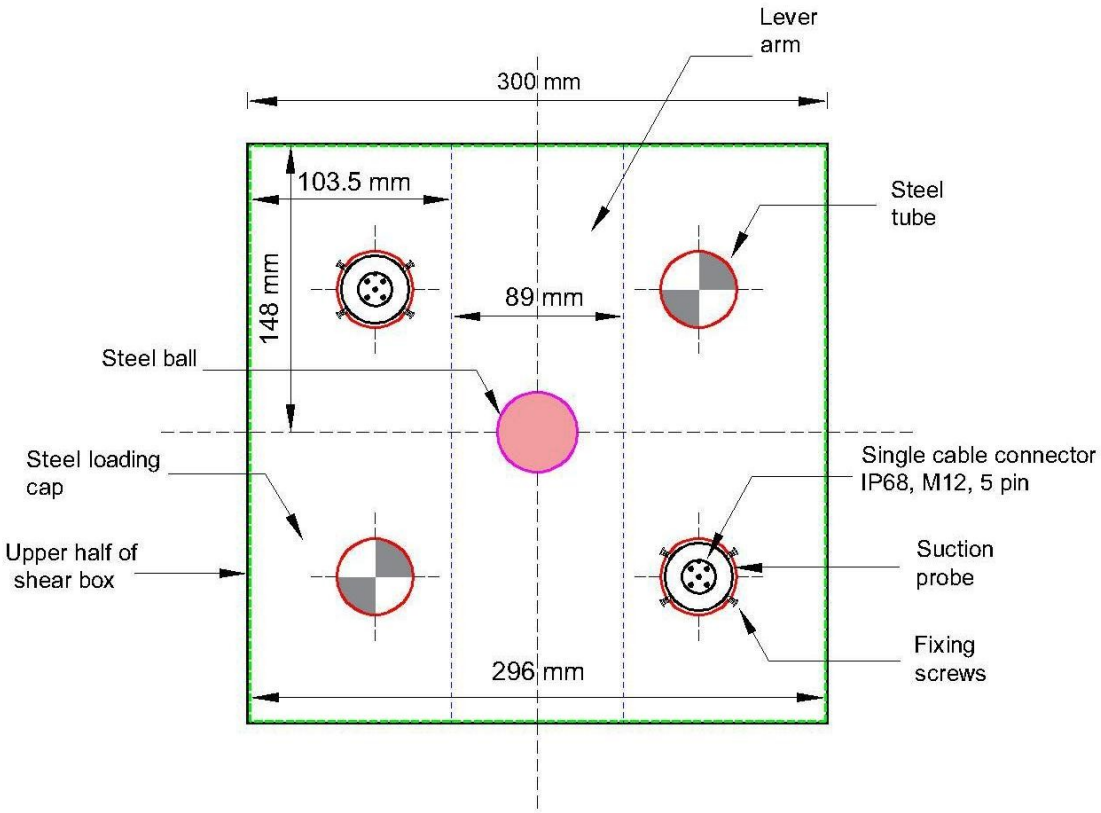

Figure 4.14: Schematic drawing of the modified steel loading cap used for soil and interface direct shear tests under constant water content condition (top view).

Four holes were machined opposite each other in the loading steel cap so that the suction probes can be inserted easily as shown in Figure 4.14. Each hole has a diameter of 42 mm, which is slightly greater than the diameter of the suction probe. In this study, only two holes were used during all experimental tests while the other two holes were sealed tightly. The two holes were selected in which one suction probe is inserted at the front of the specimen and the other at the rear. The location of the holes allowed to investigate any suction changes along the length of the soil specimen during the testing stages. During design process, an open-end steel tube with internal diameter of 42 mm, wall thickness of 3 mm, and a height of 65 mm was welded diametrically above each hole in order to provide the necessary housing for the suction probe (see Figure 4.15). A plot of the schematic cross section view of shear box cell for soil and interfaces (smooth and rough) direct shear specimens are shown in Figures 4.15(a), (b) and (c), respectively.

To avoid the movement of the suction probe during consolidation and shearing stages, each steel tube was provided with six holes at different levels of the steel tube to fix the suction probe by screws. It is worth noting that before running the real experiments, several pilot tests had been carried out to select the appropriate length of suction probe that will be inserted inside the soil specimen to avoid possible interference especially with the concrete pad during consolidation and shearing stages.

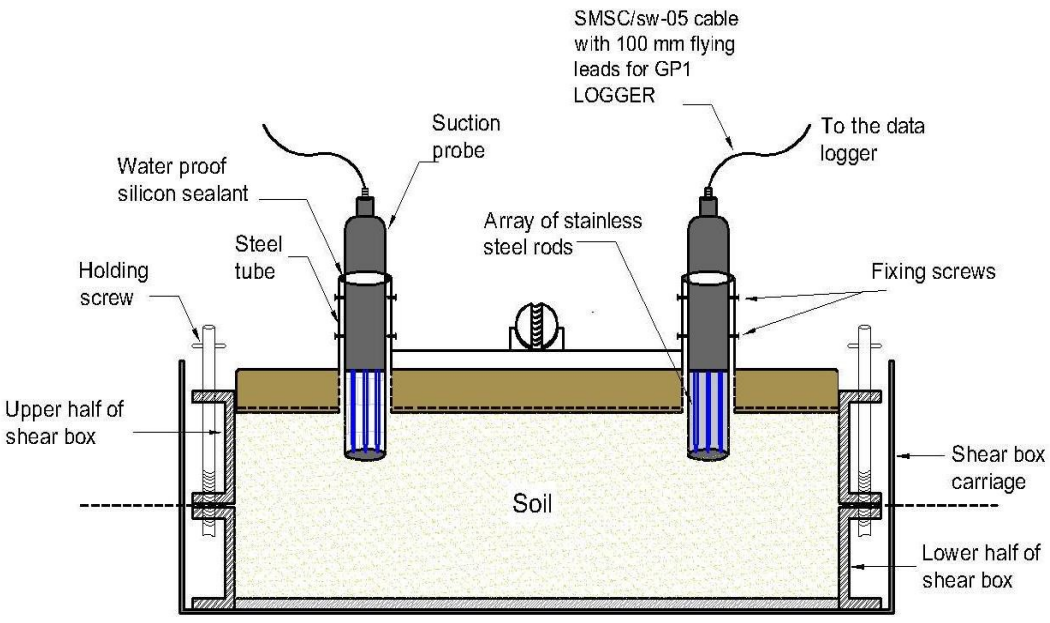

(a)

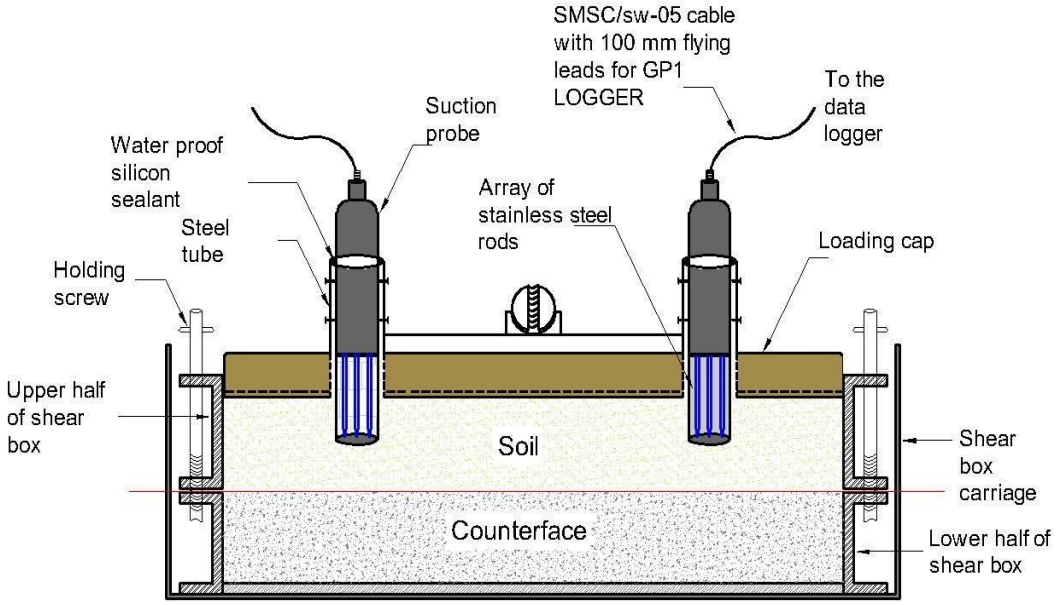

(b)

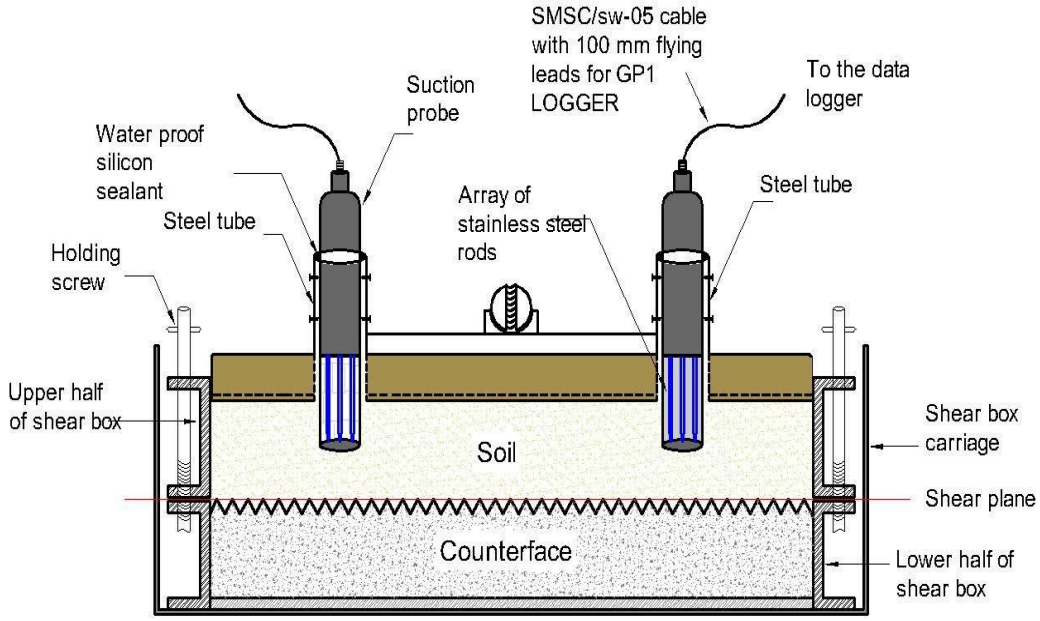

(c)

Figure 4.15: Schematic diagram of large-scale shear cell for constant water content tests: **(a)** soil-soil test, **(b)** soil-smooth interface and (c) soil-rough interface (not to scale).

Two holes having diameter coincide with the diameter of the suction probe were made in the soil sample. After that, many trials have been done to select the proper length for all the tested samples. In each trial, consolidation and shearing stages have been carried out under different levels of applied vertical stress and void ratios used in this study. At the end of the test, each sample was checked to ensure that there is no considerable soil disturbance. Due to cap rotation during shearing stage, it was necessary to check that the front and the back suction probes do not disturb the soil surrounding them during shearing process. In order to prevent the rotation of the loading cap during shearing stage, the upper edge of the steel ball (Figure 4.15) was fixed by screw in the loading steel arm whereas the lower edge was fixed in the loading cap. Subsequent direct shear tests appeared that the introduced length of the suction probe did not affect the specimen during shearing.

4.4.4 Suction measurement

In order to measure the matric suction in the soil specimen, two commercial available Equitensiometer suction probes (EQ3) were employed for this purpose. The (EQ3) Equitensiometer is designed and manufactured by Delta-T Devices Ltd (Cambridge, UK) as shown in Figure 4.16. The typical applications of this type of suction probe are:

- Measurement of matric suction of the soil in the laboratory and in the field.
- Measurement of soil temperature.

The EQ3 consists of a precision soil moisture sensor (the ML3 ThetaProbe) whose measuring rods are embedded in a porous material (the equilibrium body). This material has a known and stable relationship between water content and matric suction. When the probe is inserted into the soil, the matric suction within the equilibrium body equilibrates to that of the surrounding soils. The water content of the matric material is measured directly by the ML3 ThetaProbe, and this can be converted into the matric potential of the surrounding soil using the calibration curve supplied with each Equitensiometer. The EQ3 probe firstly submerged in de-aired water for 24 hours before use.

When power is applied to the EQ3 probe, a 100 MHz waveform is created. The waveform is applied to an array of stainless steel sensor, which transmit an electromagnetic field into the porous material (i.e. equilibrium body). The permittivity of the porous material has a strong influence on the applied field, which is detected by

the probe, resulting in a stable voltage output that acts as a sensitive measure of the soil sample matric suction.

The EQ3 probe has a 5-pin single cable connector IP68, M12 which is connected to the GP1 Data Logger by EXT/5W-05 cable. The recorded data of the soil suction and temperature by the GP1 Data Logger are downloaded to the PC through a serial port using DeltaLINK 3.6.2 Software. It is important to mention that the suction probes have the following specifications:

- Measuring range of soil matric suction from 0 kPa to 1000 kPa with accuracy of ±10 kPa.
- The suction probe is suitable to use for all non-saline soil types.
- Measuring soil temperature to ±0.5 °C over 0 to 40 °C.

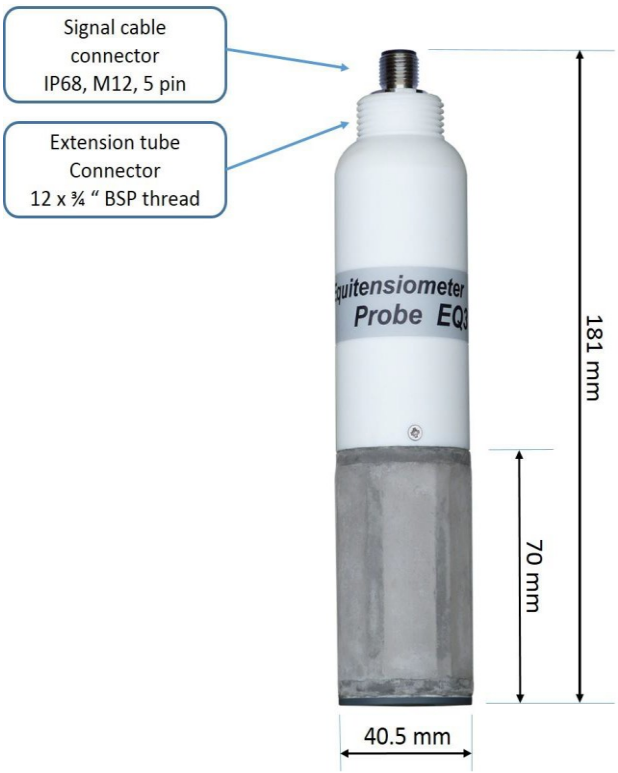

Figure 4.16: The EQ3 Equitensiometer used for suction measurement.

4.5 Summary and concluding remarks

The physical properties of the tested material and the interfaces are presented in this chapter. It describes the preliminary preparation required before starting the testing programme, which includes preparing the testing apparatus and casting the concrete pad with different surface roughness for interface tests. In addition, it illustrates the performance of anti-evaporation system used for constant water direct shear tests. The procedure of specimen preparation of soil direct shear test and soil-concrete tests is explained in details. Finally, the details of the apparatus used and the testing procedures for this research project are presented. Table 4-6 presents a summary of all the tests performed in this study.

Table 4-6: Summary of all the tests performed in this study

Test	Test specification	Purpose of the tests	Total number of performed tests	
			Target tests	Replicated tests
Particle size distribution	Sieve analysis, (BS 1377:1990)	To determine the particle size distribution of the test materials	2	1
Compaction	Standard and modified Proctor, (BS 1377-4:1990)	To determine the compaction characteristics of synthetic silty sand	Standard (4)‡‡ Modified (2)	Standard (4)+ Modified (-)
Atterberg limits	Soil consistency, (BS 1377-2:1990)	To determined the moisture contents to defined boundaries between states of consistency (liquid, plastic and solid)	(3)	(3)
Maximum density	Vibratory table method, (ASTM D 4253-00)	To determine the maximum densities of the test materials	(2)	(2)
Minimum density	a funnel pouring method, (ASTM D 4253-00)	To determine the minimum densities of the test materials	(3)	(2)
Specific gravity	Water pycnometer method, (BS 1377-2:1990)	To determine the specific gravity of soil solids	(5) ⁂	(5)†
Saturated direct shear (small-scale)	Small shear box test (BS 1377-7: 1990)	To study the effect of shear box size on the shear strength behaviour under different test conditions, void ratios, and level of vertical stress	(6)	(2)
Constant water content direct shear (small-scale) ⏚	Small shear box test (BS 1377-7: 1990)		(6)	(3)

Test	Test specification	Purpose of the tests	Total number of performed tests	
			Target tests	Replicated tests
Saturated direct shear (large-scale)	Large shear box test (BS 1377-7: 1990)	To determine shear strength response of the tested material at different void ratios and levels of vertical stress	(6)	(6)*
Constant water content direct shear (large-scale) ‡	Large shear box test (BS 1377-7: 1990)	To determine the effect of matric suction on the shear strength response of the tested material under different vertical stress level and void ratios	(6)	(6)*
Saturated interface (smooth surface)	Large shear box test (BS 1377-7: 1990)	To determine the effect of surface roughness on the interface shear strength of the tested material at different void ratios and levels of vertical stress	(6)	(6)*
Saturated interface (rough surface)	Large shear box test (BS 1377-7: 1990)		(6)	(6)*
Constant water content interface direct shear (smooth surface) ‡	Large shear box test (BS 1377-7: 1990)	To determine the effect of surface roughness, void ratio and vertical stress level on the evolution of matric suction	(6)	(6)*
Constant water content direct shear interface (rough surface) ‡	Large shear box test (BS 1377-7: 1990)		(6)	(6)*

ǂ No matric suction measurements.
‡ Suction measured by EQ3 Equitensiometer suction probe.
* Repeatability was made due to: **(i)** samples were compacted manually and **(ii)** variation in initial water content. Therefore, a variation in initial dry density occurred, which may affect the results of two samples tested at the same stress
⁑ Manual compaction.
+ Compaction machine.
⁂ Entrapped air was removed by heating the density bottle on a water bath.
† Entrapped air removed by applying a partial vacuum to the contents.

CHAPTER FIVE

SOIL SHEAR BEHAVIOUR UNDER SATURATED AND CONSTANT WATER CONTENT CONDITIONS

5.1 Introduction

A series of laboratory large-scale (300 mm x 300 mm) direct shear tests were carried out on the compacted silty sand specimens (e_i = 0.6 and 1.0) under applied vertical stresses of 100, 200, or 400 kPa. In this chapter, the obtained results of the direct shear tests conducted under saturated and constant water content conditions are presented and discussed.

5.2 Direct shear tests on saturated specimens (e_i = 0.6 and 1.0)

A total of 12 saturated direct shear tests were carried out. The soil specimens were prepared at water content of 8% ±1 and statically compacted inside the shear box (detailed information on procedures is presented in Chapter 3).

Table 5-1 shows the initial and final conditions of the tested specimens during saturation stage. Unlike the dense specimens (e_i = 0.6), the loose specimens (e_i = 1.0) exhibited collapse behaviour during saturation stage under nominal surcharge load (i.e. steel pad, equivalent of vertical stress of 1.33 kPa). Based on these observations, it can be concluded that the soil presents collapse behaviour under very low level of applied vertical stress when at low density around 13.3 kN/m^3 (e_i = 1.0), the magnitude of the observed collapse potential ranged from 6.20 to 7.85%. According to ASTM D 5333 – 92, the observed collapse potential of the tested soil can be classified as moderate to severe.

Table 5-1: Void ratio before, e_i and after e_f saturation stage and calculated collapse potential (soil-soil samples)

e_i	0.597	0.600	0.596	1.000	0.997	0.995
e_f	0.597	0.600	0.596	0.869	0.840	0.871
CP (%)	0	0	0	6.55	7.85	6.20

Table 5-2 presents the volume variation during consolidation stage. At any stress level, the specimens compacted at e_i = 1.0 showed higher volume reduction in comparison to those prepared at e_i = 0.6, as expected. This behaviour is consistent with the observations of many previous researchers (e.g. Evgin and Fakharian, 1996; Wang et al., 2013; Wang et al., 2014). The higher the studied void ratio, the larger is the vertical displacement and as a consequence the bigger is the volume reduction. As shown graphically in Figure 5.1, the volume reduction increased with the increase of the applied vertical stress for all tested specimens with both studied void ratios (e_i = 0.6 and 1.0).

Table 5-2: Sample void ratio before, e_i and after $e_{f\ cons}$ consolidation stage (saturated state)

Vertical stress, σ_v (kPa)	Initial condition	Consolidation stage		Volume reduction (%)
	e_i	$e_{f\ cons}$	Δ_e	
100	0.597	0.526	0.071	3.69
200	0.600	0.489	0.111	5.95
400	0.596	0.438	0.158	9.17
100	1.000	0.725	0.275	12.99
200	0.997	0.655	0.342	15.50
400	0.995	0.626	0.369	17.92

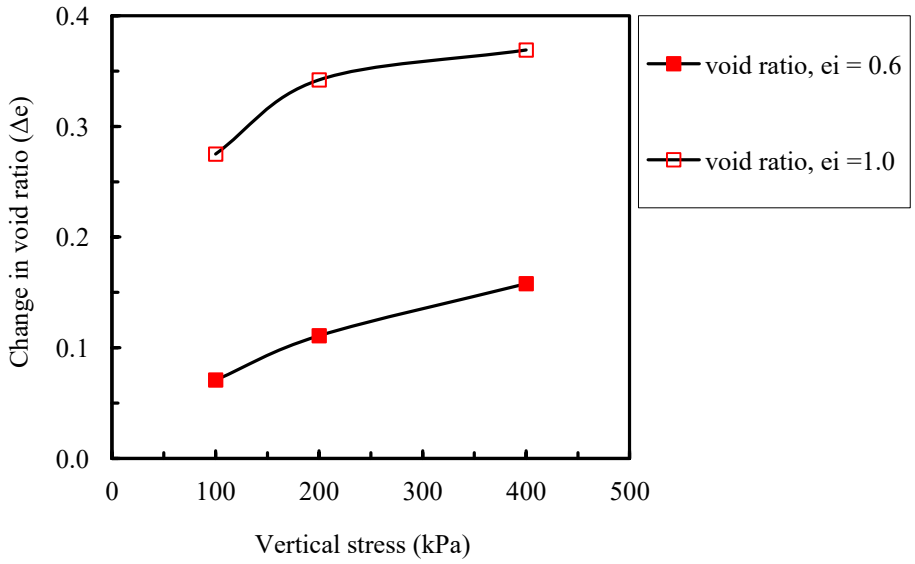

Figure 5.1: Void ratio variation against applied vertical stress for saturated tests.

Figures 5.2 (a) and (b) show the saturated shear strength behaviour and the volume changes of the studied materials at e_i = 0.6 and 1.0. It is worthy to mention that the shear strength corresponding to each increment of the horizontal displacement was calculated based on the corrected cross sectional area of the sheared specimen. It should be noted here that, for both studied void ratios, two tests were performed for each level of applied vertical stress used in this study.

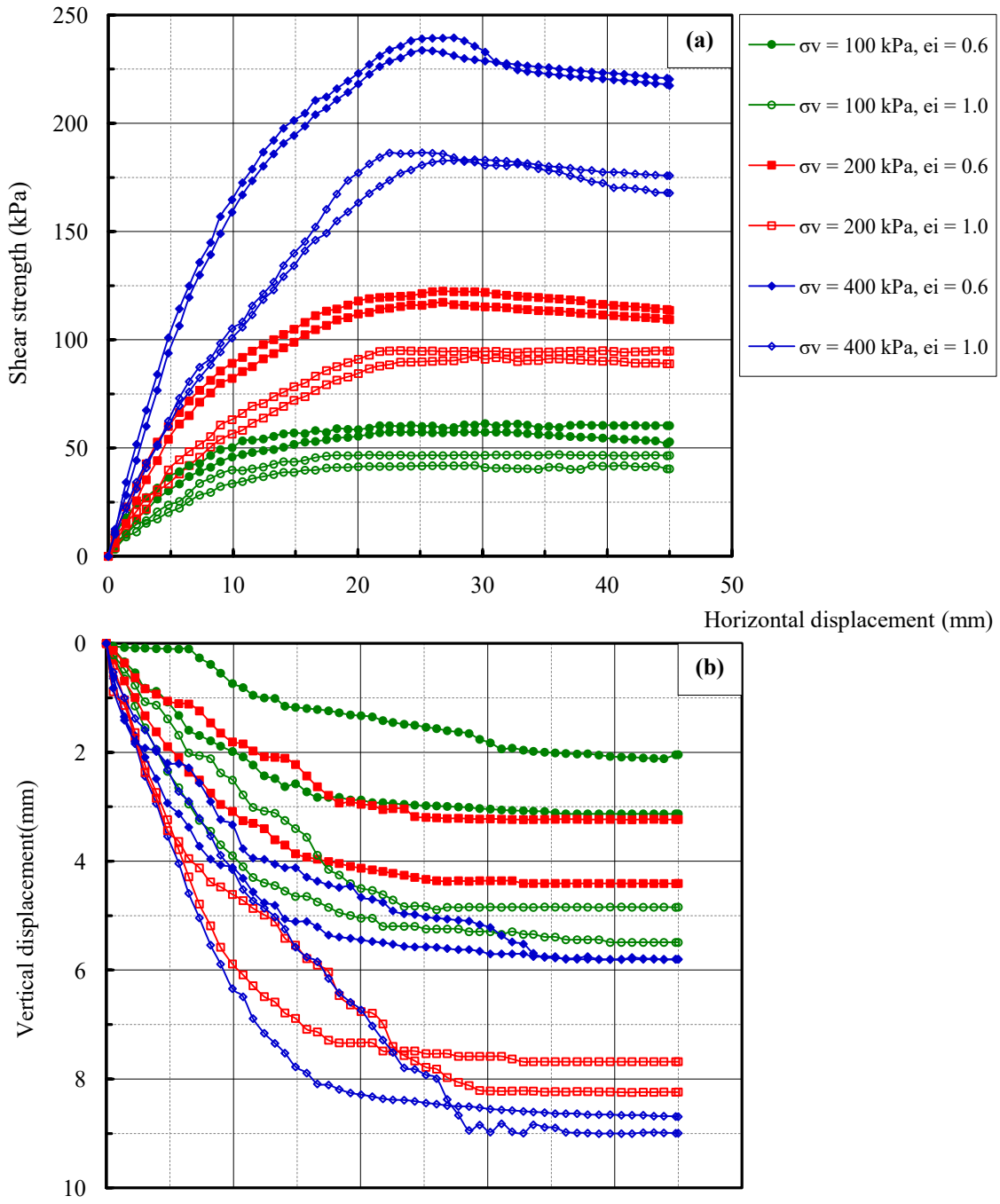

Figure 5.2: Direct shear results of silty sand samples for e_i = 0.6 and 1.0: **(a)** shear strength; **(b)** volumetric behaviour (saturated state).

As expected, the results in Figure 5.2(a) indicate that the shear strength of the tested material, at both void ratios, increased with the increasing the vertical stress level. The soil becomes more plastic with the increase of applied vertical stress. The higher the vertical stress, the greater the shear force required to overcome the intergranular forces, and larger the obtained shear strength. Similar behaviour can be found in the literature including the works of Wang et al., 2008, Wu et al., 2008, Dadkhah et al., 2010, Moayed et al., 2010, Hosseini and Jesmani, 2016.

Figure 5.2(a) reveals that the initial stiffness of the tested specimens has a clear dependency on both void ratio and the level of applied vertical stress. For specimens that have e_i = 0.6, tested under 200 and 400 kPa and e_i = 1.0, tested under 400 kPa, strain softening behaviour became pronounced. Whereas specimens e_i = 0.6 and 1.0 tested at 100 kPa and e_i = 1.0 tested at 200 kPa, the vertical stress showed hardening-softening behaviour after reaching the peak/maximum shear strength. This behaviour could be attributed to the shearing mechanism which is governed by sliding of soil particles over each other rather than interlocking (Sowers and Sowers, 1970). A noticeable peak shear strength was more pronounced only in the specimens carried out at 400 kPa vertical stress for both e_i = 0.6 and 1.0. It can also be noticed from Figure 5.1 (a) and Table 5-3, for all samples, that with increasing the level of applied vertical stress, the horizontal displacement corresponding to the peak/maximum shear strength shifted forward. From Table 5-3, as expected the horizontal displacements of specimens at e_i = 0.6 corresponding to the peak/ maximum shear strength are greater than those of e_i = 1.0 specimens.

Vertical displacement versus horizontal displacement curves of both studied void ratios are shown in Figure 5.2(b). At the beginning of shearing process, all specimens exhibited decrease in the volume until the horizontal displacement slightly before the horizontal displacement corresponding to the peak/maximum shear strength. After that the specimens begin to dilate and/or remain steady state until the soil reaches the residual shear strength. As expected, all specimens exhibited a tendency to increase in the vertical displacement (volume reduction) with increasing the level of applied vertical stress. The specimens of e_i = 1.0 exhibited greater volume reductions than those of e_i = 0.6 specimens, as expected. The maximum vertical displacement of the tested specimen approximately coincided with peak/maximum shear strength point.

Table 5-3: Values of horizontal displacement corresponding to the peak/maximum shear strength for ei = 0.6 and 1.0 soil specimens (saturated state)

Vertical stress, σ_v (kPa)	Initial void ratio, e_i = 0.6	Initial void ratio, e_i = 1.0	Horizontal displacement at peak/maximum shear strength, δ_h (mm)	
	Peak/maximum shear strength, τ (kPa)	Peak/maximum shear strength, τ (kPa)	e_i = 0.6	e_i = 1.0
100	59.07	41.05	20.04	14.04
200	122.22	91.83	23.43	21.76
400	233.73	182.65	25.98	25.15

5.3 Direct shear tests on specimens (e_i = 0.6 and 1.0) under constant water content

A series of 12 direct shear tests was performed for samples prepared at e_i = 0.6 and 1.0 (ω = 8% ±1) and tested under constant water content condition. The same sample preparation procedures to those tested under saturated conditions were adopted. Prior to consolidation, all the soil specimens were controlled in terms of soil suction until stabilisation was achieved in 9 days as presented in section 3.6.2.

As expected, during consolidation the volume reduction of the specimens increased with the increase of the applied vertical stress for all samples. Moreover, at any level of vertical stress, samples prepared with high void ratio exhibited higher decrease in void ratio than those prepared at low void ratio as shown in Figure 5.3.

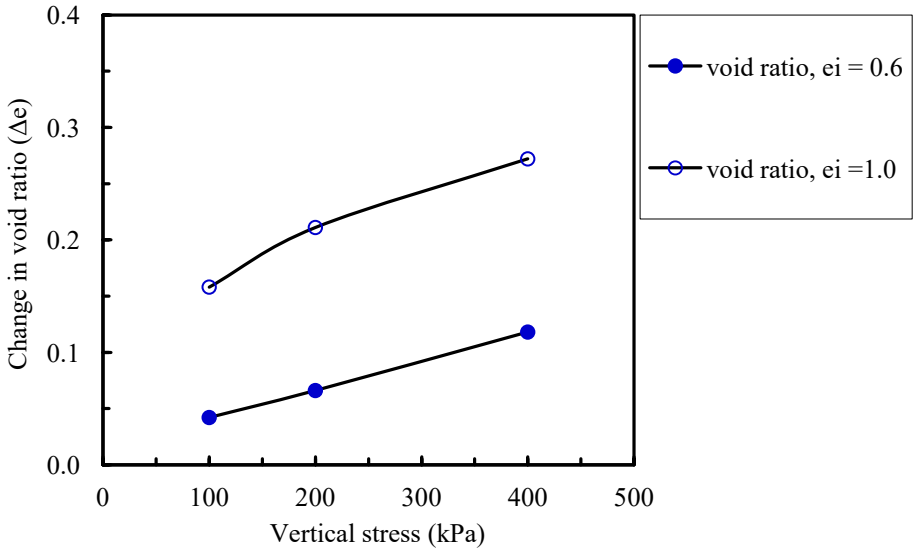

Figure 5.3: Void ratio variation against applied vertical stress for constant water content tests.

Similar behaviour was observed by Shen et al., (2009) for silty sand specimens. The results of the tested specimens at the end of the consolidation stage are tabulated in Table 5-4. From Table 5-4 during consolidation at constant water content there is a noticeable decrease in the void ratio associated with an increase in the degree of saturation for all soil specimens, as expected.

Table 5-4: Sample void ratio before, e_i and after $e_{f\ cons}$ consolidation stage (constant water content state)

Vertical stress, σ_v (kPa)	Consolidation stage							
	Initial condition			Final condition				
	e_i	S_{ri} (%)	ρ_{dry} (kg/m^3)	e_f	S_{rf} (%)	ρ_{dry} (kg/m^3)	Δ_e	ΔS_r (%)
100	0.596	35.72	1666	0.554	38.43	1711	0.042	2.71
200	0.598	35.56	1664	0.532	39.97	1736	0.066	4.41
400	0.600	35.45	1662	0.492	43.32	1782	0.108	7.78
100	0.998	21.31	1331	0.840	25.32	1445	0.158	4.01
200	1.000	21.29	1330	0.789	26.98	1486	0.211	5.69
400	0.996	21.38	1332	0.704	30.25	1561	0.292	8.87

As mentioned earlier in section 3.6.2, the consolidation stage of the tested samples performed under constant water content condition stopped when no further increase in the vertical displacement was noticed (approximately steady state). In order to understand how matric suction changes with time due to the application of vertical stress of samples with e_i = 0.6 and 1.0 the results are presented in Figure 5.4(a) and (b), respectively. It can be noticed that for both void ratios, the reduction of matric suction of the tested samples increases with the increase of the applied vertical stress. The higher is the applied vertical stress; the greater the reductions in matric suction. Looser samples (e_i = 1.0) exhibited higher measured change in matric suctions as compared to the denser samples (e_i = 0.6). This trend of behaviour was observed for all levels of vertical stress used in this study.

Test results presented in Figures 5.4(a) and (b) reveal that for both studied void ratios; the tested samples exhibited lower changes in matric suction after four hours from the beginning of consolidation test and then gradually increased with time until the end of the consolidation process. Consequently, it can be concluded that twelve hours (whole period of consolidation stage) does not offer enough time for matric suction stabilisation.

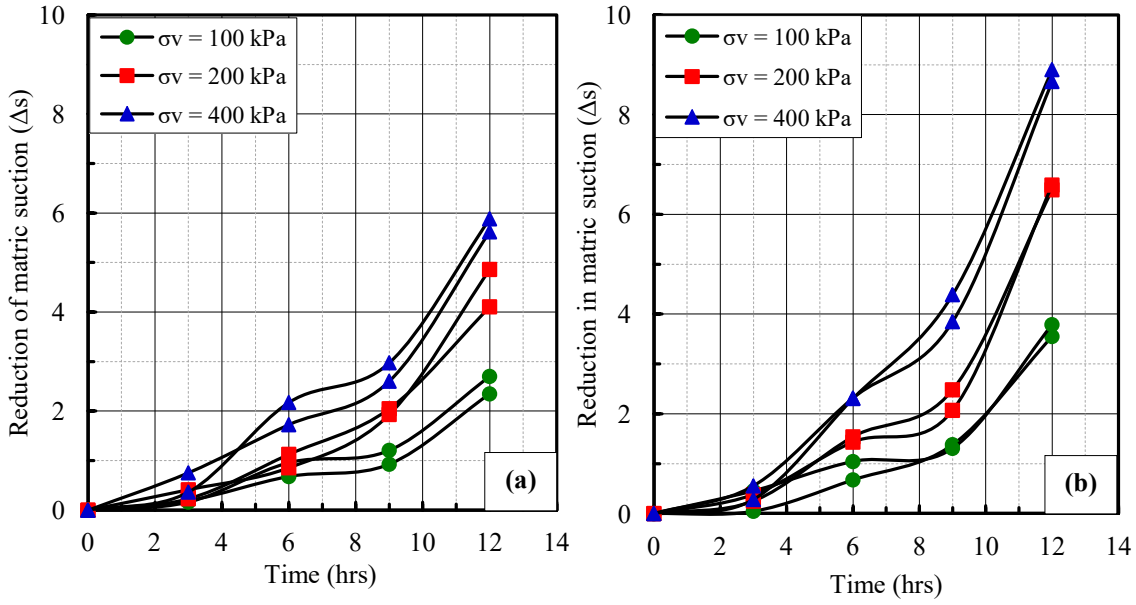

Figure 5.4: Reductions in matric suction vs. time during consolidation stage; **(a)** e_i = 0.6, **(b)** e_i = 1.0.

Figure 5.5(a) shows the shear strength against the horizontal displacement curves. The shear strength increased with the increasing of applied vertical stress. As expected, as the void ratio increased, a decrease in the shear strength was observed. This behaviour agrees with that found by many authors (e.g. Gan and Fredlund, 1988; Hamid, 2005). Likewise, test results presented in Figure 5.5(b) also shows that for both studied void ratios, a clear increase in the vertical displacement with increasing vertical stress. These observations are in agreement with the findings of other studies (Tarantino and Tombolato, 2005; Shen et al., 2009; Wang et al., 2014). In general, it can be noticed from Figure 5.5(a) that all curves of shear strength gradually increased in the pre-peak region (showing hardening behaviour) to a horizontal displacement slightly before the displacement corresponding to the peak/maximum shear strength. The other noteworthy point which can be noticed from shear strength curves is that different patterns of shear strength behaviour were observed in the post-peak region. Strain softening behaviour became pronounced with the increase in the applied vertical stress for specimens having e_i = 0.6, whereas specimens tested at e_i = 1.0 did not show any strain softening under all applied vertical stresses, in the sense that the shear strength curve showed approximately steady state after reaching the maximum strength.

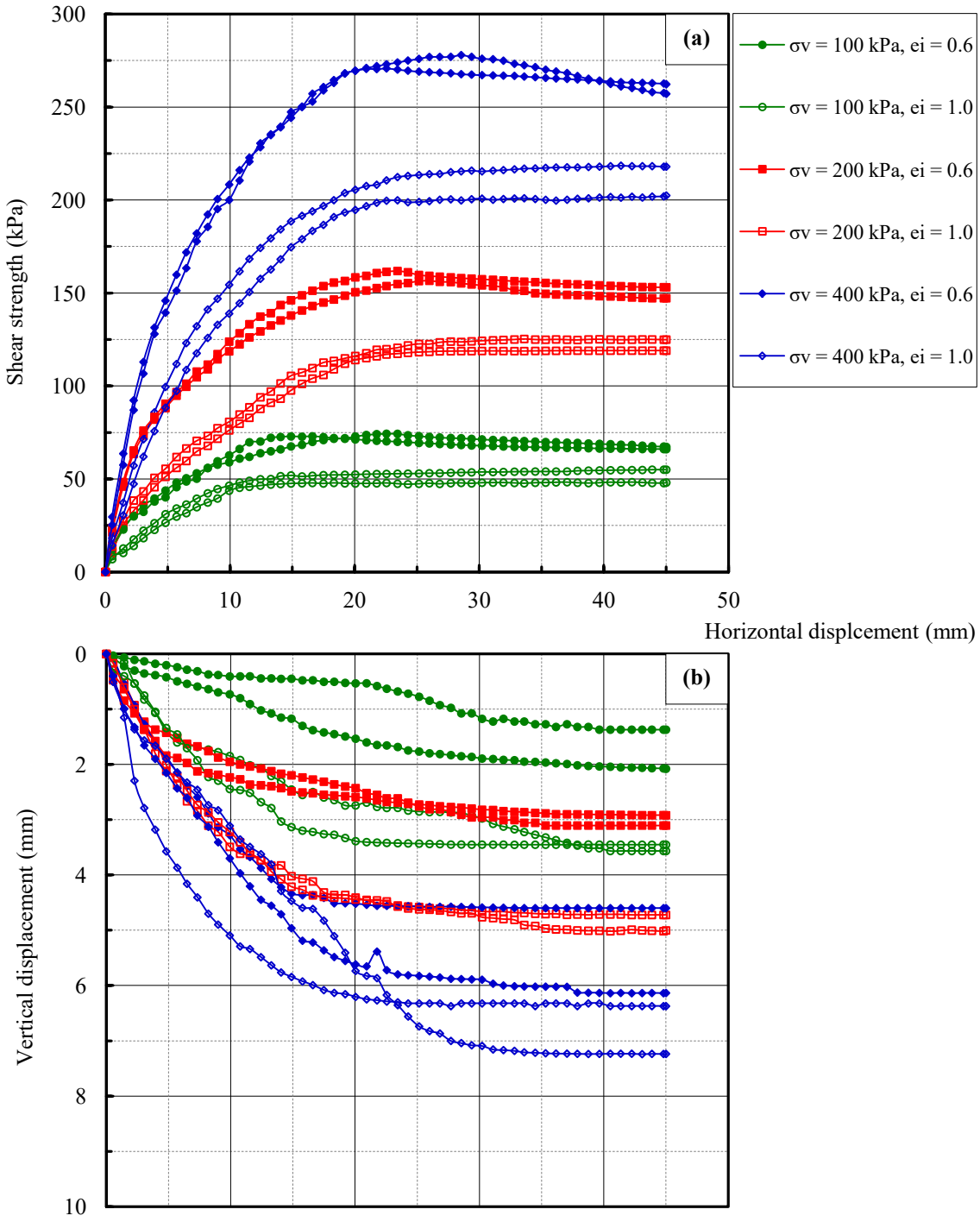

Figure 5.5: Direct shear results of silty sand samples for e_i = 0.6 and 1.0: **(a)** shear strength; **(b)** volumetric behaviour (constant water content state).

Hamid (2005) performed a series of unsaturated direct shear tests on low plasticity Minco silt. In his study, he observed that the soil suction contributed to the peak shear strength, however, the influence of suction is less important in the post-peak region. Hossain (2010) performed direct shear tests on unsaturated completely decomposed

granite soil. The author indicated three different types of shear strength behaviour in the post-peak region which are hardening, softening, and softening-hardening behaviours.

In this study, Denser specimens (e_i = 0.6) exhibited peak patterns, whereas looser specimens (e_i = 1.0) exhibited non-peak patterns. Like the shearing tests of saturated specimens, Figure 5.5(a) reveals that the horizontal displacement corresponding to the peak/maximum shear strength show clear increase with increasing of applied vertical stress, as shown in Table 5-5. Characteristics of the tested specimens at the end of the shearing stage are summarized in Table 5-6.

Table 5-5: Values of horizontal displacement corresponding to the peak/maximum shear strength for e_i = 0.6 and 1.0 soil samples (constant water content)

Vertical stress, σ_v (kPa)	Initial void ratio, e_i = 0.6	Initial void ratio, e_i = 1.0	Horizontal displacement at peak/maximum shear strength, δ_h (mm)	
	Peak/maximum shear strength, τ (kPa)	Peak/maximum shear strength, τ (kPa)	e_i = 0.6	e_i = 1.0
100	74.31	52.05	21.76	13.26
200	156.40	118.16	25.15	20.92
400	277.92	217.29	28.53	23.43

Table 5-6: Sample void ratio before, e_i and after e_f consolidation stage (constant water content state)

Vertical stress, σ_v (kPa)	Initial condition			Shearing stage			
	e_i	S_{ri} *(%)*	ω_i *(%)*	e_{she}	S_{rf} *(%)*	$\omega_{f\ she}$ *(%)*	ρ_{dry} *(kg/m^3)*
100	0.596	35.72	8.004	0.550	38.68	7.998	1716
200	0.598	35.56	7.995	0.510	41.53	7.963	1761
400	0.600	35.45	7.997	0.444	47.85	7.987	1842
100	0.998	21.31	7.996	0.801	26.45	7.967	1476
200	1.000	21.29	8.005	0.725	29.26	7.976	1542
400	0.996	21.38	8.008	0.643	32.93	7.962	1618

In order to analyse the matric suction evolution during shearing, the matric suction has been corrected to zero at the beginning of the shearing stage. Test results of samples (e_i = 0.6 and 1.0) are presented in Figure 5.6. In general, it can be noticed that the matric suction during shearing process for both studied void ratios specimens decreases with increasing the level of applied vertical stress. The higher the applied vertical stress, the denser the soil specimen, and hence the lower the matric suction is. This trend of behaviour is consistent with what was observed by Marinho and Stuermer (2000); Rao and Revanasiddappa (2002); Tripathy et al., (2003). Figure 5.6 also shows that there is a noticeable dependency of matric suction on initial value of void ratio. Samples prepared with high void ratio revealed higher matric suction than those prepared at low void ratio. This trend of behaviour was observed for all levels of vertical stress. As the horizontal displacement increased, the measured matric suction either remained unchanged or increased slightly in the post-peak region. The values of matric suction corresponding to the peak and residual shear strengths are listed in Table 5-7.

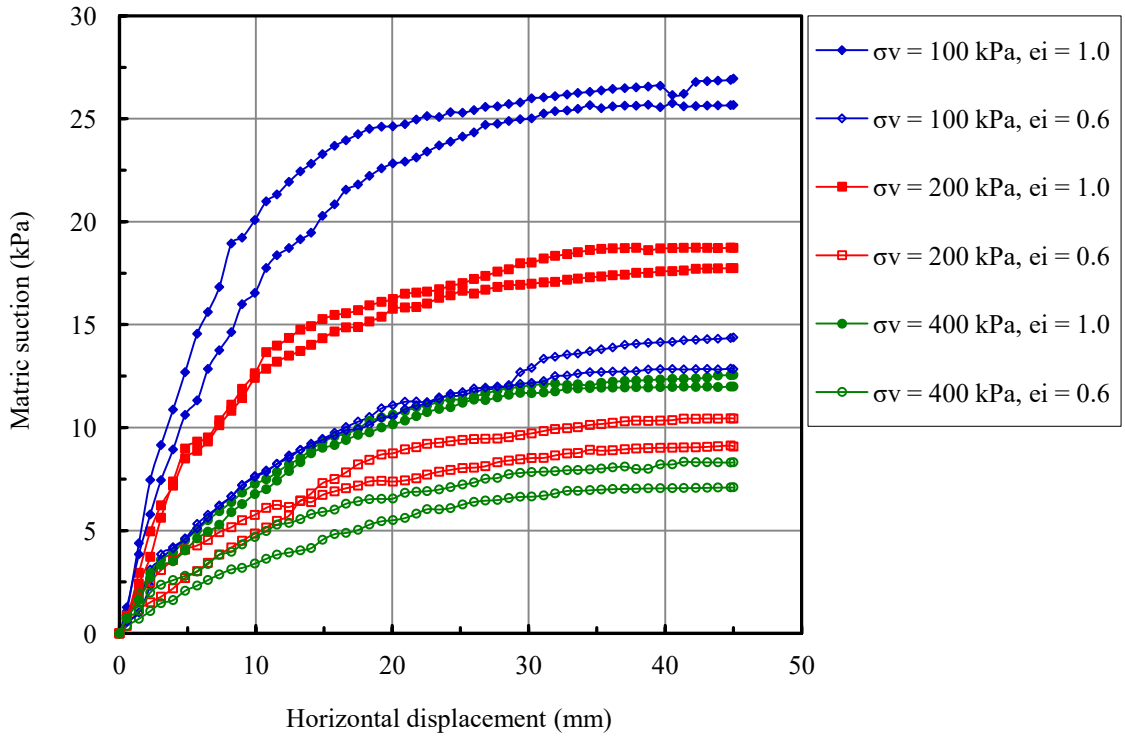

Figure 5.6: Evolution of matric suction with horizontal displacement during shearing process of soil samples at e_i = 0.6 and 1.0.

Table 5-7: Values of measured suction corresponding to peak and residual shear strengths of soil samples (constant water content)

Initial void ratio, e_i	Vertical stress, σ_v (kPa)	Peak/maximum shear strength (kPa)	Ψ_{peak} (kPa)	$\Psi_{residual}$ (kPa)
0.596	100	74.31	11.464	14.345
0.598	200	156.40	7.430	9.074
0.600	400	277.92	4.548	7.098
0.998	100	52.05	25.569	26.879
1.000	200	118.16	16.640	17.741
0.996	400	217.29	11.069	12.551

5.4 Comparison of the saturated and constant water content states

Figure 5.7 shows the volume variation during consolidation stage for samples tested under saturated and constant water content conditions. At any stress level, the specimens compacted at e_i = 1.0 showed higher volume reduction in comparison to those prepared at e_i = 0.6, as expected. Also, for both studied void ratios, the saturated samples exhibited larger volume reduction than those tested under constant water content. This behaviour is due to the fact that, in samples performed at constant water content, the normal force is induced by the capillary tension of water meniscus clinging to the contact point of the soil particles and acts so as to connect the soil particles tightly and hence reduces the volume reduction (Karube and Kawai, 2001).

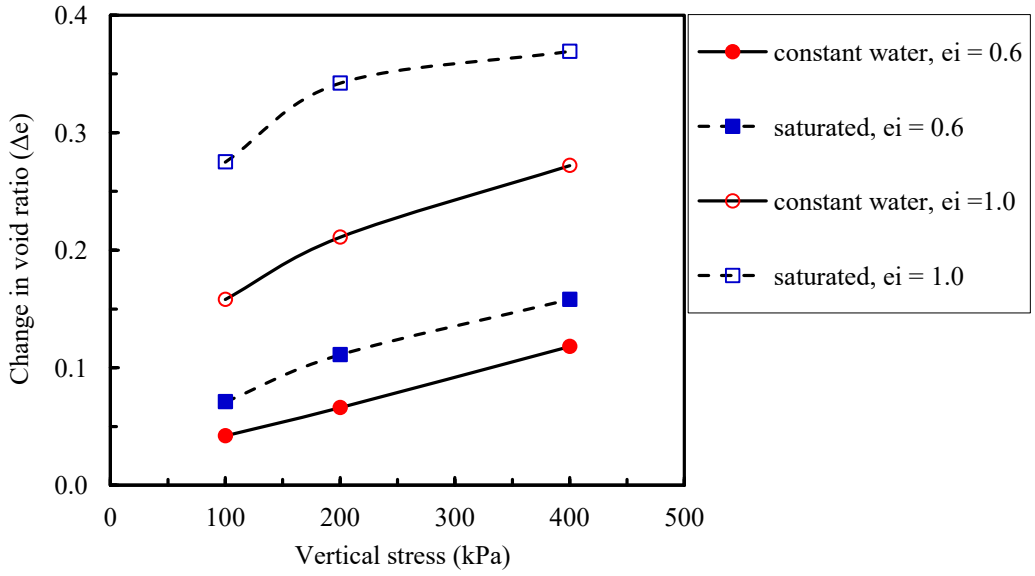

Figure 5.7: Void ratio variation against applied vertical stress for saturated and constant water content conditions.

It can also be noted from Figure 5.7 that the change in void ratio (volume reduction) of dense samples (e_i = 0.6) increased linearly with increasing applied vertical stress. This trend of behaviour was observed when samples tested under saturated and constant water content conditions. In contrast, samples that have e_i = 1.0 showed a clear non-linear volume reduction with increasing the vertical stress level. Moreover, the significant role of matric suction in decreasing the volume variation during consolidation is more obvious especially when the tested samples compacted at e_i = 1.0 (i.e. lower initial degree of saturation). At any level of vertical stress, the differences between the results of the saturated tests and that of constant water content are greater for samples at e_i = 1.0 than those at e_i = 0.6.

From the observation of Figures 5.8 and 5.9, for both studied void ratios, the obtained shear strength of specimens under constant water content are found to be distinctly greater than those obtained from saturated samples. This illustrates the significant role of soil suction on the shear strength behaviour of the tested material, as expected and vastly shown in the literature (e.g. Hossain, 2010; Moayed et al., 2010, Hosseini and Jesmani, 2016). This behaviour can be attributed to the fact that, in saturated soil, the pore spaces are filled with water that potentially can acts as lubricant agent between particles, and hence reduce the shear strength (Lambe, 1958; Terzaghi an Peck, 1967; Craig, 1974; Das, 2008).

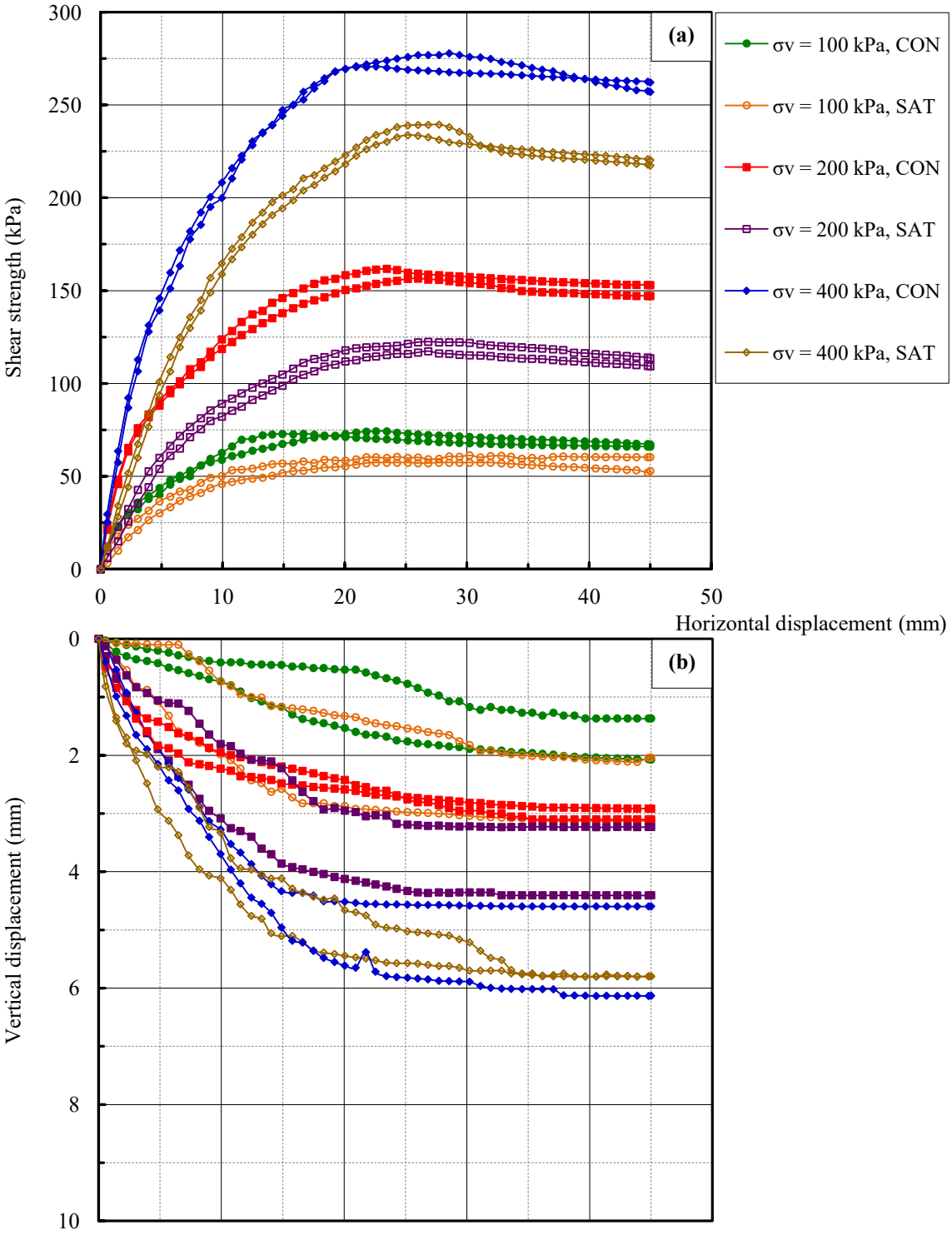

Figure 5.8: Direct shear results of silty sand samples for e_i = 0.6: effect of test condition on **(a)** shear strength; **(b)** volumetric behaviour.

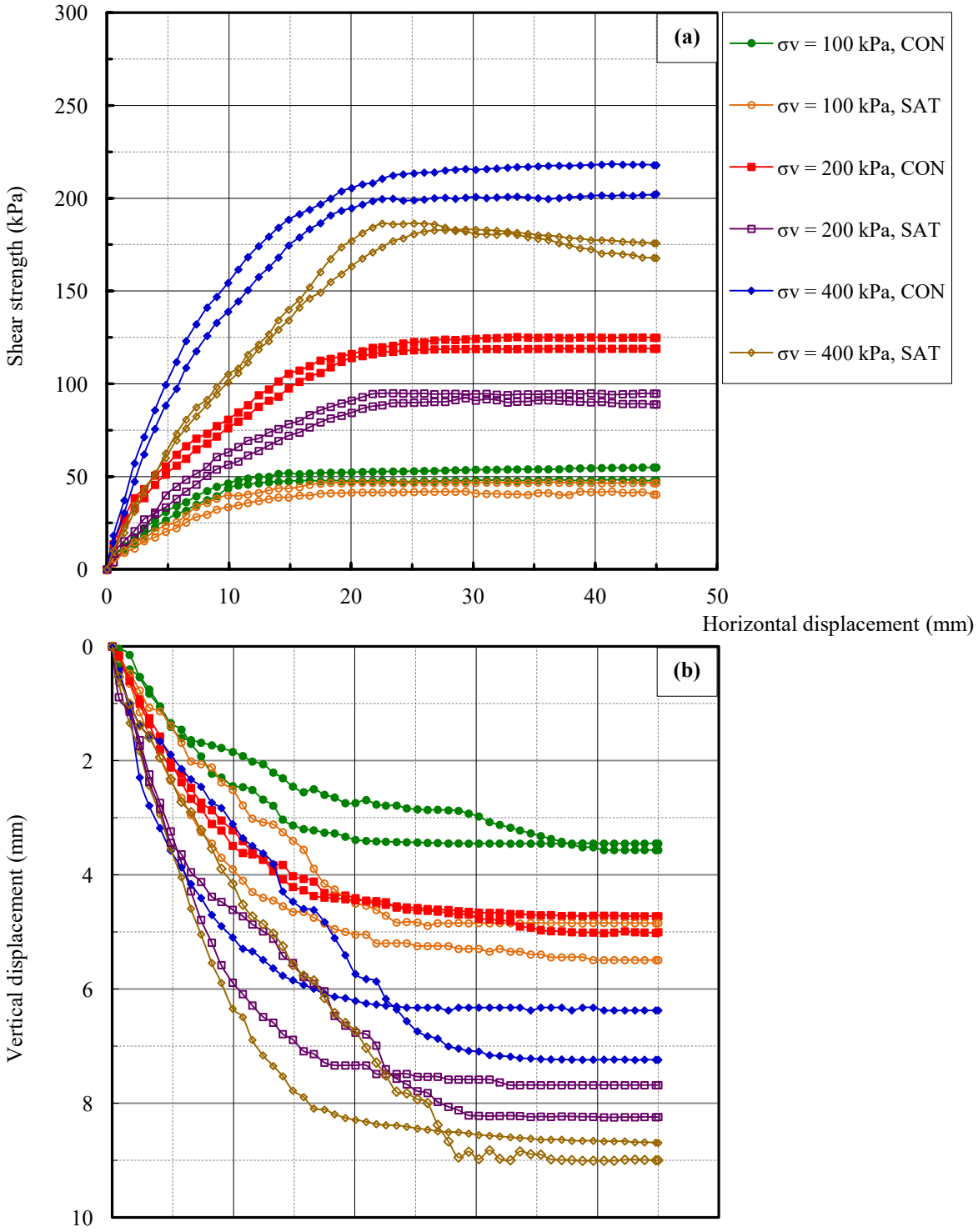

Figure 5.9: Direct shear results of silty sand samples for e_i = 1.0: effect of test condition on **(a)** shear strength; **(b)** volumetric behaviour.

As opposed to the saturated samples, at constant water content the matric suction generated due to menisci of water formation increase in the shear strength and stiffness of the tested specimens (Wheeler and Karube, 1996). Similar trend of behaviour has been observed by many researchers such as Miller and Nelson, 1993; Melinda et al., 2004; Oh et al., 2008; Maleki and Bayat, 2012; Tiwari and Al-Adhadh, 2014; Ismael and Behbehani, 2016. In this study, this behaviour was observed for all tested levels of vertical stress.

Test results presented in Figure 5.8(a) for initial void ratio of 0.6 and Table 5-8 reveal that the maximum/peak shear strength for the tested specimens under constant water content was mobilized at larger horizontal displacement when compared with those observed on saturated specimens. This behaviour can be attributed primarily to the effect of matric suction on increasing the stiffness of the specimens. No clear correlation (Figure 5.9(a) for initial void ratio 1.0) was found between the horizontal displacements corresponding to the maximum/peak shear strength.

Table 5-8: Values of horizontal displacement corresponding to the peak/maximum shear strength for e_i = 0.6 and 1.0 samples (saturated and constant water content)

Vertical stress, σ_v (kPa)	Test condition	Initial void ratio, e_i = 0.6	Initial void ratio, e_i = 1.0	Horizontal displacement at peak/maximum shear strength, δ_h (mm)	
		Peak/maximum shear strength, τ (kPa)	Peak/maximum shear strength, τ (kPa)	e_i = 0.6	e_i = 1.0
100	Saturated	59.07	41.05	20.04	14.04
200		122.22	91.83	23.43	21.76
400		233.73	182.65	25.98	25.15
100	Constant water	74.31	52.05	21.76	13.26
200		156.40	118.16	25.15	20.92
400		277.92	217.29	28.53	23.43

In Figure 5.8(a), denser specimens (e_i = 0.6) tested under saturated and constant water content conditions exhibited strain softening behaviour (peak shear strength pattern). In contrast, looser specimens (e_i = 1.0) showed clear hardening behaviour after reaching the maximum shear strength for all tested samples (non-peak shear strength pattern) except samples sheared under 400 kPa vertical stress as shown in Figure 5.9(a). By considering the results presented in Figures 5.8(a) and 5.9(a), it can be concluded that

the role of the matric suction in the post peak shear strength region is less significant in the sense that the shear strength curves exhibited different patterns of behaviour (i.e. strain softening or strain hardening behaviour). This trend of behaviour has been observed by many researchers such as Hamid 2005; Hossain 2010; Borana 2014. It can be noticed from Figures 5.8(b) and 5.9(b), for the range of applied vertical stresses, the constant water content specimens have shown lower value of vertical displacement in comparison with the corresponding saturated one.

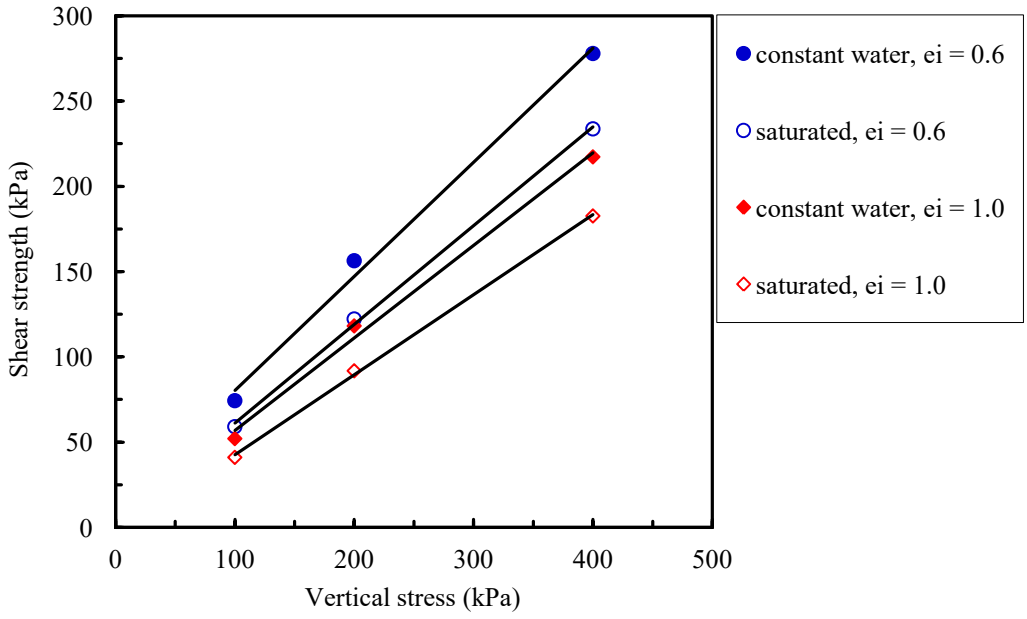

Figure 5.10: Failure envelopes of e_i = 0.6 and 1.0 soil samples: test condition effect.

In Figure 5.10, it can be noted that the slope of the linear envelopes increases with decreasing the degree of saturation of the tested samples. Consistent trend corresponding to different void ratios (e_i = 0.6 and 1.0) was also noticed in the sense that the slope of failure envelopes changes with changing void ratio; the lower the void ratio, the steeper the failure envelope. The shear strength parameters, ϕ' and c', are presented in Table 5-9.

From the analysis of Table 5-9, it can be noted that the effective cohesion, c' of the e_i = 0.6 samples increased by twofold when performed at constant water content condition in comparison with the saturated samples, while at e_i = 1.0, the effective cohesion was zero for the saturated condition and 4.5 kPa at constant water content (almost ¼ of the c' at constant water content). This shows a coupled influence of saturation state together

with the density of the tested samples. At constant water content, there is an apparent increase in the bonding between soil particles due to the negative pressure generating matric suction at the contact points in between particles. It can also be seen from Table 5-9 that there is a noticeable dependency of the effective friction angle on the test conditions (saturated or constant water). Similar to c′ the friction angle ϕ′ of both studied void ratios exhibits noticeable increase as the degree of saturation of the tested samples decreased. Moreover, the shear strength parameters (ϕ′ and c′), were noticeably increased with decreasing the studied void ratios. In brief, it can be concluded that the matric suction has a clear effect on the shear strength parameters. These results match those observed in relevant studies (e.g. Hossain 2010; Zhou and Xu, 2016).

Table 5-9: Shear strength parameters for different values of void ratio samples (saturated and constant water content)

Initial void ratio, e_i	Test condition	ϕ'/ϕ (Degree)	c'/c (kPa)	R^2
0.6	Saturated	31	7.5	0.9990
1.0		26.5	0	0.9992
0.6	Constant water	36.5	16	0.9938
1.0		29	4.5	0.9943

5.5 The effect of shear box size on the shear strength behaviour

In the current study, in addition to the large-scale tests shown in sections 5.1 to 5.4, small-scale direct shear tests (60 mm x 60 mm) were carried out on the samples (initial sample parameters e_i = 0.6 and 1.0) to examine the effect of shear box size on the shear behaviour of the silty sand soil. All tests were performed under the same saturated and constant water content conditions. The shear strength versus horizontal displacement curves and the corresponding vertical displacement versus horizontal displacement curves are presented in Figure B, Appendix B. Figures 5.11(a) and (b) show clearly that the horizontal displacement corresponding to the peak/maximum shear strength is not constant for the two shear box sizes. Hence, the comparison between the results is difficult. To overcome this problem, the shear strength is plotted against relative lateral strain (horizontal displacement/shear box length) instead of horizontal displacement (Moayed and Alibolandi, 2016).

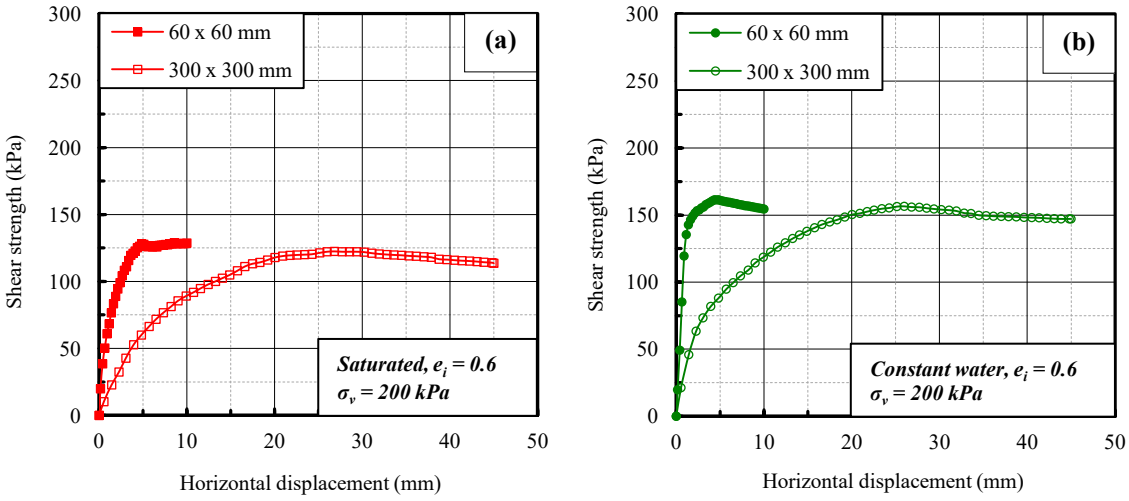

Figure 5.11: Comparison of the shear strength curves using two different shear box sizes under **(a)** saturated; **(b)** constant water content (e_i = 0.6, σ_v = 200 kPa).

In Figures 5.12(a) and (b), the same results shown in Figures 5.11(a) and (b), are redrawn, but plotting the x-axis as a relative lateral strain (horizontal displacement divided by shear box length). It can be seen that the peak shear strength slightly decreases with increasing the shear box size. Moreover, peak strengths are approximately reached at similar relative lateral strain.

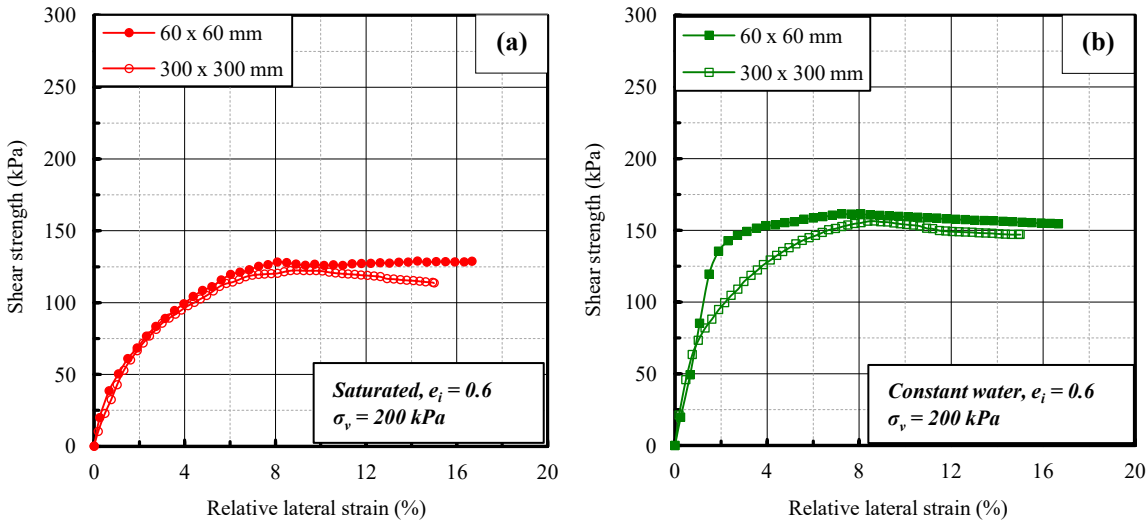

Figure 5.12: Shear strength versus relative lateral strain curves: comparison using two different shear box sizes under **(a)** saturated; **(b)** constant water content (σ_v = 200 kPa).

This trend of behaviour is mostly observed for both studied void ratios performed under saturated and constant water content conditions as shown in Figures 5.13 and 5.14.

These figures also show that the effect of shear box size on residual shear strengths was found to be insignificant. This is in agreement with experimental results that were obtained in the literature including the works of Palmeira and Milligan (1989); Matsushima and Tatsuoka (2007); Shakri et al., (2017). Table 5-10 shows the values of peak/maximum shear strength and the corresponding strength parameters obtained from two different shear box sizes.

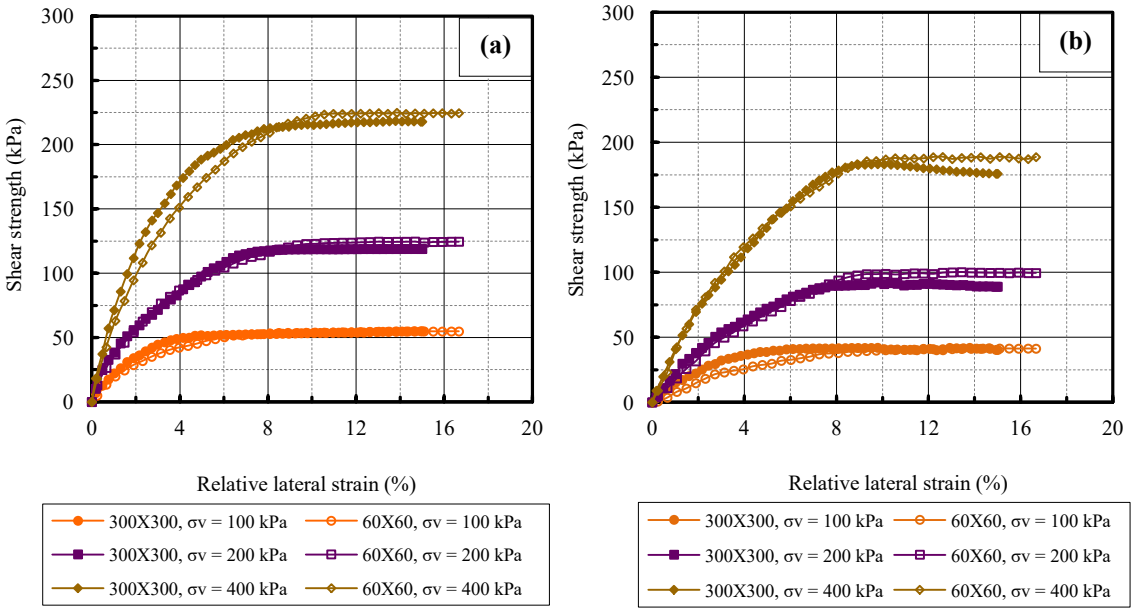

Figure 5.13: Comparison of the shear strength curves using two different shear box sizes under saturated condition **(a)** e_i = 0.6 ; and **(b)** e_i = 1.0.

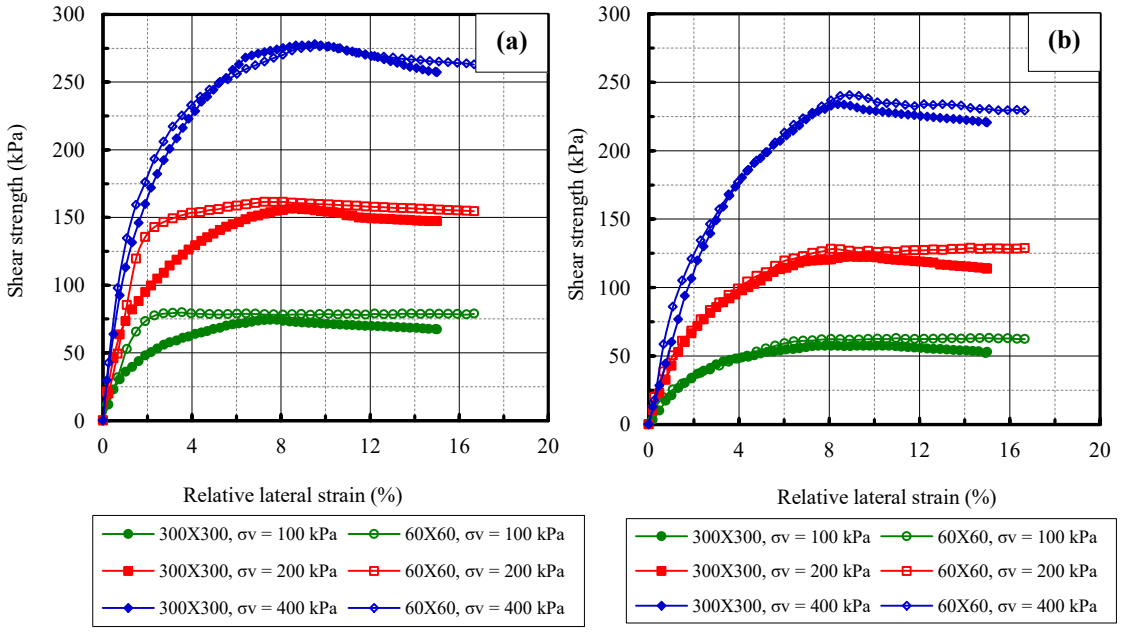

Figure 5.14: Comparison of the shear strength curves using two different shear box sizes under constant water content condition **(a)** e_i = 0.6 ; and **(b)** e_i = 1.0.

Figure 5.15 in conjunction with Table 5-10 show that there is no much significant difference in angle of friction for the specimen tested in direct shear test by two devices (i.e. small-scale and large-scale). However Table 5-10 shows same differences in the results. The angle of internal friction values obtained from small-scale shear box apparatus are higher (1.5° to 2.5°) as compared to large-scale shear box. Moreover, except for the samples prepared at e_i = 0.6 and tested under constant water content (cohesion decreased as the shear box size increased), Table 5-10 shows that the shear box size does not have a clear effect on the cohesion of the other samples.

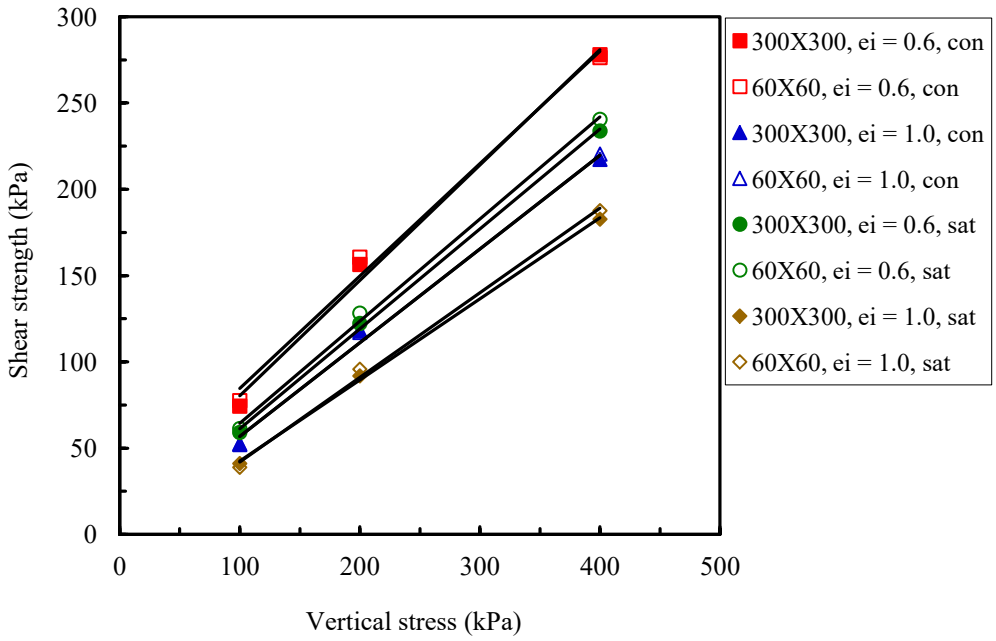

Figure 5.15: Failure envelopes for different shear box sizes of specimens (e_i = 0.6 and 1.0) performed under saturated and constant water content conditions.

Table 5-10: Effect of shear box size on the strength parameters of the tested specimens

Test condition	e_i	σ_v (kPa)	τ_f (kPa)		ϕ' (deg)		c' (kPa)		$\Delta\tau_f$ (%)	$\Delta\phi'$ (%)	$\Delta c'$ (%)
			60x60	300x300	60x60	300x300	60x60	300x300			
Saturated	0.6	100	61.31	59.07	32.5	31	5.5	7.5	3.65	4.61	-------
		200	128.10	122.20					4.60		
		400	240.40	233.70					2.78		
	1.0	100	38.86	41.05	28	26.5	0	0	-------	5.35	-------
		200	98.70	91.83					6.96		
		400	187.50	182.60					2.61		
Constant water	0.6	100	77.49	74.31	36.5	36	21	16	4.10	1.37	23.80
		200	160.60	156.40					2.61		
		400	276.20	277.90					-------		
	1.0	100	52.48	52.05	31	29	3	4.5	0.82	6.45	-------
		200	117.00	118.10					-------		
		400	220.30	217.20					1.40		

5.6 Concluding remarks

The shear strength and volumetric behaviour of silty sand soil have been presented and shown to be prevailing of the behaviour of saturated and constant water content soils reported by many researches. For both studied void ratios, the obtained shear strength of specimens under constant water content is found to be distinctly greater than those obtained from saturated samples. The results showed that the samples compacted at e_i = 1.0 exhibited collapse behaviour during saturation stage, whereas the same samples did not show any volume change during stabilisation stage when tested under constant water content condition. It can also be seen from the test data that the specimen size is of secondary importance as there is no significant difference in shear strength parameters with increasing the shear box size. It was therefore recommended that the small-scale shear box can more efficient because less material is needed to determine the shear strength properties of cohesionless soil under saturated and constant water content conditions.

The next chapter will state the direct shear test results of soil-concrete interface (smooth and rough), and their interpretations with discussions.

CHAPTER SIX

SOIL-CONCRETE INTERFACE SHEAR BEHAVIOUR UNDER SATURATED AND CONSTANT WATER CONTENT CONDITIONS

6.1 Introduction

In this chapter, the results of direct shear tests on the soil-concrete (two concrete roughness) interface are presented. The experimental campaign has been designed based on concrete that is most commonly used in foundation material in Iraq. The two most popular types are the pre-cast foundation, for example, driven piles and the cast in-situ foundation, such as isolated foundation. The first one generates a pre-cast interface in which the surrounding soil is compressed during the installation process, while the second type generates a cast in-situ interface when the concrete is placed over previously prepared trench.

The large-scale direct shear tests (300 mm x 300 mm) were performed for the following constant applied vertical stresses: 100, 200, or 400 kPa and void ratio of e_i = 0.6 and 1.0 under saturated and constant water content conditions. The effect of void ratio and vertical stress level on the soil shear strength and corresponding volumetric changes are presented in the first part of this chapter. In the second part, the effect of surface roughness (smooth and rough) on the interface shear strength and volumetric characteristics are discussed in detail. The influence of soil suction on the interface shear strength behaviour of the tested material is also presented at the end of the current chapter.

6.2 Saturated interface test results and interpretations

6.2.1 Soil-smooth concrete interface shear tests of e_i = 0.6 and 1.0

A series of experimental direct shear tests were performed using the procedure that was explained in details in sections 4.5.2 and 4.6. A total of 12 direct shear tests were performed on initially saturated soil-smooth interface samples having e_i = 0.6 and 1.0, respectively. The specimens were prepared at a water content of 8±1%, saturated, consolidated, and then sheared under a constant vertical load and a constant rate of horizontal displacement of 0.05 mm/min. The results and the main achievements are shown in the followings.

Adequate saturation of all the tested samples took 24 hours (see section 4.6.1). Similar to the soil samples performed under saturated condition (Chapter 5), all the soil-smooth concrete samples compacted at e_i = 1.0, showed collapse behaviour during saturation process under nominal surcharge load (i.e. steel pad, equivalent of vertical stress of 1.33 kPa), while no collapse was observed for specimens compacted at e_i = 0.6. The initial and final conditions of the tested specimens during saturation stage as well as the observed collapse potential are presented in Table 6-1. It should be pointed out that the collapse potential has been calculated by applying nominal surcharge load (loading steel pad) to the sample at its initial water content. The soil has been subsequently flooded with water and left to settle until no further increase of vertical displacement has been recorded (Medero et al., 2009).

Table 6-1: Void ratio before, e_i and after e_f saturation stage and calculated collapse potential (soil-smooth samples)

Initial void ratio, e_i	Nominal stress, σ_n	Void ratio at end of saturation, e_f	Collapse potential, *CP* (%)
0.597	1.33	0.597	0
0.600		0.600	0
0.595		0.595	0
0.998		0.856	7.10
0.995		0.872	6.16
0.998		0.868	6.50

Based on these observations, it can be concluded that the soil presents collapse behaviour under very low level of applied vertical stress when compacted at e_i = 1.0,

and the magnitude of the observed collapse potential ranged from 6.16 to 7.10%. According to ASTM D 5333 – 92, the observed collapse potential of the tested soil can be classified as moderate to severe.

Figure 6.1 describes the volume variation during consolidation stage. For both studied void ratios, the volume reduction increased with increasing the level of applied vertical stress for all samples, as expected. Furthermore, at any stress level, samples prepared with high void ratio exhibited higher volumetric reduction than those prepared at low void ratio. This behaviour agrees with that found by other researchers (e.g. Wang et al., 2013; Tiwari and Al-Adhadh, 2014). The initial and final conditions of the soil-smooth samples during consolidation stage are summarized in Table 6-2.

Table 6-2: Soil-smooth samples void ratio before, e_i and after $e_{f\ cons}$ consolidation stage (saturated state)

Vertical stress, σ_v (kPa)	Initial condition	Consolidation stage		Volume reduction (%)
	e_i	e_f	Δ_e	
100	0.597	0.536	0.061	4.57
200	0.600	0.499	0.101	6.89
400	0.595	0.466	0.129	8.98
100	0.998	0.806	0.192	17.19
200	0.995	0.761	0.234	19.42
400	0.998	0.720	0.278	21.47

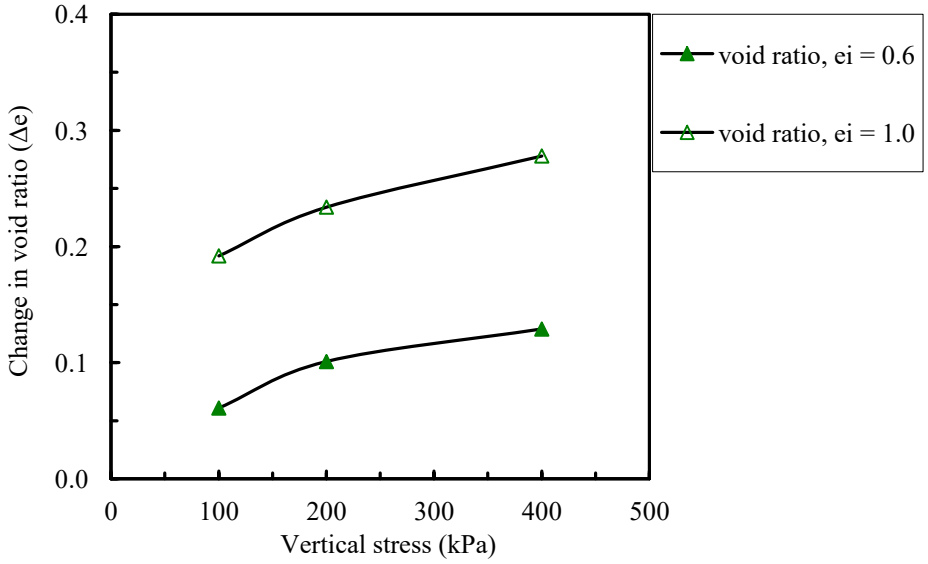

Figure 6.1: Void ratio variation against applied vertical stress during consolidation for saturated tests (soil-smooth samples).

The interface direct shear test results are best illustrated through the plots of the interface shear strength versus horizontal displacement and the related plots of vertical displacement versus horizontal displacement. Figures 6.2(a) and (b) show these relationships of the studied materials at e_i = 0.6 and 1.0.

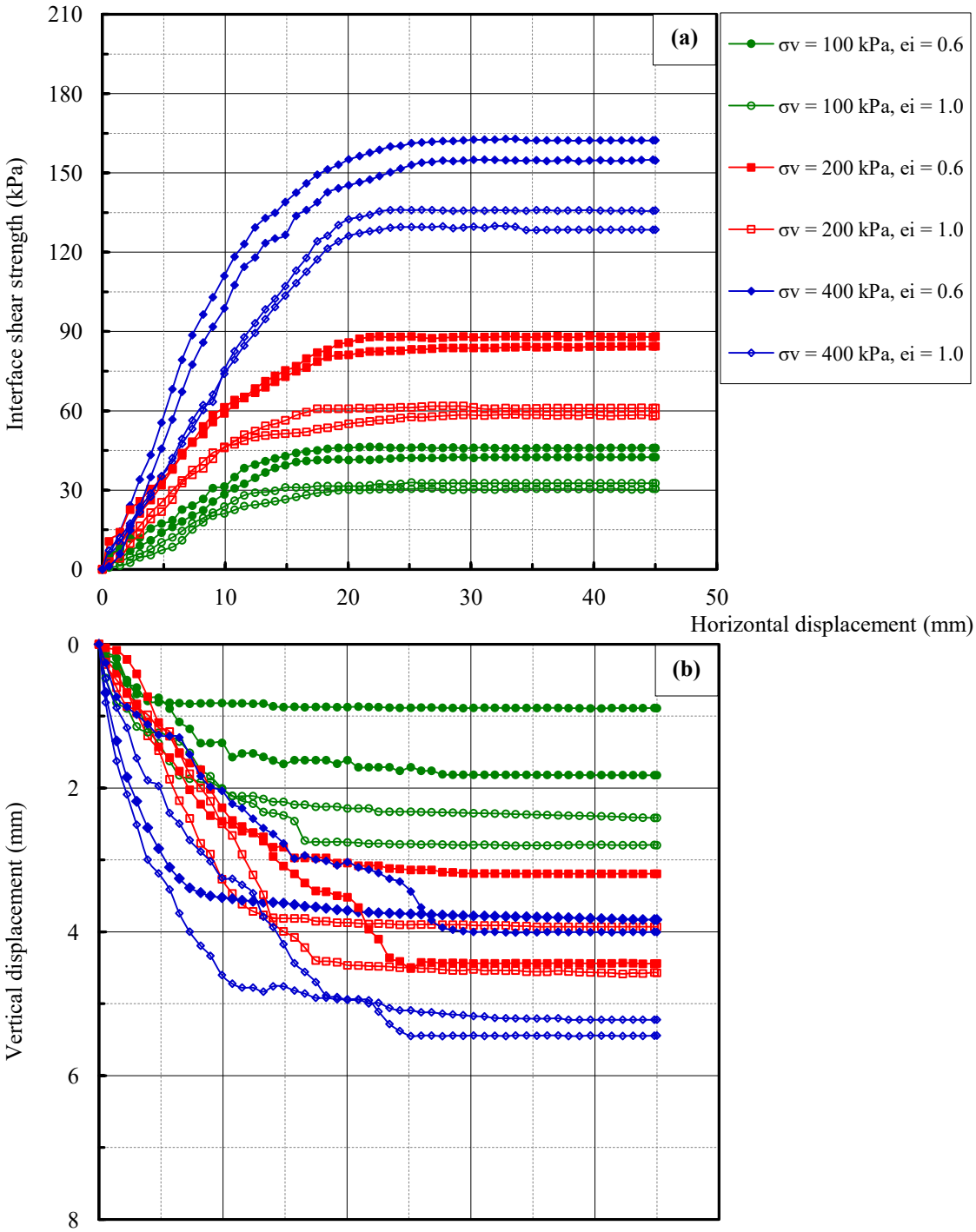

Figure 6.2: Direct shear results of soil-smooth interface samples for e_i = 0.6 and 1.0: **(a)** shear strength; **(b)** volumetric behaviour (saturated state).

For both studied void ratios, the shear strength is clearly influenced by the level of applied vertical stress. The higher the vertical stress, the larger is the obtained interface shear strength. At any stress level, denser specimens (e_i = 0.6) had a larger contact area and stronger interlocking at the interface resulting in a higher peak/maximum interface shear strength, while the looser specimens (e_i = 1.0), on the contrary, showed smaller shear strength. The later phenomenon for saturated soil-smooth interface tests was also noted by other researchers such as Potyondy 1961; Panchanathan and Ramaswamy, 1964; Kulhawy and Peterson, 1979; Desai et al, 1985; Fakharian and Evgin, 1996; Chu and Yin, 2005.

Moreover, Figure 6.2(a) also reveals that the shear displacement corresponding to the peak/maximum interface shear strength increases with increasing the applied vertical stress. This means that the specimen stiffness increases as the vertical stress level is increased. The horizontal displacement corresponding to the peak/maximum interface shear strength of specimens at e_i = 0.6 and 1.0 tested under different vertical stress levels are presented in Table 6-3. As expected, the horizontal displacements of specimens at e_i = 0.6 corresponding to the peak/ maximum shear strength are greater than those of e_i = 1.0 specimens. This behaviour agrees with that found by Kalhor 2012; Ismail and Behbehani 2014; Farooq et al., 2015.

Referring to Figure 6.2(a), it can be clearly seen that the loose and dense specimens show no clear interface peak shear strengths, indicating mostly strain hardening behaviour. In other words, the peak and residual shear strengths are approximately the same. The corresponding curves of vertical displacement and horizontal displacement show approximately steady state behaviour (i.e. little to no change in vertical displacement) in the post peak region for both studied void ratios specimens (Figure 6.2(b)). This behaviour can be attributed to the sliding of the soil particles which was the predominant mechanism in the post-peak region at the interface of the smooth concrete surface. This observation was also made by several researchers (e.g. Kulhawy and Peterson, 1979; Uesugi and Kishida, 1986; Iscimen, 2004; Al-Mhaidib, 2006).

In terms of volume changes, as expected, a clear increase in the vertical displacement as the applied vertical stress increase can be observed as shown in Figure 6.2(b). This trend of behaviour was noticed for both studied void ratios. The higher the void ratio, the greater volume change is observed.

Table 6-3: Values of horizontal displacement corresponding to the peak/maximum shear strength for e_i = 0.6 and 1.0 specimens (soil-smooth interface)

Vertical stress, σ_v (kPa)	Initial void ratio, e_i = 0.6	Initial void ratio, e_i = 1.0	Horizontal displacement at peak/maximum shear strength, δ_h (mm)	
	Peak/maximum shear strength, τ (kPa)	Peak/maximum shear strength, τ (kPa)	e_i = 0.6	e_i = 1.0
100	39.34	26.61	14.88	12.42
200	80.96	59.23	18.32	16.60
400	159.96	126.15	23.43	20.04

6.2.2 Soil-rough concrete interface shear tests of e_i = 0.6 and 1.0

As mentioned earlier, one of the main interesting factors for many researchers and particularly of this research is the surface roughness of the structural material (i.e. concrete) which dominates the interface shear strength behaviour. The test procedure and calculations of soil-rough concrete interface specimens were performed by following the same procedure adopted in the previous section (section 6.2.1).

During saturation stage, the soil-rough interface specimens at e_i = 1.0 showed similar behaviour (i.e. collapse phenomenon under very low level of applied vertical stress) to the soil-smooth interface tests, which was expected as the collapse response is defined by the soil. The initial and final conditions of the soil-rough concrete interface specimens during saturation stage as well as the observed collapse potential CP are presented in Table 6-4.

Table 6-4: Void ratio before, e_i and after e_f saturation stage and calculated collapse potential (soil-rough specimens)

Initial void ratio, e_i	Nominal stress, σ_n	Void ratio at end of saturation, e_f	Collapse potential, *CP* (%)
0.600	1.33	0.600	0
0.595		0.595	0
0.597		0.597	0
0.994		0.872	6.11
0.998		0.866	6.60
0.996		0.851	7.25

As in the soil-smooth concrete interface tests, the results of soil-rough tests during consolidation stage showed the same behaviour, in the sense that the volume reduction increased with increasing the applied vertical stress level for all samples as shown in Figure 6.3. Moreover, at any stress level, the specimens compacted at e_i = 1.0 showed higher volume reduction in comparison to those prepared at e_i = 0.6, as expected. The characteristics of the saturated soil-rough interface specimens before and after consolidation stage are presented in Table 6-5.

Table 6-5: Soil-rough samples void ratio before, e_i and after $e_{f\,cons}$ consolidation stage (saturated state)

Vertical stress, σ_v (kPa)	Initial condition	Consolidation stage		Volume reduction (%)
	e_i	e_f	Δ_e	
100	0.600	0.528	0.072	6.61
200	0.595	0.497	0.098	8.62
400	0.597	0.480	0.117	9.67
100	0.994	0.823	0.171	17.83
200	0.998	0.764	0.234	20.66
400	0.996	0.727	0.269	22.60

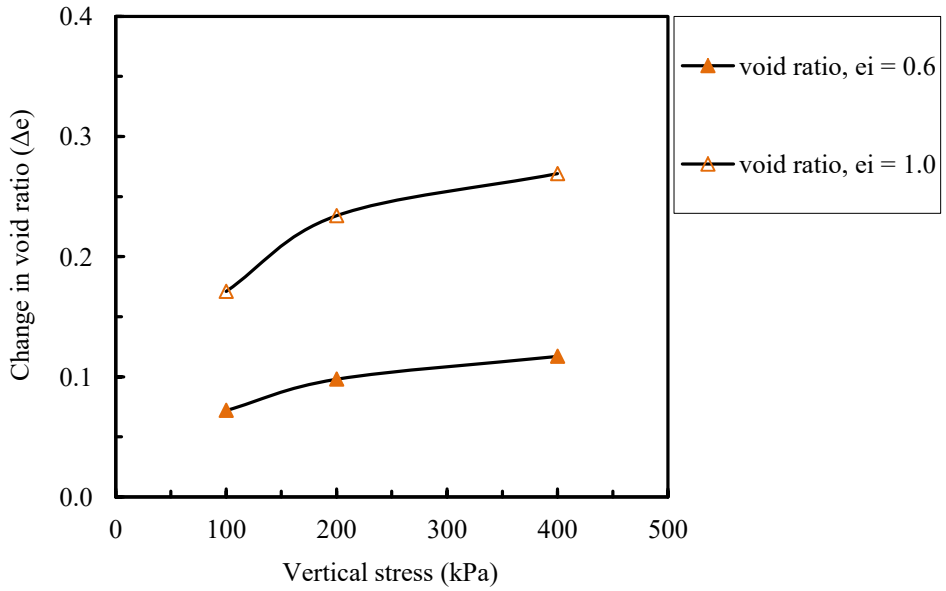

Figure 6.3: Void ratio variation against applied vertical stress during consolidation for saturated tests (soil-rough samples).

The maximum interface shear strength of the soil-rough specimens, for both studied void ratios, increased with the increasing level of applied vertical stress as shown in Figure 6.4(a).

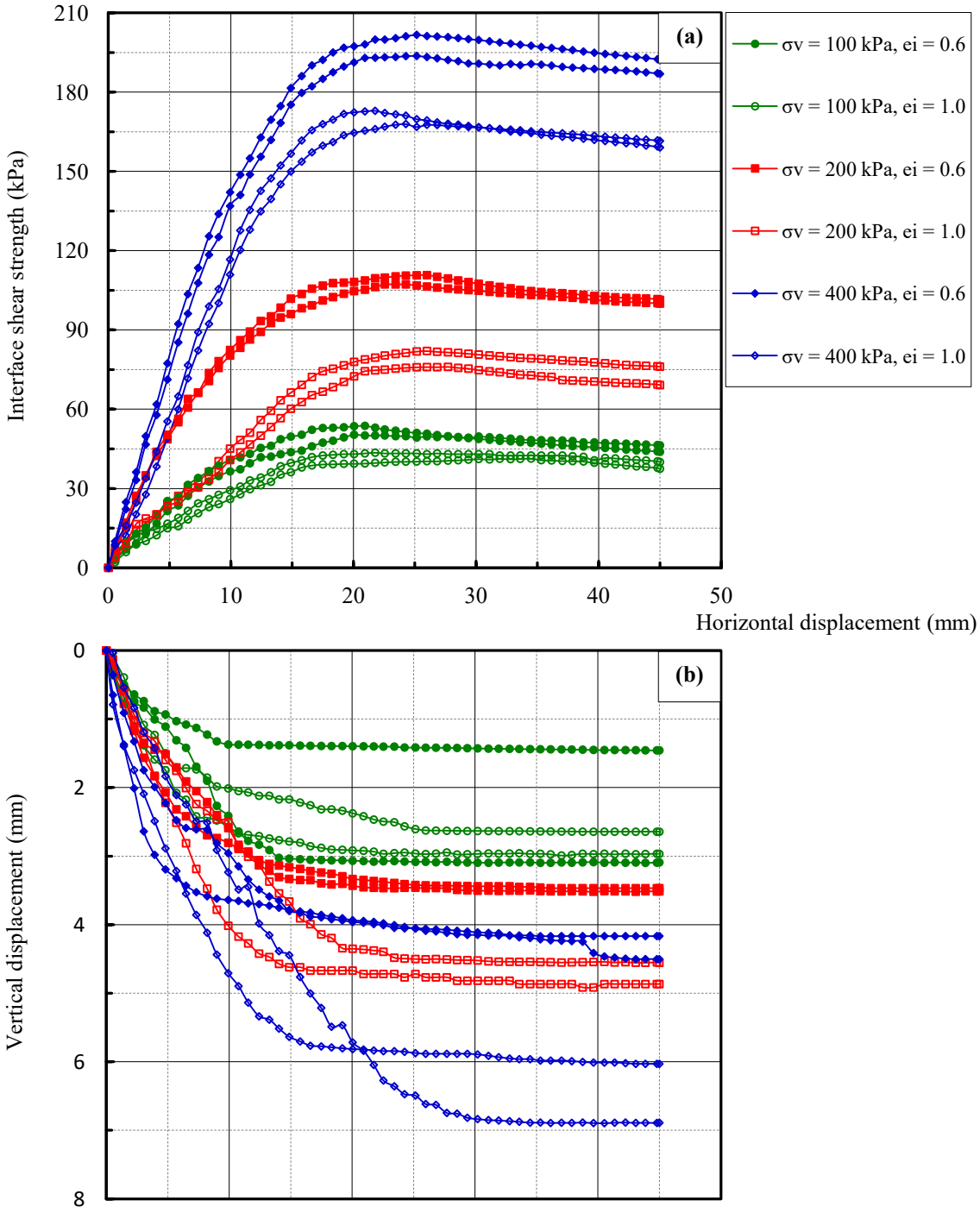

Figure 6.4: Direct shear results of soil-rough interface samples for e_i = 0.6 and 1.0: **(a)** shear strength; **(b)** volumetric behaviour (saturated state).

The test results presented in Figure 6.4 revealed that the shear strength is clearly influenced by the value of the initial void ratio of the tested samples. As expected, as the void ratio increased, a decrease in the shear strength was observed. All curves of the interface shear strength and horizontal displacement gradually increased (showing hardening behaviour) in the pre-peak region until the peak strength point. This agrees with the observation made by other researchers such as Potyondy 1961; Uesugi et al., 1990; Paikowsky et al., 1995; Chu and Yin, 2006; Tiwari and Al-Adhadh, 2014. For both studied void ratios, the interface shear strength curves of the specimens tested under 100 kPa applied vertical stress changed gradually from hardening behaviour (without showing any noticeable peak shear strength) to a gentle hardening-softening behaviour (Figure 6.4(a)).

Strain softening behaviour becomes noticeable with the increasing level of applied vertical stress (i.e. 200 and 400 kPa) for samples that have e_i = 0.6 and 1.0. A smooth peak shear strength is achieved and followed by a gradual reduction in the shear strength. In other words, the shearing behaviour of the tested samples changed from stiff behaviour to ductile behaviour when tested under high levels of vertical stress. Looking at Figure 6.4(a), it can be seen that the results are similar to those obtained with smoother concrete interface, in the sense that the horizontal displacement corresponding to the peak and/or maximum shear strength increased with the increase of the applied vertical stress. This trend of behaviour was observed for both studied void ratios specimens as shown in Table 6-6. It can also be noted from Table 6-6 that at any stress level, the horizontal displacement corresponding to the peak and/or maximum shear strength shows a clear decrease with increasing the void ratio of the tested samples.

To better understand the interface shear strength behaviour, the volumetric response associated with the shearing process needs to be closely considered. As expected, all specimens exhibited a tendency to increase in the vertical displacement (volume reduction) with increasing the level of applied vertical stress. At any stress level, Figure 6.4(b) shows that the specimens of e_i = 1.0 exhibited greater volume reduction than that of e_i = 0.6 specimens, as expected. The higher the vertical stress, the bigger is the volume reduction. This behaviour was also found by several researchers such as Chu and Yin, 2006 and Tiwari and Al-Adhadh, 2014. It can also be seen from Figures 6.4(a) and (b) that the shear strength-horizontal displacement curves maximum are almost consistent with their corresponding vertical displacement-horizontal displacement

curves (Figure 6.4(b)) in which the peak shear strength point approximately coincided with the maximum interface shear strength point.

Table 6-6: Values of horizontal displacement corresponding to the peak/maximum shear strength for e_i = 0.6 and 1.0 samples (soil-rough interface)

Vertical stress, σ_v (kPa)	Initial void ratio, e_i = 0.6	Initial void ratio, e_i = 1.0	Horizontal displacement at peak/maximum shear strength, δ_h (mm)	
	Peak/maximum shear strength, τ (kPa)	Peak/maximum shear strength, τ (kPa)	e_i = 0.6	e_i = 1.0
100	50.32	40.92	19.20	17.48
200	107.20	81.82	23.43	21.76
400	201.64	163.64	25.15	23.43

6.3 Influence of surface roughness (smooth versus rough)

As described earlier in Chapter 2, a number of influencing factors primarily governed the saturated interface shear behaviour. Among all the factors, the surface roughness of the construction material is the most important factor which may influence the mechanical behaviour of the interface. All previous interface studies in the literature emphasised the important role of the surface roughness.

Typical plots for the effect of surface roughness (smooth and rough) on the strength and volumetric behaviour of the interface are shown in Figures 6.5 and 6.6. The presented results indicate that the surface roughness significantly affected the peak and the residual shear strength as well as the volumetric behaviour of the tested samples. Several important observations can be made from these plots regarding the influence of the surface roughness and are listed in the following:

1- The peak/maximum interface shear strength is dependent on the surface roughness of the concrete. For both studied void ratios, a smooth peak shear strength was observed for soil-rough surface samples when tested under 200 and 400 kPa vertical stress.

2- The shear strength and the corresponding vertical displacement for the rough interface were larger than those of the smooth interface for both studied void ratios specimens and for all applied vertical stress levels used in this study, as

expected and found in the literature (e.g. Panchanathan and Ramaswamy, 1964; Bosscher and Ortiz, 1987; Uesugi et al., 1990; Chu and Yin, 2006.

3- Peak and/or maximum shear strength for the soil-rough interface was mobilized at larger horizontal displacement in comparison with soil-smooth specimens, illustrating an increase in the degree of interlocking between soil particles and concrete interface with increasing surface roughness (See Table 6-3 and Table 6-6) and thereby an increase in the horizontal displacement to reach the failure point.

4- At the beginning of the shearing process, both smooth and rough interfaces showed similar trend of behaviour until the peak shear strength was achieved. In the post-peak region, the smooth interface exhibited a steady state without showing any noticeable change in the vertical displacement (strain hardening behaviour). Conversely, the rough interface showed a clear decrease in the shear strength (strain softening behaviour) with the progress of horizontal displacement until the residual shear strength was achieved. This can be attributed to the differences in the shearing mechanisms between rough and smooth interfaces. This behaviour agrees with that found by many researchers (e.g. Al-Mhaidib, 2006 Hossain 2010; Jing et al., 2016).

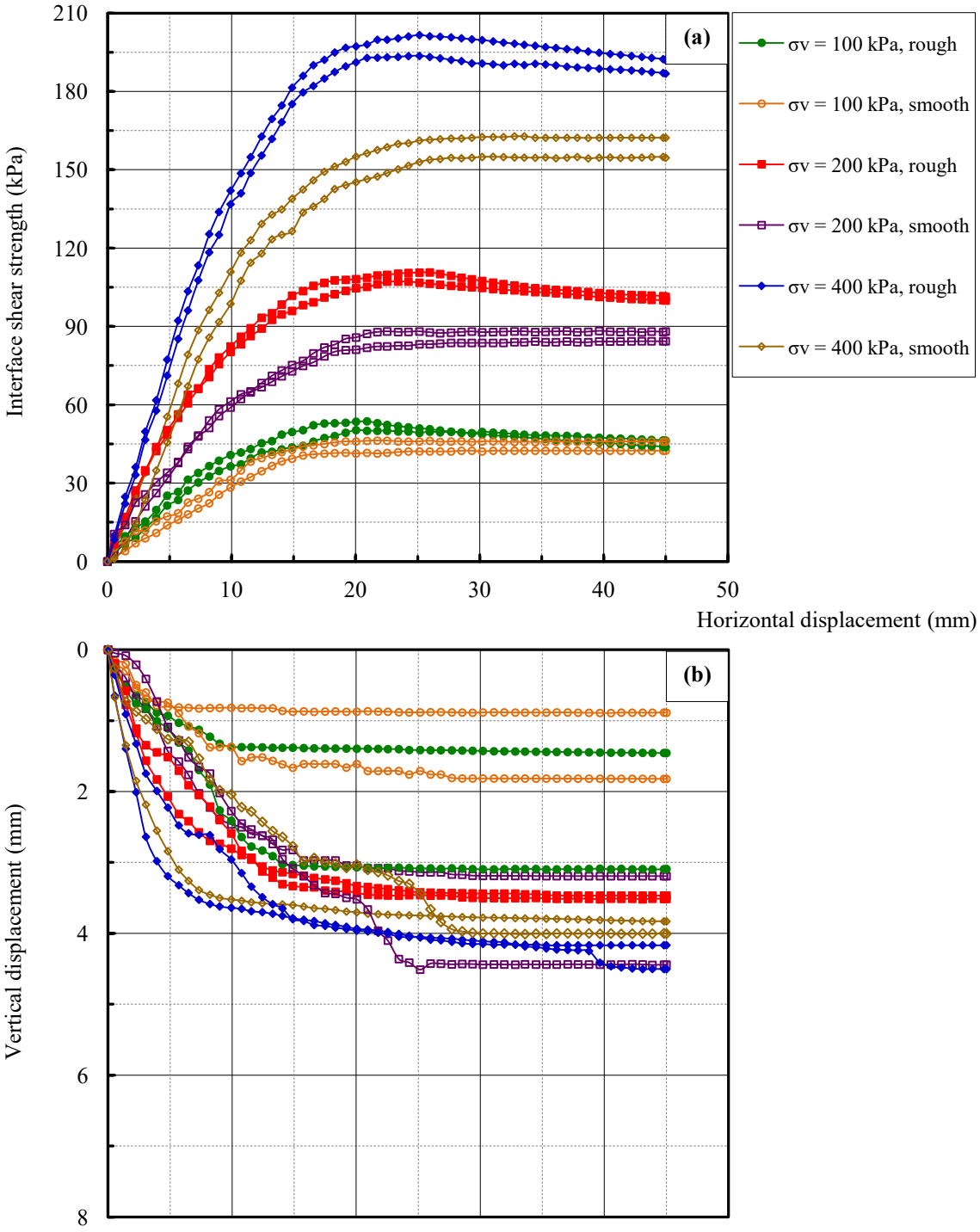

Figure 6.5: Results showing effect of surface roughness on **(a)** interface shear strength and **(b)** volumetric behaviour of samples at $e_i = 0.6$.

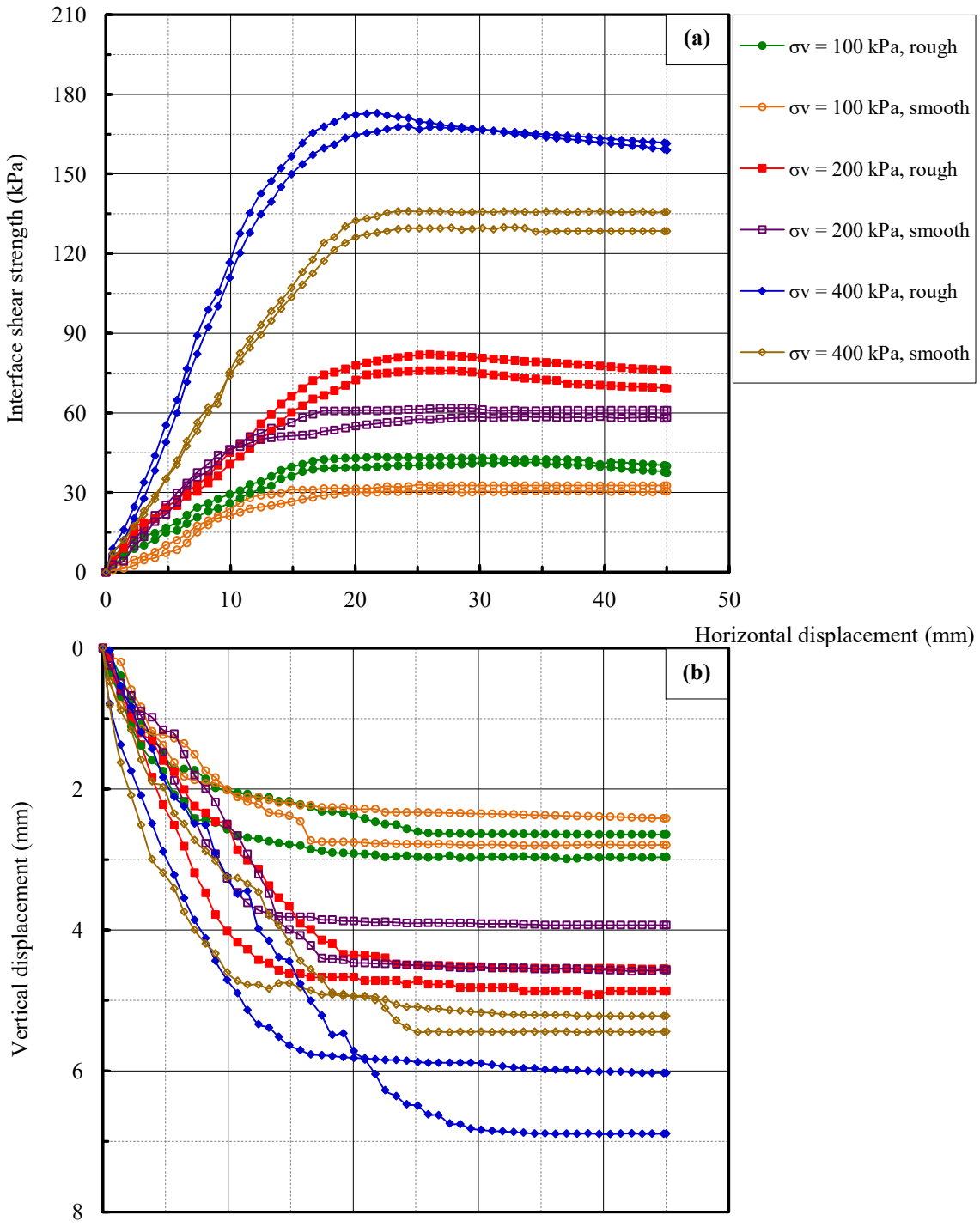

Figure 6.6: Results showing effect of surface roughness on **(a)** interface shear strength and **(b)** volumetric behaviour of samples at e_i = 1.0.

6.4 Interface test results and interpretations of specimens under constant water content

6.4.1 Soil-smooth concrete interface shear tests of e_i = 0.6 and 1.0

As with the soil tests (Chapter 5), the time required to attain soil suction stabilisation state was adopted equal to nine days. Unlike the saturated specimens at e_i = 1.0, the soil-smooth interface samples did not show any changes in the void ratio (volume reduction) after the end of suction stabilisation stage. During consolidation stage, a similar behaviour was seen for soil-smooth interface as was seen for the soil, in the sense that the reduction of matric suction of the tested samples decreased with increase of the vertical stress and continued until the end of the consolidation stage as shown in Figures 6.7 (a) and (b). Looser samples (e_i = 1.0) exhibited higher reduction in the matric suction as compared to the denser samples (e_i = 0.6). This trend of behaviour was observed for all levels of vertical stress considered in this study. It can be seen from Table 6-7 that there was a noticeable decrease in the void ratio associated with an increase in the degree of saturation, as expected. Note that tests described in this section were undertaken using large-scale direct shear apparatus and the matric suction was measured during all stages of the experimental procedure.

Table 6-7: Soil-smooth sample void ratio before, e_i and after e_{fshe} consolidation stage (constant water content)

Vertical stress, σ_v (kPa)	Consolidation stage							
	Initial condition			Final condition				
	e_i	S_{ri} (%)	ρ_{dry} (kg/m^3)	e_f	S_{rf} (%)	ρ_{dry} (kg/m^3)	Δ_e	ΔS_r
100	0.597	35.63	1665	0.564	37.71	1700	0.033	2.08
200	0.593	35.89	1669	0.535	39.78	1732	0.058	3.89
400	0.600	35.45	1662	0.515	41.31	1755	0.085	5.86
100	0.995	21.38	1333	0.892	23.85	1405	0.103	2.47
200	0.998	21.33	1331	0.798	26.67	1479	0.200	5.34
400	1.000	21.27	1330	0.758	28.06	1513	0.242	6.79

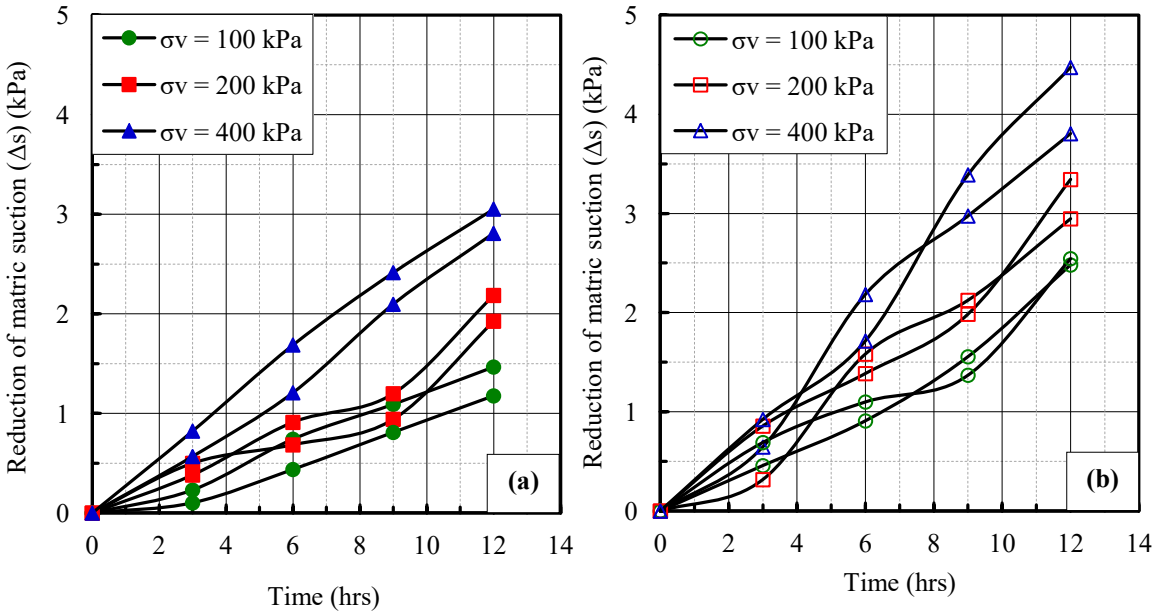

Figure 6.7: Reduction of matric suction vs. time during consolidation stage; **(a)** e_i = 0.6, **(b)** e_i = 1.0 (soil-smooth samples).

Figure 6.8 shows that the volume reduction of the tested soil-smooth samples during consolidation, for both studied void ratios, increased noticeably with the increase of the applied vertical stress during consolidation stage. At any stress level, looser samples (e_i = 1.0) revealed higher volume reduction than the denser samples (e_i = 0.6), as expected.

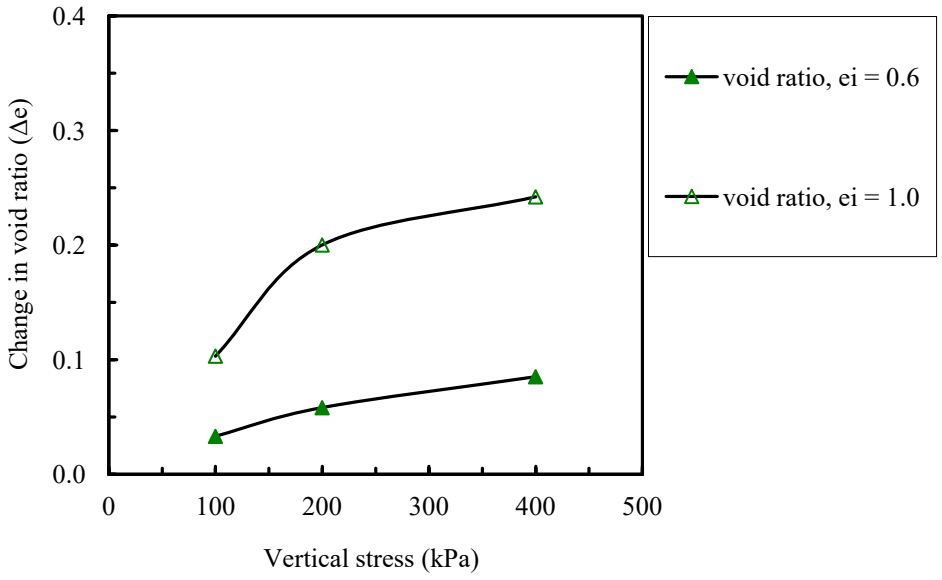

Figure 6.8: Void ratio variation against applied vertical stress during consolidation for constant water content tests (soil-smooth samples).

The test results of the interface shear strength versus horizontal displacement of the tested materials (soil-smooth) at e_i = 0.6 and 1.0 are presented in Figure 6.9(a). For both studied void ratios, as the vertical stress is increased, the interface shear strength increases, as expected. It is clear from the analysis that, at any stress level, the tested samples (e_i = 0.6 and 1.0) exhibited little to no strain softening behaviour in the post-peak region. The smooth interface shear strength increased gradually up to the maximum shear strength followed by a steady state behaviour (non-peak shear strength pattern). This behaviour can be attributed to the reason that the smooth interface exhibited stick-slip phenomenon after the maximum shear strength was achieved. The hardening stick-slip behaviour continued until the end of the shearing process. Hamid (2005) and Borana (2014) conducted laboratory tests to investigate the effects of different surface roughness on the shear strength and volumetric behaviour for different types of soil. Their findings revealed a noticeable stick-slip behaviour followed by peak/maximum shear strength when the soil specimens sheared against smooth counterface. They postulated that the shearing mechanism for the smooth interface is governed by sliding rather than interlocking between soil particles and smooth steel interface.

As with the observations of the soil tests (Chapter 5), the soil-smooth interface samples showed an increase in the horizontal displacement corresponding to the maximum and/or peak shear strength with the increasing of vertical stress level as shown in Table 6-8. This trend of behaviour was observed for both studied void ratios. Test results presented in Figure 6.9(a) and Table 6-8 reveal that the maximum/peak shear strength for the tested specimens at e_i = 0.6 was mobilized at larger horizontal displacement when compared with those observed on samples at e_i = 1.0.

Table 6-8: Values of horizontal displacement corresponding to the peak/maximum shear strength for e_i = 0.6 and 1.0 specimens (soil-smooth interface)

Vertical stress, σ_v (kPa)	Initial void ratio, e_i = 0.6	Initial void ratio, e_i = 1.0	Horizontal displacement at peak/maximum shear strength, δ_h (mm)	
	Peak/maximum shear strength, τ (kPa)	Peak/maximum shear strength, τ (kPa)	e_i = 0.6	e_i = 1.0
100	52.11	38.44	14.04	10.75
200	101.74	76.58	16.60	12.42
400	193.62	154.62	18.32	14.04

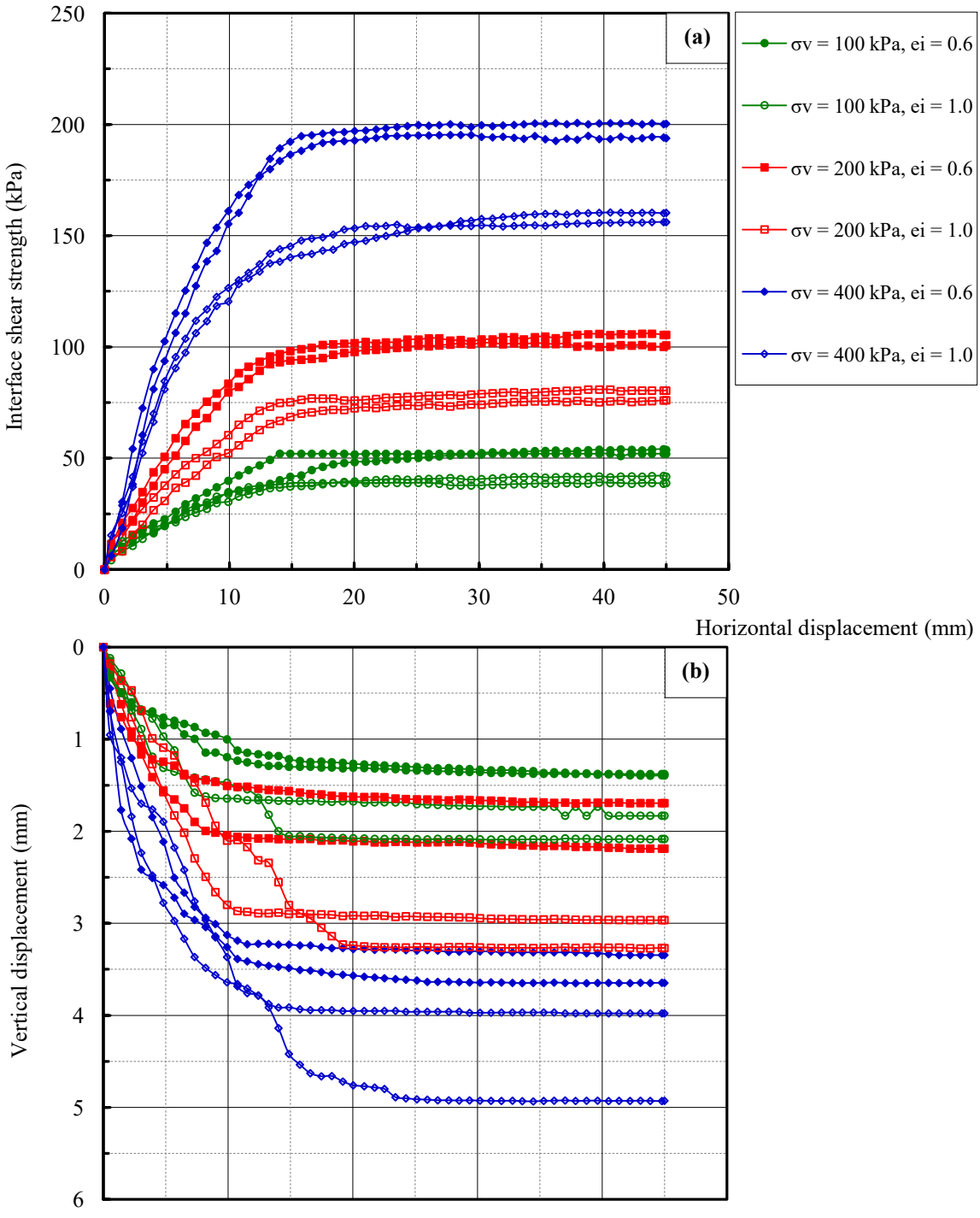

Figure 6.9: Direct shear results of soil-smooth interface samples at e_i = 0.6 and 1.0: **(a)** shear strength; **(b)** volumetric behaviour (constant water content).

Corresponding vertical displacement versus horizontal displacement curves of specimens at e_i = 0.6 and 1.0 are shown in Figure 6.9(b). These curves showed that all the tested specimens showed an increase in the volume reduction until the horizontal displacement slightly before the horizontal displacement corresponding to the maximum

shear strength. After that the specimens remained at steady state until the soil reached the residual shear strength. Moreover, at any stress level, the specimens with e_i = 1.0 exhibited greater volume change than those with e_i = 0.6, as expected.

Similar to soil tests (Chapter 5), the matric suction has been corrected to zero at the beginning of the shearing stage. The matric suction evolution during shearing is plotted against the horizontal displacement and presented in Figure 6.10. Similar to the soil tests, for both studied void ratios, the soil suction during shearing process decreased with increasing the applied vertical stress level. This figure also shows that the horizontal displacement corresponding to the maximum matric suction approximately coincided with the horizontal displacement corresponding to the maximum shear strength. This behaviour means that there is clear contribution of the matric suction in increasing the shear strength in the pre-peak region associated with an increase in the applied vertical stress, similar to the observations of soil tests.

It can also be noticed that for both studied void ratios, a little increase in the matric suction occurred after reaching the maximum shear strength. This behaviour agrees with that found by Hamid (2005) who mentioned that the role of the matric suction is less significant after the peak shear strength. The values of measured suction corresponding to the peak and residual shear strengths are presented in Table 6-9. Figure 6.10 also shows that there is a noticeable dependency of matric suction on the initial value of void ratio. Samples prepared at e_i = 1.0 revealed higher matric suction than those prepared at e_i = 0.6. This trend of behaviour was observed for all levels of vertical stress.

Table 6-9: The values of measured suction at peak and residual shear strengths of soil-smooth samples (constant water content)

Initial void ratio, e_i	Vertical stress, σ_v (kPa)	Peak/maximum shear strength (kPa)	Ψ_{peak} (kPa)	$\Psi_{residual}$ (kPa)
0.597	100	52.11	3.512	4.313
0.593	200	101.74	6.716	7.493
0.600	400	193.62	9.268	10.189
0.995	100	38.44	2.969	3.087
0.998	200	76.58	4.509	5.816
1.000	400	154.62	7.856	8.897

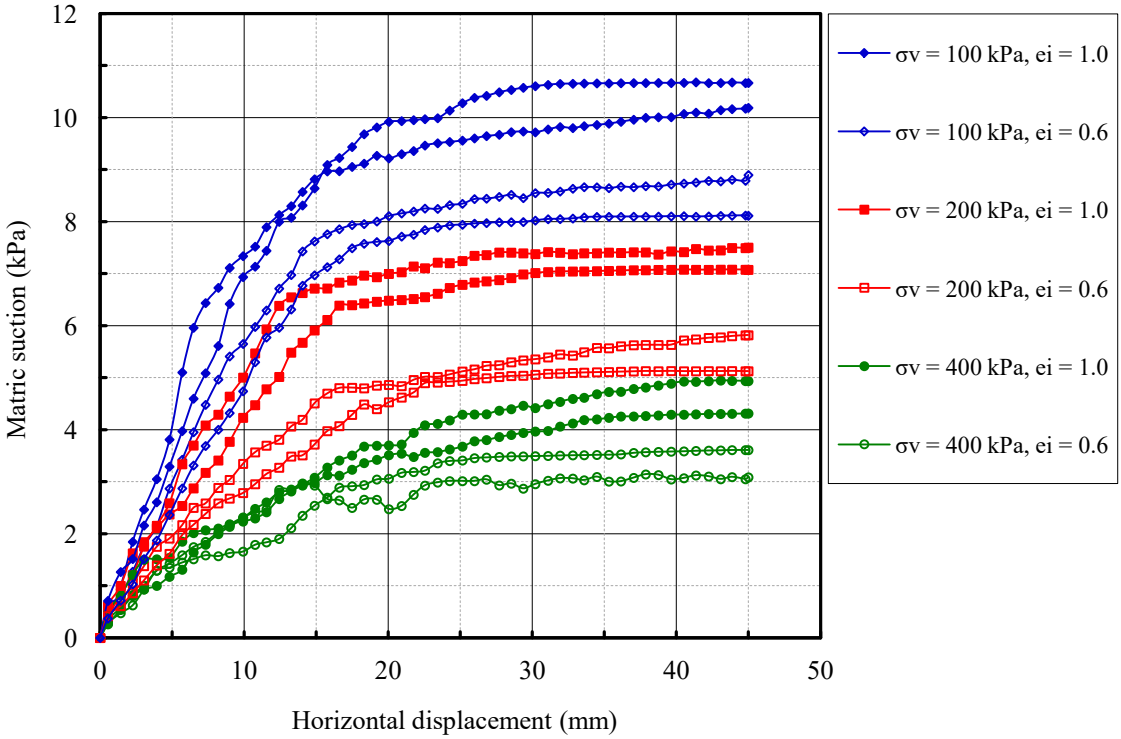

Figure 6.10: Evolution of matric suction with horizontal displacement during shearing process of soil-smooth samples at e_i = 0.6 and 1.0.

6.4.2 Soil-rough concrete interface shear tests of e_i = 0.6 and 1.0

The soil-rough interface samples exhibited similar trend of behaviour as the one of the smooth interface during suction stabilisation stage for samples with e_i = 1.0. Figure 6.11 shows the change in void ratio versus applied vertical stress for e_i = 0.6 and 1.0 samples during consolidation stage.

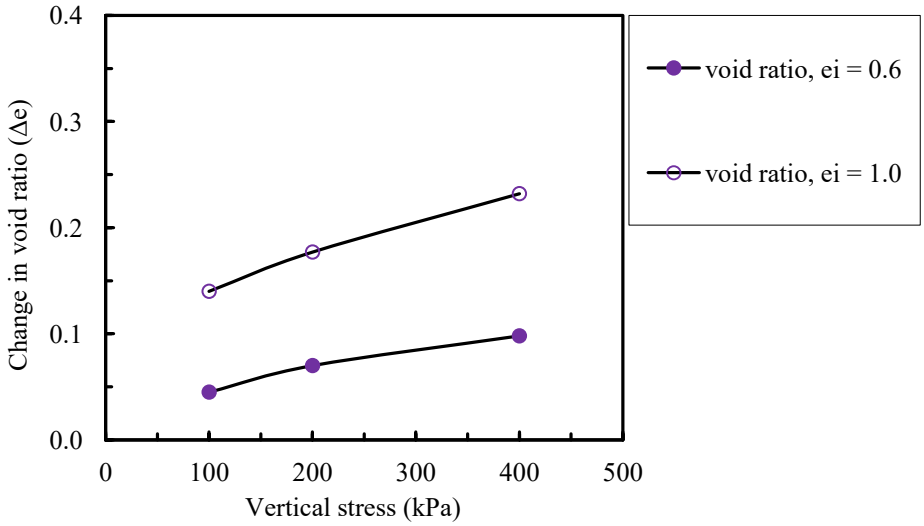

Figure 6.11: Void ratio variation against applied vertical stress for constant water content tests (soil-rough samples).

The volume reduction increased with increase of the applied vertical stress for all tested specimens with both studied void ratios. At any stress level, samples prepared with e_i = 1.0 exhibited higher decrease in void ratio than those prepared with e_i = 0.6. Table 6-10 presents the values of void ratios before e_i and after e_f consolidation stage. Similar to soil-smooth interface tests, the soil-rough interface specimens exhibited gradual reduction in the matric suction with increase of the applied vertical stress, as shown in Figure 6.12. This trend of behaviour was observed for both studied void ratios and for all levels of applied vertical stress.

Table 6-10: Soil-rough sample void ratio before, e_i and after e_{fshe} consolidation stage (constant water content)

Vertical stress, σ_v (kPa)	Consolidation stage							
	Initial condition			Final condition				
	e_i	S_{ri} (%)	ρ_{dry} (kg/m^3)	e_f	S_{rf} (%)	ρ_{dry} (kg/m^3)	Δ_e	ΔS_r
100	0.594	35.80	1668	0.549	38.73	1717	0.045	3.27
200	0.598	35.59	1664	0.528	42.32	1740	0.070	4.85
400	0.593	35.86	1669	0.495	45.25	1779	0.098	7.50
100	0.997	21.32	1331	0.857	28.45	1432	0.140	3.48
200	1.000	21.26	1330	0.823	29.82	1459	0.177	4.58
400	0.994	21.41	1334	0.762	32.65	1509	0.232	6.52

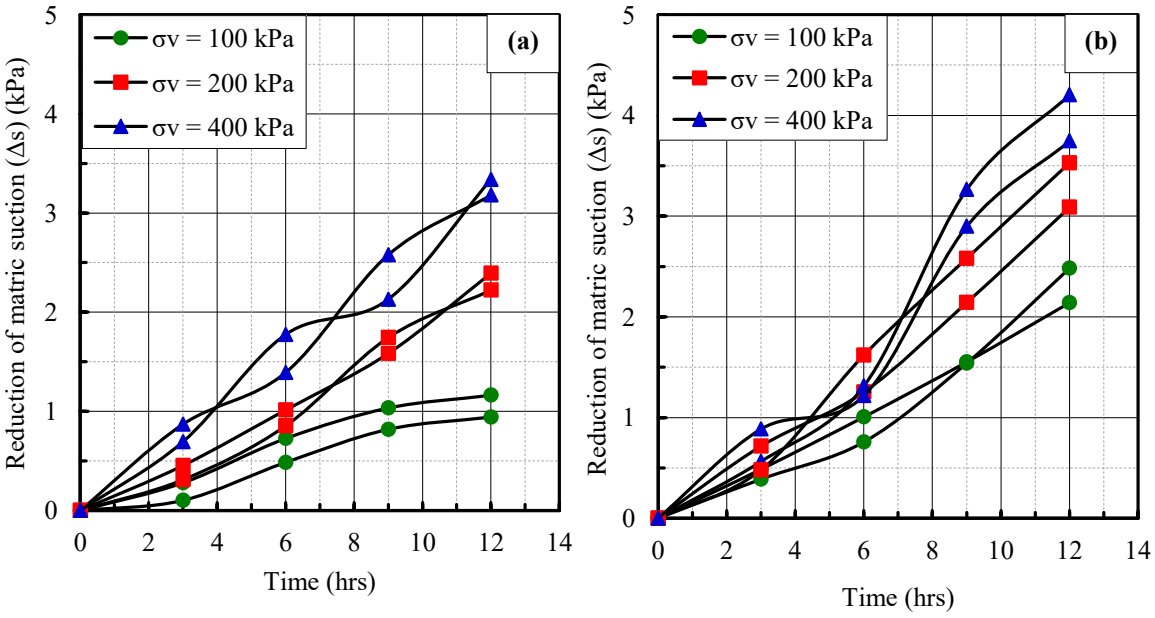

Figure 6.12: Reduction of matric suction vs. time during consolidation stage; **(a)** e_i = 0.6, **(b)** e_i = 1.0 (soil-rough samples).

Figure 6.13(a) shows that for both studied void ratios, the shear strength of the soil-rough interface samples was increased as the level of the applied vertical stress increased. All the shear strength curves presented gradual hardening behaviour to a horizontal displacement slightly before the peak strength point. For samples with e_i = 0.6 tested under 100, 200 and 400 kPa vertical stress, a noticeable strain softening behaviour was observed after the peak shear strength was attained. Dense samples exhibit a more brittle strain softening behaviour with increasing the level of applied vertical stress.

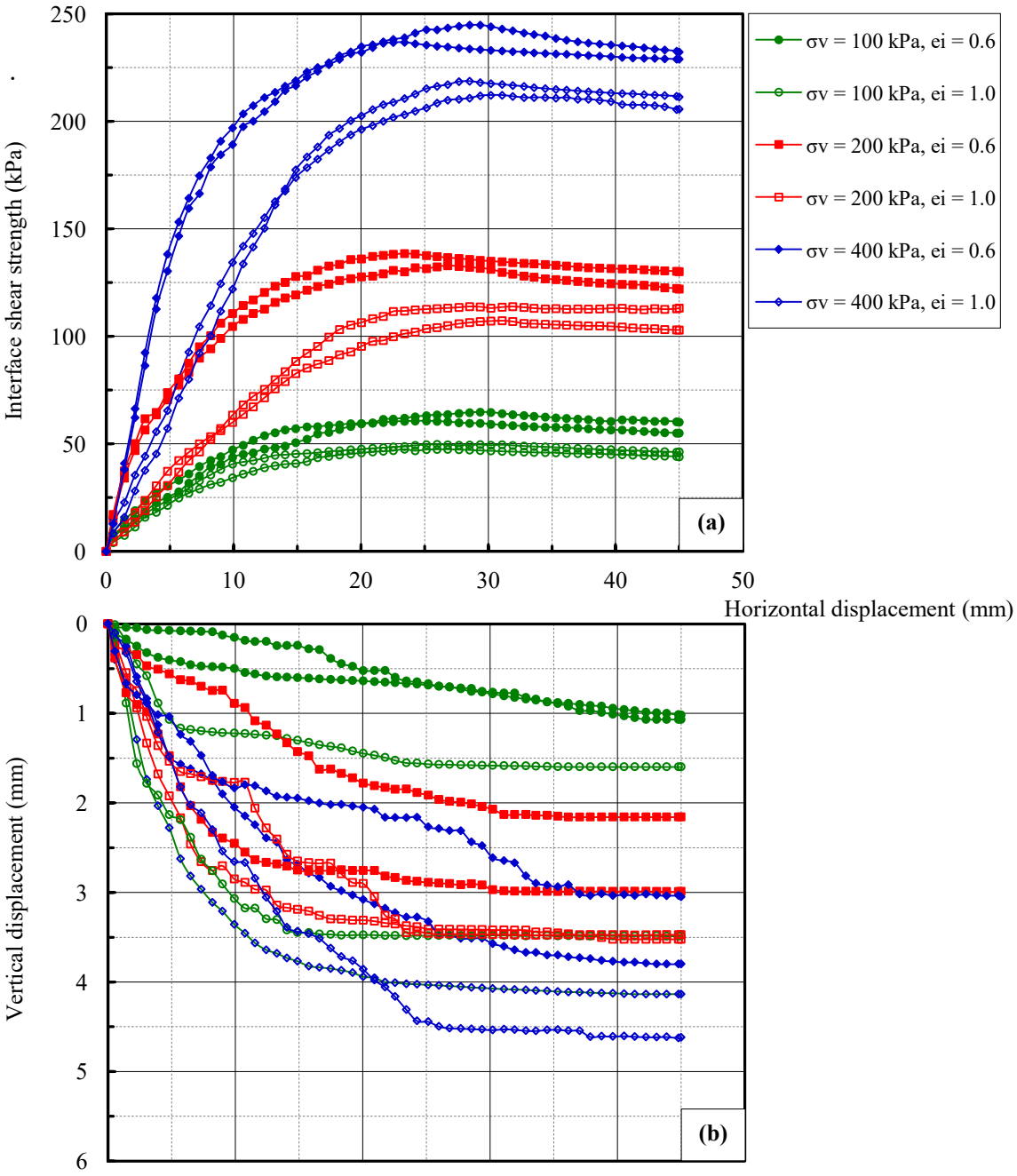

Figure 6.13: Direct shear results of soil-rough interface samples at e_i = 0.6 and 1.0: **(a)** shear strength; **(b)** volumetric behaviour (constant water content).

Similar strain softening trend could be noticed as well with shearing of loose samples at 400 kPa vertical stress. At higher vertical stress level (i.e. 400 kPa), the contraction becomes more pronounced for samples with e_i = 1.0 and hence, the soil behaves as a dense sample and shows strain softening behaviour in the post-peak region. Whereas, specimens with e_i = 1.0, tested at 100 and 200 kPa vertical stress exhibited no to a little reduction in the shear strength with increasing horizontal displacement beyond the peak shear strength (softening-hardening behaviour). Test results presented in Figure 6.13(a) also showed that at any stress level, the peak/maximum shear strength of the soil-rough interface samples decreases as the void ratio is increased, as expected and shown in the literature (e.g. Murad et al., 2007; Muthukkuumaran 2011; Tiwari and Al-Adhadh, 2014;).

Similar to the observations for soil and soil-smooth interface specimens, the horizontal displacement corresponding to the peak shear strength increased with increasing the level of the applied vertical stress as shown in Table 6-11. This trend of behaviour was seen for both studied void ratios (e_i = 0.6 and 1.0). Corresponding vertical displacement versus horizontal displacement curves are shown in Figure 6.13(b). These curves highlight that all specimens exhibited a tendency to increase in the vertical displacement (volume reduction) with increasing the level of applied vertical stress. The specimens with e_i = 1.0 exhibited greater volume reduction than those of with e_i = 0.6 specimens, as seen for soil and smooth-interface specimens.

Table 6-11: Values of horizontal displacement corresponding to the peak/maximum shear strength for e_i = 0.6 and 1.0 specimens (soil-rough interface)

Vertical stress, σ_v (kPa)	Initial void ratio, e_i = 0.6	Initial void ratio, e_i = 1.0	Horizontal displacement at peak/maximum shear strength, δ_h (mm)	
	Peak/maximum shear strength, τ (kPa)	Peak/maximum shear strength, τ (kPa)	e_i = 0.6	e_i = 1.0
100	60.22	47.73	23.43	20.04
200	132.43	106.28	25.98	25.15
400	244.71	211.43	29.37	27.70

Figure 6.14 shows the evolution of matric suction with the horizontal displacement during shearing process for soil-rough specimens. For both studied void ratios, the

matric suction decreased as the vertical stress increased. It can also be noted from Figure 6.14 that at any stress level, the measured matric suction of samples at e_i = 1.0 is greater than that of samples at e_i = 0.6, as expected considering the samples have larger pores with e_i = 1.0 and for both studied void ratios the specimens prepared with same initial degree of saturation. The values of measured suction corresponding to the peak and residual shear strengths are presented in Table 6-12.

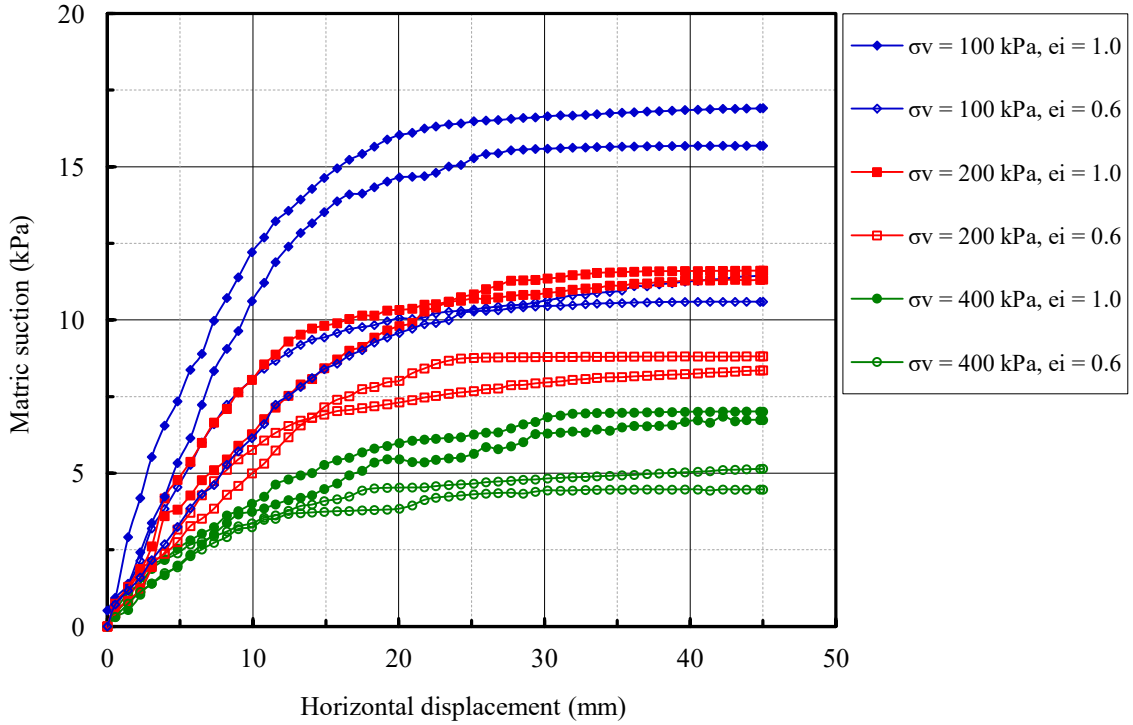

Figure 6.14: Evolution of matric suction with horizontal displacement during shearing process of soil-rough samples at e_i = 0.6 and 1.0.

Table 6-12: Values of measured suction at peak and residual shear strengths (soil-rough samples)

Initial void ratio, e_i	Vertical stress, σ_v (kPa)	Peak/maximum shear strength (kPa)	Ψ_{peak} (kPa)	$\Psi_{residual}$ (kPa)
0.594	100	60.22	5.483	6.731
0.598	200	132.43	9.416	10.046
0.593	400	244.71	14.710	15.00
0.997	100	47.73	4.529	5.144
1.000	200	106.28	7.678	8.351
0.994	400	211.43	10.480	11.443

6.5 Influence of surface roughness: (rough versus smooth)

Test results for the effect of surface roughness on the shear strength and volume change behaviour of the interface are shown in Figures 6.15 and 6.16. The obtained results indicate that the shear strength was found to be strongly influenced by the surface irregularity of the interface Based on the results presented in Figures 6.15 and 6.16, the following conclusions can be drawn:

1- A noticeable peak shear strength was observed only for the rough interface specimens tested at e_i = 0.6 under different levels of applied vertical stress. Whereas, for both studied void ratios, smooth interface specimens did not show any peak pattern.

2- The shear strength showed a remarkable increase with increasing of the surface roughness, for all levels of applied vertical stress, and this trend of behaviour was consistent for all the tested samples at e_i = 0.6 and 1.0.

3- The peak shear strength of rough interface samples was observed at larger horizontal displacement than those of the smooth interface, for both studied void ratios, and at all considered stress levels.

4- A pronounced stick-slip phenomenon was observed after the maximum shear strength for the smooth surface, whereas slipping, rolled, moved vertically and rearrangement of the soil particles at the interface of the rough surface did not show stick-slip behaviour.

5- Figures 6.15(b) and 6.16(b) show that both rough and smooth interfaces exhibited similar behaviour in the sense that the vertical displacement increased (compression) with the horizontal displacement until the peak shear strength was achieved. After that, the smooth interface revealed approximately steady state behaviour in the post-peak region until the end of the shearing process. In contrast, the rough interface showed an increase in the vertical displacement after reaching the peak shear strength.

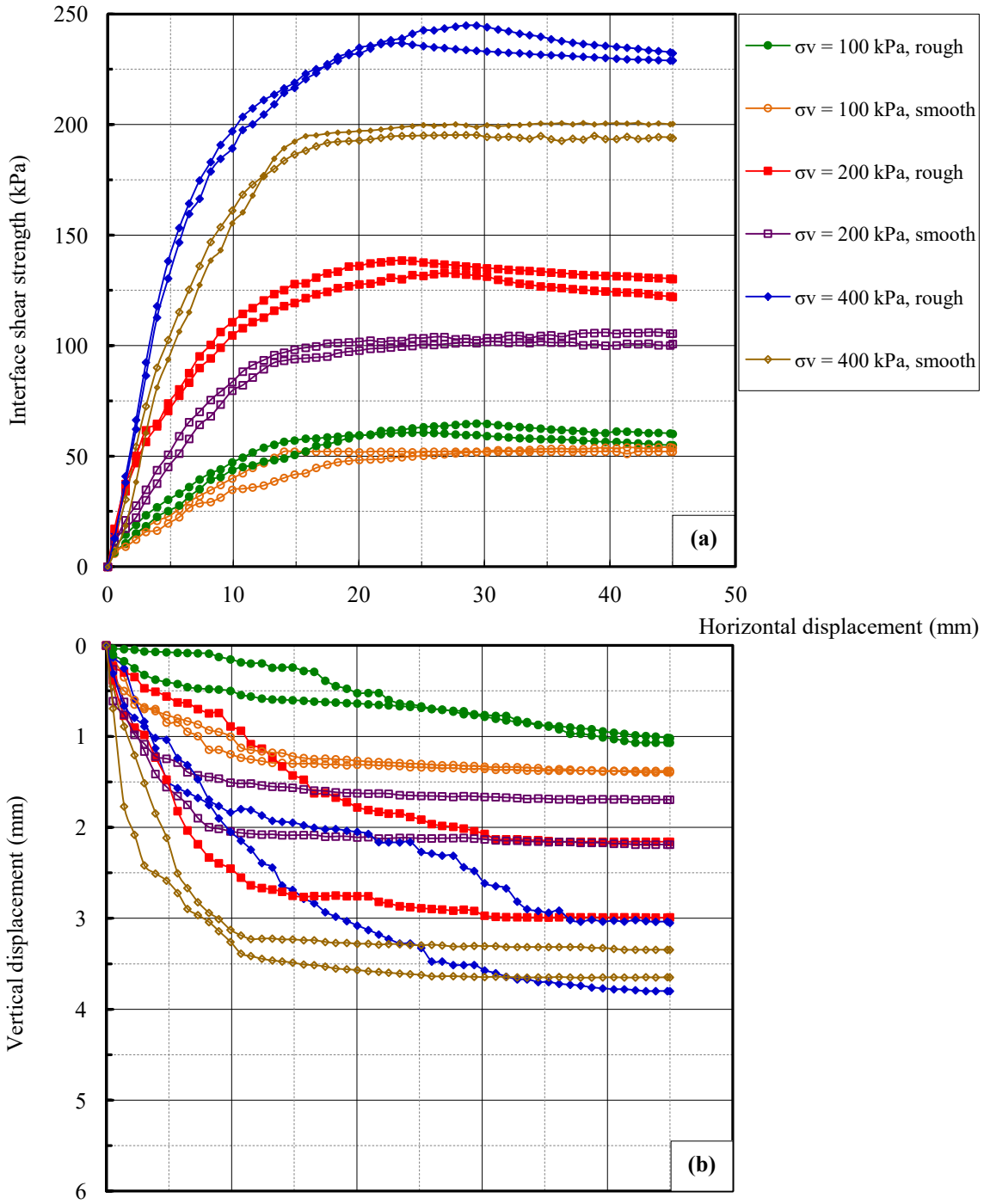

Figure 6.15: Results showing effect of surface roughness on **(a)** interface shear strength and **(b)** volumetric behaviour of samples at e_i = 0.6 (constant water content).

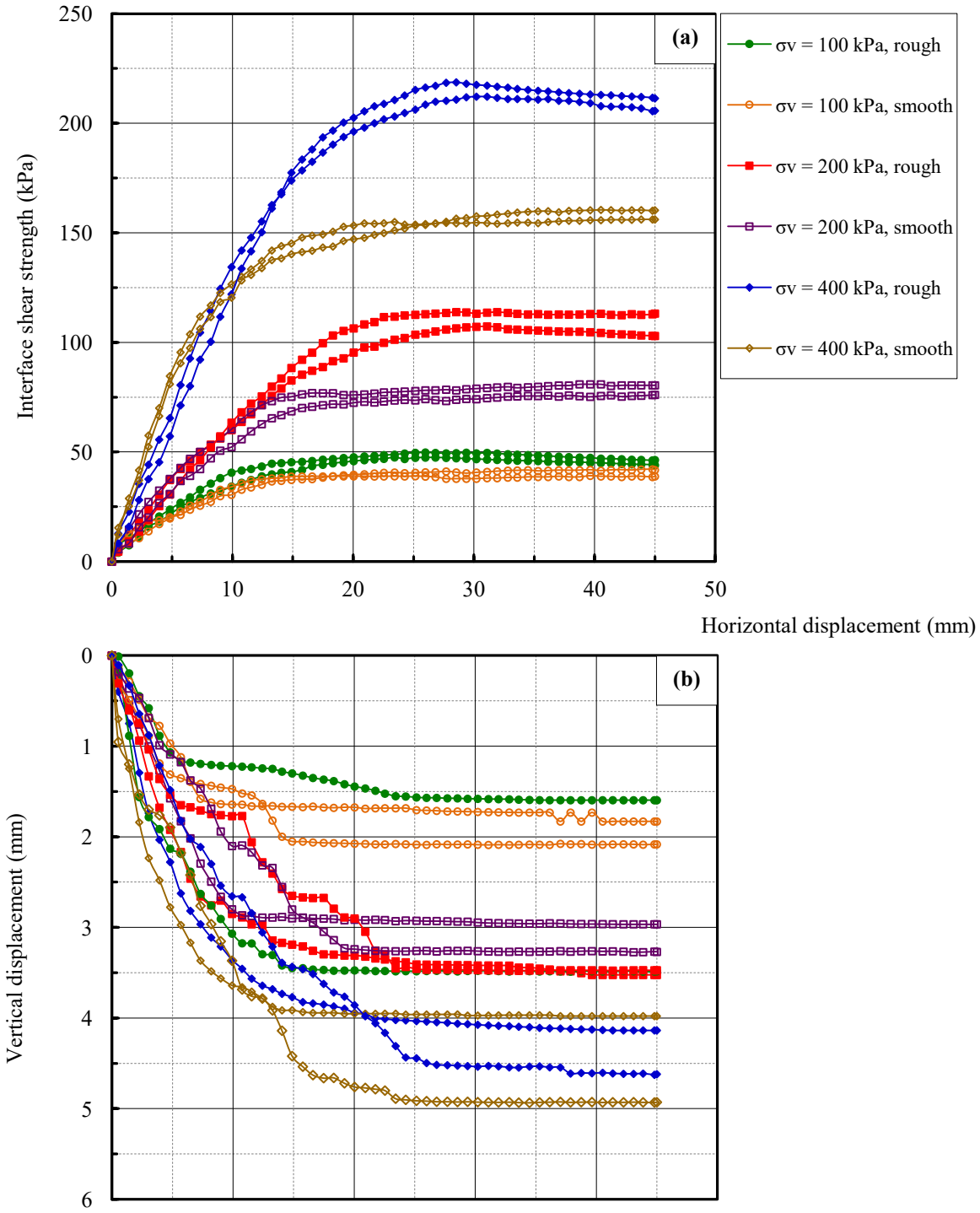

Figure 6.16: Results showing effect of surface roughness on **(a)** interface shear strength and **(b)** volumetric behaviour of samples at e_i = 1.0 (constant water content).

6.6 Comparison of the saturated and constant water content conditions of interface specimens

6.6.1 Soil-rough interface specimens

Figure 6.17 shows the volume variation during consolidation stage for samples tested under saturated and constant water content conditions. For both test conditions, the volume reduction of the soil-rough interface samples during consolidation stage increased with increasing the applied vertical stress level. This trend of behaviour was observed for both void ratios used in this study. Also, for both studied void ratios, the saturated samples exhibited larger volume reduction than those tested under constant water content. This behaviour was expected due to the effect of soil suction on the unsaturated samples. Moreover, as the void ratio increased, the volume reduction of the soil-rough interface samples increased markedly. As with the soil tests, the important role of matric suction is more obvious for samples with e_i = 1.0 that those with e_i = 0.6.

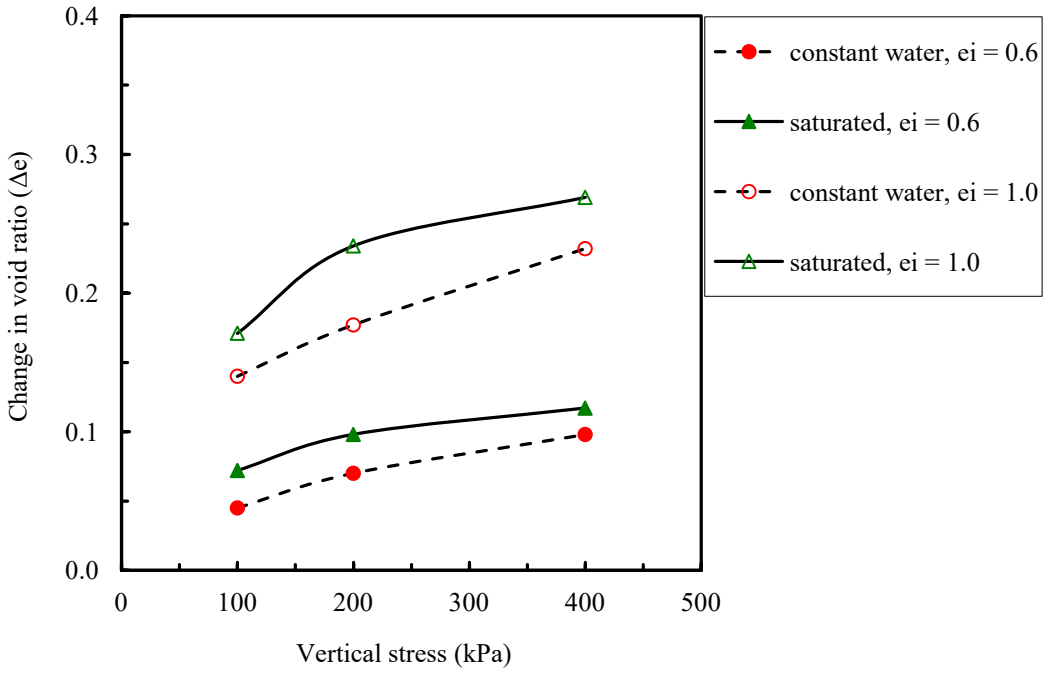

Figure 6.17: Void ratio variation against applied vertical stress for soil-rough interface samples performed saturated and constant water content conditions.

The analysis of test results presented in Figures 6.18(a) and 6.19(a) illustrate that for both studied void ratios, the shear strength of soil-rough interface samples increased with increasing the applied vertical stress level. This trend of behaviour was observed for all samples tested under saturated and constant water content conditions. As

expected, at any stress level, the obtained shear strength of specimens under constant water content is found to be distinctly greater than that obtained from saturated samples. This observed behaviour illustrates the significant role of soil suction on the shear strength behaviour of the tested material, as expected. Similar trends have been reported by Hossain, 2010; Dafalla, 2013 and Borana, 2014.

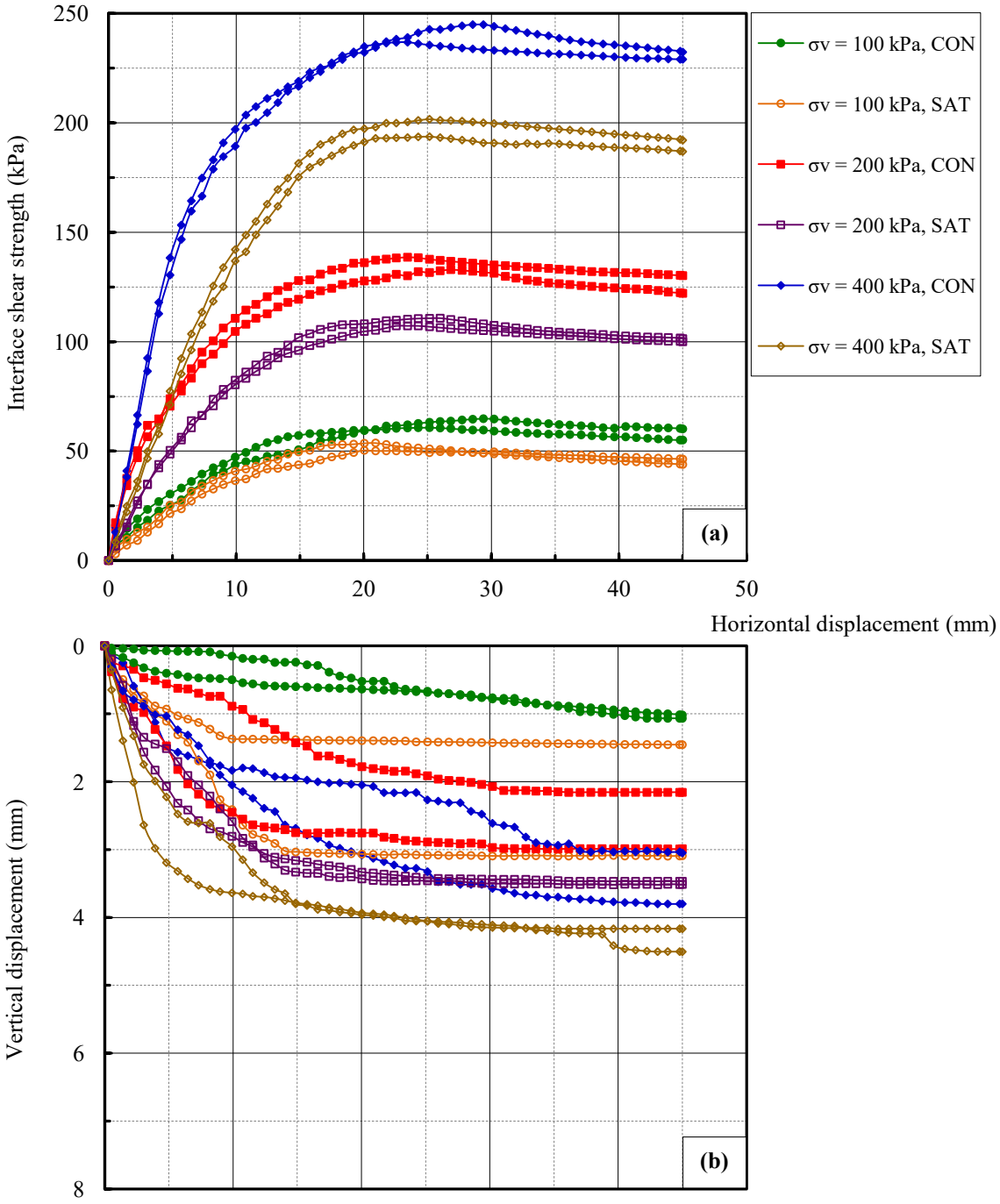

Figure 6.18: Results showing effect of test condition on **(a)** interface shear strength, and **(b)** volumetric behaviour of soil-rough interface samples at $e_i = 0.6$.

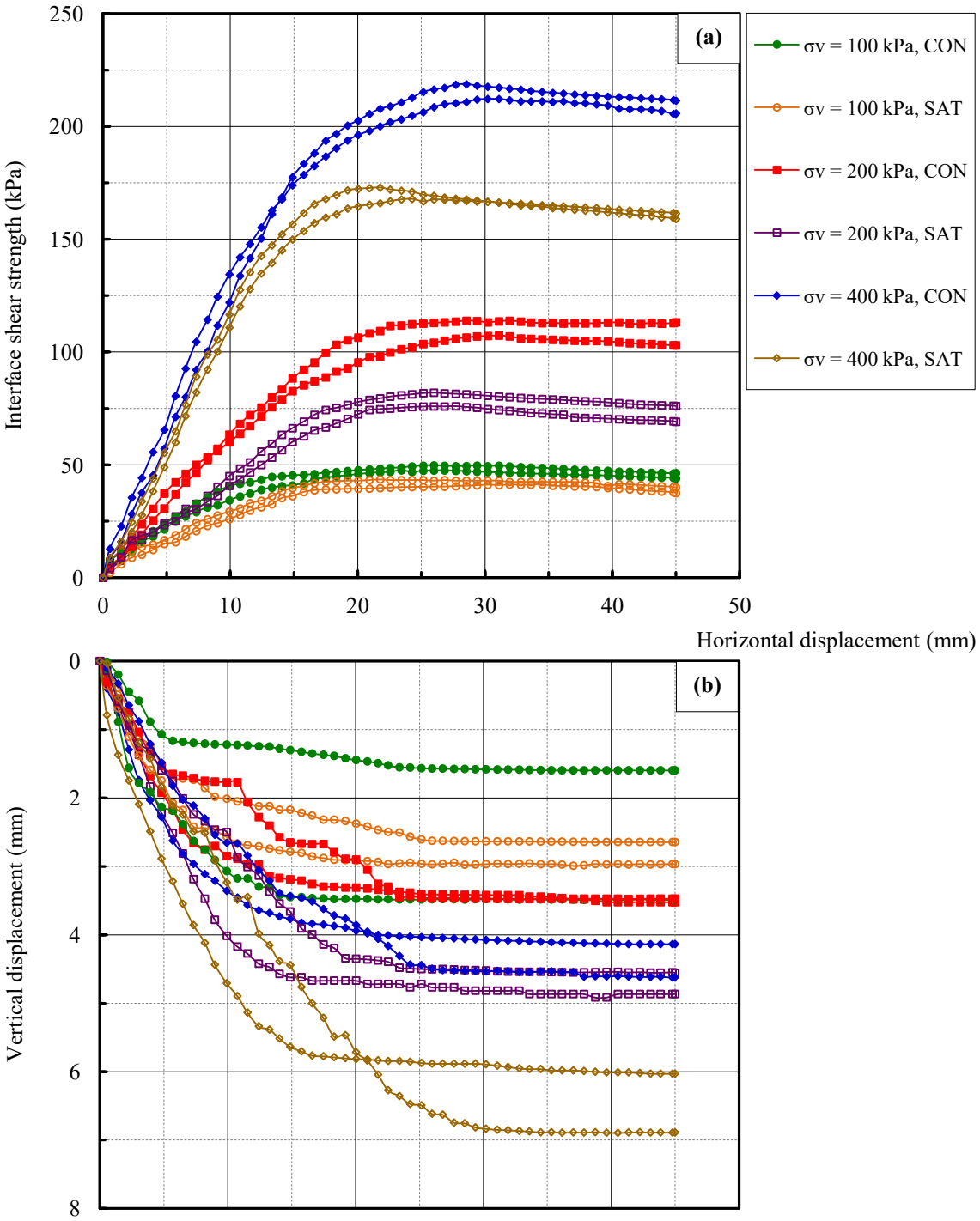

Figure 6.19: Results showing effect of test condition on **(a)** interface shear strength, and **(b)** volumetric behaviour of soil-rough interface samples at e_i = 1.0.

Furthermore, for both test conditions, it was noticed that there is a clear dependency of the interface shear strength on the initial void ratio of the tested samples. As expected, as the void ratio increased, a decrease in the shear strength was observed. Similar trend

of behaviour has been observed by many researchers such as Hossain 2010; Borana 2013. The test results presented in Figures 6.18(a) and 6.19(a) show also that, for both test conditions, the horizontal displacement corresponding to the peak/maximum interface shear strength increased with increasing the applied vertical stress regardless of the test condition. Similar to soil specimens, the rough interface showed two different shearing patterns in the post-peak region, strain softening behaviour (with noticeable peak shear strength) and strain hardening behaviour (with no clear peak shear strength). Whereas, soil-smooth interface samples at e_i = 0.6 and 1.0 showed only strain hardening behaviour for both test conditions. Moreover, it can be noted that, at any stress level, the horizontal displacement corresponding to the peak/maximum interface shear strength increased with decreasing the degree of saturation of the tested samples (meaning increased soil suction). This trend of behaviour was observed for two void ratios used in this study (e_i = 0.6 and 1.0).

The vertical displacement versus horizontal displacement plots Figures 6.18(b) and 6.19(b), reveal that there is an obvious dependency of the change in vertical displacement (volume reduction) on the level of applied vertical stress, void ratio, and test condition. As expected, for the range of applied vertical stresses, the constant water content specimens have shown lower value of vertical displacement in comparison with the corresponding saturated one. This behaviour can be directly related to the effect of soil suction on the volumetric behaviour of the tested specimens. Furthermore, for both test conditions, all interface specimens exhibited a tendency to increase the vertical displacement with increasing the void ratio.

The test results presented in Figure 6.20 in conjunction with Table 6-13 show that the interface friction angle δ_a' of the soil-rough interface is primarily influenced by the initial degree of saturation and the initial density of the tested samples, while the effective adhesion c_a' seems to be slightly affected by these parameters. The latter behaviour may be attributed to the reason that the physio-chemical and capillary forces between soil particles and rough interface along the shear plane are relatively weak (Hamid, 2005; Hossain, 2010). Moreover, for both test conditions, the interface shear strength parameters (δ_a' and c_a'), noticeably increased with decreasing the studied void ratios.

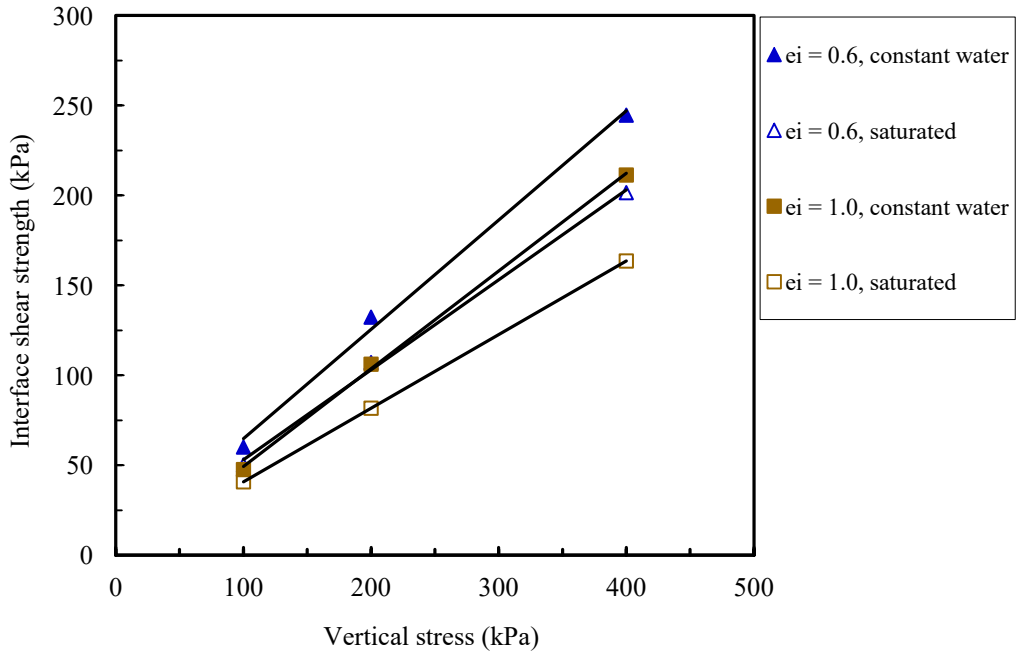

Figure 6.20: Failure envelopes of e_i = 0.6 and 1.0 soil-rough samples: test condition effect.

Table 6-13: Shear strength parameters of soil-rough samples under different test conditions

Initial void ratio, e_i	Test condition	δ_a'/δ_a (Degree)	c_a'/c_a (kPa)	R^2
0.6	Saturated	29	4	0.9977
1.0		24	0	1.000
0.6	Constant water	33.5	7	0.9957
1.0		29	0	0.9993

6.6.2 Soil-smooth interface behaviour

The test condition (saturated and constant water content) and void ratio (e_i = 0.6 and 1.0) were observed to have the same effect on the soil-smooth interface samples as for soil-rough interface test during consolidation stage as shown in Figure 6.21.

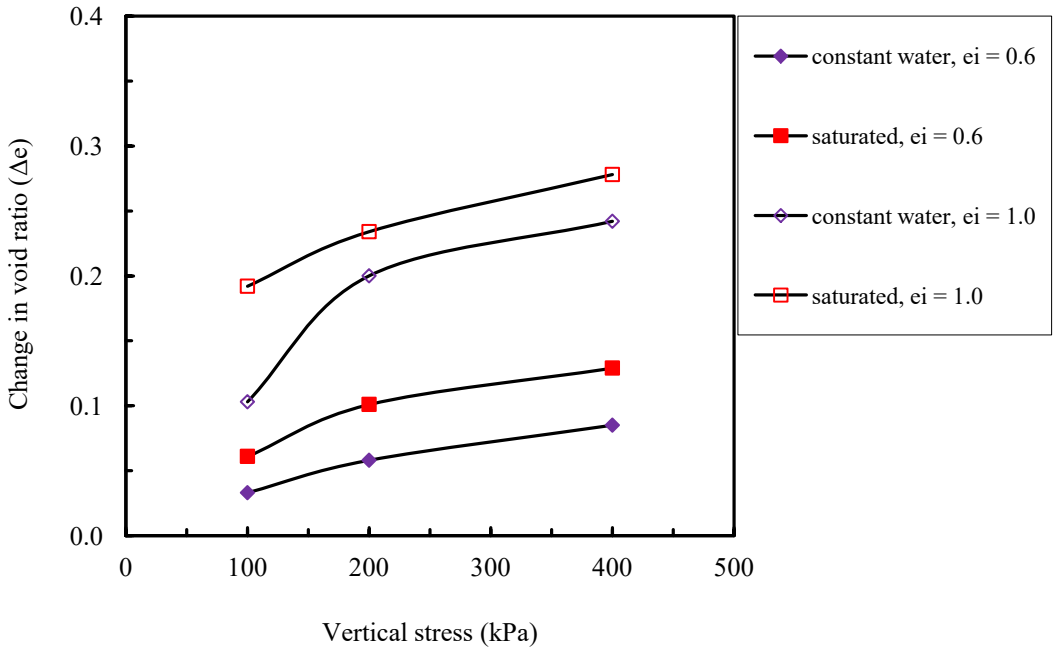

6.21: Void ratio variation against applied vertical stress for soil-smooth interface samples performed saturated and constant water content conditions.

The shear strength of soil-smooth interface specimens increased with increasing of applied vertical stress as well as no strain softening behaviour was seen followed by the maximum interface shear strength. This trend of behaviour was observed for both studied void ratios tested under saturated and constant water content conditions as shown in Figures 6.22 and 6.23. Also, similar to the soil-rough interface specimens, at any stress level, the horizontal displacement corresponding to the maximum interface shear strength increased with decreasing the degree of saturation of the tested samples.

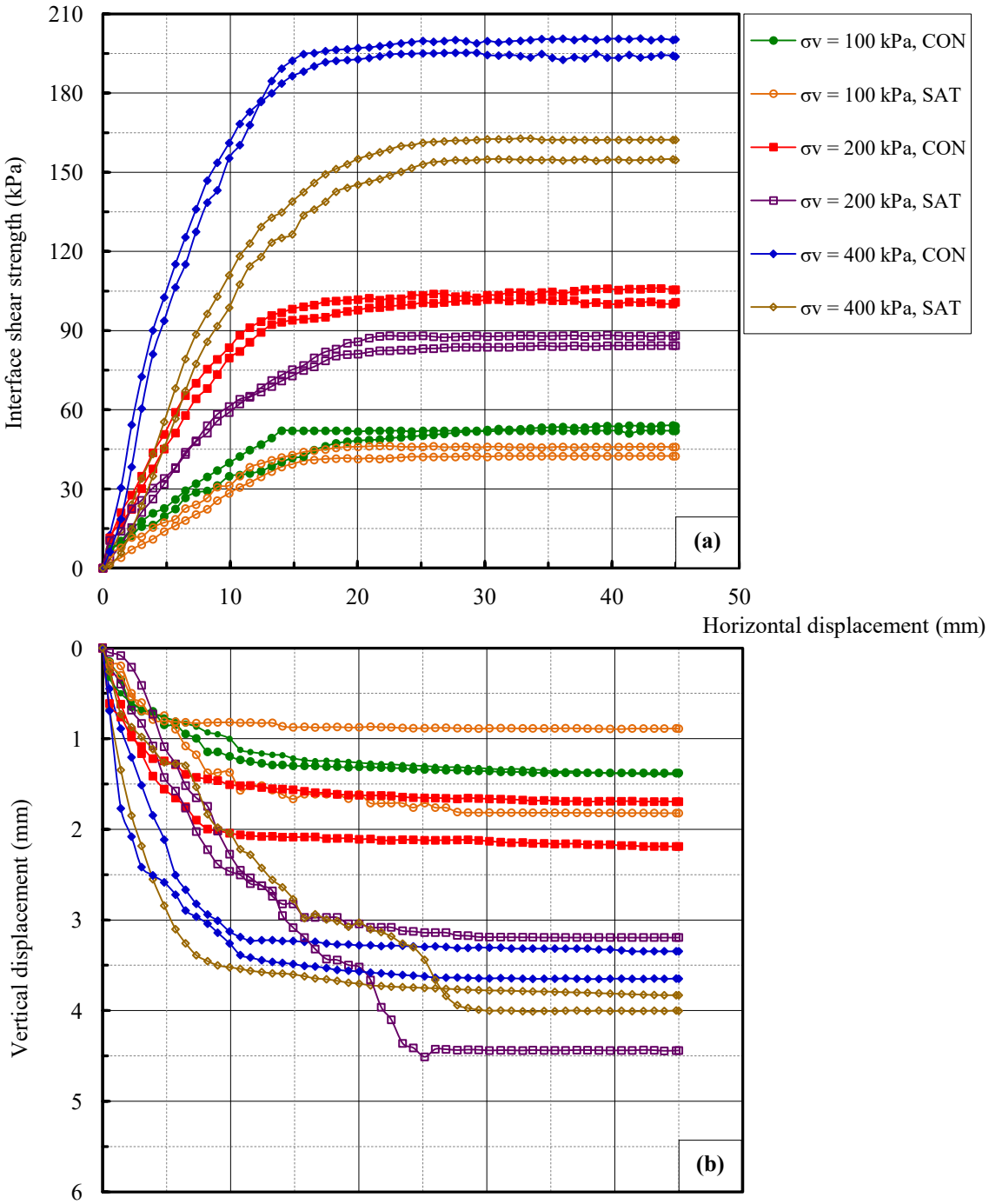

Figure 6.22: Results showing effect of test condition on **(a)** interface shear strength, and **(b)** volumetric behaviour of soil-smooth interface samples at $e_i = 0.6$.

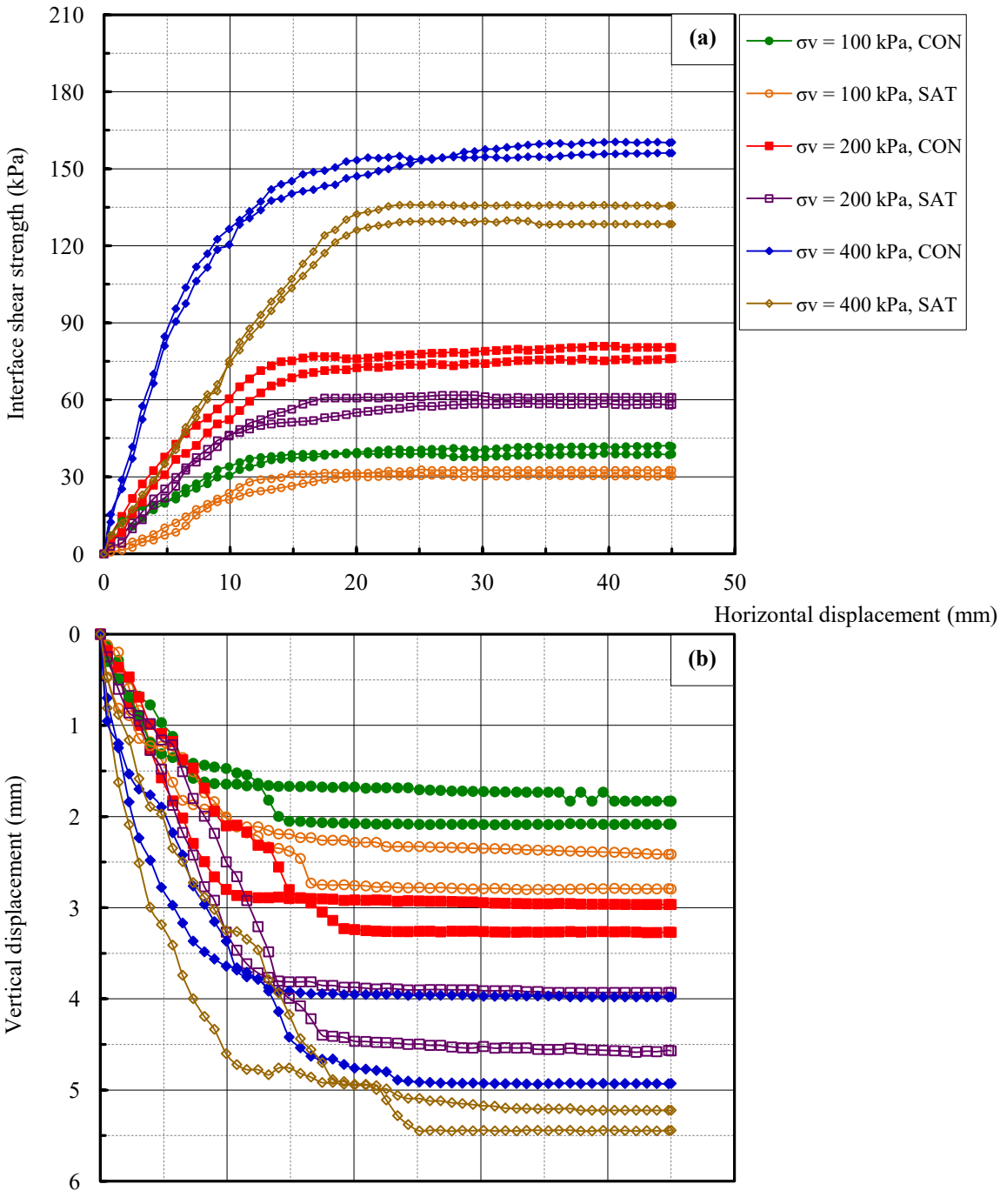

Figure 6.23: Results showing effect of test condition on **(a)** interface shear strength, and **(b)** volumetric behaviour of soil-smooth interface samples at e_i = 1.0.

Figure 6.24 shows the failure envelopes of the soil-smooth interface specimens with e_i = 0.6 and 1.0 performed under saturated and constant water content conditions. The presented test results indicate that the soil suction has significant effects on the interface friction angle, δ_a', at different levels of applied vertical stress in the sense that δ_a'

increased with decreasing the degree of saturation of the tested samples, as expected and also observed by Hossain, 2010; Borana 2014; Zainal and Abbas 2016. The interface adhesion c_a' showed slight increase only for specimens that have e_i = 0.6 (see Table 6-14).

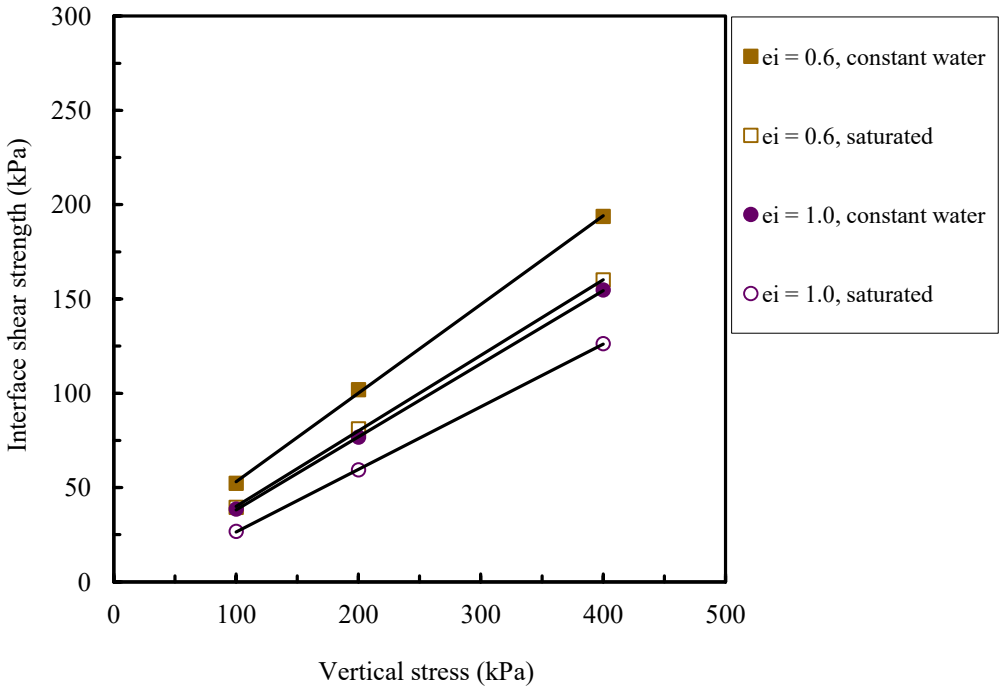

Figure 6.24: Failure envelopes of e_i = 0.6 and 1.0 soil-smooth samples: test condition effect.

Table 6-14: Interface shear strength parameters of soil-smooth samples under different test conditions

Initial void ratio, e_i	Test condition	δ_a'/δ_a (Degree)	c_a'/c_a (kPa)	R^2
0.6	Saturated	22.5	0	0.9998
1.0		19.5	0	1.000
0.6	Constant water	26	3.5	0.9996
1.0		22	0	1.000

6.7 Concluding remarks

The behaviour of soil-concrete interface specimens for two types of surface roughness (smooth and rough) in terms of shear strength and volume change has been presented. The test results obtained from saturated and constant water content direct shear tests had been evaluated and discussed with reference to results indicated by previous researchers of the related materials. This thesis presents, for the first time, the evolution of matric suction during consolidation and shearing process of soil-interface specimens using large-scale direct shear apparatus. It has been shown that the time adopted for consolidation stage did not offer enough time for matric suction equalisation. For both smooth and rough surfaces, the constant water content specimens have shown higher value of shear strength in comparison with the corresponding saturated one. It was observed that there is a clear increase in the peak/maximum shear strength with increasing the surface roughness, and consequently this causes the shear strength parameters to increase proportionally, as well. For both test conditions, there was a tangible tendency that shear strength curves to have peak behaviour (strain softening) when the soil was sheared against a rough surface, whereas a smooth surface did not show any peak strength behaviour (strain hardening). Therefore, it can be concluded that the role of the matric suction in the post peak shear strength region is less significant. It can also be seen that the smooth interface exhibited maximum shear strength at a smaller horizontal displacement than the rough interface for all specimens with both studied void ratios tested under saturated and constant water content conditions.

CHAPTER SEVEN

COMPARISON OF SHEAR BEHAVIOUR OF SOIL AND SOIL-CONCRETE INTERFACE

7.1 Introduction

This chapter starts with a comparison of the soil and interfaces under saturated conditions, and then a similar comparison is made when the specimens are tested under constant water content conditions. Finally, concluding remarks are presented to highlight the implications of the observed behaviour in consideration of the previously presented test results.

7.2 Comparison between soil and interface behaviour under saturated conditions

The behaviour of soil and soil-concrete interfaces (smooth and rough) for both studied void ratios (e_i = 0.6 and 1.0) during saturation stage are compared and presented in Figures 7.1(a) and (b). From comparison, it can be observed that the interfaces behaved in a similar way to the soil in the sense that the values of collapse potential of specimens with e_i = 1.0 are almost the same. This behaviour can be attributed to the fact that before the start of the direct shear tests, the collapse response of the interfaces is governed by the soil behaviour. In contrast, specimens with e_i = 0.6 showed non-collapse behaviour during saturation stage. Table 7-1 summarizes the initial and final conditions of the tested specimens during saturation stage. The difference in collapse potential may be attributed to the variation in specimen preparation process which would result in different values of collapse potential.

Table 7-1: Void ratio before, e_i and after e_f saturation stage and calculated collapse potential of soil, soil-smooth and soil-rough samples

Type of test		Soil – soil			Soil – smooth			Soil – rough		
Vertical stress, σ_v (kPa)		100	200	400	100	200	400	100	200	400
CP (%)	$e_i = 0.6$	0	0	0	0	0	0	0	0	0
	$e_i = 1.0$	6.55	7.85	6.20	7.10	6.16	6.50	6.11	6.60	7.25

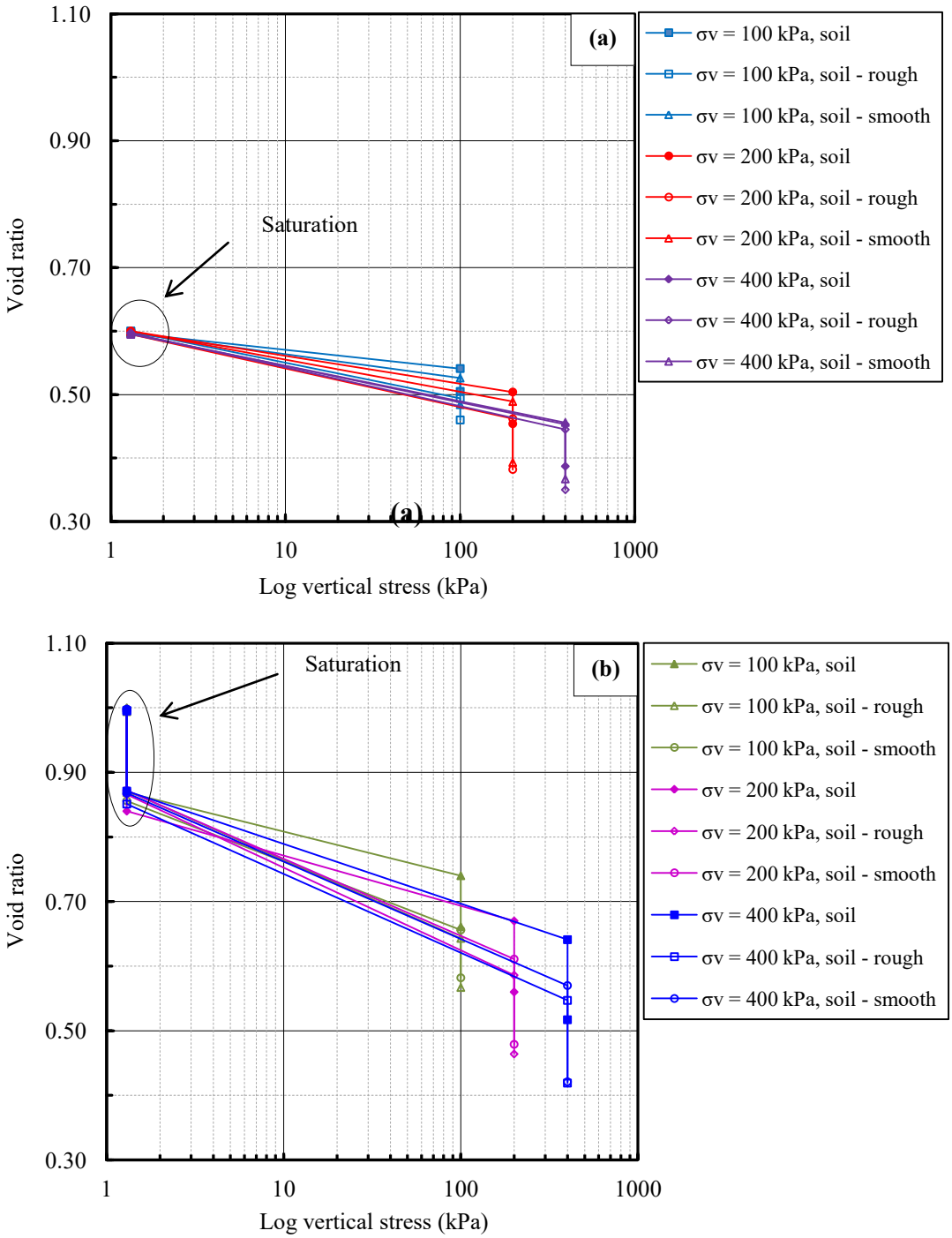

Figure 7.1: Collapse behaviour during saturation stage of soil and interfaces at **(a)** e_i = 0.6 and **(b)** e_i = 1.0.

The comparison of shearing behaviour between soil and both interfaces (smooth and rough) for e_i = 0.6 and 1.0 specimens are presented in Figures 7.2(a) and 7.3(a).

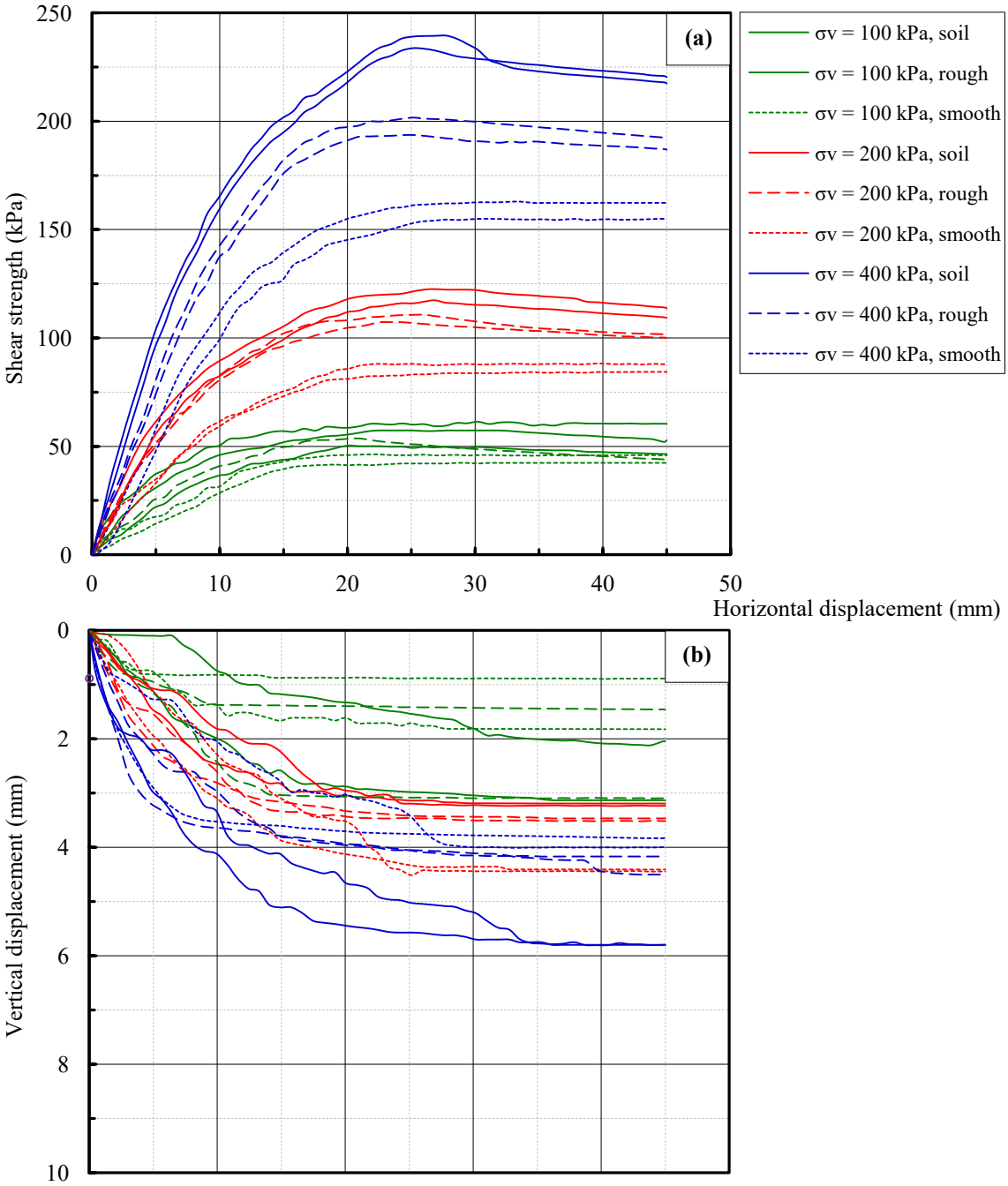

Figure 7.2: Comparison of soil, soil-smooth and soil-rough interfaces shear strength results at e_i = 0.6: **(a)** shearing behaviour and **(b)** volumetric response under saturated condition

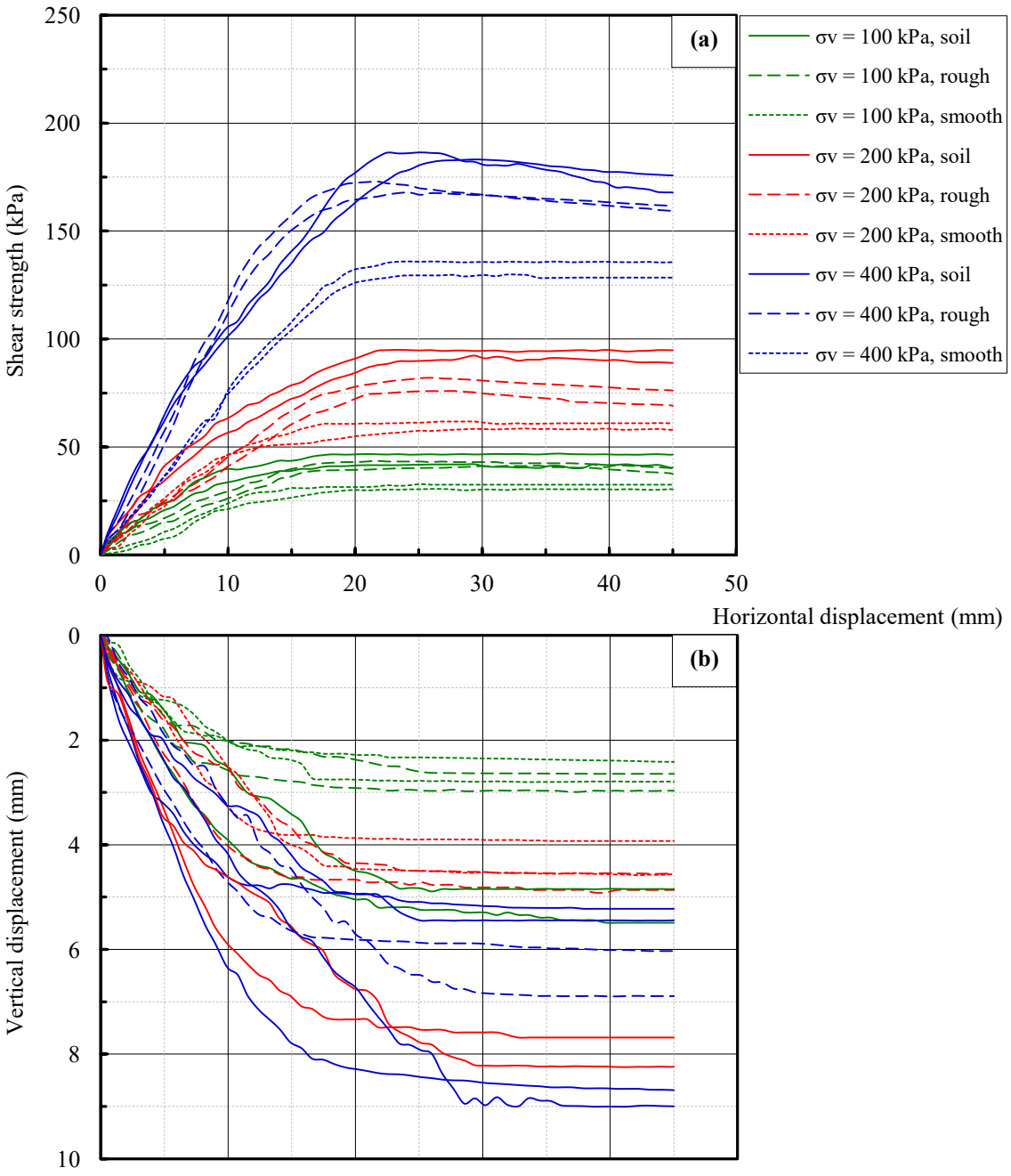

Figure 7.3: Comparison of soil, soil-smooth and soil-rough interfaces shear strength results at e_i = 1.0: **(a)** shearing behaviour and **(b)** volumetric response under saturated condition

As expected, at any stress level, it is obvious that the shear strength of soil was higher than the rough and smooth interfaces for both studied void ratios, whereas, the smooth interface showed lower values of shear strength of all the tested samples. This behaviour agrees with that found by Kulhawy and Peterson (1979) and Borana (2014) for sand-to-concrete and silty sand-to-steel interface tests, respectively.

For specimens that have e_i = 0.6 and 1.0 tested under 200 and 400 kPa applied vertical stress, the shear strength of soil and soil-rough interface specimens exhibited strain

softening behaviour in the post-peak region (showing a noticeable peak shear strength). Also, similar trend of behaviour was observed for samples with e_i = 1.0 tested under 400 kPa vertical stress. However, for both studied void ratios, the smooth interface showed strain hardening behaviour (steady state) after reaching the peak shear strength. The test results presented in Figures 7.2(a) and 7.3(a) in conjunction with Table 7-2 highlight for all samples that with increasing the level of applied vertical stress, the horizontal displacement corresponding to the peak/maximum shear strength increased. It can be noted that the maximum shear strength for the smooth interface was mobilised at smaller horizontal displacement than that of the soil and rough interface. The latter phenomenon could be attributed to the surface roughness which started dominating the shearing behaviour of the smooth interface specimens at a smaller horizontal displacement (Fakharian and Evgin, 1996; Borana, 2014; Jing et al., 2016). The values of horizontal displacement corresponding to peak/maximum shear strength for the soil, soil-smooth, and soil-rough samples are listed in Table 7-2.

Corresponding vertical displacement versus horizontal displacement curves of soil, soil-rough and soil-smooth samples are shown in Figures 7.2(b) and 7.3(b). As expected, obvious dependency of volume change of the tested samples on the level of applied vertical stress and void ratio was noticed. It is clear from these figures, for both studied void ratios, that the volume change of soil samples is greater than that occurred for smooth and rough interfaces. This trend of behaviour was observed for all stress levels. Also, slight differences were found between the volume reduction of smooth and rough interface.

Table 7-2: Values of horizontal displacement corresponding to the peak and/or maximum shear strength of soil and interfaces e_i = 0.6 and 1.0 (saturated state)

Type of test	Vertical stress, σ_v (kPa)	Initial void ratio, e_i = 0.6	Horizontal displacement, δ_h (mm)	Initial void ratio, e_i = 1.0	Horizontal displacement, δ_h (mm)
Soil – soil	100	0.597	20.04	1.000	14.04
	200	0.600	23.43	0.997	21.76
	400	0.596	25.98	0.995	25.15
Soil - smooth	100	0.597	14.88	0.998	12.42
	200	0.600	18.32	0.995	16.60
	400	0.595	23.43	0.998	20.04
Soil – rough	100	0.600	19.20	0.994	17.48
	200	0.595	23.43	0.998	21.76
	400	0.597	25.15	0.996	23.43

Plots of peak shear strength versus vertical stress corresponding to failure for soil, soil-smooth and soil-rough interface specimens are shown in Figure 7.4. It is obvious that the shear strength envelopes of the tested specimens showed good linearity over the vertical stress range of 100 to 400 kPa.

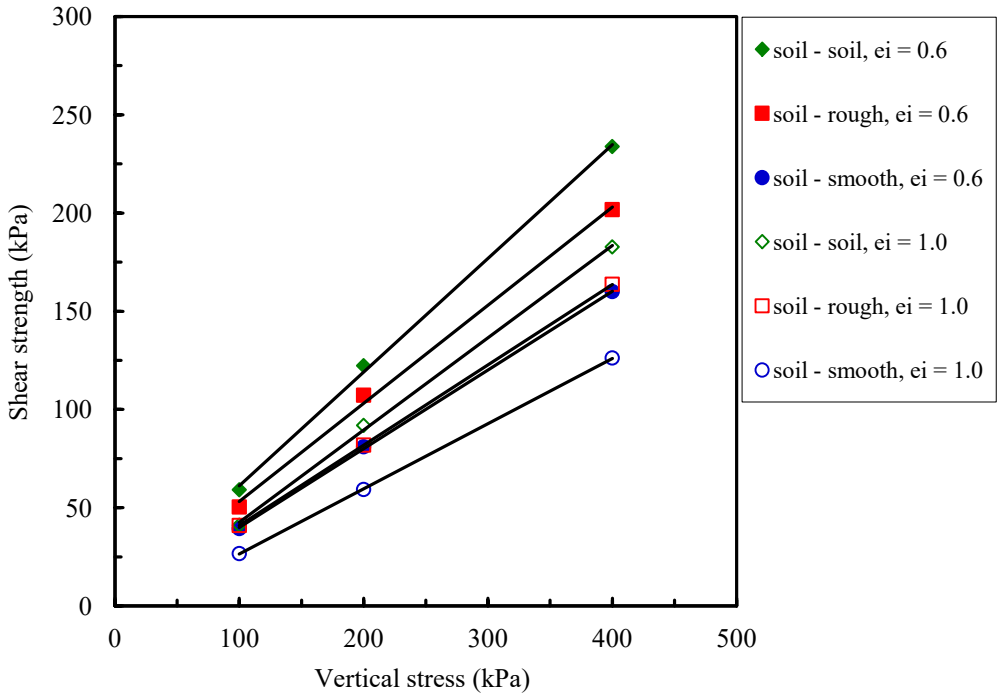

Figure 7.4: Mohr-Coulomb failure envelopes for soil, rough and smooth interface shear tests at e_i = 0.6 and 1.0 under saturated condition.

Furthermore, Figure 7.4 revealed that the interface friction angle is higher in the case of rough interface with respect to the case of smooth interface, but lower than the corresponding soil friction angle, which indicates that the interlocking between soil particles themselves is stronger than the interlocking between soil particles and interfaces. This behaviour is consistent with the observations of many previous researchers (e.g. Potyondy, 1961; Kulhawy and Peterson, 1979; Hossain, 2010; Borana, 2013).

It can be noted, for both studied void ratios, that the interface friction angle δ_a' increased with increasing the surface roughness of the interface. Moreover, as can be seen from the data presented in Table 7-3, for dense specimens (e_i = 0.6), the value of soil cohesion c' is slightly greater than the value of interface adhesion c_a' of the rough interface. This behaviour can be attributed to the fact that the cohesion forces between

soil particles themselves are stronger than the adhesion forces between soil and rough interface. Whereas, for both studied void ratios, the interface adhesion c_a' of the smooth interface was equal to zero. Also, the R-square values of the shear envelopes are indicated in the tables to verify the linearity of the relations. In brief, both of the void ratios and the surface roughness of the interface have a clear effect on the shear strength of the tested specimens which in turn caused a clear increase in the soil and interface friction angles.

Table 7-3: Saturated shear strength parameters of soil and interfaces specimens

Type of test	Void ratio	ϕ' *and/or* δ_a'	c' *and/or* c_a'	R^2
	e_i	(Degree)	(kPa)	
Soil	0.6	31	7.5	0.9990
	1.0	26.5	0	0.9992
Rough interface	0.6	29	4	0.9977
	1.0	24	0	1.0000
Smooth interface	0.6	22.5	0	0.9998
	1.0	19.5	0	1.0000

7.3 Comparison between soil and interface behaviour under constant water content

The comparison of behaviour between soil and interfaces during consolidation stage for both studied void ratios in terms of volume variation is presented in Figure 7.5. As expected, at any stress level, the looser samples (e_i = 1.0) showed higher volume reduction in comparison to the dense samples (e_i = 0.6). Also, soil samples showed larger volume reduction than those of interfaces. This trend of behaviour was observed for both studied void ratios. It can also be noted that, for the range of applied vertical stress used in this study, the smooth and rough interfaces showed some differences in the magnitude of volume reduction. In general, the differences in volume reduction do not show any clear pattern. These differences can be attributed to many factors such as the variation in sample preparation and the difference in initial water content of the tested samples.

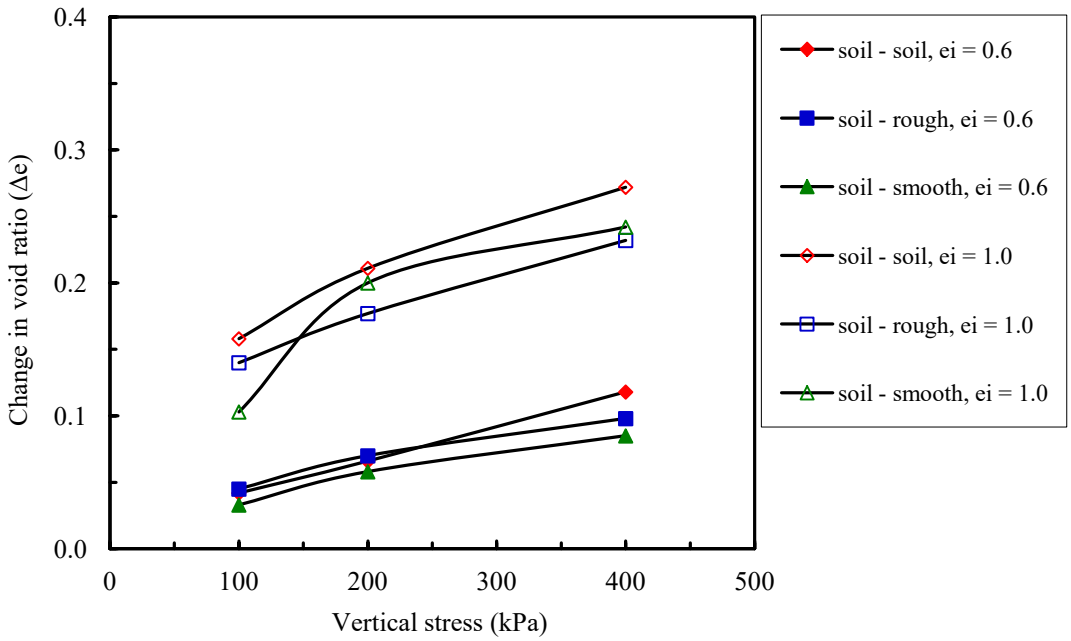

Figure 7.5: Void ratio variation against applied vertical stress for soil and interfaces under constant water content.

The matric suction development associated with the confining pressure was also observed by Oliveria et al., (2016). They studied the influence of soil structure on the matric suction development in the compacted specimens of a residual gneiss from Brazil using conventional triaxial testing equipment under constant water content condition (CW). Their results suggested that the matric suction changes in the soil under CW condition depend mainly on the volume change behaviour, which is influenced by the level of confining pressure, the degree of saturation and soil structure. The authors concluded that the higher confining pressure produces more volume contraction, and hence there will be greater increase in the degree of saturation and greater reduction in the matric suction of the soil specimen.

In this study, similar trend of behaviour during consolidation stage was seen for the tested specimen with e_i = 0.6 and 1.0 as shown in Figures 7.6(a) and (b). It can be noticed that the reduction of matric suction increased with the increase of applied vertical stress. The larger is the applied vertical stress, the higher is the observed volume reduction and, as a consequence, with constant water content, there is an increase in the

degree of saturation that generated a decrease in soil suction. However, the soil samples revealed greater reduction in matric suctions as compared to the interfaces (smooth and rough). This trend of behaviour was seen for all investigated vertical stress levels. In addition, all the tested samples showed a larger reduction in the matric suction as the void ratio increased (i.e. e_i = 1.0).

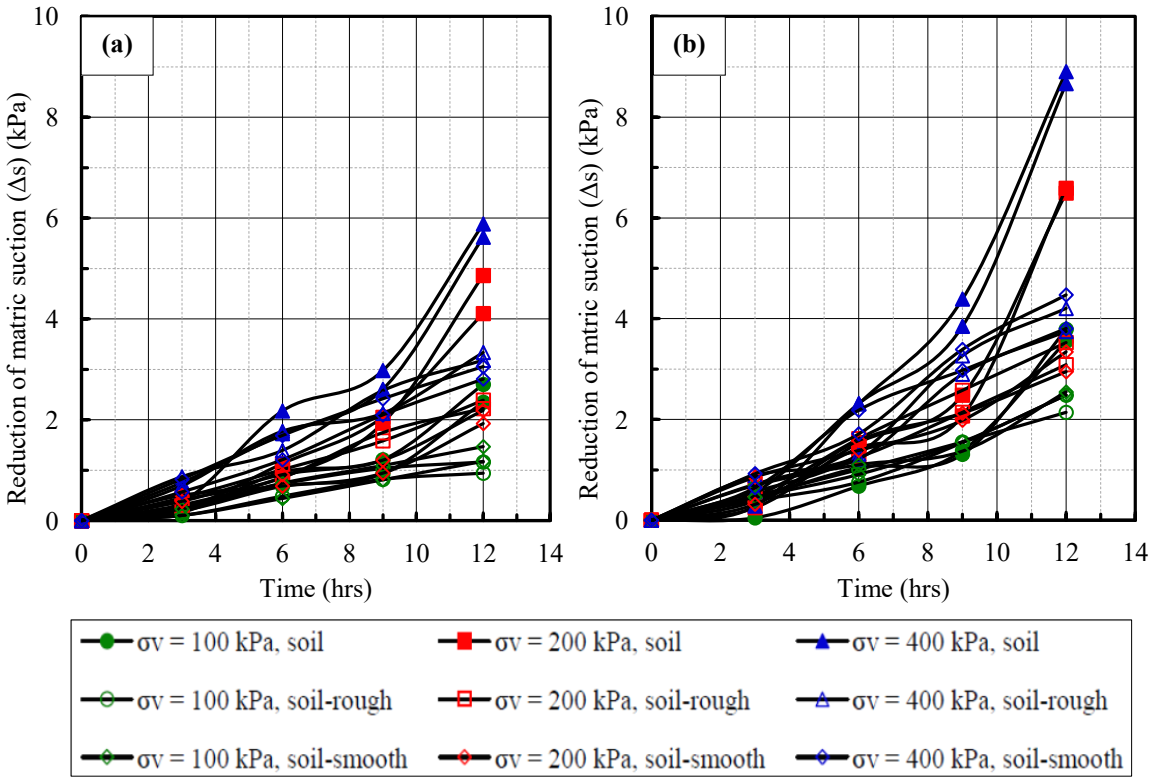

Figure 7.6: Reductions in matric suction vs. time during consolidation stage for soil and interfaces; **(a)** e_i = 0.6, **(b)** e_i = 1.0.

It is interesting to note that, in addition to the level of the confining pressure, Oliveria et al., (2016) reported that the matric suction change also depends on the initial matric suction in the soil specimen. The authors reported that the coefficient of suction change due to applying a confining pressure (ratio of matric suction change to the initial matric suction) decreased with increasing the initial matric suction. The higher the initial matric suction, the lower the coefficient of suction change.

In this study, Figure 7.7 shows the relationship between the coefficient of suction change versus initial matric suction of the soil, soil-rough, and soil-smooth interface

specimens. From the analysis of the figure it can be seen that the specimens with higher initial matric suction showed lower coefficient of suction change.

Also, a logarithm equation was used for best-fitting the test results presented in this figure, with R-square values almost higher than 0.94, except the soil and soil-rough interface specimens tested under 100 kPa vertical stress showed R-square value lower than 0.83. Moreover, it can be noted from Figure 7.8 that the coefficient of suction change increased with increasing the level of applied vertical stress. This trend of behaviour was observed for soil and interface specimens. Similar behaviour can be found in the literature including the works of Thu et al., (2006) and Oliveira et al., (2016).

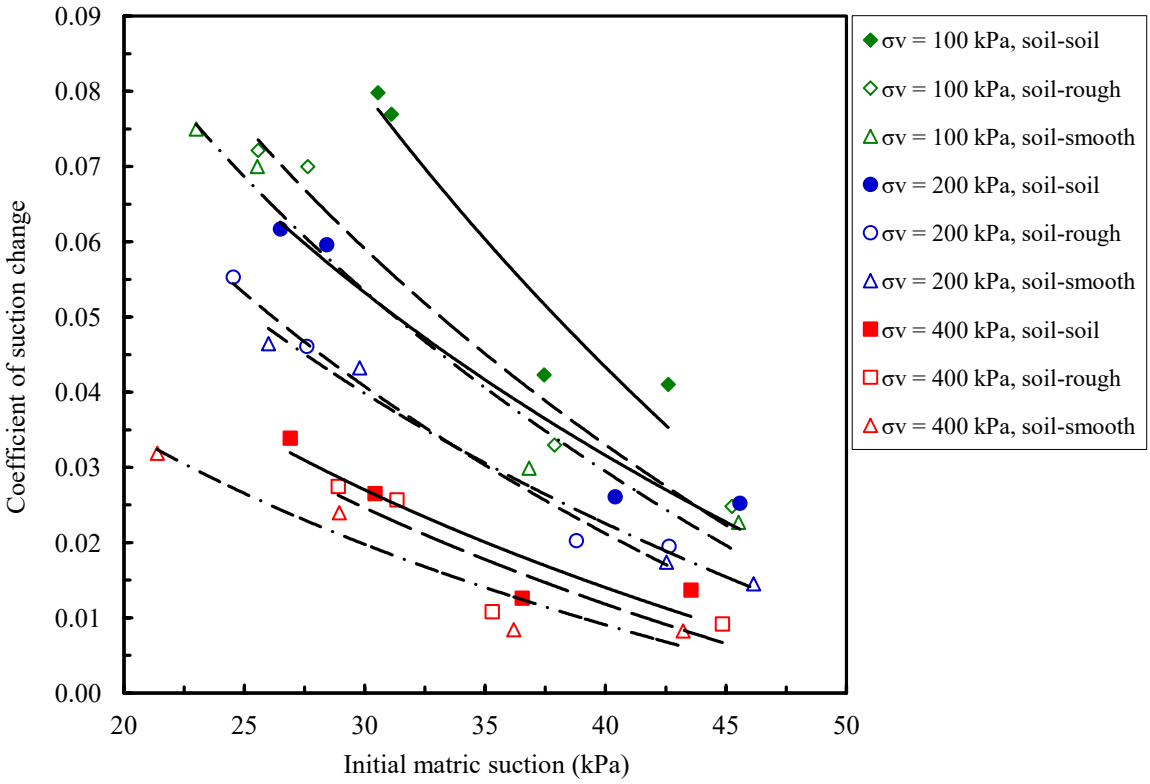

Figure 7.7: Variation of coefficient of suction change under different levels of applied vertical stress with respect to the initial suction of the tested specimens.

The direct shear test results of soil and interface (smooth and rough) are compared in terms of shear strength and volumetric behaviour as shown in Figures 7.8 and 7.9. It is evident from Figures 7.8(a) and 7.9(a) that for both studied void ratios, the shear strength of soil and interfaces increased as the level of applied vertical stress increased.

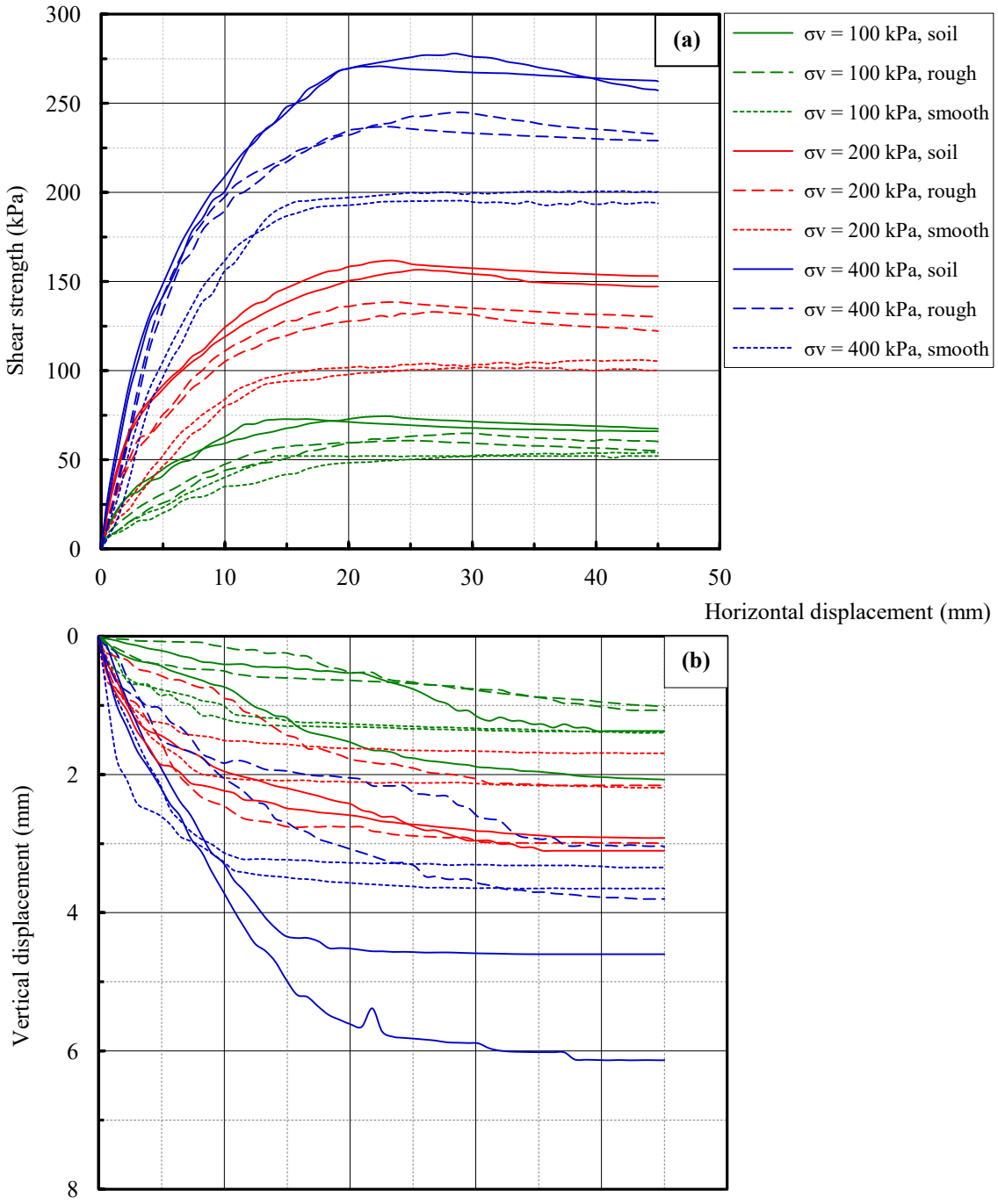

Figure 7.8: Comparison of soil, soil - smooth and soil - rough interfaces shear strength results at e_i = 0.6: **(a)** shearing behaviour and **(b)** volumetric response under constant water content.

Moreover, the test results presented in Figures 7.8(a) and (b) also indicated that the shear strength of the soil and interfaces increased as the void ratio of the tested samples decreased from 1.0 to 0.6. The former and the latter behaviour were expected and seen for all values of applied vertical stress. Figure 7.8(a) showed that the specimens with e_i

= 0.6 sheared under 100 kPa vertical stress for the soil and soil-rough interface specimens had almost similar behaviour in the sense that the shear strength curves exhibited strain softening pattern after the peak shear strength.

In contrast, for the case of smooth interface, the shear strength curve exhibited steady state behaviour followed by the maximum shear strength without showing any noticeable change in the corresponding vertical displacement (Fig. 7.8(b)). Peak shear strength is more pronounced for the soil and soil-rough specimens with increasing the level of applied vertical stress (i.e. 200 and 400 kPa), whereas, no peak shear strength was observed for the smooth interface specimen (showing hardening stick-slip behaviour) at the same vertical stress without showing any significant change in the corresponding vertical displacement (Figure 7.8(b)).

Also, it can be seen from Figure 7.8(a) for vertical stress of 400 kPa, the rough interface showed similar trend of behaviour to the soil until the horizontal displacement reached 9.92 mm. This can be attributed to the rough interface which is governed by the overlain compacted soil in this region and both have almost the same stiffness and vertical displacement (Figure 7.8(b)). After that, the shear strength and the vertical displacement of the soil increased with increasing horizontal displacement, whereas the rough interface shear curve deviated from the soil and showed moderate increase in the shear strength followed by the peak point.

Based on the observations mentioned above, it can be concluded from Figure 7.8(a) that the surface roughness clearly affected the pattern of the shear strength behaviour in the post-peak region. In addition, different patterns of shearing behaviour observed in the post-peak region indicated that the role of matric suction was not of major significance. This behaviour is consistent with findings reported by Hamid (2005); Hossain (2010); Borana (2013). Figure 7.8(a) in conjunction with Table 7-4 indicates that, for all levels of vertical stress, the smooth interface presented maximum shear strength at smaller horizontal displacement than the soil and rough interface. This means that the surface roughness started governing the shear strength behaviour of the smooth interface earlier than the soil and rough surface.

Table 7-4: Values of horizontal displacement corresponding to the peak and/or maximum shear strength of soil and interfaces at e_i = 0.6 and 1.0 (constant water content)

Type of test	Vertical stress, σ_v (kPa)	Initial void ratio, e_i = 0.6	Horizontal displacement, δ_h (mm)	Initial void ratio, e_i = 1.0	Horizontal displacement, δ_h (mm)
Soil - soil	100	0.596	21.76	0.998	13.26
	200	0.598	25.15	1.000	20.92
	400	0.600	28.53	0.996	23.43
Soil - smooth	100	0.597	14.04	0.995	10.75
	200	0.593	16.60	0.998	14.04
	400	0.600	18.32	1.000	17.48
Soil – rough	100	0.594	23.43	0.997	20.04
	200	0.598	25.98	1.000	25.15
	400	0.593	29.37	0.994	27.70

The comparison of shearing behaviour between soil and interface of samples with e_i = 1.0 is presented in Figures 7.9(a) and (b). Similar to the dense specimens (e_i = 0.6), the shear strength and the corresponding vertical displacement of the loose specimens (e_i = 1.0) increased with increasing the applied vertical stress. However, test results of soil specimens showed higher shear strength than those of interfaces (smooth and rough).

Shear strength curves of the soil-smooth and soil-rough specimens revealed compatible trends of behaviour to each other in the pre-peak region and this behaviour continued until the horizontal displacement reached 11.54 mm as shown in Figure 7.9(a). This means that at any stress level, the surface roughness did not significantly influence the shear strength of the tested specimens and the shearing behaviour of the interfaces in this region is controlled by the soil overlain the concrete pad. Beyond this value of horizontal displacement (i.e. 11.54 mm), the smooth interface curves bent away from the rough interface and showed relatively steady state behaviour until the end of the shearing stage without showing any noticeable peak shear strength (i.e. no to little change in the vertical displacement), whereas, the shear strength and the corresponding vertical displacement of rough interface increased up to the peak strength, then a slight decrease in the shear strength was observed especially for 200 and 400 kPa applied vertical stress.

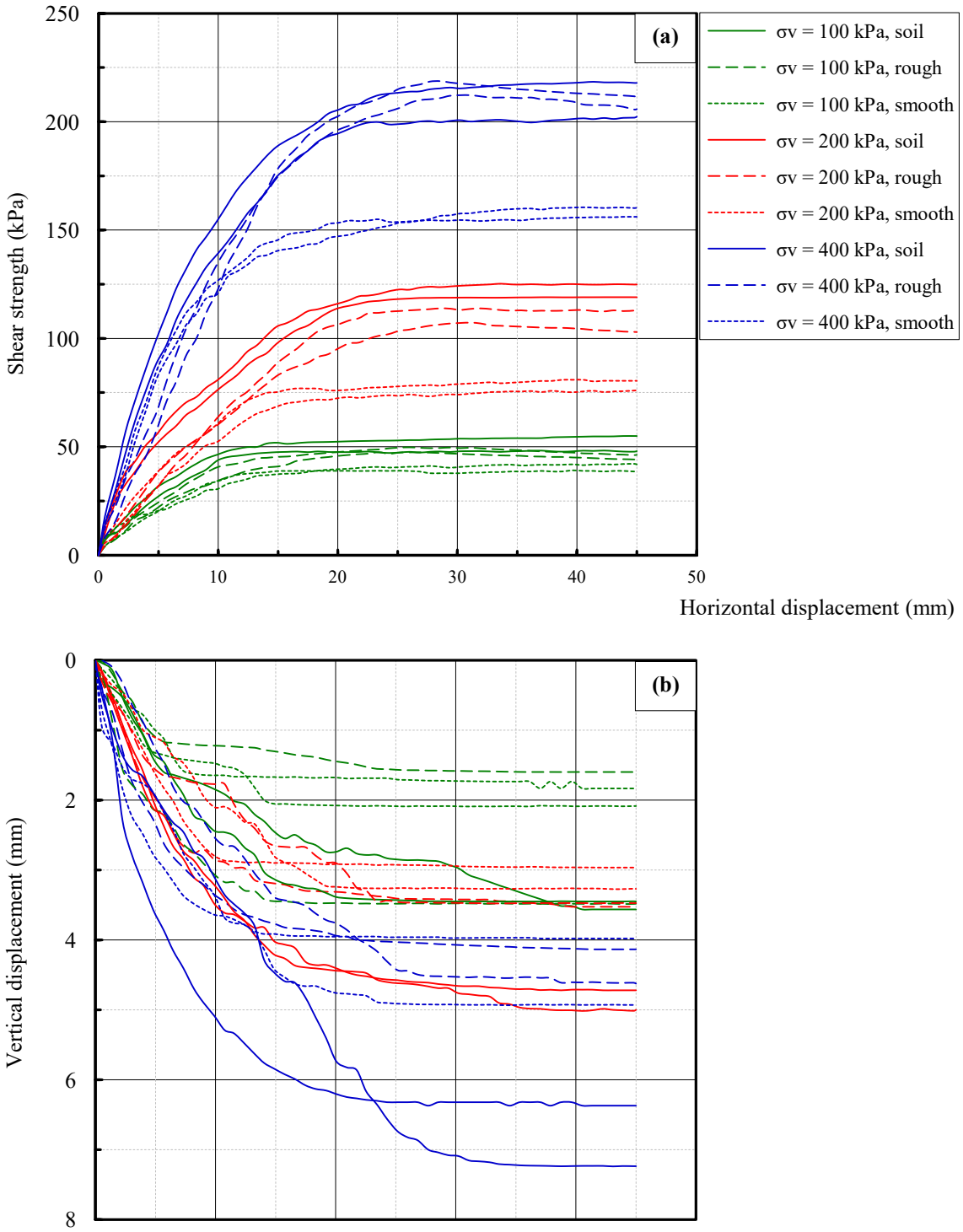

Figure 7.9: Comparison of soil, soil - smooth and soil - rough interfaces shear strength results at e_i = 1.0: **(a)** shearing behaviour and **(b)** volumetric response under constant water content.

It can also be seen from Figure 7.9(a) that the shear strength of the soil specimens exhibited steady state shear strength behaviour followed by the maximum shear strength

(hardening behaviour). Like the dense specimens (e_i = 0.6), the horizontal displacement corresponding to the peak and/or maximum shear strength of loose specimens increased with increasing of vertical stress. In addition, at any stress level, the smooth surface started governing the shear strength of the tested specimens at a smaller horizontal displacement than the soil and rough surface. This trend of behaviour was seen for all levels of vertical stress used in this study as presented in Table 7-4. Similar to the dense specimens, insignificant contribution of matric suction to shear strength in post-peak region was also noted.

Plots of shear strength versus vertical stress corresponding to failure for soil, rough and smooth interfaces are shown in Figure 7.10. This figure indicates that the slope of shear strength envelopes for soil and interfaces generally tends to increase as the void ratio decreased. Furthermore, it can be seen that the interface friction angle δ_a increased as the roughness of the interface increased, whereas, the interface adhesion component c_a showed a slight increase.

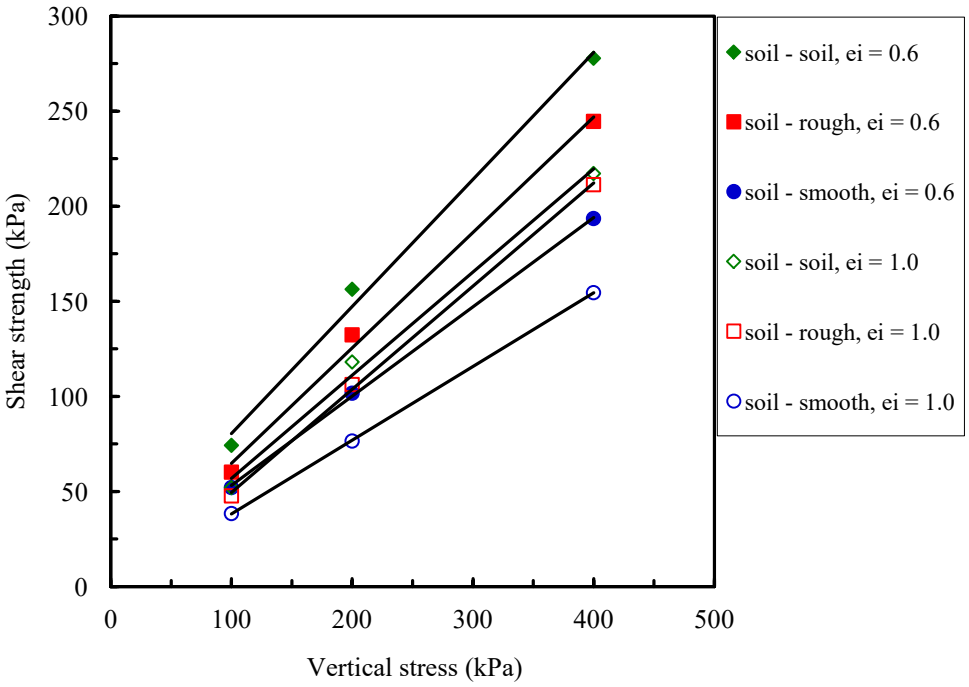

Figure 7.10: Mohr-Coulomb failure envelopes for soil, rough and smooth interface shear tests at e_i = 0.6 and 1.0 under constant water content.

As is shown in Table 7-5, for both studied void ratios, the interface friction angle, δ_a, and adhesion, c_a, of rough interface are greater than the values of δ_a and c_a of the smooth

interface. However, for the case of smooth interface, the values of δ_a and c_a are smaller than those of soil and rough interface. Examining Table 7-5 closely, it can be observed that the values of ϕ and δ_a are the same for soil and soil-rough interface specimens with $e_i = 1.0$. This means that the interlocking between soil particles themselves is similar to the interlocking between rough surface and the soil particles of the interface layer.

One of the noticeable points, which can be noted from Table 7-5, is that for both studied void ratios, the cohesion of soil c, is greater than the adhesion δ_a of rough and smooth interfaces. This behaviour is due to the fact that the normal force is induced by the capillary tension of water meniscus (cohesion forces) clinging to the contact point of the soil particles is stronger than the adhesion forces between soil and interfaces (Hamid, 2005; Hossain; 2010). In addition, the interface adhesion, c_a, of smooth and rough interfaces is equal to zero for specimens with $e_i = 1.0$. This is due to the weaker bonding between soil particles and the interfaces. The R-square values of the shear envelopes are presented in Table 7-5 to verify the linearity of the relations. It is clear that the shear strength envelopes of the tested specimens showed good linearity over the vertical stress range of 100 to 400 kPa. A very little amount of scattering was noticed regarding the R-square values of the first order failure envelope lines of different void ratios specimens for soil and interfaces, which ranged from 0.9938 to 1.0000. This can be attributed to many factors such as the rigour adopted during the preparation method of the tested specimens and performing the laboratory tests under controlled conditions to some extent.

Table 7-5: Shear strength parameters of soil and interfaces specimens under constant water content

Type of test	Void ratio	*ϕ and/or δ_a*	*c and/or c_a*	R^2
	e_i	(Degree)	(kPa)	
Soil	0.6	36.5	16	0.9938
	1.0	29	4.5	0.9943
Rough interface	0.6	33.5	7	0.9957
	1.0	29	0	0.9993
Smooth interface	0.6	26	3.5	0.9996
	1.0	22	0	1.0000

The curves of matric suction evolution versus horizontal displacement for soil and interfaces (rough and smooth) during shearing process are shown in Figures 7.11(a) and

(b). The general trend of these curves showed a clear increase in the soil suction associated with increasing the horizontal displacement. This trend of behaviour was seen for both studied void ratios under different applied vertical stress levels. The most important matric suction evolution occurred before the achieved horizontal displacement corresponding to the peak/maximum shear strength. As horizontal displacement increased, the matric suction did not show significant evolution. The latter observation interprets different patterns of shear behaviour (strain softening and strain hardening) in the post-peak region of soil and interfaces. Similar behaviour was noticed by Tarantino and Tombolato (2005) and Curuso and Tarantino (2004) on compacted Speswhite kaolin. They reported clear increases in the matric suction during shearing stage with increasing the horizontal displacement and/or increasing the applied vertical stress.

Furthermore, it can be seen from Figures 7.11(a) and (b) that the soil samples with e_i = 0.6 and 1.0 exhibited higher matric suction evolution than the smooth and rough interfaces. This behaviour is due to the water meniscus bonding caused by the physico-chemical and capillary forces between the soil particles in the soil specimen which is stronger than those bonding the soil particles and the interfaces (Hamid and Miller, 2009). However, at any stress level, the soil specimens sheared against smooth interface showed lower values of matric suction than the soil and rough interface.

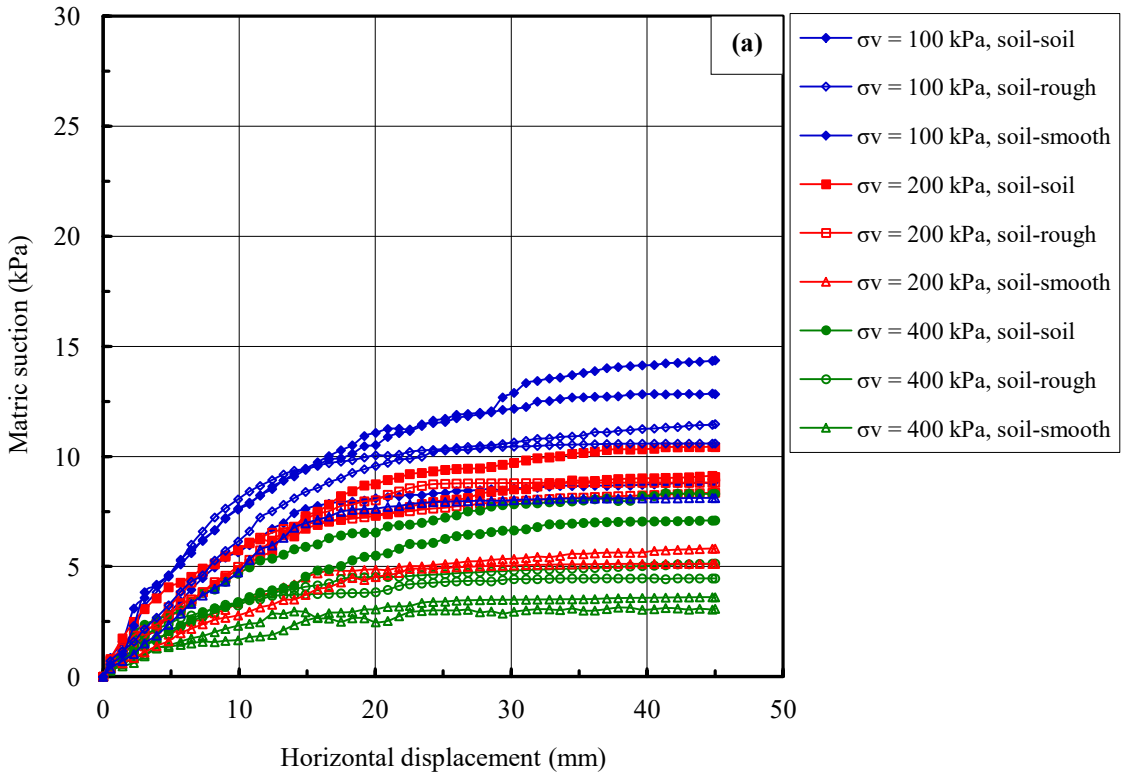

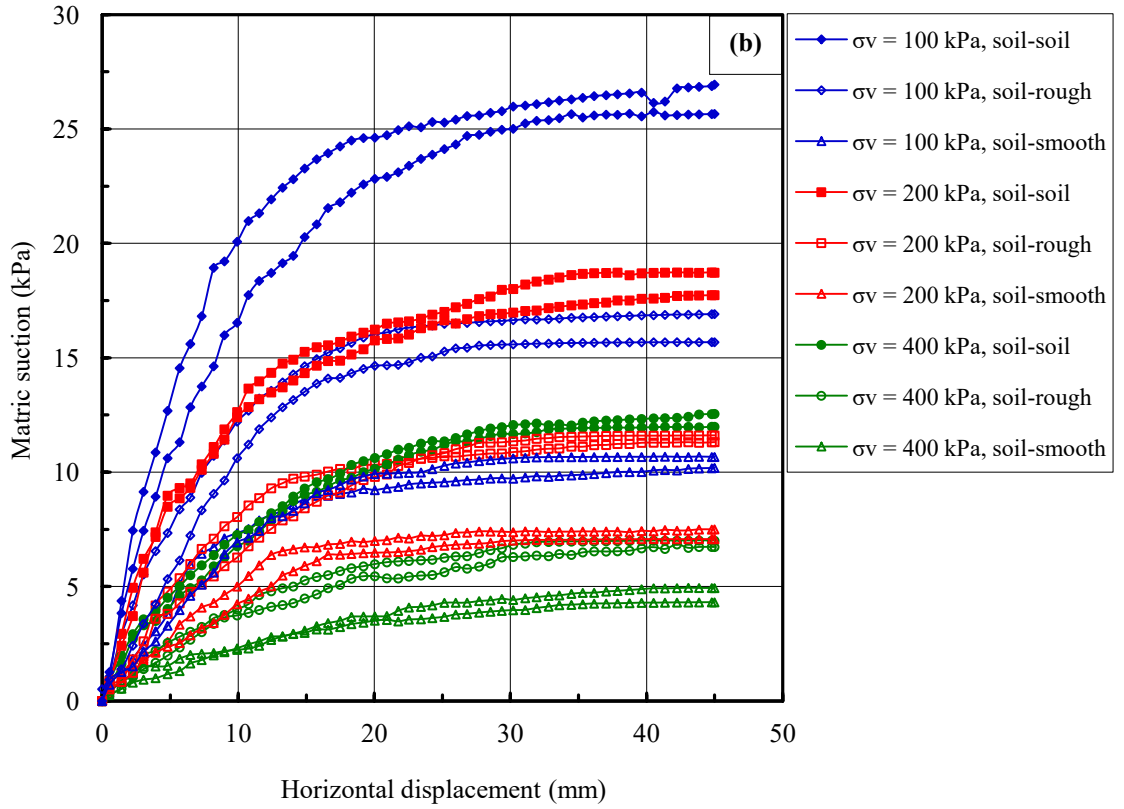

Figure 7.11: Evolution of matric suction during shearing stage for soil and soil-interface specimens (smooth and rough) of: **(a)** $e_i = 0.6$ and **(b)** $e_i = 1.0$.

7.4 Concluding remarks

In this chapter, a comparison between the direct shear test results of soil and interfaces (smooth and rough) is made. The results showed that the soil specimens exhibited higher shear strength than the interfaces for all levels of vertical stress and for both test conditions (saturated and constant water content). It was observed that shear strength decreases with increasing degree of saturation of the soil and interfaces as would be expected when degree of saturation increases, the matric suction decreases. Although the shear strength of the soil was higher than the rough interface for all values of vertical stress, shear strength behaviour of soil and the rough interface was similar as both showed strain softening behaviour (smooth peak pattern) for dense specimens (e_i = 0.6) suggesting that the matric suction is less important in the post-peak region. However, smooth interface showed steady state behaviour (non-peak pattern) for both studied void ratios after reaching maximum shear strength. In addition, the maximum shear strength of smooth interface was less than the soil and rough interface for all values of vertical stress used in this study. This observation supports the argument that the shearing mechanism of the smooth interface is governed by sliding between soil particles and smooth concrete pad rather than interlocking (i.e. stick-slip behaviour). It can also be noticed that the smooth interface exhibited maximum shear strength at a smaller horizontal displacement than the soil and rough interface and for all specimens, which indicates that the surface roughness of initiated governing the shearing behaviour of the smooth interface at a smaller horizontal displacement.

The comparison of test results showed that the angle of friction, ϕ', and cohesion, c', of soil is greater than the interface friction angle, δ', and adhesion, c_a', of rough and smooth interfaces. The values of δ' and c_a' between soil and smooth interface are smaller than those of the case of rough interface for all vertical stress levels and under different test conditions (saturated and constant water). From the test results, it can be concluded that the matric suction reduction during consolidation stage of soil samples was higher than that of the interfaces. Furthermore, at any stress level, specimens (soil, soil-smooth, soil-rough) with higher initial matric suction showed lower coefficient of suction reduction. The larger is the change in volume, the larger is the reduction in matric suction.

The increase in matric suction with horizontal displacement during shearing stage, as observed in the case of soil and rough interface, can also be observed for the smooth

interface. However, an increase in matric suction in the case of the smooth interface is less pronounced than the soil and rough interface suggesting that the water meniscus bonding due to physico-chemical and capillary forces between soil particles and smooth surface is weaker and hence lower matric suction.

CHAPTER EIGHT

CONCLUSIONS AND RECOMMENDATIONS

8.1 Introduction

This research represents one of the first attempts to investigate the interface shearing behaviour of Iraqi soils. A primary objective of this thesis was to study experimentally the effect of void ratio, the level of applied vertical stress, surface roughness, and test conditions (saturated and constant water content) on the shear strength and volumetric characteristics of soil-concrete interfaces and soil specimens. A conventional large-scale direct shear device was used for performing the experimental program to achieve the objectives of this study.

The testing programme consisted of three main parts. The first part was devoted to determine the index properties of the prepared soil and some conventional standard relevant tests to characterise the adopted soil for the investigation. The shear strength and volumetric behaviour of compacted soil-soil specimens were investigated in the second part. The third part focused on the detailed investigation on the shear strength characteristics of the soil-concrete interface specimens. Based on the analysis of the experimental results presented in Chapters 4 to 7, the major conclusions corresponding to each part of the testing programme are described in the following sections.

8.2 Conclusions from soil – soil direct shear tests

The large-scale direct shear apparatus used for saturated soil tests was upgraded for the direct shear tests of soil specimens under constant water content condition. The major conclusions are drawn based on the experimental data and their interpretations presented in Chapter 5. They are listed below:

1. For the studied silty sand soil, the loose specimens (e_i = 1.0) performed under saturated condition exhibited collapse behaviour during saturation stage under very low level of applied vertical stress (1.33 kN/m^2). Whereas same samples did not show any volume change during suction equalisation stage (9 days period prior to start consolidation stage) when tested at constant water content condition. It was therefore concluded that the samples prepared with e_i = 1.0 presented an open metastable structure and are collapsible. Moreover, the same sample showed that the matric suction has an important effect on the samples response to load and shear.

2. The level of applied vertical stress was found to highly influence the shear strength characteristics of the compacted soil specimens. As vertical stress was increased, the shear strength and the corresponding vertical displacement increased for both test conditions, demonstrating the important role of the level of vertical load applied on the soil.

3. It can be concluded that the initial void ratio and test conditions have an important influence on the shear strength of the tested specimens. From analysis of the results, it was clearly seen that the specimens with e_i = 0.6 revealed greater shear strength in comparison with those prepared with e_i = 1.0. It was observed that the specimens with e_i = 1.0 exhibited greater volume reduction than those with e_i = 0.6 specimens. Furthermore, the results showed that the obtained shear strength of specimens under constant water content are found to be distinctly greater than those obtained from saturated samples, as it was expected due to the effect of matric suction increasing the apparent strength of the soil. Therefore, it was concluded that the shear strength behaviour of the studied material was primarily dependent on initial void ratio and matric suction level.

4. The horizontal displacement corresponding to peak/maximum shear strength depends on the level of applied vertical stress, void ratio and test conditions (saturated or constant water content). The magnitude of horizontal displacement increased with the increase of applied vertical stress. From the analysis of the obtained results, it can be also noted that the tested specimens showed larger

horizontal displacement as void ratio decreased. The results also show that the maximum/peak shear strength for the tested specimens under constant water content was mobilized at larger horizontal displacement when compared with those observed on saturated specimens. This behaviour can be attributed primarily to the effect of matric suction on increasing the apparent stiffness of the specimens.

5. The strain softening behaviour of the tested material is significantly influenced by the initial void ratio of specimens tested under saturated and constant water content conditions. Strain softening behaviour (peak strength pattern) became pronounced with the increase in applied vertical stress for specimens with e_i = 0.6, whereas specimens tested with e_i = 1.0 did not show any strain softening (i.e. hardening behaviour without showing peak strength) under all applied vertical stresses and the shear strength curve exhibited approximately steady state after reaching the maximum strength (non-peak strength pattern), and this is due to the density of the samples at the start of the shearing.

6. Shear strength-horizontal displacement curves of the constant water content samples showed two different patterns in the post-peak region. Dense samples (e_i = 0.6) showed strain softening behaviour after a smooth peak shear strength, whereas, samples with e_i = 1.0 showed no peak shear strength followed by steady state (hardening behaviour) suggesting that within this region the role of matric suction is less significant.

7. Failure envelopes plotted in shear strength-vertical stress plane showed good linearity for the range of applied vertical stress used in this study. The influence of void ratio and test conditions (saturated or constant water content) on angle of friction, ϕ', and soil cohesion, c', of the tested material were investigated. From analysis of the results, for both test conditions, it can be perceived that the angle of friction increases with decreasing the void ratio and degree of saturation of specimens. Furthermore, the results showed that the soil cohesion of saturated specimens increased slightly with decreasing void ratio, while the cohesion increased by fivefold when soil specimens are tested at constant water content condition, demonstrating the significant effect of the matric suction.

8. The effect of shear box size on the shear strength behaviour of silty sand soil performed under saturated and constant water content conditions was

investigated in this study. The shear strength results obtained from two different shear box sizes (60 mm x 60 mm and 300 mm x 300 mm) were compared. It was observed that the peak/maximum shear strength decreases slightly with increasing the size of shear box and, as a consequence, the angle of friction of the samples decreases. While no clear correlation was found between soil cohesion and different shear box sizes.

The conclusions 2 to 8 are in agreement with the findings reported in the literature and highlighted throughout the thesis.

9. A new loading steel cap for large-scale direct shear apparatus (300 mm x 300 mm) was designed for understanding the evolution of matric suction during equalisation, consolidation and shearing stages. For this purpose, two commercial suction probes were employed, inserted into the modified loading steel cap and fixed by screws. From the results, it was observed that the initial matric suction has a clear dependency on the void ratio of the specimens. As the value of void ratio increased, so did the matric suction. The obtained experimental results also showed that, during consolidation stage, the reduction in matric suction increased with the increase of void ratio and the level of applied vertical stress.

10. During shearing process, the evolution of matric suction increased with the increase in horizontal displacement until the peak shear strength is attained. As the horizontal displacement increased, the measured matric suction either remained unchanged or increased slightly in the post-peak region. It was also observed that the matric suction of both studied void ratios specimens decreased with increasing the level of applied vertical stress. Furthermore, the test results showed that the samples prepared with high void ratio revealed higher matric suction than those prepared at low void ratio, as it was expected and vastly shown in the literature.

8.3 Conclusions from soil – concrete interface direct shear tests

The direct shear apparatus used for soil tests under constant water content condition was employed for investigating the interface behaviour between silty sand soil and concrete interface. Cast in-situ interface was formed between soil and concrete counterface with different surface roughness (smooth and rough). Based on the findings reported in Chapter 5, the following conclusions were drawn:

1. The shear strength characteristics of soil-concrete interface performed under saturated and constant water content conditions get significantly affected by the level of applied vertical stress and initial void ratio. Interface shear strength and the corresponding vertical displacement are noted to increase with increasing the vertical stress. The results also showed the tested specimens compacted at a lower void ratio (i.e. e_i = 0.6) exhibited higher interface shear strength. Furthermore, the comparison of shearing behaviour between soil and both interfaces (smooth and rough) showed that the shear strength of soil was higher than the rough and smooth interfaces for both studied void ratios, whereas, the smooth interface showed lower values of shear strength of all the tested samples, which indicates that the interlocking between soil particles themselves is stronger than the interlocking between soil particles and interfaces.

2. The shearing behaviour of the soil-concrete interfaces has shown to be dependent on the test conditions (saturated or constant water content). Similar to soil tests, the obtained interface shear strengths of specimens under constant water content were found to be distinctly greater than those obtained from saturated samples. This illustrates the significant role of matric suction on the shear strength behaviour of the tested material.

3. The surface roughness of the concrete has a noteworthy influence on the interface shear strength for the particular void ratios and applied vertical stress tested under saturated and constant water content conditions. From the results, it was observed that the interface with greater counterface roughness (rough interface) showed a higher peak shear strength, while the interface with smooth counterface showed lower peak shear strength. This behaviour is due to the fact that the inter-particle friction increases with surface roughness and hence on the shear strength.

4. It was shown that the contribution of matric suction to the interface shear strength after reaching the peak/maximum shear strength is not of large significance. Dense samples (e_i = 0.6) sheared against rough interface showed strain softening behaviour (with a noticeable peak strength), whereas, strain hardening behaviour (with no peak strength) was only observed for samples with e_i = 1.0 under 200 and 400 kPa applied vertical stress. Furthermore, shear strength-horizontal displacement curves of samples with e_i = 0.6 and 1.0 tested against smooth interface attained steady state behaviour (strain hardening with no peak strength) in the post-peak region. It was therefore concluded that the surface roughness of the counterface and initial void ratio of the samples are controlling the shear strength behaviour of the interfaces in this region.

5. The interface shear strength failure envelopes plotted in shear strength-vertical stress plane are almost linear for the range of applied vertical stress used in this study. The results revealed that the interface friction angle, δ_a', increased with an increase in the surface roughness of the counterface and a decrease in the initial void ratio of samples. It was also observed that the interface adhesion, c_a', of constant water content samples increased slightly with decreasing the void ratio. From the test results, reducing the degree of saturation increased the shear strength parameters (δ_a' and c_a') of the interface samples. In addition, interface friction angle is higher in the case of rough interface with respect to the case of smooth interface, but lower than the corresponding soil friction angle, which indicates that the interlocking between soil particles themselves is stronger than the interlocking between soil particles and interfaces. The results also showed that the cohesion of soil, c', is greater than the adhesion of the interfaces, c_a' (smooth and rough) suggesting that the cohesion forces clinging to the contact point of the soil particles are stronger than the adhesion forces between soil and interfaces.

6. Similar to soil tests, this study results have shown that the horizontal displacement corresponding to peak/maximum shear strength of the interfaces increased with the increase in the level of applied vertical stress and a decrease in void ratio of the tested samples. However, the smooth interface exhibited maximum shear strength at smaller horizontal displacement than the rough interface. The results showed that the peak strength for soil samples mobilized at

larger horizontal displacement than the interfaces. Another relevant point, it was also observed that the horizontal displacement increases with decreasing the degree of saturation of samples suggesting that stronger bonding forces were associated with lower water content and hence an increase in the horizontal displacement to attain the failure point.

7. The evolution of matric suction during consolidation stage was investigated for the interfaces (smooth and rough). From analysis of the obtained results, it can be observed that the void ratio has a noticeable effect on initial matric suction of the tested material. The matric suction of the compacted samples increased as the value of void ratio increased from 0.6 to 1.0. As for soil tests, the experimental results showed that the reduction of matric suction during consolidation stage depends mainly on the level of applied vertical stress and the initial void ratio. For both void ratios used in this study, specimens consolidated under high level of vertical stress exhibited greater reduction in matric suction. The comparison of soil and interface behaviour during consolidation showed that, for both studied void ratios, the suction reduction was more pronounced for soil than for the interfaces. The larger is the volume contraction, the larger would be the matric suction reduction in a compacted sample. From the obtained experimental results, it was also noted that, for soil and interfaces, specimens with the higher initial matric suction (e_i = 1.0) showed lower coefficient of suction change (i.e. the lower reduction with respect to the initial matric suction) in comparison to those prepared at e_i = 0.6.

8. Test results revealed clearly that there is a remarkable increase in matric suction during shearing stage with increasing the level of applied vertical stress for all investigated samples (e_i = 0.6 and 1.0). However, at any level of vertical stress, the matric suction obtained from soil-smooth samples was less than those of soil and soil-rough interface. This is due to the weaker bonding between soil particles and the smooth interface and hence lower evolution of matric suction. The curves of matric suction evolution versus horizontal displacement for both interfaces (smooth and rough) showed a clear increase in the matric suction associated with increasing the horizontal displacement. It was noted that the most important matric suction evolution occurred before the horizontal displacement corresponding to the peak/maximum shear strength reached. As horizontal displacement increased, the matric suction did not show significant

changes. From the analysis of the results, it can be remarked that the soil samples at e_i = 0.6 and 1.0 exhibited higher matric suction evolution than the smooth and rough interfaces suggesting that the water meniscus bonding the soil particles themselves is stronger than that bonding the soil particles and the interfaces.

8.4 Recommendations for Future Work

1. The experimental results showed clearly that the void ratio plays a remarkable role in the mechanical behaviour of soil and interfaces. Therefore, it is recommended to investigate the influence of different initial soil characteristic (e.g. water content, relative compaction) on the behaviour of soil and interfaces performed under constant water content conditions.

2. The current thesis examined the shear strength and volumetric behaviour between compacted silty sand soil (disturbed samples) and interfaces. It is recommended to investigate the interface behaviour between undisturbed samples (natural soil) and the counterface, because it is very widespread throughout the world and the behaviour of these natural soils may be very different to that of compacted soil (because of the different soil structures).

3. In this study, the soil and interfaces samples were investigated under different levels of applied vertical stress ranged from 100 to 400 kPa. It is recommended to explore the effect of various which range of vertical stress than used in this study. It is also recommended to investigate the effect of different rate of shear displacement on the shear strength and volumetric behaviour of soil and soil-interface samples under constant water content condition.

4. For soil-interface direct shear tests, the concrete was used in this study as a counterface with different surface roughness (smooth and rough). An experimental programme is recommended to study the influence of different interface materials such as steel, wood and geosynthetics on the geotechnical characteristics of the soil-interface samples performed under constant water content condition.

5. In this study, the compacted soil was tested using two different shear box sizes, large-scale (300 mm x 300 mm) and small-scale (60 mm x 60 mm), to investigate the shear strength characteristics of silty sand soil. The experimental tests were carried out under saturated and constant water content conditions. Further studies can be conducted to explore the shear strength of different types of soils (e.g. clayey and silty soils).

APPENDICES

Appendix: A

Matric suction behaviour during stabilisation stage for soil and interfaces

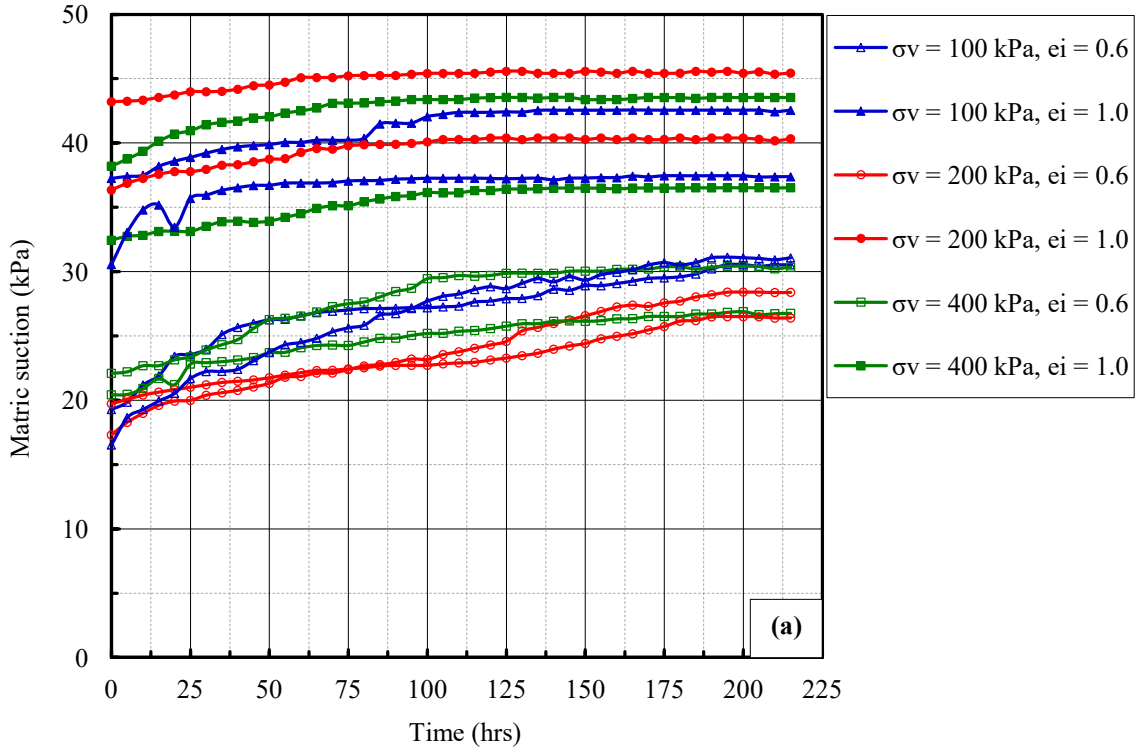

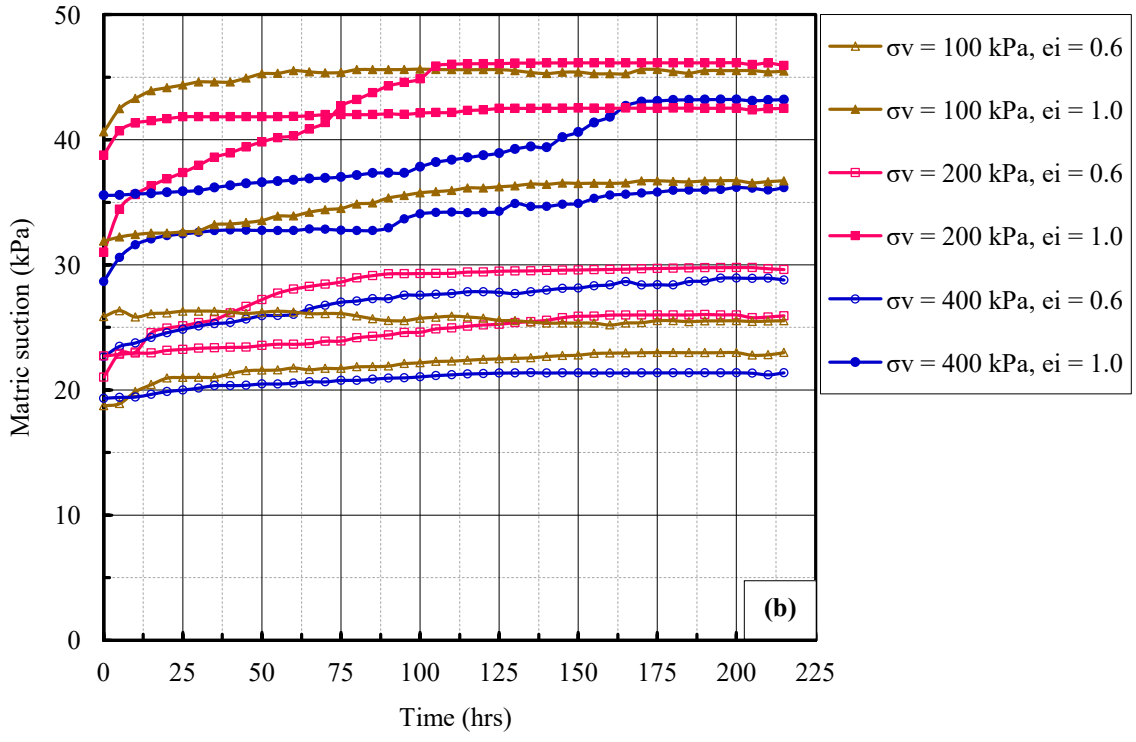

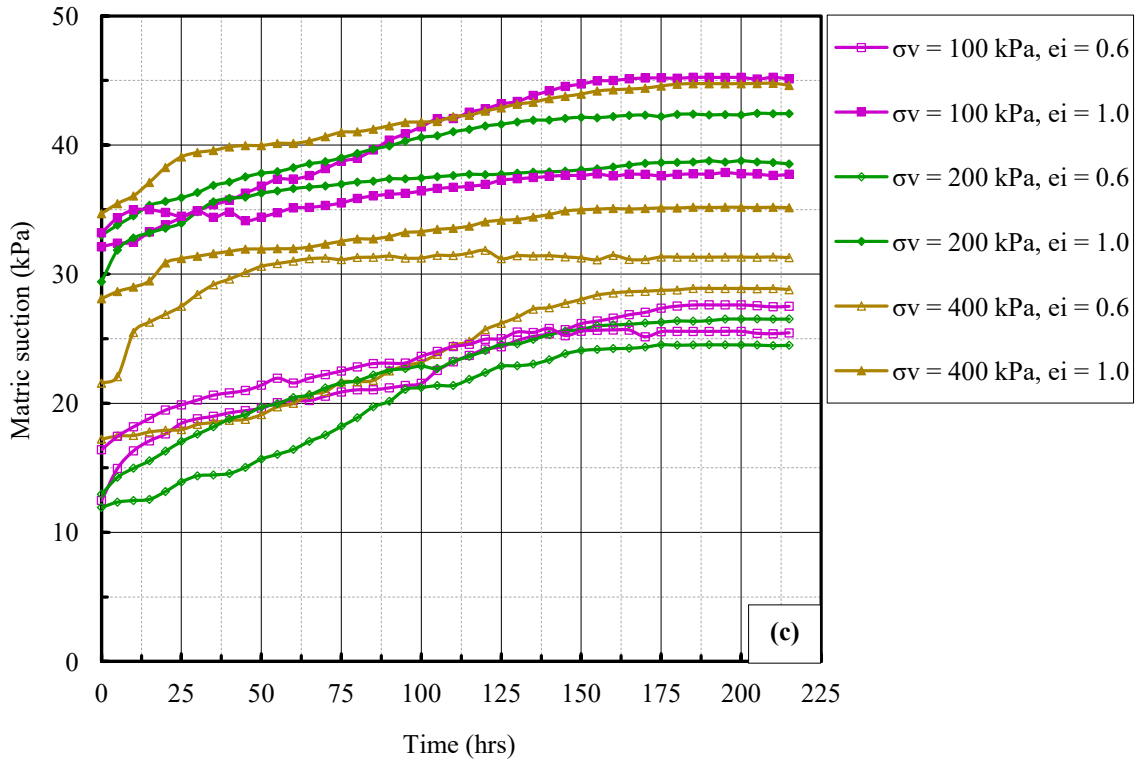

Figure 1A: Matric suction behaviour during stabilisation stage of e_i = 0.6 and 1.0: **(a)** soil, **(b)** soil-smooth and **(c)** soil - rough

Appendix: B

Direct shear test results of small-scale (60 mm x 60 mm) apparatus

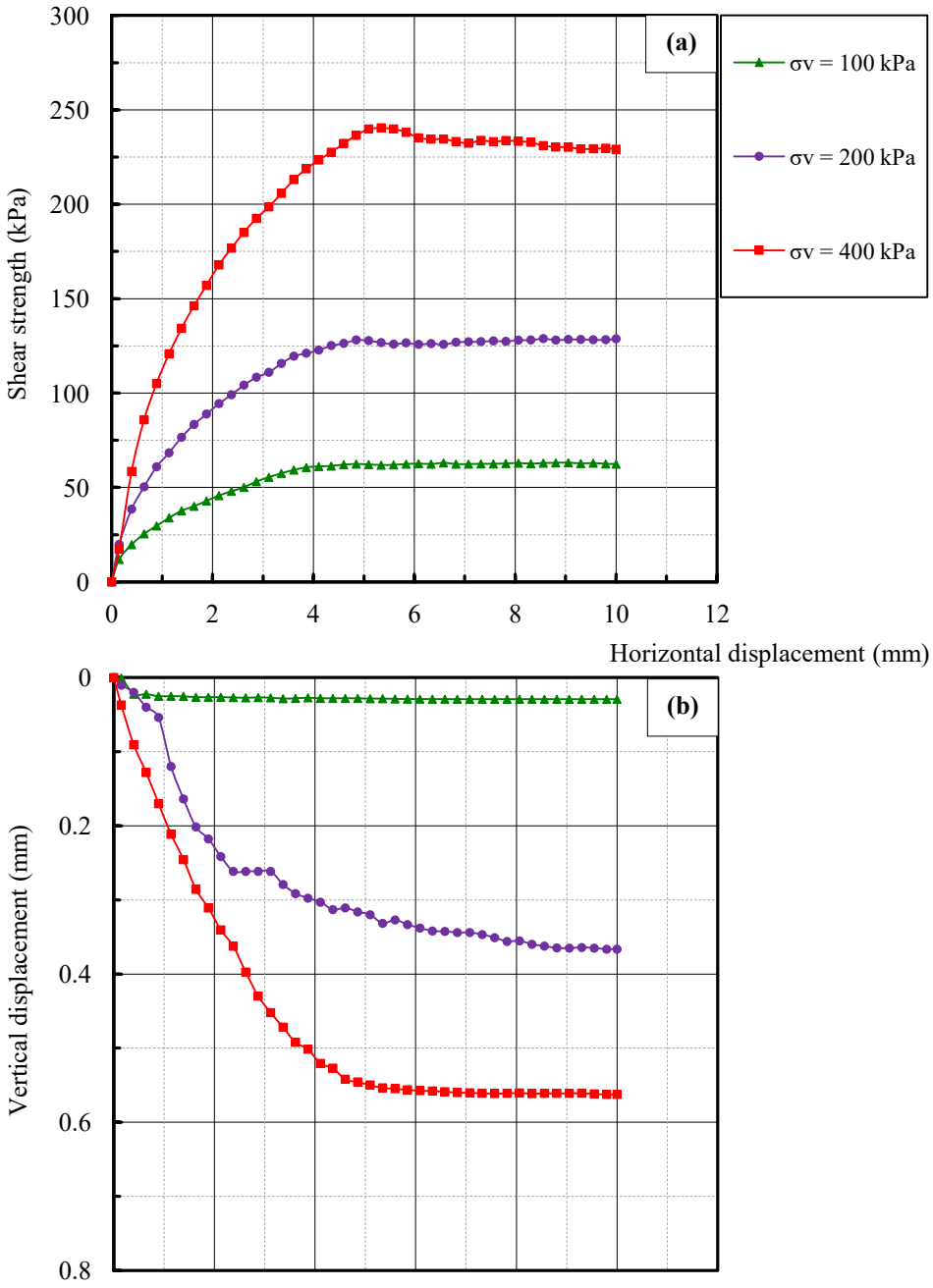

Figure 1B: Direct shear results of silty sand samples for e_i = 0.6: **(a)** shear strength; **(b)** volumetric behaviour (saturated state).

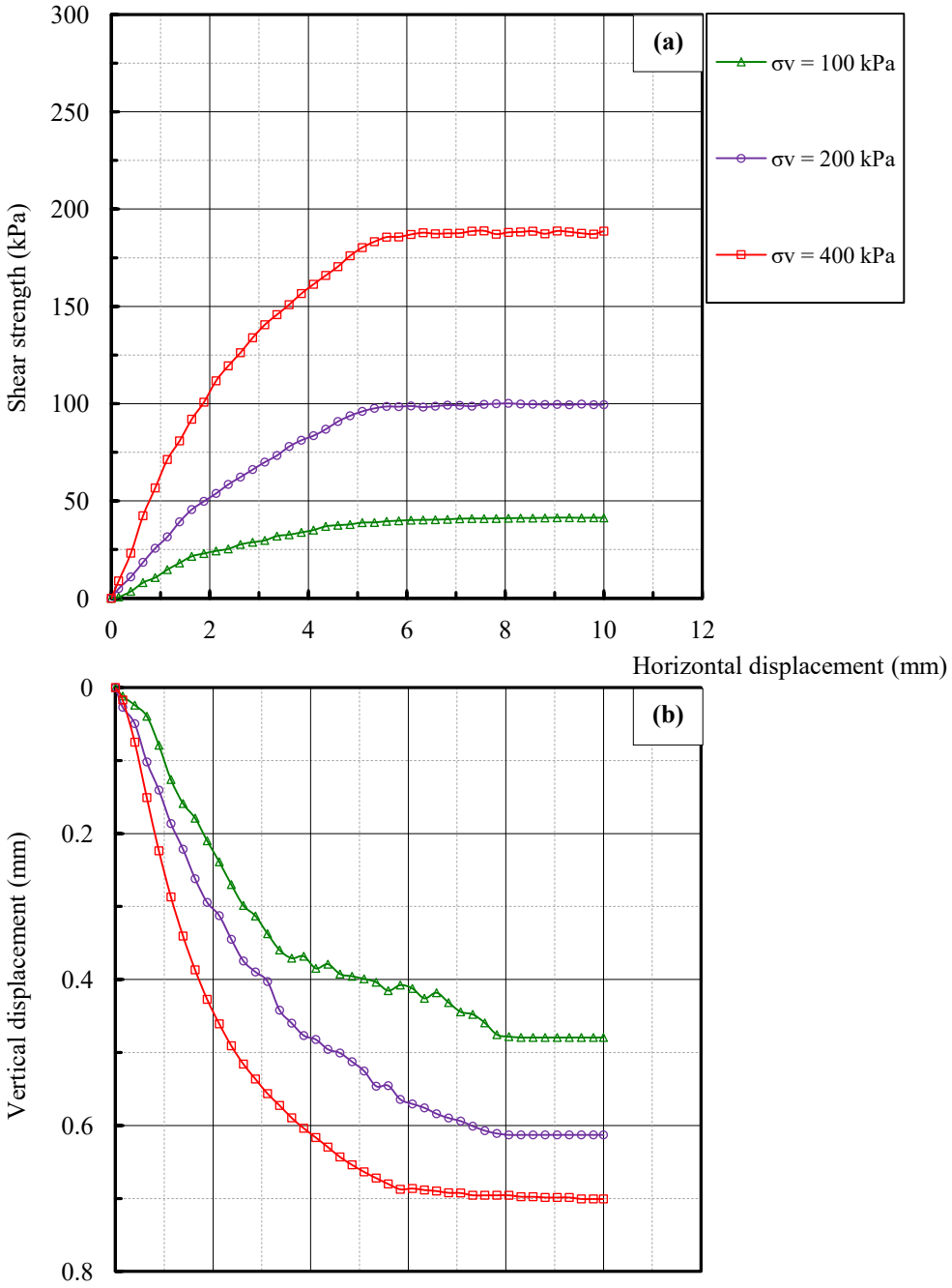

Figure 2B: Direct shear results of silty sand samples for e_i = 1.0: **(a)** shear strength; **(b)** volumetric behaviour (saturated state).

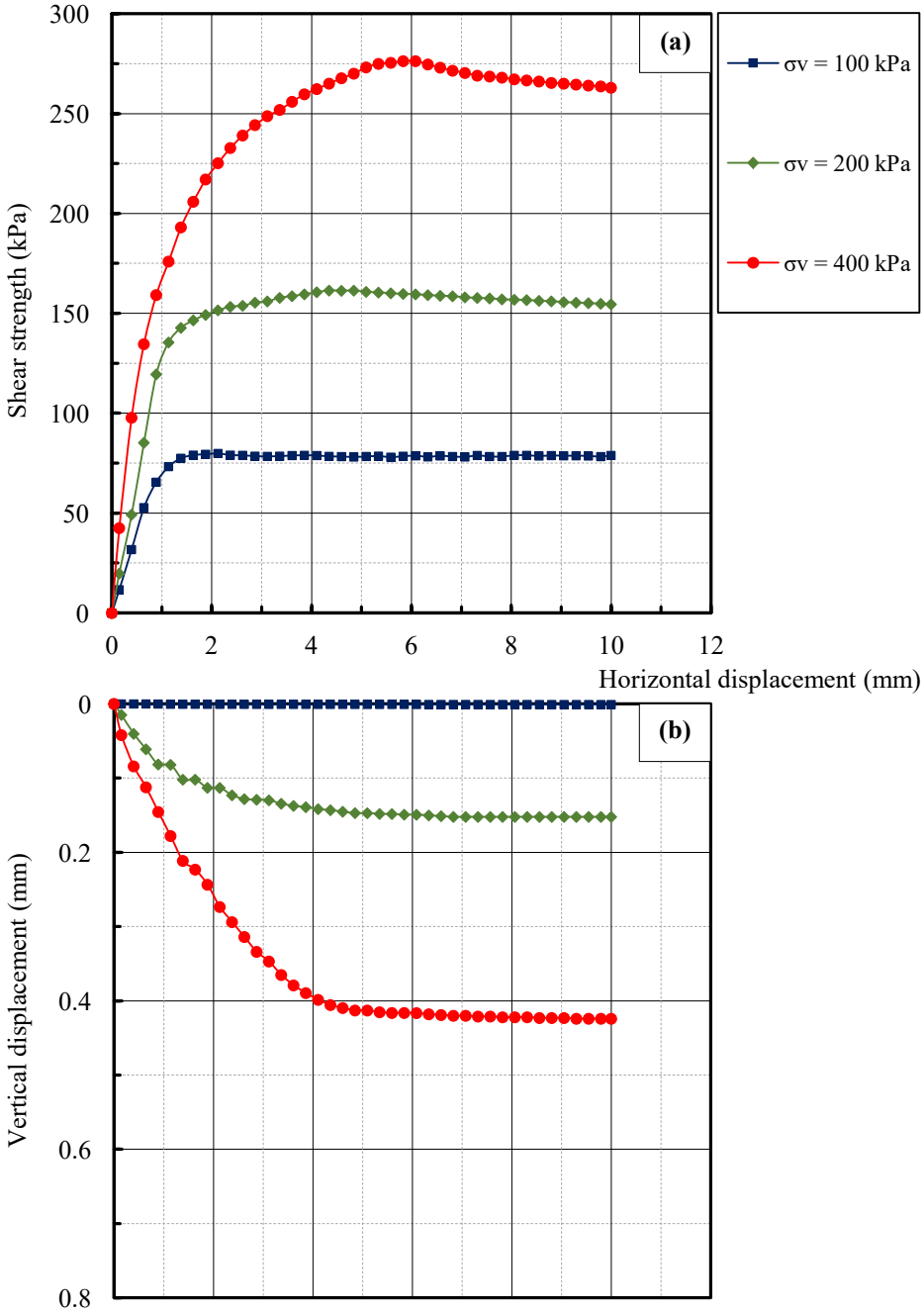

Figure 3B: Direct shear results of silty sand samples for e_i = 0.6: **(a)** shear strength; **(b)** volumetric behaviour (constant water content state).

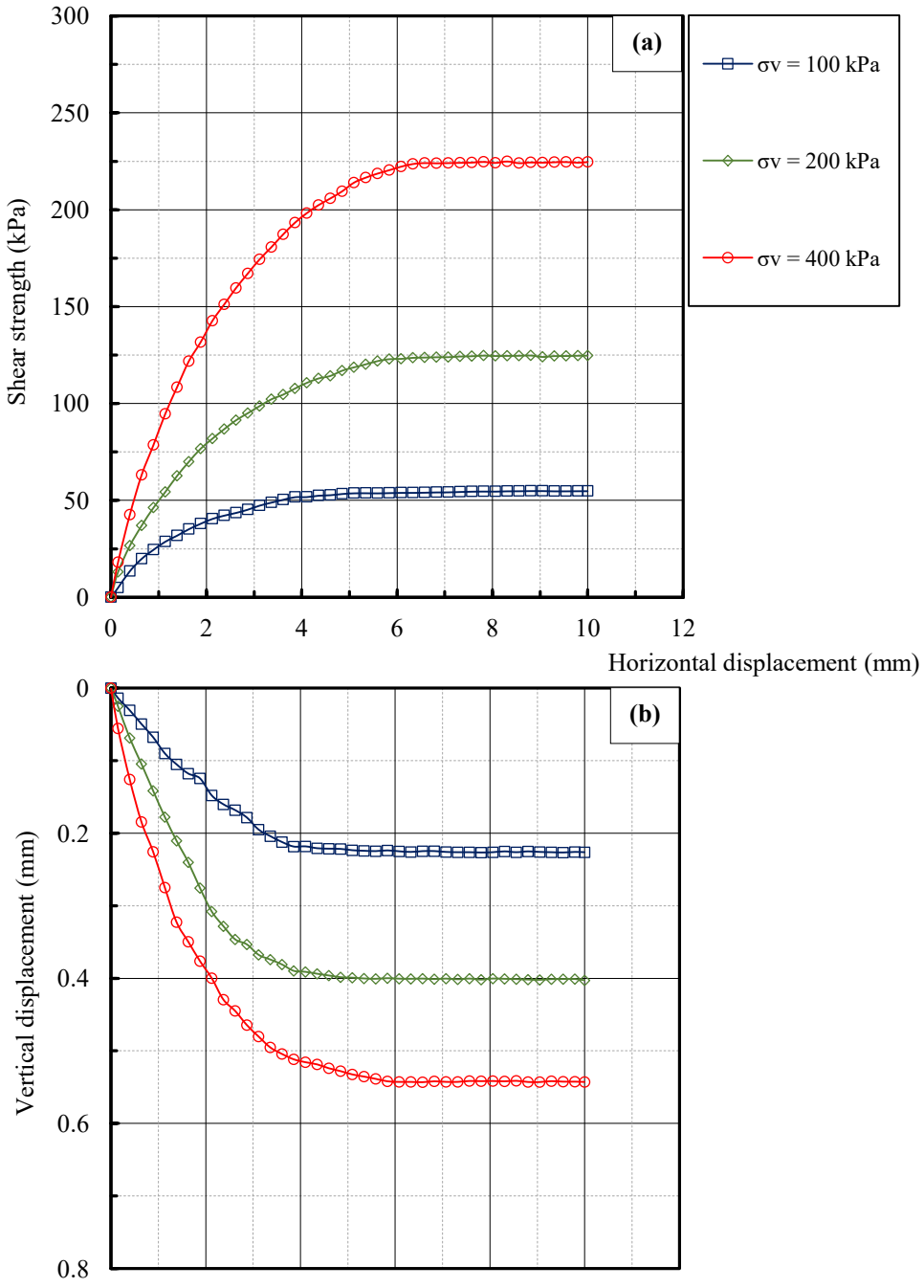

Figure 4B: Direct shear results of silty sand samples for e_i = 1.0: **(a)** shear strength; **(b)** volumetric behaviour (constant water content state).

Table B-1: Values of horizontal displacement corresponding to the peak/maximum shear strength for e_i = 0.6 and 1.0 specimens (saturated condition)

Vertical stress, σ_v (kPa)	Initial void ratio, e_i = 0.6	Initial void ratio, e_i = 1.0	Horizontal displacement at peak/maximum shear strength, δ_h (mm)	
	Peak/maximum shear strength, τ (kPa)	Peak/maximum shear strength, τ (kPa)	e_i = 0.6	e_i = 1.0
100	61.31	38.86	3.61	4.35
200	128.17	98.70	4.84	5.09
400	240.48	187.58	5.58	5.58

Table B-2: Values of horizontal displacement corresponding to the peak/maximum shear strength for e_i = 0.6 and 1.0 specimens (constant water content condition)

Vertical stress, σ_v (kPa)	Initial void ratio, e_i = 0.6	Initial void ratio, e_i = 1.0	Horizontal displacement at peak/maximum shear strength, δ_h (mm)	
	Peak/maximum shear strength, τ (kPa)	Peak/maximum shear strength, τ (kPa)	e_i = 0.6	e_i = 1.0
100	77.49	52.48	1.63	3.61
200	160.60	117.02	4.10	4.84
400	276.29	220.36	6.08	5.83

Table B-3: Shear strength parameters for different initial void ratio specimens (saturated condition)

Initial void ratio, e_i	ϕ'	c'	R^2
	(Degree)	(kPa)	
0.6	32.5	5.5	0.9980
1.0	28	0	0.9939

Table B-4: Shear strength parameters for different initial void ratio specimens (constant water content condition)

Initial void ratio, e_i	ϕ'	c'	R^2
	(Degree)	(kPa)	
0.6	36	21	0.9909
1.0	31	3	0.9967

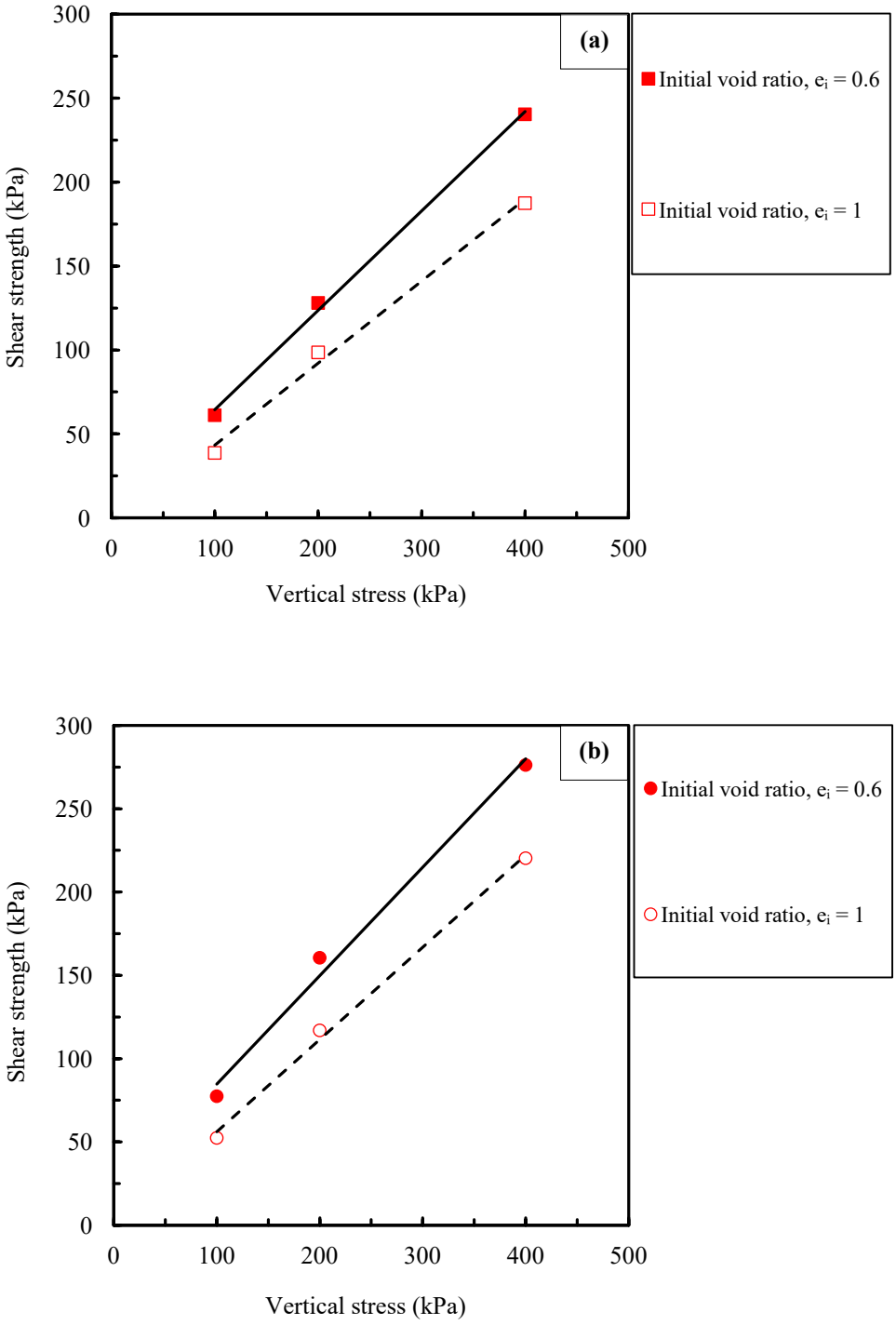

Figure 5B: Failure envelopes corresponding to different void ratios (e_i = 0.6 and 1.0): **(a)** saturated condition; **(b)** constant water content condition.

Appendix: C

Calibration of direct shear components

C.1. Small-scale apparatus

In order to provide correct and accurate measurements, which will be used in the analysis and interpretation, the calibrations and the adjustment of the direct shear device and its components used in this study were determined and presented in the following sections.

The small-scale direct shear tests were carried out using an ELE International, 26-2114, Digital Direct/Residual Shear Apparatus (Figure 1C). A GDU 8 Channel Data Acquisition (ELE International) was used for logging the recorded shear tests data, and the ELE Geotechnical Analysis Software, DS7 (DataSystem 7) was used to transfer the recorded data from data acquisition to a PC. The direct shear apparatus equipped with three measuring devices. There are two Linear Variable Differential Transducers (LVDTs) for measuring horizontal and vertical displacements. Each of these transducers had maximum displacement capacities of 15 mm. The load cell with a capacity of 5 kN was used for measuring the horizontal shear load. It should be noted that the calibrations data for all the LVDTs and load cell were prepared and submitted by the manufacture. However, the calibrations were performed in the Geotechnical laboratory before commencement of the tests.

The horizontal and vertical LVDT were calibrated by using a slidecaliperse, whereas the load cell was calibrated by applying compressive load of 0 to 5 kN through a universal testing machine. The concept of calibration can be summarized by subjecting several different increments of displacement or force to it and these increments were measured by using well-calibrated reference device. After completing the calibration process, pairs of readings were recorded corresponding to each increment, a digital (voltage) reading from the transducer and a physical reading from the reference device with

known units. Figures 2C (a), (b) and (c) show the calibration curves of the LVDTs and load cell respectively and linear regression line drawn.

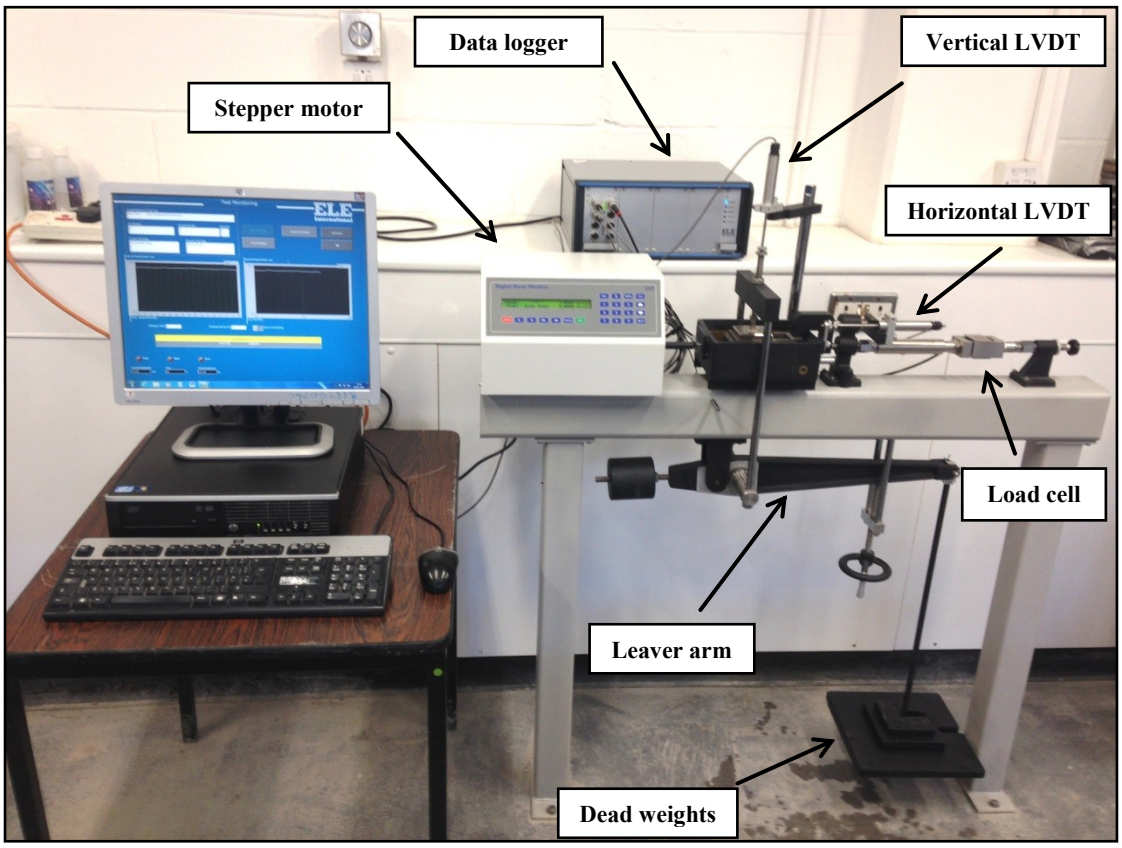

Figure 1C: Photograph of small-scale direct shear apparatus.

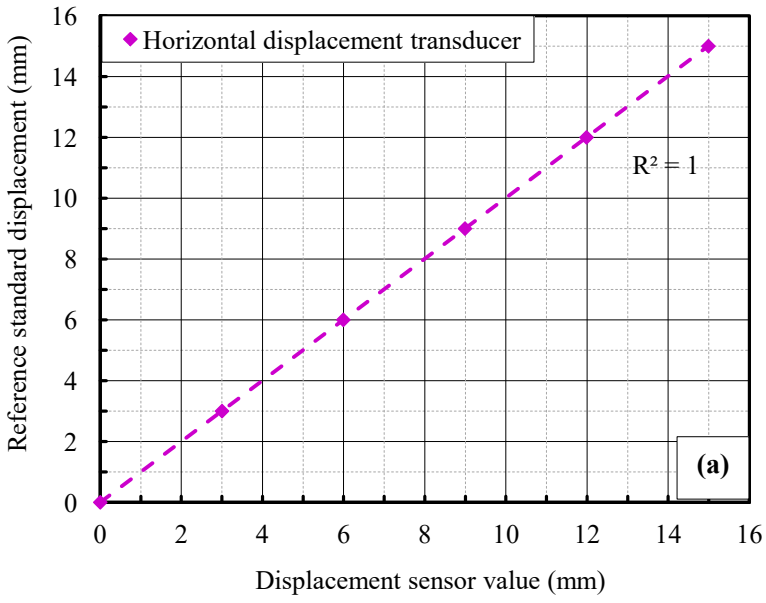

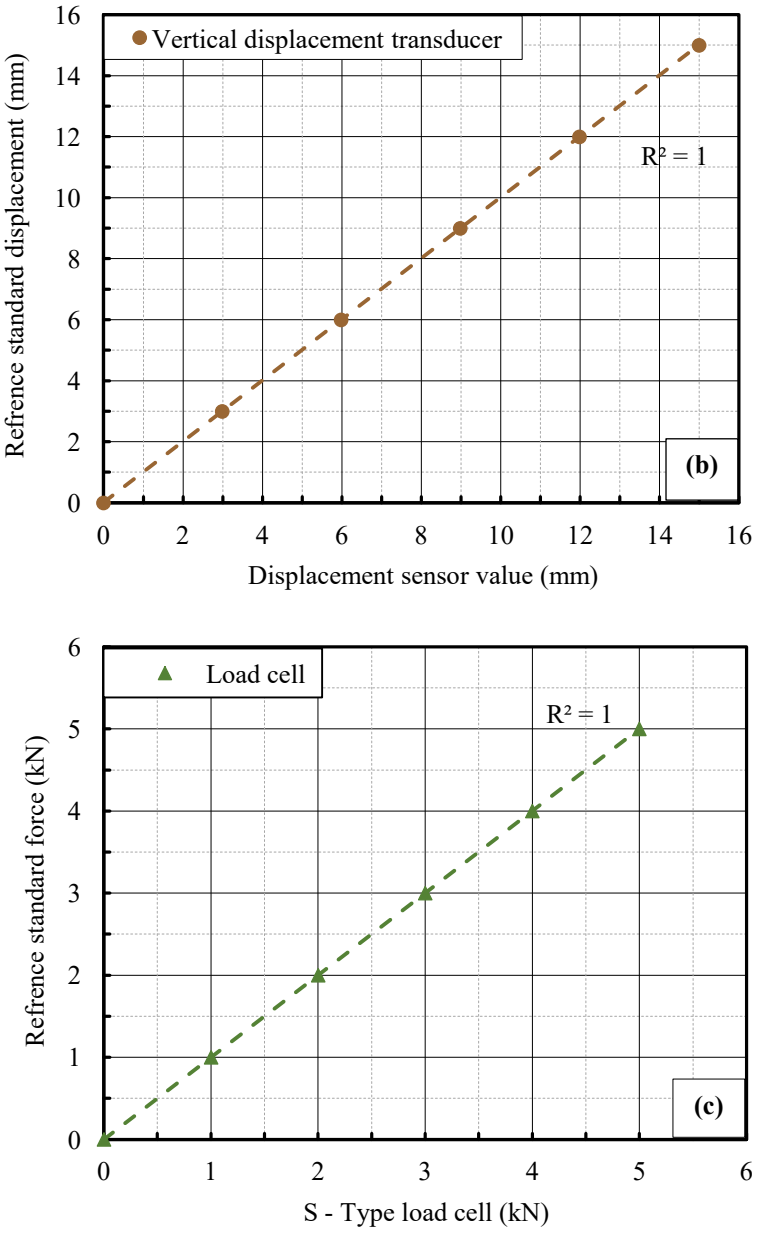

Figure 2C: Calibration curves of: **(a)** Horizontal LVDT; **(b)** Vertical LVDT; **(c)** load cell (small-scale direct shear)

C.2. Large-scale apparatus

A general view of the large-scale direct shear apparatus used for soil-soil and soil-concrete tests is shown in Figures 3C (a), (b), (c) and (d). Large shear box was used for this experimental campaign with a square cross section of 300 mm by 300 mm and a height of 140 mm. The apparatus was provided by Wykeham Farrance Engineering Ltd., Model WF 40200, 100 kN Stepless Shear Box Machine. The machine is equipped with two LVDTs which was used for measuring the horizontal and vertical displacements. One load cell having capacity of 100 kN is installed for measuring the

horizontal shear force. It is worthy to mention here that the LVDTs and the load cell were calibrated following the same procedure adopted in C.1. Figures 4C (a), (b) and (c) show the calibration curves for the horizontal and vertical LVDTs and the load cell, respectively.

Figure 3C: Photographs of the components of large-scale direct shear apparatus: **(a)** shear box; **(b)** hydraulic pressure machine; **(c)** data loggers; **(d)** PC.

The software's TracerDAQ and DASWizard were used to measure and record the displacements (or load) measured by LVDTs (or load cell) during testing stages. The recorded data of the direct shear test was done using USB-1208FS data acquisition (DAQ) device provided by (MESURMENT COMPUTING$_{TM}$, MC) as shown in Figure 3C (c). For recording the evolution of matric suction, the software, called DeltaLINK 3.6.2 was installed on PC. The soil suction data as well as the temperature were transferred from the data logger (GP1) to the computer using this software. Two EQ3s can connect to each data logger (GP1), as shown in Figure 3C (c).

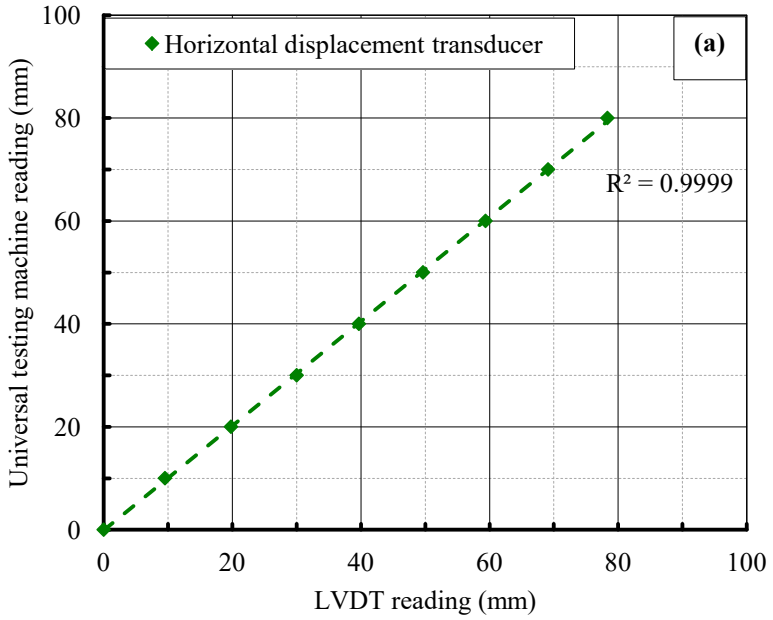

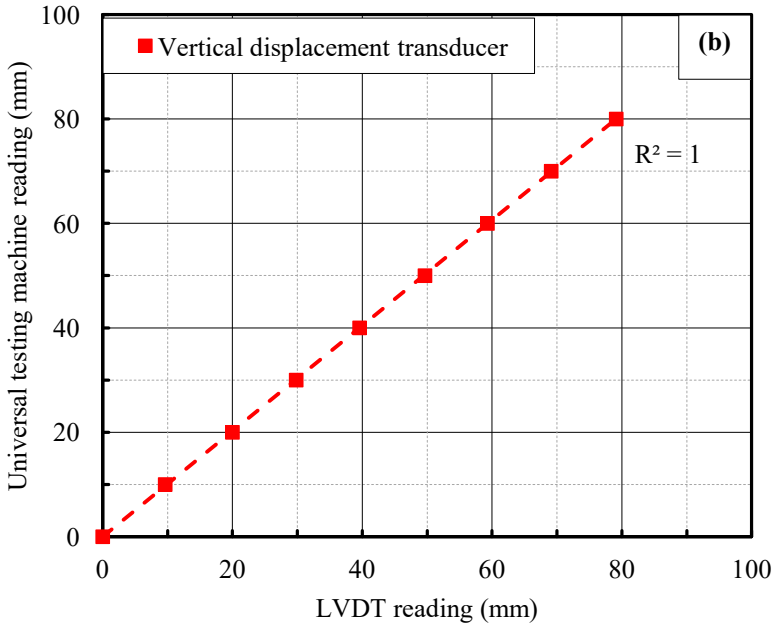

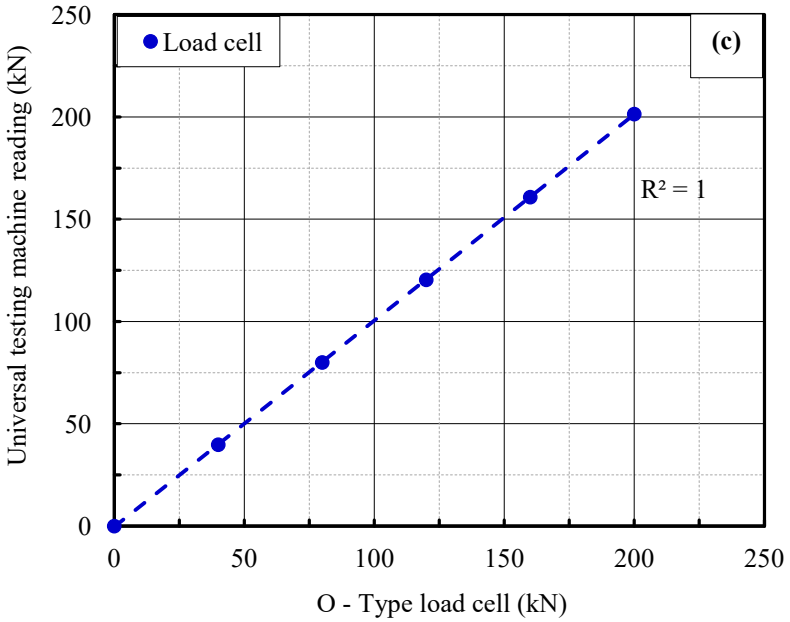

Figure 4C: Calibration curves of: **(a)** Horizontal LVDT; **(b)** Vertical LVDT; **(c)** load cell (large-scale direct shear).

REFERENCES

Acar Y., Durgunoglu H., and Tumay M., 1982, *Interface Properties of Sand*. Journal of Geotechnical Engineering, ASCE, Vol. 108, No. GT4, pp 648 - 654.

Ahmed K. I., 2013, *Effect of gypsum on the hydro-mechanical characteristics of partially saturated sandy soil*, Ph.D. thesis: Cardiff University, UK.

Aitchison G.D., and Donald I.B., 1956, *Some preliminary studies of unsaturated soils*. *In* Proceedings of the 2nd ANZ Conference SMFE, Technical Publications for the New Zealand Institution of Engineers, Wellington, New Zealand. pp 192 – 199.

Aitchison G., 1961, *Relationships of Moisture Stress and Effective Stress Functions in Unsaturated Soils,* In Proceedings of the Conference on Pore Pressure and Suction in Soils, Butterworths, London, UK, pp 47 - 52.

Al-Mhaidib A., 2006, Influence of shearing rate on interfacial frictional between sand and steel, Engineering Journal of the University of Qatar, Vol. 19, pp 25 - 35.

Arunasalam R., 2009, *Coupling of mechanical behaviour and water retention behaviour in unsaturated soils.* PhD thesis, University of Glasgow.

Aubertin M, Ricard J., and Chapuis R., 1998, *A Predictive Model for The Water Retention Curve: Application to Tailings from Hard-Rock Mines*, Canadian Geotechnical Journal, **35 (1)**, pp 55 - 69.

Aubertin M., Mbonimpa M., Bussière M., and Chapuis R.P., 2003, *Development of a model to predict the water retention curve using basic geotechnical properties*, Technical Report EPMRT-2003-01. École Polytechnique de Montréal, pp 51.

Aziz A., Ali F., Heng C., Mohammed T., and Huat B., 2006, *Collapsibility and Volume Change Behaviour of Unsaturated Residual Soil*, American Journal of Environment Sciences, **2(4)**, pp 161 - 166.

Babu B. R., Rastogi N. K.., and Raghavarao K. S. M. S., 2006, *Mass transfer in osmotic membrane distillation of phycocyanin colorant and sweet-lime juice*. Journal of Membrane Scienc*e*, **272** (1–2), pp 58 – 69.

Baker R., and Frydman S., 2009, *Unsaturated soil mechanics: critical review of physical foundations*. Engng Geol. **106**, No. 1, pp 26 – 33.

Barbour S., 1998, *Nineteenth Canadian Geotechnical Colloquium: The Soil Water Characteristic Curve: A Historical Perspective*, Can. Geotech. J., Vol. 35, pp 873 – 894.

Barden L., and Sides G. R., 1970, *Engineering Behaviour and Structure of Compacted Clay*, Journal of Soil Mechanics and Foundation Engineering, ASCE, No.96, SM4, pp 1171 - 1201.

Bear J., 1972, *Dynamics of Fluids in Porous Media*, American Elsevier, New York, NY.

Birle E., Heyer D., and Vogt N., 2008, *Influence of the initial water content and dry density on the soil-water retention curve and the shrinkage behavior of a compacted clay*, Acta Geotech., **3**, pp 191 - 200.

Bishop A., 1959, *The Principle of Effective Stress*, Lecture Delivered in Oslo, Norway, in 1955; *published in Teknik Ubeblad*, **106(39)**, pp 859 - 863.

Bishop A., and Donald I., 1961, *The Experimental Study of Partially Saturated Soils in the Triaxial Apparatus*, Proceedings of the 5th ICSMFE, Paris, Vol.1, pp 13 - 21.

Bishop A.W., and Blight G.E., 1963, *Some aspects of effective stress in saturated and partly saturated soils*, Géotechnique, **13 (3)**, pp 177 - 197.

Blight G.E., 1967, *Effective stresses evaluation for unsaturated soil*, J. of Soil Mechanics and Foundations Division, ASCE, USA, **93**, pp 125 - 148.

Borana L., Yin J., Singh D., and Shukla S., 2013, *A Modified Suction-Controlled Direct Shear Device for Testing Unsaturated Soil and Steel Plate Interface*, Marine and Georesources and Geotechnology, **33**, pp 289 - 298.

Borana T. B., 2014, *Study on the interface behaviour between unsaturated soil and steel surface*, Ph.D. thesis, The Hong Kong Polytechnic University, Hong Kong.

Bosscher P. J., and Ortiz G. C., 1987, Frictional properties between sand and various construction materials, Journal of Geotechnical Engineering, ASCE, **113(90)**, pp 1035 - 1039.

Brumund W. F., and Leonards G. A., 1973, Experimental study of static and dynamic friction between sand and typical construction materials, Journal of testing evaluation, JTEVA, **1(2)**, pp 162 - 165.

Buckingham E., 1907, *Studies On The Movement of Soil Moisture*, Bulletin 38. USDA Bureau of soils. Washington. DC.

Bulut R., and Leong E. C., 2008, *Indirect measurement of suction*, Geotechnical and Geological Engineering, DOI 10.1007/s10706-008-9197-0.

Burland J., 1965, *Soma Aspects of the Mechanical Behaviour of Partially Saturated Soils*, Moisture Equilibrium and Moisture Changes in Soils beneath Covered Area, A symposium in Print, Butterworth Sidney, Australia.

Buringh P., 1960, *Soils and Soil Conditions in Iraq*, Ministry of Agriculture, Baghdad.

Caruso A., and Tarantino A., 2004, *A shear box for testing unsaturated soils from medium to high degrees of saturation*. Geotechnique **45(4)**, pp 281 – 284.

Cerato A. B., and Lutenegger A. J., 2006, *Specimen size and scale effects of direct shear box tests of sands*, Geotechnical Testing Journal, **29(6)**, pp 1 – 10.

Chandler R., 1968, *Shaft Friction of Piles in Cohesive Soils in Terms of Effective Stress*. Civil Engineering, **63(738)**, pp 48-49+51.

Cui Y., and Delage P., 1996, *Yielding and Plastic Behaviour of Unsaturated Compacted Silt*, Géotechnique 46, pp. 291 - 311.

Dadkhah R., Ghafoori M., Ajalloeian R., and Lashkaripour G. R., 2010, *The effect of scale direct shear test on the strength parameters of clayey sand in Isfahan city, Iran*, Journal of Applied Sciences, 10(18): pp 2027 – 2033.

De Campos T.M.P., and Carrillo C.W., 1995, *Direct shear testing on an unsaturated soil from Rio de Janeiro*. Proc. 1st Int. Conference on Unsaturated Soils, Paris (1), 31-38.

Desai C. S., Drumm E. C., and Zaman M. M., 1985, *Cyclic Testing and Modeling of Interfaces*, ASCE, Journal of Geotechnical Engineering, Vol.111, No.6, pp.793 - 815.

Dregne H. E., 1986, *Desertification of Arid Lands*, In: El-Baz F., Hassan M.H.A. (eds) Physics of desertification.

Elgabu H., 2013, *Critical evaluation of some suction measurement techniques*, Ph.D. thesis: Cardiff University, UK.

Escario V., 1980, *Suction Controlled Penetration and Shear Tests*, Proceedings, 4th International Conference on Expansive Soils, Vol. 2, pp. 781 - 797.

Escario V., Sáez J., 1986, *The shear strength of partly saturated soils*, Géotechnique **36(3)**, pp 453 - 456.

Escario V., and Juca J.F.T., 1989, *Strength and deformation of partly saturated soils*, Proceedings of the 12th International Conference on Soil Mechanics and Foundation Engineering (ICSMFE), Rio de Janeiro, Brazil, pp. 43 – 46.

Estabragh A., and Javadi A., 2012, *Effect of Suction on Volume Change and Shear Behaviour of an Overconsolidated Unsaturated Silty Soil*, Geomechanics and Engineering, **4(1)**, pp. 55 - 65.

Fakharian K. and Evgin E., 1996, *An Automated Apparatus for Three-Dimensional Monotonic and Cyclic Testing of Interfaces*, Geotechnical Testing Journal, Vol. 19, No. 1, pp. 22 - 31.

Fakharian K., 1996, *Three-Dimensional Monotonic and Cyclic Behaviour of Sand-Steel Interfaces: Testing and Modelling*, Ph.D. dissertation submitted to Department of Civil Engineering, University of Ottawa.

Farooq K., Rogers J. D., and Ahmed M. F., 2015, *Effect of densification on the shear strength of landslide material: A case study from salt range, Pakistan*, Earth Science Research, **4(1)**, pp 113 – 125.

Feuerharmel C., Pereira A., Gehling W. Y. Y., and Bica A. V. D., 2006, *Determination of the shear strength parameters of two unsaturated colluvium soils using the direct shear test*, in Proceedings The fourth international conference on unsaturated soils, Carefree, Arizona, Volume 2, ASCE, pp 1181 - 1190.

Fleming I.R., Sharma J.S., Jogi M.B., 2006, *Shear strength of geomembrane-soil interface under unsaturated conditions*, Geotextiles and Geomembranes, **24**, 274 - 284.

Food and Agriculture Organization, 1990, http://www.fao.org/iraq/en/

Fredlund D. W., 1975, *A diffused air volume indicator for unsaturated soils*, Canadian Geotechnical Journal, **12(4)**, 533 – 539.

Fredlund D.G., Morgenstern N.R., 1977, *Stress State Variables for Unsaturated Soils*, Journal of Geotechnical Engineering Division, **103**, pp. 447 - 466.

Fredlund D.G., Morgenstern N.R., and Widger R.A, 1978. *Shear Strength of Unsaturated Soils*, Canadian Geotechnical Journal, Vol. 15, No. 3, pp. 313 - 321.

Fredlund D., Rahardjo H., 1993, *Soil Mechanics for Unsaturated Soils*, John Wille & Sons, New York.

Fredlund D., Xing A., and Huang S., 1994, *Predicting the Permeability Function for Unsaturated Soils using the Soil-Water Characteristic Curve*, Canadian Geotechnical Journal, **31 (3)**, pp. 533 - 546.

Fredlund M., Fredlund, D., and Wilson, G., 2000, *An Equation to Represent Grain-size Distribution*. Canadian Geotechnical Journal, Vol. 37, pp. 817 - 827.

Fredlund D.G., Rahardjo H., and Fredlund M.D., 2012, *Unsaturated soil mechanics in engineering practice*, John Wiley & Sons.

Frost J., and Han J., 1999, *Behaviour of Interfaces between Fiber-Reinforced Polymers and Sands*. Journal of Geotechnical and Geoenvironmental Engineering, ASCE, **125(8)**, pp. 633-640.

Gachet P., Klubertanz G., Vulliet L., and Laloui L., 2003, *Interfacial Behaviour of Unsaturated Soil with Small- Scale Models and Use of Image Processing Techniques*, Geotechnical Testing Journal, Vol. 26, No.1.

Gallage C., and Uchimura T., 2010, *Effects of Dry Density and Grain Size Distribution on Soil-Water Characteristic Curves of Sandy Soils*, Soil and Foundations, **50(1)**, pp. 161 - 172.

Gallipoli D., Gens A., Sharma R. S. and Vaunat J., 2003, *An elasto-plastic model for unsaturated soil incorporating the effect of suction and degree of saturation on mechanical behaviour*, Géotechnique **53**, No. 2.

Gan J.K.M., 1986, *Direct shear testing of unsaturated soils*, M.Sc. thesis, University of Saskatchewan, Saskatoon, Sask.

Gan K.J., Fredlund D.G., 1988, *Multistage direct shear testing of unsaturated soils*, Geotechnical Testing Journal **11(2)**, pp 132 - 138.

Gan, J., Fredlund, D. and Rahardjo, H. 1988, *Determination of the Shear Strength Parameters of an Unsaturated Soil Using the Direct Shear Test*, Canadian Geotechnical Journal, **25(3)**, pp. 500 - 510.

Gan J. K-M., and Fredlund D. G., 1992, *Direct Shear Testing of a Hong Kong Soil under Various Applied Matric Suctions*, GEO Report No. 11, Geotechnical Engineering Office, Civil Engineering Department, Hong Kong, 587 pp.

Gan J. K-M., and Fredlund D. G., 1996, *Shear Strength Characteristics of Two Saprolitic Soils*, Submitted to Canadian Geotechnical Journal.

Gardner, W., and Widtsoe, J., 1921, *The Movement of Soil Moisture*, Soil Science Journal, Vol. 11, pp. 215 – 232.

Garven E. A., and Vanapalli S. K. 2006, *Evaluation of empirical procedures for predicting the shear strength of unsaturated soils*. In Unsaturated Soils 2006 (eds G. A. Miller, C. E. Zapata, S. L. Houston and D. G. Fredlund), Geotechnical Special Publication no. 147, pp. 2570 – 2581. Reston, VA, USA: American Society of Civil Engineers.

Geiser F., Laloui L., and Vulliet L., 2000, *On the volume measurement in unsaturated triaxial test*, In Unsaturated soils for Asia, Edited by H. Rahardjo, D.G. Toll, and E.C. Leong. A.A. Balkema, Rotterdam, The Netherlands, pp. 669 - 674.

Gireesha N.T., and Muthukkumaran K., 2011, Study on soil structure interface strength property", Int. J. Earth Sci. Eng., **4(6)**, pp 89 - 93.

Hamid T. B., 2005, *Testing and modelling of unsaturated interfaces*, Ph.D. thesis, University of Oklahoma, Oklahoma, United States.

Hamid T. B., and Miller G. A., 2008, *A constitutive model for unsaturated soil interfaces*, International Journal for Numerical and Analytical Methods in Geomechanics, **32(13)**: pp 1693 – 1714.

Hamid T. B., and Miller G. A., 2009, *Shear strength of unsaturated soil interfaces*, Canadian Geotechnical Journal, **46(5)**, pp 595 – 606.

Hamidi A., Habibagahi G., and Ajdari M., 2013, *Shear behaviour of Shiraz silty clay Determined using osmotic direct shear box*, Proceeding of the 5th Asian-Pacific Conference on Unsaturated soils, At Pattaya, Thailand, Volume: 2.

Hillel D., 1998, *Environmental Soil Physic*, Academic Press, San Diego, USA.

Ho D. Y. F., and Fredlund D. G., 1982, *Increase in strength due to suction for two Hong Kong soils*, Reproduced with permission from the proceedings, ASCE Geotechnical conference on Engineering and Construction in Tropical and Residual soils, Honolulu, Hawaii, pp 263 – 295.

Hossain M. A., 2010, *Experimental study on the interface behaviour between unsaturated completely decompose granite soil and cement grout*, Ph.D. thesis, The Hong Kong Polytechnic University, Hong Kong.

Hossain M. A., and Yin J. H., 2010, *Shear strength and dilative characteristics of an unsaturated compacted completely decomposed granite soil*, Canadian Geotechnical Journal, **47(10)**, pp 1112 – 1126.

Huat B., Ali H., Heng A., and Choong F., 2006, *Effect of Loading Rate on the Volume Change Behaviour of Unsaturated Residual Soil*. Geotechnical and Geological Engineering, **24**, pp. 1527 - 1544.

Hu P., Yang Q., and Li P. Y., 2010, *Direct and indirect measurement of soil suction in the laboratory*, Electronic Journal of Geotechnical Engineering, 15, Band A, pp 2 – 14.

Ismael N. F., and Behbehani M., 2014, *Influence of relative compaction on the shear strength of the compacted surface sands*, International Journal of Environmental Science and Development, **5(1)**, pp 8-11.

Jassim S. Z. and Goff J. C., 2006, *Geology of Iraq*, Engineering, **8**(8), Czech Republic, Brno, pp 341 – 352.

Jing X. Y., Zhou W. H., and Li Y., 2016, *Interface Direct Shearing Behavior between Soil and Saw-tooth Surfaces by DEM Simulation*, 1st International Conference on the Material Point Method, MPM 2017, pp 1-7.

Jennings J., Burland J., 1962, *Limitations to the Use Effective Stresses in Partly Saturated Soils*, Géotechnique, **12(2)**, pp. 125-144.

Josa A., Alonso E.E., Gens A., and Lloret A., 1987, *Stress-Strain Behaviour of Partially Saturated Soils*, Proc. 9 Eur. Conf. Soil Mech. and Found. Eng., pp. 561 - 564.

Kalhor A., 2012, *The Shear Strength Analyses of Soil with Various Compactions under Vertical Load in Direct Shear Test*, International Research Journal of Applied and Basic Sciences, **3**(S): pp 2815-2821.

Karube D., 1988, *New Concept of Effective Stress in Unsaturated Soil and its Proving Test*, Donaghe R.T., Chaney R.C., Silver M.L. (Eds), Advanced Triaxial testing of Soil 230 and Rocks, ASTM STP 977, American Society for Testing and Materials, Philadelphia, pp 539 - 555.

Karube D., and Kawai K., 2001, *The role of pore water in mechanical behaviour of unsaturated soil, Geotechnical and Geological engineering*, **19(3)**: pp 211 - 241.

Kasangaki G.J., 2012, *Experimental Study of Hydro-Mechanical Behaviour of Granular Materials*, Ph.D Thesis, Heriot-Watt University.

Katte V. Y., and Blight G. E., 2012, *The roles of solute suction and surface tension in the strength of unsaturated soils*, (ed.), Mancuso, C., Jommi, C &D′Onza F., Heildeberg: Springer.

Kawai K., Karube D., and Kato S., 2000, *The Model of Water Retention Curve Considering Effects of Void Ratio*, In: Rahardjo, H. Toll, D. G. and Leong, E. C. (Eds), Unsaturated Soils for Asia, Balkema, Rotterdam, pp. 329-334.

Khoury C. N., Miller G. A., and Hatami K., 2010, *Unsaturated soil geotextile interface behaviour, Journal of Geotextile and Geomembrane*, **29(1)**, pp 613 – 624.

Krahn J., and Fredlund D., 1972, *On Total Matric and Osmotic Suction*, Journal of soil science, **114 (5)**, pp. 339 - 348.

Kulhawy F. H. and Peterson M. S., 1979, *Behaviour of sand-concrete interfaces*, In Proceedings of 6th Pan-American Conference on Soil Mechanics and Foundation Engineering, Vol. 7, pp 225 – 236.

Lashkari A., 2010, *Sanisand Model with Anisotropic Elasticity*. Soil Dynamics and Earthquake Engineering, **30**, pp. 1462–1477.

Laskar A.H., and Dey A.K., 2011, *A study on deformation of the interface between sand and steel plate under shearing*, Proceeding of Indian Geotechnical Conference, Kochi, India, December, pp. 895 - 898.

Lee I., Sung S., and Cho, G., 2005, *Effect of Stress State on the Unsaturated Shear Strength of a Weathered Granite*, Canadian Geotechnical Journal, Vol. 42, pp. 624 - 631.

Lemos L. J. L., and Vaughan P. R., 2000, *Clay-interface shear resistance*, Géotechnique, **50(1)**, pp 55 - 64.

Leong E. C., Tripathy S., and Rahardjo H., 2003, *Total suction measurement of unsaturated soils with a device using the chilled-mirror dew-point technique*, Géotechnique, **53(2)**, pp. 173–182.

Lloret A., and Alonso E. E., 1985, *State surfaces for partially saturated soils*, Proc. 11th Int. Conf. Soil Mech. Fdn Engng, San Francisco, **2**, pp 557 - 562.

Long X., 2006, *Prediction of shear strength and vertical movement due to moisture diffusion through expansive soils*, Ph.D Thesis, TEXAS A&M University.

Lourenço S. D. N., Gallipoli D., Toll D. G., Evans F. D. 2006, *Development of a commercial tensiometer for triaxial testing of unsaturated soils*. In Miller et al. (eds.). ASCE Geotechnical Special Publication No. **147(2)**: pp 1875 - 1886.

Lu N., Likos W.J., 2004, *Unsaturated Soil Mechanics*, John Wiley and Sons, Inc., New Jersey, USA.

Lyklema, J., 2000, *Fundamental of Interface and Colloid Science*, Vol. III, Academic, New York.

Malaya C., and Sreedeep S., 2010, *A Study on the Influence of Measuring Procedures on Suction-Water Content Relationship of a Sandy Soil,* Journal of Testing and Evaluation, ASTM, Vol. **38 (6)**, pp. 1 - 9.

Malaya C., and Sreedeep S., 2012, *Critical Review on the Parameters Influencing Soil-Water Characteristic Curve*, Journal of Irrigation and Drainage Engineering, ASCE, **138(1)**.

Maleki M., and Bayat M., 2012, *Experimental Evaluation of Mechanical Behaviour of Unsaturated Silty Sand under Constant Water Content Condition*, Engineering Geology **(141–142)**, pp 45 – 56.

Marinho F. A. M., and Pinto C. D. S., 1997, *Soil suction measurement using a tensiometer*. In Almeida (ed.), Recent developments in Soil and Pavement Mechanics 1:249 - 254. Rotterdam: Balkema.

Marshal T., 1959, *Relations between Water and Soil*, Technical communication No. 50, Commonwealth Bureau of soils Harmondsworth, United Kingdom.

Matyas E., Radhakrishna H., 1968, *Volume Change Characteristics of Partially Saturated Soils*, Géotechnique, **18(4)**, pp. 432 - 448.

Medero G. M., Schnaid F., Gehling W. Y. Y., and Gallipoli D., 2005, *Analysis of the Mechanical Response of an Artificial Collapsible Soil*, Journal of Geotechnical and Geoenvironmental Engineering, **134(1)**: pp 9 - 15.

Miao L., Liu S, and Lai Y., 2002, *Research of Soil-water Characteristics and Shear Strength Features of Nanyang Expansive Soil*, Engineering Geology Vol. 65, pp. 261 – 267.

Miguel M. G., and Vilar O. M., 2009, *Study of Water Retention Properties of a Tropical Soil*, Can. Geotech. J., **46**, 2009.

Miller D. J., and Nelson J. D., 1993, *Osmotic suction as a valid stress state variables in unsaturated soil mechanics*, unsaturated soils, Geotechnical Special Publication, No. 30, pp 64 – 76.

Miller E., and Miller R., 1956, *Physical Theory for Capillary Flow Phenomena*, Journal of applied physics, **4(27)**, pp 324 - 332.

Miller C., Yesiller N., Yaldo K., and Merayyan S., 2002, *Impact of Soil Type and Compaction Conditions on Soil Water Characteristic*, Journal of Geotechnical and Geoenvironmental Engineering ASCE, **128(9)**, pp 733 – 742.

Moayed R. Z., Alibolandi M., and Alizadeh A., 2012, *Specimen size effects on direct shear test of silty sand*, International Journal of Geotechnical Engineering, **11(2)**: pp 1 – 8.

Murray E., and Sivakumar V., 2010, *Unsaturated Soils a Fundamental Interpretation of Soil Behaviour*, Wiley-Blackwell, United Kingdom.

Nam S., Gutierrez M., Diplas P., Petrie J., Wayllace A., Lu N., and Munoz J., 2009, *Comparison of Testing Techniques and Models for Establishing the SWCC of Riverbanksoils,* Engineering Geology, Volume 110, issue 1-2, pp 1 - 10.

Ng C. W. W., and Pang Y. W., 2000, *Influence of stress state on soil–water characteristics and slope stability*, Journal of geotechnical and Geoenvironmental Engineering, ASCE, Vol. 26, No. 2, pp. 157–166.

Ng C. W. W., and Chiu A. C. F., 2001, Behaviour of a loosely compacted unsaturated volcanic soil, Journal of Geotechnical and Geoenvironmental Engineering, **127(12)**, pp 1027 – 1036.

Ng C. W. W., Zhan I. T., and Cu Y. J., 2002, *A new simple system for measuring volume changes in unsaturated soils*, Canadian Geotechnical Journal, **39(3)**, pp 757 – 764.

Ng C., Menzies B., 2007, *Advanced Unsaturated Soil Mechanics and Engineering*, Taylor and Francis, Abingdon, United Kingdom.

Nishimura T., and Toyota h., 2002, *Interpretation of the direct shear strength of desiccated compacted soil in high soil suction ranges*, Environmental Geomechanics, Monte Verita, pp 201 - 206.

Paikowsky S. G., Player C. M., and Connors P. J., 1995, *A Dual Apparatus for Testing Unrestricted Friction of Soil Along Solid Surfaces*, Geotechnical Testing Journal, Vol. 18, No. 2, pp 168 - 193.

Palmeira E. M., and Milligan G. W. E., 1989, *Scale effects in direct shear tests on sand*, Proceedings of the 12th International Conference on Soil Mechanics and Foundation Engineering, **1(1)**: pp 739 – 742.

Parsons J. D., 1936, *Progress Report on an Investigation of the Shearing Resistance of Cohesionless Soils*, Proceedings of the 1st International Conference on Soil Mechanics and Foundation Engineering, **2**, pp 133– 138.

Pan H., Quing Y., Pei-Yong L., 2010, *Direct and indirect measurement of soil suction in the laboratory*, Electron. J. Geotech. Eng. (EDGE), **15 (1)**, pp 1 - 14.

Potyondy J. G., 1961, *Skin Friction Between Various Soils and Construction Materials*, Géotechnique, Vol. 11, No. 4, pp 831 - 853.

Rahardjo H., and Fredlund D. G., 1996, *Consolidation Apparatus for Testing Unsaturated Soils*, Geotechnical Testing Journal, Vol.19, No.4, pp 341-353.

Rahardjo H., Ong B. H., and Leong E. C., 2004, *Shear strength of a compacted residual soil from consolidated drained and constant water content triaxial tests*, Canadian Geotechnical Journal, June, **41(3)**, pp 421 - 436.

Rassam D., and Williams D., 1999, *A Relationship Describing the Shear Strength of Unsaturated Soils*. Canadian Geotechnical Journal, **36(2)**, pp 363 - 368.

Ridley A. M., 1993, *The measurement of soil moisture suction*, Ph.D. dissertation, Imperial College, University of London.

Ridley A. M., and Burland J. B., 1995, *A pore pressure probe for the in situ measurement of soil suction*, Proceedings of conference on advances in site investigation practice, London.

Ridley A.M., and Wray W.K., 1995, *Suction measurement: a review of current theory and practices*, In Proceedings of the 1st International Conference on Unsaturated Soils (UNSAT 95), Paris,1995 (Eds. E.E. Alonsoand P. Delage), Balkema, Rotterdam: pp 1293 - 1322.

Rojas E., 2008*, Equivalent stress equation for unsaturated soils*, I: Equivalent stress, International Journal of Geomechanics **8**: pp 285 - 290.

Romero E., and Vaunat J., 2000, *Retention curves of deformable clays*, Proc. Int. Workshop on Experimental evidence and theoretical approaches in unsaturated soils, 91-106, Trento (Italy), Balkema, Rotterdam.

Rouaiguia A., 2010, *Residual shear strength of clay-structure interfaces*, International Journal of Civil & Environmental Engineering, **10(3)**, pp 6 - 18.

Schofield R., 1935, *The pF of the Water in Soil*, Trans. 3rd Int. Congress soil Sci., Vol. 2, pp 37 - 48.

Sowers G. F. and Sowers G. B., 1970, *Introductory soil mechanics and foundations: geotechnical engineering*, New York.

Take W. A., and Bolton M. D., 2003, *Tensiometer saturation and the reliable measurement of soil moisture suction*. Géotechnique **53(2)**, pp 159 - 172.

Terzaghi K., 1936, *The Shearing Resistance of Saturated Soils*, Proc. 1st Int. Conf. on Soil Mechanics, Cambridge, pp 54 – 56.

Thu T., Rahardjo H., and Leong E., 2007, *Soil-Water Characteristic and Consolidation behaviours of Compacted Silt*, Canadian Geotechnical Journal, Vol.44, pp 266 - 275.

Tinjum J., Benson C, and Blotz, L., 1997, *Soil-Water Characteristic Curves for Compacted Soils*, Journal of Geotechnical and Geoenvironmental Engineering, Vol. 11, pp 1060 - 1069.

Tiwari B., and Al-Adhadh, A., 2014, *Influence of Relative Density on Static Soil Structure Frictional Resistance of Dry and Saturated Sand*. Geotechnical and Geological Engineering **32 (2)**, pp 411 - 427.

Toll D., 1990, *A Framework for Unsaturated Soil Behaviour*. Géotechnique, **40(1)**, pp 31 - 44.

Uesugi M., and Kishida H., 1986, *Influential Factors of Friction Between Steel and Dry Sands*. Soils and Foundation, **26(2)**, pp 29 – 42.

Vanapalli S., Fredlund D., Pufhal D., and Clifton A., 1996, *Model for the Prediction of Shear Strength With Respect to Soil Suction*. Can Geotech J., **33**, pp 379 - 392.

Vanapalli S., Fredlund D., and Pufhal D., 1999, *The Influence of Soil Structure and Stress History on the Soil-Water Characteristics of a Compacted Till*, Géotechnique, **49(2)**, pp 143 - 159.

Wang Y. H., and Fredlund D. G., 2003, *Towards a better understanding of the role of the contractile skin*, Proceedings of the 2nd Asian Conference on Unsaturated Soils, pp 15 - 17.

Wheeler S., and Karube D., 1995, *Constitutive Modelling*, Proceedings of the First International Conference on Unsaturated Soils, Paris, pp 1323-1350.

Wheeler S. J., 1986, *The stress-strain behaviour of soils containing gas bubbles*, D. Phil. Thesis, University of Oxford, UK.

Wheeler S. J., Sharma R. S., and Buisson M. S. R., 2003, *Coupling of hydraulic hysteresis and stress-strain behaviour in unsaturated soils*, Géotechnique **53(1)**, pp 41 – 54.

White N. F., Duke H. R., Sunada D. K., and Corey A. T., 1970. *Physicsof desaturation in porous materials*, J. Irr. Div. Am. Soc. Civ. Eng. Proc.JR-2: pp165 - 191.

Wilson W., 1990, *Soil Evaporative Fluxes for Geotechnical Engineering Problems*, PhD dissertation, University of Saskatchewan, Saskatoon, Sask., Canada, pp 464.

Yang H., Rahardjo H., and Fredlund D., 2004, *Factors Affecting Drying and Wetting Soil Water Characteristic Curves of Sandy Soils*, Canadian Geotechnical Journal, **41(5)**, pp 908 - 920.

Yoshimi Y., and Kishida T., 1981, *Friction between Sand and Metal Surface*. Proceedings, 10th International Conference on Soil Mechanics and Foundation Engineering, Vol. 1, pp. 831-834.

Zainal A. K. E., and Abbas M. F., 2016, *Effect of Variation of Degree of Saturation with depth on Soil–Concrete Pile Interface in Clayey Soil*, Journal of Engineering, 22(4), pp 1-17.

Zhen l., Yi-chuan X., 2006, *Effects of dry density and percent fines on shearing strength of sandy cobble and broken stone*. Rock and Soil Mechanics, **27(12)**, pp 2255 - 2260.